



# Al-Mustansiriyah

## ISSN 1814 - 635X

Journal of Science

Vol. 23, No. 6, 2012



Issued by College of Science - Mustansiriyah University

Vol. 23  
No. 6  
2012

# **Al-Mustansiriyah**

## **Journal of Science**

Issued by College of Science, Al-Mustansiriyah  
University, Baghdad, Iraq

### **Editor -in-chief**

Prof. Dr. Redha I. AL-Bayati

### **Manager Editor**

Prof. Dr. Khudhur H. Ali

### **Editorial Board**

Dr. Inaam Abdul-Rahman	Member
Dr. Fatin Fadhil	Member
Dr. Iman Natiq	Member
Dr. Ahmed Azeez	Member
Dr. Muneam Hakeem	Member
Dr. Omar Abbas	Member
Dr. Kareem Qasim	Member
Dr. Saad Owaid	Member

### **Consultant Committee**

Dr. Tariq Salih Abdul-Razaq	Member
Dr. Hasan Hashim	Member
Dr. Tariq Suhail Najim	Member
Dr. Ali Hussein Dehya	Member
Dr. Abd Al-Muneam Salih	Member
Dr. Layla Salih	Member

Mobile: 07711184399

e-mail: [mustjsci@yahoo.com](mailto:mustjsci@yahoo.com)

## INSTRUCTION FOR AUTHORS

1. The journal accepts manuscripts in Arabic and English languages. Which had not been published before.
2. Author (s) has to introduce an application requesting publication of his manuscript in the journal. Four copies (one original) of the manuscript should be submitted. Should be printed by on the computer by laser printer and re produced on A4 white paper in three coppice with floppy disc should be also submitted.
3. The title of the manuscript together with the name and address of the author (s) should typed on a separate sheet in both Arabic and English. Only manuscripts title to be typed again with the manuscript.
4. For manuscripts written in English, full name (S) of author (s) and only first letters of the words (except prepositions and auxiliaries) forming title of the manuscript should be written in capital letters. Author (s) address (es) to be written in small letters.
5. Both Arabic and English abstracts are required for each manuscript. They should be typed on two separate sheets (not more then 250 words each).
6. References should be denoted by a number between two bracket on the same level of the line and directly at the end of the sentence. A list of references should be given on a separate sheet of paper, following the interactional style for names and abbreviations of journals.
7. Whenever possible, research papers should follow this pattem: INTRODUCTION, EXPERIMENTAL (MATERIALS AND METHODS), RESULTS AND DISCUSSION, and REFERENCES. All written in capital letters at the middle of the page. Without numbers or underneath lines.
8. The following pattern should be followed upon writing the references on the reference sheet: Sumame (s), intials of author (s), title of the paper, name or abbreviation of the journal, volume, number, pages and (Year). For books give the author(s) name(s), the title, edition, pages, publisher, place of publication and (Year).
9. A publication fees in the amount of ID. 50 thousand is charged upon a Receipt of the paper and 25 thousand upon the acceptance for publication for their ID. 75 thousand should be paid for the editorial board.

## CONTENTS

ITEM	Page No.
Comparison of Antimicrobial Activities of Methanol Extracts of <i>Juglans regia</i> against <i>Staphylococcus aureus</i> , & <i>Streptococcus mutans</i> with Ciprofloxacin: <i>In Vitro</i> Najah Ali Mohammed, Yehi Kassem Hossien, and Kifah Ahmed Jassim	1-6
Insecticidal Activity of Aqueous and Methanol Extracts of Apricot <i>Prunus armeniaca</i> L. Kernels in the Control of <i>Tribolium confusum</i> Duval (Coleoptera: Tenebrionidae) Hind S. Abdulhay	7-18
Epidemiological Study on <i>Fasciola Hepatica</i> In Children and Animals At Babylon City Rafid abdalwahed abdalnabi	19-26
Effect of Phoenix dactylifera Pollen on In Vitro Sperm Activation of Infertile Men Saad S. AL-Dujaily <sup>1</sup> , Nahla J. AL-Shahery, and Areeg	27-34
Detection of <i>Chlamydia trachomatis</i> Using polymerase chain reaction (PCR) Shatha T. Al	35-42
Autoimmune Haemolytic Anemia Associated With Some Diseases Amany Mohammed Jasim and Safa A. Fadil	43-52
The Extraction and Purification Of Gallic Acid from the Pomegranate Rind Entessar H.A. Al-Mosawe and Iman I. Al- Saadi	53-60
Study the effect of Insulin Resistance on visfatin, Total Anti oxidant Capacity and other Anti oxidants in Females with Chronic renal Failure [Stage 3] Atheer Awad Mehde	61-74
Synthesis Of Some Pyranopyrazoles-6-One Derivatives By Microwave Method Redha I,H,AL-Bayati, Foad .M, Saed and Wassan B, Ali	75-82
Synthesis of new pyrazole derivatives derived from 4-hydroxy coumarin and evaluation of their biological activity Redha I. H. Al-Bayati, Ammar A.R. Kubba and Mahdi H. Radi	83-92
Preparation Of New 2-Imino-hexahydro-1,3-Thiazepine Derivatives Hamed Jassim Jaffar and Ahmed Qassim Abdul-Hussein	93-116
Study of Some <i>Mirabilis jalapa</i> L. Leaves Components and Effect of Their Extracts on Growth of Pathogenic bacteria Mustafa Taha Mohammed	117-124
Unifying Technique for Multisource Remote Sensing Images Firas Abdulrazzaq Hadi And Rawnaq Adil Abdulwahhab	125-136
Fitting a Two Parameters of Weibull Distribution Using Goodness of Fit Tests Rasha Abdul Hussein Ali	137-148



Investigation of Reciprocity of Energy Loss in Gases and Solid Materials	Baida Mohsen Ahmed	149-158
Study the Design of Dielectric Chirped Mirror	Elham Jasim Mohammad	159-172
Studies on Physical Properties of SnO <sub>2</sub> : Co Nano-crystalline Thin Films Prepared by Spray Pyrolysis Technique	Ali Jasim AL-Jabiry	173-182
Study Some Of Physical Properties Of Gan/Si(100) For Solar Cell Applications	Wisam Jafer Aziz	183-188
Design Fast Feed Forward Neural Network to Solve Initial Value Problems	Luma. N. M. Tawfiq and Yaseen. A. Oraibi	189-196
On Optimal Codes	Najm A. M. AL-Seraji	197-204
A Not on Fully (m,n)-stable modules relative to ideal	Muna Jasim Mohammed Ali	205-210
Using Semi – Analytic Technique for Solving Heat Conduction Problem in the Human Head	Luma N. M. Tawfiq and Heba W. Rasheed	211-218
On Feebly Door spaces	Qays R. Shakir	219-224
The Rate of multi Approximation of Unbounded Functions by Means of K-Functional	Saheb Al-Saidy and Ban Mohommed Hassen	225-230
A Remark on Generalized Semi- Preregular Closed Sets	Adhiya K. Hussain	231-232
Multi Spectral Scanner “MSS” and Panchromatic Components Difference of Al- Haditha Dam Region Using GIS and Remote Sensing Techniques	Israa J. Muhsin, Faleh Hassan Mahmood and Fouad K. Mashee	233-242

## Comparison of Antimicrobial Activities of Methanol Extracts of *Juglans regia* against *Staphylococcus aureus*, & *Streptococcus mutans* with Ciprofloxacin: *InVitro*

Najah Ali Mohammed<sup>1</sup>, Yehi Kassem Hossien<sup>2</sup>, and Kifah Ahmed Jassim<sup>3</sup>

<sup>1,2</sup>Science Microbiology, Assistant professors, Technical medical institute  
Consultant, Health central laboratories

Received 6/5/2012 – Accepted 20/6/2012

### الخلاصة

يعتبر التسوس من بين مجموعة المشكلات السنية المزمنة والخطيرة أيضاً، وهو مرض مايكروبي مؤدي إلى تكلس أنسجة الاسنان وأن البلاك البكتيري يلعب دور أساسي في الأمراض، في هذا البحث تم مقارنة الفعالية البكتيرية لخلاصة قشور السيقان لنبات الجوز الميثانولية ضد اثنين من بكتريا الموجبة لصبغة كرام (العنقوديات الذهبية والمسبحيات الميوتنسية). اجري الاختبار لفعالية خلاصة النبات على البكتريا المعزولة من نماذج اللعاب لمرضى يعانون من تسوس الاسنان والتهاب اللثة وباستخدام طريقة التنافذ بالحفر ومقارنة منطقة التثبيط مع المضاد البكتيري سيروفلوكساسين.

تم في هذه الدراسة تقييم الفعالية البكتيرية لخلاصة قشور السيقان لنبات الجوز الميثانولية ضد اثنين من بكتريا الموجبة لصبغة كرام (العنقوديات الذهبية والمسبحيات الميوتنسية). وكانت منطقة التثبيط 8.7 ملم و 7.2 ملم للمسبحيات الميوتنسية والعنقوديات الذهبية على التوالي، بينما كانت منطقة التثبيط للمضاد البكتيري سيروفلوكساسين 15.1 ملم و 15.52 ملم و 15.1 ملم ضد كل من المسبحيات الميوتنسية والعنقوديات الذهبية على التوالي.

### ABSTRACT

Among several dental problems caries process (cavitation) is deadly serious and chronic too. It is an irreversible microbial disease of calcified tissues of teeth. Bacterial plaque plays the primary role in the pathogenesis of the disease. This work compares the antibacterial activities of methanol extracts of stem bark of *Juglans regia* against two Gram positive bacteria (*Staphylococcus aureus*, *Streptococcus mutans*). The efficacy of the plant extracts has been assessed by testing on salivary samples of patients suffering from dental carries and gingivitis by antimicrobial assay was carried out using well diffusion method and compared the zone of inhibition of the extracts with ciprofloxacin (antibacterial).

The present study, antibacterial activities (zone of inhibition in mm) of methanol extracts of bark stem of *Juglans regia* against *S. mutans*, *S. aureus* was evaluated. methanolic bark extract of *Juglans regia* was effective in inhibiting the two bacteria with zone of inhibition 7.2mm and 8.7mm against *S. mutans*, *S. aureus* respectively while the inhibition zone of Ciprofloxacin 15mm and 15.52mm, 15.1mm against *S. mutans*, *S. aureus* respectively.

Key words: *Juglans regia*, medicinal plant, antimicrobial activity, well diffusion

### INTRODUCTION

The advancement in biological and engineering research is bringing a medical revolution to dentistry. Among several dental problems caries process (cavitation) is deadly serious and chronic too. It is an irreversible microbial disease of calcified tissues of teeth, characterized by demineralization of inorganic portion of teeth and destruction of organic substance of teeth (1). It was established that mutans group of Streptococci are the key agents causing dental caries (2).

The increasing failure of chemotherapeutics and antibiotic resistance exhibited by pathogenic microbial infectious agents has led to the screening of several medicinal plants for potential antimicrobial activity, and the plant extracts were found to have potential against microorganisms (3, 4).

Over the past few decades, there has been much interest in natural products as sources of new antimicrobial agents. Different extracts from traditional medicinal plants have been tested (5). Many reports show the effectiveness of traditional herbs against microorganisms. As a result, plants have become one of the bases of modern medicine (6).

There is a continuous need of new antimicrobial components due to rapid emergence of multidrug-resistant pathogens and explosive dreadful infectious diseases (7). Plants are natural source of antibacterial agents. Plant-derived medicines have been a part of our traditional health care system, and the antimicrobial properties of plant derived compounds are well documented. Herbal medicines are more effective and less harmful as they have negligible side effects. They exhibit low mammalian toxicity and can be handled (6, 8). In Ayurvedic system of medicines *Juglans regia* is reported to have potent activity for dental complaints. The juice of the green husks, boiled with honey, is a good gargle for a sore mouth and inflamed throat. A piece of the green husks put into a hollow tooth, eases the pain. Decoction of the stem bark is useful in dental complaints (9). Antifungal, antibacterial and antioxidant activities of this plant have also been described by (10, 11). The health benefits of walnuts are usually attributed to their chemical composition. Walnuts are a good source of essential fatty acids and tocopherols (12).

In the present investigation, the methanolic stem bark extracts of *Juglans regia* were evaluated for antimicrobial activity against common human pathogen

## MATERIALS AND METHODS

### Preparation of methanol extract:

Twenty five grams of the material was soaked in 100 ml of methanol and allowed to stand for 24 hrs followed by boiling until the volume was reduced to one-third. The extracts were obtained by filtration and stored in a refrigerator at 4°C .

### Inoculums preparation:

The tested bacteria firstly isolated from saliva patients suffering from dental carries and gingivitis on mitis salivarius + bacitracin medium and identification by API-20 Strep. system (bioMérieux, France) for *S. mutans*, and on Brain Heart Infusion agar for *S. aureus* (13). Seven colonies of the strains were inoculated to Brain Heart Infusion broth and

incubated at 37°C for 22–24 h. The turbidity was adjusted with sterile broth to correspond to the 0.5 McFarland standards.

#### Agar well diffusion method

Antibacterial activity of methanolic stem bark extracts were tested using agar well diffusion method (14). The microbial inoculum was standardized at 0.5 McFarland. 200µl of bacteria were aseptically introduced and spread using cotton swabs on surface of Muller Hilton agar plates. A well of about 6.0mm diameter with sterile cork borer was aseptically punched on each agar plate. 50µl of the methanolic stem bark of *J. regia* were introduced into the wells in the plates. A negative control well was too made with 50µl of the extracting solvent (methanol). Ciprofloxacin was used as positive control. Plates were kept in laminar flow for 30 minutes for pre diffusion of extract to occur and then incubated at 37°C for 24 hours. After incubation all the plates were observed for zones of inhibition and the diameters of these zones were measured in millimeters. All tests were performed under sterile conditions. Finally the diameter of the zone of inhibition were recorded and expressed in mm (15).

**Statistical analysis:** The results were calculated as mean diameter of zone of inhibition in mm  $\pm$  standard deviation (mean  $\pm$  SD). By ANOVA analysis.

## RESULTS AND DISCUSSION

In the present study, antibacterial activities (zone of inhibition in mm) of methanol extracts of bark stem of *Juglans regia* were studied against two gram positive bacteria *S. mutans*, *S. aureus* was evaluated. methanolic bark extract of *Juglans regia* was effective in inhibiting the two bacteria with zone of inhibition ,7.2mm and 8.7mm against *S. mutans*, *S. aureus* respectively while the inhibition zone of Ciprofloxacin 15mm to 15.52mm against *S. mutans*, *S. aureus* respectively Table (1) and (Figure 1 &2).

Table-1: Inhibition zone (mm) of methanolic bark extract of *Juglans regia* against *S. mutans* compared with Ciprofloxacin.

Agent or inhibitor	The mean of inhibition zone mm averages $\pm$ SD)	
	<i>mutans</i>	<i>Staph. aureus</i>
<i>jugules reja</i> L.	7.2 $\pm$ 2.1	8.7 $\pm$ 2.7
Ciprofloxacin.	15.52 $\pm$ 3.10	15.1 $\pm$ 3

\*=significant at0.05



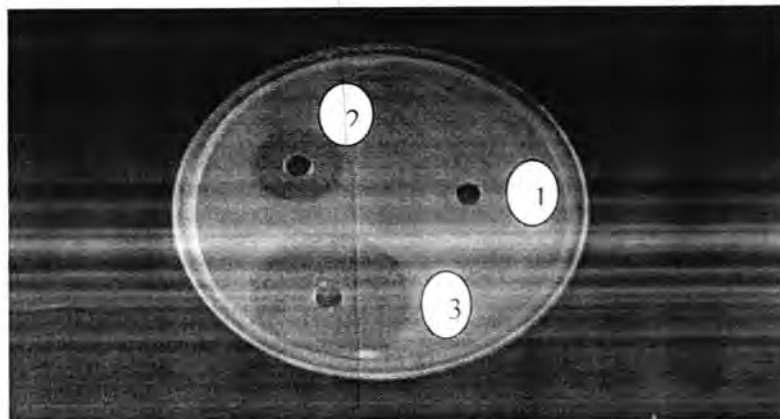


Figure-1: Inhibition zone (mm) of methanolic bark extract of *Juglans regia* against *S. mutans* compared with Ciprofloxacin.

1=negative control. 2= *Juglans regia*. 3= Ciprofloxacin.

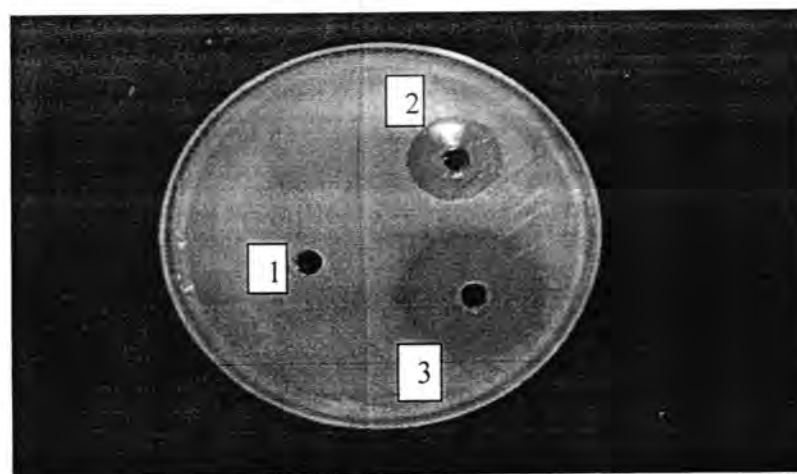


Figure-2: Inhibition zone (mm) of methanolic bark extract of *Juglans regia* against *S. aureus* compared with Ciprofloxacin.

1=negative control. 2= *Juglans regia*. 3= Ciprofloxacin.

Antimicrobial activities of various other parts of *Juglans regia* have already been studied with different microorganisms. (16) reported the growth inhibition effect of *Juglans regia* bark extract against gram positive (*S. aureus* and *S. mutans*), gram negative (*E. coli* and *P. aeruginosa*) and pathogenic yeast (*C. albicans*). (17) studied the antimicrobial activity of *Juglans regia* leaf extracts, in which they reported the zone of inhibition ranged from 15.8–17.6 mm against *P. acnes*, 11.3–15.7 mm against *S. aureus* and 12.9–15.5 mm against *S. epidermidis* by disc diffusion method. The chemical composition, antioxidant potential and antimicrobial activity were studied in the fruits of six walnuts (*Juglans regia*) cultivars Franquette, Lara, Marbot, Mayette, Mellanaise and Parisienne) produced in Portugal. Their

antimicrobial activities were checked against gram positive (*Bacillus cereus*, *Bacillus subtilis*, *Staphylococcus aureus*) and gram negative bacteria (*Pseudomonas aeruginosa*, *Escherichia coli*, *Klebsiella pneumoniae*) and fungi (*Candida albicans*, *Cryptococcus neoformans*), revealing activity against the different tested microorganisms(18,19). Antibacterial properties of the plant material may be due to the presence of phenolic compounds, terpenoids, alkaloids, flavonoids and steroids (20). It is reported that leaves from *J. regia* L. contain monoterpenes and sesquiterpenes, and the bark contains ketones like juglone, regiolone, sterol and flavonoid(21,22).

Methanol extract was found to be more effective of the extracts as anti-microbial against the oral microflora. This study has confirmed the antimicrobial potentials of the plant, thus supporting its folklore application as a preventive remedy for various microbial diseases of hard tissues in the oral cavity.

### RERERANCES

1. Antony E. Winston and Sindu N. Bhaskar. Low sucrose levels promote extensive *S. mutans*-induced dental caries. Journal of American Dental Association, vol.129, Nov. (1998).
2. Jason M. Tanzer. "Bacterial Genomics-*Streptococcus mutans*", National Academy of Sciences, USA, vol 99.No. 22, pp: 14434-14439 (2002).
3. Kafaru E. Immense Help Formative Workshop. In: Essential. Pharmacology, 1st edn. pp.11-14. Elizabeth Kafaru Publishers, Lagos, Nigeria. 125(1994).
4. Jason M. Tanzer, *Streptococcus salivarius* FruA Inhibits *Streptococcus mutans* biofilm formation. Journal of Dental Research vol.74, pp:1536 (1995).
5. Pizsolitto A.C, Mancini and B., Fracalanza L. Determination of antibacterial activity of essential oils officialized by the Brazilian pharmacopeia, 2nd edition. Chem. Abstr. 86:12226s(1977).
6. Evans, C.E., A. Bansa and O.A. Samuel. Efficacy of some medicinal plants against *Salmonella typhi*: an in vitro study. J. Ethnopharmacology.80:21-24(2002).
7. Jones,G.,and Moellering R.C. Increasing antibiotic resistance among methicillin-resistant *Staphylococcus aureus* strains. Clin. Infect. Dis. 46 Suppl 5: 360-367 (2004).
8. Ahmad I, Mehamood Z, Mohammad F. Screening of some Indian medicinal plants for their antimicrobial properties. J. Ethnopharmacol. 62: 183-193(1998).
9. Argueta and Cano. Phytotherapy Research, Vol 22 Issue 4, 13 Mar.2008, pp.557-559 (1994).

10. Locher C.P., Burch M.T., Mower H.F., Berestecky J., Davis H. Anti- microbial activity and anti-complement activity of extracts obtained from selected Hawaiian medicinal plants. *J. Ethnopharmacol.* 49(1): 23-32(1995).IVSL.
11. Fadi Qa'dan, Abdul-Jalil Thewaini, Dalia A. Ali, Rana Afifi, Abdalla Elkhawad and Khalid Z. Matalaka. The antimicrobial activities of *Psidium guajava* and *Juglans regia* leaf extracts to acne-developing organisms. *The American Journal of Chinese Medicine*, 33: 197-204(2005).
12. Al-Bayati F.A. and Sulaiman K. D. Efficacy of Aqueous and Methanol Extracts of Some Medicinal Plants for Potential Antibacterial Activity. *Turk J. Biol.*, pp.57-62 (2008).
13. Hosseinzadeh H, Bazzaz BSF, Haghi MM. Anti-bacterial activity of total extracts of *Juglans regia* in Mice. *Pharmacol.*, 2007; 2: 429-435.
14. Alkhawajah, A.M. Studies on antimicrobial activity of *Juglans regia*. *Am. J. Chin. Med.*, 25: 175-180(1997).
15. Lino A, Deogracious O. The in-vitro antibacterial activity of *Annona senegalensis*, *Securidacca longipendiculata* and *Steanotaenia araliacea*- Ugandan Medicinl plants. *Afri. Health Sci.* 6(1): 31-35. (2006).
16. Oliveira, I., A. Sousa, I.C. Ferreira, A. Bento, L. Estevinho and J.A. Fereira. Total phenols, antioxidant potential and antimicrobial activity of walnut (*Juglans regia* L.) green husks. *Food and Chem. Toxicol.*, 46: 2326-2331(2008).
17. Inbaraj and Chignell. Screening of some traditionally used medicinal plants for potential antibacterial activity. *Toxicology and applied Pharmacology*, Vol.209, Issue 1, 15 Nov. pp.1-9 (2005).
18. Bandow J. E., Brotze H., Leichert LIO, Pharmacological and toxicological properties of *Juglans regia* .*Antimicorb. Agents Chemother*, Vol 47, pp. 948-955 (2003).
19. Duke J. A. *Handbook of Energy Crops*, pp.269. 9(1983).
20. Pereira, J.A., I. Oliveira, A. Sousa, I.C.F.R. Ferreira, A. Bento and L. Estevinho. Bioactive properties and chemical composition of six walnut (*Juglans regia* L.) cultivars. *Food and Chemical Toxicology*, 46: 2103-2111(2008).
21. Vijay K. J., Hari P. D., and Xianghe Yan. Novel Natural Food Antimicrobials. *Annual Review of Food Science and Technology* Vol. 3: 381-403 (2012).IVSL.
22. Rauha, J.-P., S. Remes, M. Heinonen, A. Hopia, M. Kahkonen, T. Kujala, K. Pihlaja, H. Vuorela and P. Vuorela. Antimicrobial effects of Finnish plant extracts containing flavonoids and other phenolic compounds. *Int. J. Food Microbiol.*, 56: 3-12(2000).

## Insecticidal Activity of Aqueous and Methanol Extracts of Apricot *Prunus armeniaca* L. Kernels in the Control of *Tribolium confusum* Duval (Coleoptera: Tenebrionidae)

Hind S. Abdulhay

Department of Biology, College of Science, University of Baghdad, Baghdad, Iraq

Received 27/2/2012 – Accepted 20/6/2012

### الخلاصة

بيّنت الدراسة فاعلية المستخلصين المائي والميثانولي لبذور المشمش *Prunus armeniaca* L. في هلاك خنفساء الطحين المحيرة *Tribolium confusum* Duval. حضّرت تراكيز 2.5، 5، 10، 15، 20 ملغم / مل لكلا المستخلصين وتم الاعتماد على طريقتين: الأولى مزج كل من المستخلص المائي والميثانولي مع غذاء البالغات الصناعي والآخرى تضمنت معاملة يرقات الطور الرابع والبالغات مباشرة. تباينت استجابة الحشرات تبعاً لنوع المستخلص والتركيز، إذ بلغت قيم التركيز القاتل 50% بعد 7 أيام و 54.854 و 4.192 ملغم / مل فيما بلغت 77.079 و 2.384 ملغم / مل بعد 14 يوماً لكل من المستخلص المائي والميثانولي على التوالي. وجد أن يرقات وبالغات خنفساء الطحين المحيرة أكثر حساسية للمستخلص الميثانولي قياساً مع المستخلص المائي. كما أشارت النتائج إلى وجود علاقة طردية بين زيادة التركيز ورمز التغذية وبين زيادة سمية المستخلصات على الحشرة. فيما أظهرت نتائج المعاملة المباشرة سمية عالية على خنفساء الطحين المحيرة ولكلا المستخلصين. وكان معدل هلاك اليرقات لجميع التراكيز أعلى من البالغات. تُعد الدراسة الأولى في بحث فاعلية بذور المشمش ضد الحشرات ودلت نتائجها على أن مستخلصات بذور المشمش قد تكون واعدة في مكافحة خنفساء الطحين المحيرة فضلاً عن كونها آمنة بيئياً.

### ABSTRACT

The present study revealed the insecticidal activity of aqueous and methanol extracts of apricot *Prunus armeniaca* L. kernels on confused flour beetle *Tribolium confusum* Duval. Extracts were prepared in the rate of 2.5, 5, 10, 15 and 20 mg ml<sup>-1</sup>. Two methods were adopted: the first one consists on an incorporation of water and methanol extracts in the artificial diet of adults and the second concerns an abdominal application on 4<sup>th</sup> instar larvae and adults. Insect responses varied according to extract and concentration. After 7 days, the LC<sub>50</sub> values were estimated to be 54.854 and 4.192 mg ml<sup>-1</sup> while, after 14 days were 77.079 and 2.384 mg ml<sup>-1</sup> respectively for aqueous and methanol extracts. It was found that *T. confusum* larvae and adults were more susceptible to the methanol extract compared with aqueous extract. Increasing the concentration and ingestion time increased the toxicity of extract on insect. Extracts topically applied on *T. confusum* revealed high toxicity caused by methanol and aqueous *P. armeniaca* kernels extracts. Also, methanol extracts was more active compared to the aqueous extracts. For all extracts, mortality was higher for larvae than adults. It is the first work undertaken on apricot kernels insecticidal activity and its results suggest that apricot kernel extracts could be promising for managing populations and environmentally safe for control confused flour beetle.

### INTRODUCTION

Apricot (*Prunus armeniaca* L.) is a member of the Rosaceae family, along with apple, pear, peach, and other stone fruits. Apricot fruit, being a rich source of carbohydrates, organic acids, mineral elements and



vitamins, is one of the most familiar crops worldwide [1]. It has been used in folk medicine as a remedy for various diseases including hemorrhages, infertility, eye inflammation and spasm [2]. Apricot is a quite valuable fruit that can be processed into numerous different products (e.g. jam and fruit juice). The seeds of its kernel are by-products of the apricot processing industry. The kernels are used in the treatment of asthma, coughs, acute or chronic bronchitis and constipation. Also, kernel oil has been used in cosmetics as a pharmaceutical agent [3,4].

Apricot kernels contain amygdalin D(-)-mandelonitrile  $\beta$ -gentiobioside [5,6] belongs to cyanogenic glycoside, which are phytoanticipins widely distributed in more than 2500 different plant species [7] including economical important plants like white clover, linum, almond, sorghum, rubber tree and cassava [8]. Also, it is found in most stone fruit seeds and bitter almonds, they are considered to have an important role in plant defense against herbivores due to bitter taste and release of toxic hydrogen cyanide upon tissue disruption [9]. D-amygdalin is the main component of apricot seed extract [10] which contains various amounts of amygdalin depending on cultivars. It is reported that bitter cultivars contain higher amygdalin than sweet cultivars [5]. Overconsumption of seeds containing high amount of cyanogenic glycoside might cause acute or chronic toxicity in human beings and animals [11]. However, recently, interest in amygdalin is gradually increasing due to a derivative of amygdalin, that is, laetrile (vitamin B17), which use as secondary cancer chemotherapy and antineoplastic agent has been encouraged [10,12]. Nevertheless, the cancer-preventive efficiency of laetrile has not been proved yet, and it is reported that no permission could be obtained from the U.S. Food and Drug Administration for the use of vitamin B17 as a drug in the treatment of patients [13] while, in traditional Chinese medicinal amygdalin can be used in medicine for preventing and treating migraine, hypertension, chronic inflammation, and other reaction source diseases, most important of all, amygdalin is used as a medicament for the treatment of cancer [14]. Amygdalin, which has been isolated from a large number of species, is primarily restricted in the generative parts of the plants, the fruits and seeds of Rosaceae [5,15]. Small quantities of amygdalin have, previously been reported from foliage [16].

Numerous reports concerning the physicochemical characteristics of apricot seeds are available in the literature [17,18], but lacks the insecticidal activities of apricot kernels. Thus, the objective of the present study was to determine the insecticidal activities of aqueous and methanol extracts of *P. armeniaca* L. kernels on confused flour beetles *Tribolium confusum* Duval (Coleoptera: Tenebrionidae), which is one of

the most abundant and injurious insect pest milled grain and stored products, such as flour, cereals, meal, beans, spices, pasta, and even dried museum specimens, both adults and larvae feed on grain dust and broken kernels, but not the undamaged whole grain kernels [19]. It also showed a resistance to several traditional synthetic insecticides commonly used as grain protectants [20,21]. The insecticidal activity of many plant derivatives against several stored-product pests has been demonstrated [22,23,24,25].

## MATERIALS AND METHODS

### INSECTS REARING

Cultures of *T. confusum* were obtained from a laboratory rearing maintained on artificial diet of wheat flour mixed with yeast (95:5 w/w) at a constant temperature of  $30 \pm 1^\circ\text{C}$  and  $70 \pm 5\%$  r.h, in darkness [26]. The adults were moved to new rearing medium every 2 days, this procedures allowed us to obtain *T. confusum* larvae and adults used in tests.

### PLANT MATERIAL

Fresh Apricot fruits (*P. armeniaca* L.) were collected at their optimum commercial maturity in Baghdad, Iraq in 2010. Apricot flesh was removed from fruits; the apricot outer shell was washed with tap water and air-dried at  $34 \pm 1^\circ\text{C}$  for about 2 weeks, the outer shell of apricot was cracked manually to obtain the kernel, which were dried then pulverized to powder using an electrical grinder, and packaged in plastic bags for preservation until used.

### PREPARATION OF EXTRACTS

Aqueous extracts were prepared by adding (20g) of pulverized kernel to (200 ml) distilled water in a glass flask, and mixed for 15 minutes on a rotary shaker (200 rpm). The solution was incubated for 24 h at  $25^\circ\text{C}$ . Thereafter, it was filtered through Whatman No.1 filter paper, then the extracts was taken to dryness on oven at  $40^\circ\text{C}$ . Following the same steps for the preparation of methanol extract except replacing distilled water by methanol and the mixture was filtered and methanol was removed by rotary evaporator to give the crude methanol extract [2]. The dried extracts were kept at  $4^\circ\text{C}$ .

In order to test the effect of the aqueous extract (2g) of dry matter were taking and dissolved in (100ml) of distilled water to obtain a final concentration of  $20\text{mg ml}^{-1}$  (2%). The control was prepared by the same way but extract application was excluded. While for testing the dry substance results from extract in methanol (2g) were taken and

dissolved in (3ml) of methanol, completed to (100ml) by distilled water to obtain the same concentration  $20\text{mg ml}^{-1}$ , control was (3ml) methanol completed to (100 ml) by distilled water. All extracts were kept in airtight bottles at  $4^{\circ}\text{C}$  for further studies.

## BIOASSAYS

Preparing the concentration 2.5,5,10,15,20  $\text{mg ml}^{-1}$ , assayed for toxicity bioassay by:

### 1. Toxicity by topical application

One microliter of each concentration and control were abdominally applied to adults aged between 10-14 days old and 4<sup>th</sup> instar larvae according to [27] on the mean 3.23mm length, and 0.40mm head capsule width (five replications). The mortality rate was recorded after 2, 4, 24, 48 and 72 hours. [28]. The calculation of mortality rate was corrected for control mortality according to Abbott's correction [29]:

$$Mo = \frac{Mt - Mc}{100 - Mc} \times 100$$

Where: Mt = mortality rate of treated insect (%), Mc = mortality rate of control(%), Mo = corrected mortality rate (%).

### 2. Toxicity by ingestion

The method described by [30] was adopted, using wafer discs prepared from artificial diet. Ten discs were treated with each concentration of apricot seeds water and methanol extract (5 $\mu\text{l}$ ). Ten other discs were treated either with water or methanol alone as control. The solvent was allowed to evaporate during 24 hours at  $27 \pm 3^{\circ}\text{C}$ . After evaporation of solvent, two treated discs were placed in each glass vial (2.5 cm diam.  $\times$  5.5 cm high) where ten unsexed adults of *T. confusum* (10-14 days old) were then introduced (five replicates). Each 7 days, the number of dead insects was recorded during 2 weeks [22, 31].

## STATISTICAL ANALYSIS

Mortality data were analyzed with SPSS software [32]. Probit analysis was used to determinate  $\text{LC}_{50}$  values. Data were analyzed using one-way analysis of variance (ANOVA) The results were expressed as means  $\pm$  Standard deviation (SD) and were statistically significant at  $p = 0.05$ , Duncan test was used.

## RESULTS AND DISCUSSION

### TOXICITY BY TOPICAL APPLICATION

During the experiment, larval and adults mortality rate increased constantly in time (Fig.1, 2, 3 and 4). Statistical analyses showed

significant effect in methanol extracts. The comparison activity between aqueous and methanol extract showed that methanol extracts were more toxic than aqueous extract in all treatments. At 20 mg ml<sup>-1</sup> concentration there was a significant toxic effect reaching 100% of all period of time on larval and adults, but for the same concentration, with aqueous extracts, mortality rate did not exceed 70% and 55% for larval and adults, respectively.

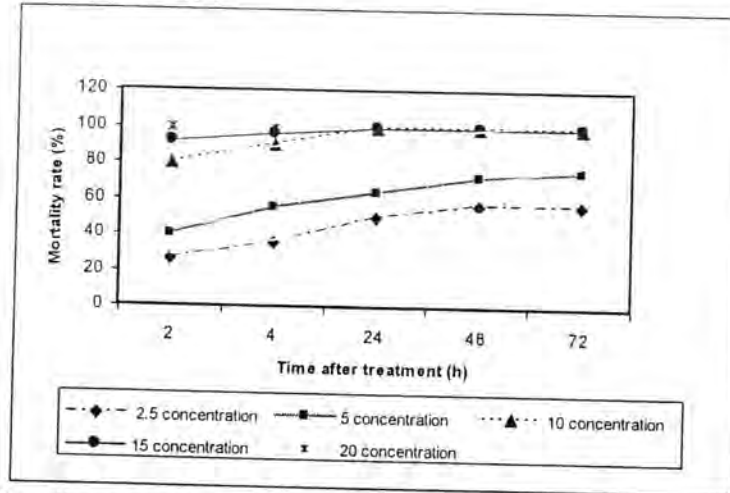


Figure-1: Mortality rate of *T.confusum* larvae treated by topical application with methanol extracts of *P.armeniaca* kernel

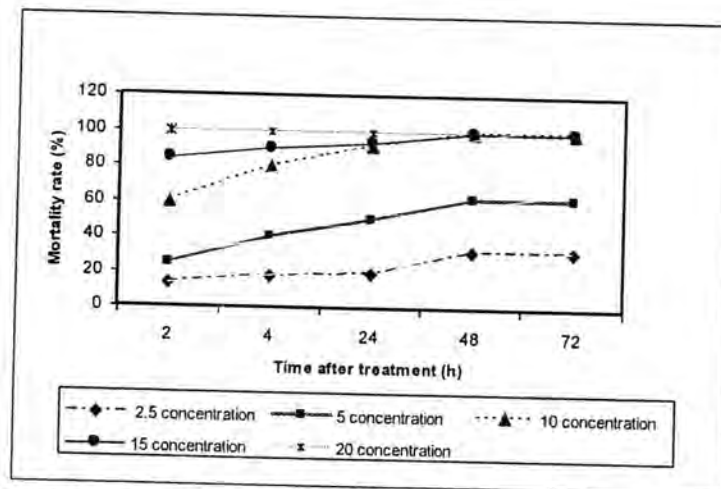


Figure-2: Mortality rate of *T.confusum* adults treated by topical application with methanol extracts of *P.armeniaca* kernel



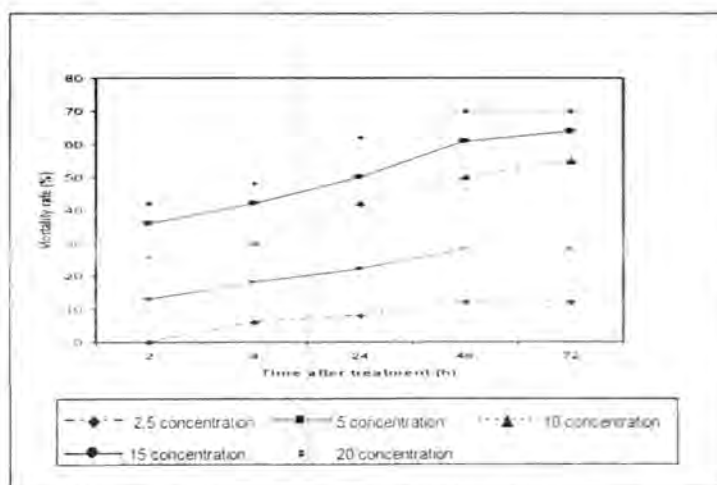


Figure-3: Mortality rate of *T. confusum* larvae treated by topical application with aqueous extracts of *P. armeniaca* kernel

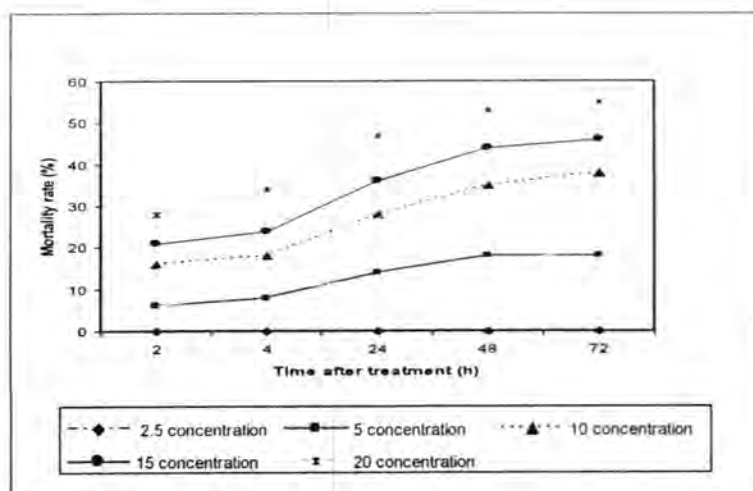


Figure-4: Mortality rate of *T. confusum* adults treated by topical application with aqueous extracts of *P. armeniaca* kernel

## TOXICITY BY INGESTION

The toxic activity of aqueous and methanol extracts against *T. confusum* adults by ingestion showed increase in adult mortality rate (Table 1). Firstly, after 7 days no mortality was noted for the aqueous extracts concentration 2.5, 5, 10 mg ml<sup>-1</sup> and were low for 15, 20 mg ml<sup>-1</sup>, compared with the highest mortality caused by methanol extracts concentration. The LC<sub>50</sub> values were estimated to be 54.854 and 4.192 mg ml<sup>-1</sup> respectively for aqueous and methanol extracts (Table 2). After two weeks, high toxicities of methanol extracts were observed, varied between 56% with 2.5 mg ml<sup>-1</sup> and 94% with 20 mg ml<sup>-1</sup>, and the LC<sub>50</sub> values were 77.079 and 2.384 mg ml<sup>-1</sup> respectively for aqueous and methanol extracts (Table 3). Hence, kernel methanol extract were more toxic than aqueous extract and *T. confusum* adults were more susceptible to methanol extract compared with aqueous extract.

Increasing the concentration and ingestion time increased the toxicity of extract on insect.

Table-1: Toxic effects caused by ingestion of flour discs treated with apricot seeds extracts in adults of *T. confusum*

Concentration (mg ml <sup>-1</sup> )	Extract	7 (days)	14 (days)
2.5	aqueous	0 ± 0 b	10 ± 1.22 b
	methanol	45 ± 7.91 ac	56 ± 5.54 ac
5	aqueous	0 ± 0 b	14 ± 3.81 b
	methanol	50 ± 7.07 a	65 ± 12.25 a
10	aqueous	0 ± 0 b	18 ± 2.80 b
	methanol	62 ± 10.37 a	76 ± 10.84 a
15	aqueous	5 ± 1.22 b	25 ± 5.25 bc
	methanol	66 ± 11.94 a	85 ± 7.91 a
20	aqueous	11 ± 4 bc	34 ± 6.75 b
	methanol	82 ± 5.71 a	94 ± 6.52 a

Values followed by the same letter within a column are not significantly different at the  $P < 0.05$  level (Duncan test).

Table-2: LC<sub>50</sub> values of apricot seeds extracts to *T. confusum* adults at 7 days

Extract	LC <sub>50</sub> (mg ml <sup>-1</sup> )	Slope (± SE)	Intercept (± SE)	R <sup>2</sup>
Aqueous	54.854	4.339 (±1.798)	-2.545 (±1.747)	0.812
Methanol	4.192	1.033 (±0.245)	4.357 (±0.238)	0.925

Table 3: LC<sub>50</sub> values of apricot seeds extracts to *T. confusum* adults at 14 days

Extract	LC <sub>50</sub> (mg ml <sup>-1</sup> )	Slope (± SE)	Intercept (± SE)	R <sup>2</sup>
Aqueous	77.079	0.897 (±0.143)	3.307 (±0.139)	0.964
Methanol	2.384	1.429 (±0.163)	4.461 (±0.159)	0.951

The results revealed insecticidal effects of apricot kernels extracts on *T. confusum*. However, methanol extracts were more toxic than aqueous. Indeed successful prediction of botanical compounds from plant material is largely dependent on the type of solvent used in the extraction procedure. In our studies we found that plant extracts in organic solvent (methanol) provided more consistent insecticidal activity compared to the extracted in water. These observations can be rationalized in terms of the polarity of the compounds being extracted by each solvent, therefore, methanol can dissolve organic compounds better and quickly than water so more toxic compounds in methanol extract, in addition to their bioactivity. In fact, [33] demonstrated apricot kernels (*P. armeniaca*) and bitter almond kernels having a content of

amygdalin of about 3–4% by weight. [34] obtain similar results for the methanol extracts of four medicinal plants, *Peganum harmala* (Zygophyllaceae), *Aristolochia baetica* (Aristolochiaceae), *Ajuga iva* (Labiatae) and *Raphanus raphanistrum* (Brassicaceae) on *Tribolium castaneum*.

Topical application on *T. confusum* showed also, after 48 hours of treatment, significant toxic effects reached to 100% caused by methanol extracts of *P. armeniaca* at concentration 10, 15, 20 mg ml<sup>-1</sup> for larvae and adults. Moreover results showed that larvae were more susceptible than the adults. The mortality rate for the larvae after 2h was 1.6 and 2.17 times more susceptible than adults for methanol and aqueous extracts respectively. Same results obtain by [21,26] tested salt marsh plants for their insecticidal activities against *Tribolium confusum*, and mentioned that larvae were more sensitive than adults, while [35,36,37] find *T. confusum* can survive at application rates of substances which are lethal for other stored-grain beetle species and slightly higher dose rates are needed to kill all larvae of this insect. Other studies revealed that a hexane extract of clove flower buds, which contains mainly eugenol, demonstrated a toxic contact effect on *Sitophilus zeamais* and *T. castaneum* and reduced their fecundity [38]. Also, [39] reported that eugenol was toxic to four stored-product coleopteran species, namely, *S. zeamais*, *Sitophilus granarius* L., *T. castaneum* and *Prostephanus truncates* Horn.

According to our results, we can suggest that *P. armeniaca* could be a source of insect growth disturbing. In fact, this study demonstrates that *P. armeniaca* methanol extracts were toxic by ingestion and by topical application (with all concentration). The use of such plant extracts in insect control is an alternative pest control method for minimizing the noxious effect of pesticides on the environment. Hence, *P. armeniaca* extracts could be developed as insecticides against *T. confusum*.

#### ACKNOWLEDGEMENTS

The author is grateful to Emeritus Prof. Dr. Mohammed A. Al-Rawy (Department of Biology, College of Science, University of Baghdad) for plant identification.

## REFERENCE

1. Ruiz D., Egea J., Gil M.I. and Tomas-Barberan F.A., Phytonutrient content in new apricot (*Prunus armeniaca* L.) varieties, *Acta. Hort.*, 717: 363-365, (2006).
2. Yiğit D., Yiğit N. and Mavi A., Antioxidant and antimicrobial activities of bitter and sweet apricot (*Prunus armeniaca* L.) kernels, *Braz. J. Med. Biol. Res.* 42(4): 346-352, (2009).
3. Dwivedi D.H. and Ram R.B., Chemical Composition of Bitter Apricot Kernels from Ladakh, India, *Acta. Hort.*, (ISHS) 765: 335-338, (2008).
4. Targais K., Stobdan T., Yadav A. and Singh S.B., Extraction of apricot kernel oil in cold desert Ladakh, India, *Indian Journal of Traditional Knowledge*, 10(2):304-306, (2011).
5. Gomez E., Burgos L., Soriano C. and Marin J., Amygdalin content in the seeds of several apricot cultivars, *J. Sci. Food Agric.*, 77:184-186, (1998).
6. Tatsuma T., Komori K., Yeoh H.H. and Oyama N., Disposable test plates with tyrosinase and b-glucosidases for cyanide and cyanogenic glycosides, *Analytica.Chimica.Acta.*, 408:233-240 (2000).
7. Zagrobelny M., Bak S. and Moller B.L., Cyanogenesis in plants and arthropods, *Phytochem.*, 69:1457-1468, (2008).
8. Bak S., Paquette S.M., Morant M., Rasmussen A.V., Saito S., Bjarnholt N. and *et al.* Cyanogenic glycosides: a case study for evolution and application of cytochromes P450, *Phytochem., Rev.* 5: 309-329, (2006).
9. Zagrobelny M., Bak S., Rasmussen A.V., Jørgensen B., Naumann C.M. and Møller B.L., Cyanogenic glucosides and plant-insect interactions, *Phytochem.*, 65:293-306, (2004).
10. Kang S.H., Jung H., Kim N., Shin D.H. and Chung D.S., Micellar electrokinetic chromatography for the analysis of D-amygdalin and its epimer in apricot kernel, *J. Chromatogr., A.* 866:253-259, (2000).
11. Silem A., Günter H.O., Einfeldt J. and Boualia A., The occurrence of mass transport processes during the leaching of amygdalin from bitter apricot kernels: detoxification and flavour improvement, *Int.J.Food Sci.Tech.*, 41:201-213, (2006).
12. Suchard J.R., Wallace K.L. and Gerkin R.D., Acute Cyanide Toxicity Caused by Apricot Kernel Ingestion, *Ann. Emergency Med.*, 32(6):742-744, (1998).
13. Asma B.M. and Misirli A., Kayısı çekirdeği, *Hasad Bitkisel Üretim*, 22(261): 55-58, (2007).



14. China Pharmacopoeia Committee, Pharmacopoeia of the People's Republic of China; 1<sup>st</sup> Division, China Chemical Industry Press: Beijing, p. 160–161, (2000).
15. Dicenta F., Martinez-Gomez P., Grane N., Martin M.L., Leon A., Canovas J.A. and Berenguer V., Relationship between cyanogenic compounds in kernels, leaves, and roots of sweet and bitter kernelled almonds, J. Agric. Food Chem., 50:2149–2152, (2002).
16. Santamour F.S., Amygdalin in *Prunus* leaves, Phytochem., 47:1537–1538, (1998).
17. Dragovic-Uzelac V., Delonga K., Levaj B., Djakovic S. and Pospisil J., Phenolic profiles of raw apricots, pumpkins, and their purees in the evaluation of apricot nectar and jam authenticity, J. Agric. Food Chem., 53: 4836-4842, (2005).
18. Rashid F., Studies on the chemical constituents of *Prunus armeniaca*, Dissertation, University of Karachi, Karachi. 152p, (2003).
19. Weston P.A. and Rattigourd P.L., Progeny production by *Tribolium castaneum* (Coleoptera: Tenebrionidae) and *Oryzaephilus surinamensis* (Coleoptera: Silvanidae) on maize previously infested by *Sitotroga cerealella* (Lepidoptera: Gelechiidae), J. Econ. Entomol., 93:533-536, (2000).
20. Zettler J.L. and Arthur F.H., Dose-response tests on red flour beetle and confused flour beetle (Coleoptera: Tenebrionidae) collected from flour mills in the United States, J. Econ. Entomol., 90:1157-1162, (1997).
21. Vayias B.J. and Athanassiou C.G., Factors affecting the insecticidal efficacy of the diatomaceous earth formulation SilicoSec against adults and larvae of the confused flour beetle, *Tribolium confusum* Duval (Coleoptera: Tenebrionidae), J. Crop Prot., 23:565-573, (2004).
22. Huang H., Lam S.L. and Ho S.H., Bioactivities of essential oil from *Elletaria cardamomum* (L.) Maton. to *Sitophilus zeamais* Motschulsky and *Tribolium castaneum* (Herbst), J. Stored Products Res., 36:107-117, (2000).
23. Fields P.G., Xie Y.S. and Hou X., Repellent effect of pea (*Pisum sativum*) fractions against stored- product insects, J. Stored Prod. Res., 37: 359-370, (2001).
24. Tripathii A. K., Prajarati V., Verm N., Baiil J.R., Bansal R.P., kiianuja S.P.S. and Kumar S., Bioactivities of the leaf essential oil of *Curcuma Longa* (Var. ch66) on three Species of stored-product beetles (Coleoptera), J. Econ. Entomol., 95:183-189, (2002).

- 25.Saidana D., Ben Halima-Kamel M., Ben Tiba B., Haouas D., Mahjoub M.A., Mighri Z. and Helal A.N., Bio-insecticidal activities of Halophylic plant extracts against *Tribolium confusum* (Coleoptera: Tenebrionidae), Comm. App. Sci. Ghent. Univ.,70:793- 798,(2005).
- 26.Saidana D. M., Ben Halima-Kamel M. . Mahjoub M.A., Haouas D., Mighri Z. and Helal A.N. Insecticidal Activities of Tunisian Halophytic Plant Extracts against Larvae and Adults of *Tribolium confusum*, Tropicultura,25(4):193-199,(2007).
- 27.Brindley T.A.,The growth and development of *Ephestia kuehniella* Zeller and *Tribolium confusum* Duval under controlled conditions of temperature and relative humidity, Annals Ent.Soc.Amer.,23:741-757,(1930).
- 28.Haouas D., Ben Halima-Kamel M. and Ben Hamouda M.H., Insecticidal activity of flower and leaf extracts from *Chrysanthemum* species against *Tribolium confusum*, Tunis J. Plant Prot., 3(2): 87-93,(2008).
- 29.Abbott W.S.,A method of computing the effectiveness of insecticides,J. Econ.Entomol.,18 : 265–267,(1925).
- 30.Bloszyk E., Szafranski F., Drozd B. and Al-Shameri K., African plants as antifeedant against stored product insect pests,J. Herbs. Spices Med. Plants, 3(1): 25-35,(1995).
- 31.Alonso-Amelot M.E., Avila J.L., Otero L.D., Mora F. and Wolff B., A new bioassay for testing plant extracts and pure compounds using red flour beetle *Tribolium castaneum* Herbst , J. Chem. Ecol., 20(5):1161-1177,(1994).
- 32.SPSS Inc., SPSS for windows user's guide release 6, Chicago IL. 320 p,(1993).
- 33.Niels T., Extraction of amygdalin from fruit kernels, Patent., No.WO 9: 620,716,(1996).
- 34.Jbilou R.,Ennabli A. and Sayah F.,Insecticidal activity of four medicinal plant extracts against *Tribolium castaneum* (Herbst)(Coleoptera:Tenebrionidae),African J.Biotech,5:936-940,(2006).
- 35.Kubo I., Screening techniques for plant-insect interactions, In K. Hostettemann (ed): Methods in Plants Biochemistry, Vol.6. Academic Press. pp179-193,(1991).
- 36.Arthur F.H.,Impact of food source on survival of red flour beetles and confused flour beetles (Coleoptera:Tenebrionidae)exposed to diatomaceous earth,J.Econ.Entomol,93:1347-1356,(2000)
- 37.Fields P. and Korunic Z., The effect of grain moisture content and temperature on the efficacy of diatomaceous earths from different

geographical locations against stored-product beetles, J. Stored Prod. Res., 36:1-13,(2000).

38. Ho S.H., Cheng L.P.L., Sim K.Y. and Tan H.T.W., Potential of cloves (*Syzygium aromaticum* (L.) Merr.) and perry as a grain protectant against *Tribolium castaneum* (Herbst) and *Sitophilus zeamais* Motsch, Postharvest. Biol. Tec., 4:179-183,(1994).
39. Obeng-Ofori D. and Reichmuth C., Bioactivity of eugenol, a major component of essential oil of *Ocimum suave* (Wild.) against four species of stored-product Coleoptera, Int. J. Pest. Manag., 43:89-94, (1997).

## Epidemiological Study on *Fasciola Hepatica* In Children and Animals At Babylon City

Rafid abdalwahed abdalnabi

Department of pharmacy, Alyarmok University College

Received 28/12/2011 – Accepted 28/2/2012

### الخلاصة

شملت الدراسة التحري عن وبائية الدودة الكبدية *Fasciola hepatica* للفترة من شهر تموز 2010 ولغاية شهر حزيران 2011 في محافظة بابل واختيرت ثلاثة مناطق واحدة في مدينة الحلة واثنان في مدينة المسيب حيث تم التحري عن الإصابة في الاطفال وكذلك عن نسبة الإصابة في المضيف الوسيط *Galba truncatula*.

ولقد كانت نسبة الإصابة في الاطفال 6.6 % اما في الحيوانات فكانت في الابقار 14.3 % والاغنام 35 % اما الماعز كانت 68.4 % اما بخصوص نسبة الإصابة في المضيف الوسيط كانت 19.2 %

### ABSTRACT

Epidemiological investigations on *Fasciola hepatica* were carried out from July 2010 to June 2011 in the Babylon after the detection of a children case. Three habitats were studied: one in El Hilla city and two in AlMusayib. The prevalence of human infection was 6.6 %. The presence of the parasite was detected through serology in 14.3 % of cattle, 35 % of sheep and 68.4 % of goats. the prevalence of the infection of the intermediate host *Galba truncatula* was 19.2 % from July 2010 to June 2011.

### INTRODUCTION

The fasciolosis caused by *Fasciola hepatica* a parasite trematode, is of considerable medical and veterinarian importance, because it contaminates the breeding of cattle, goats, horses, ovines and swines, resulting in serious losses for the cattle and as a matter of fact raising economic problems in many countries.

Compared to other helminths the life-cycle is complex, involving an intermediate host, the mud snail *Galba* (*Lymnaea*) *truncatula* and several free-living stages. The role of the snail, which prefers muddy, slightly acidic conditions, particularly areas associated with poor drainage, means that the incidence of liver fluke is far greater in the wetter areas of the country and in years when there is high summer rainfall.

With the capacity of the snail to multiply rapidly (100,000 offspring in 3–4 months) along with the multiplication of the parasite within the snail, there is potential for very large numbers of parasites [1].



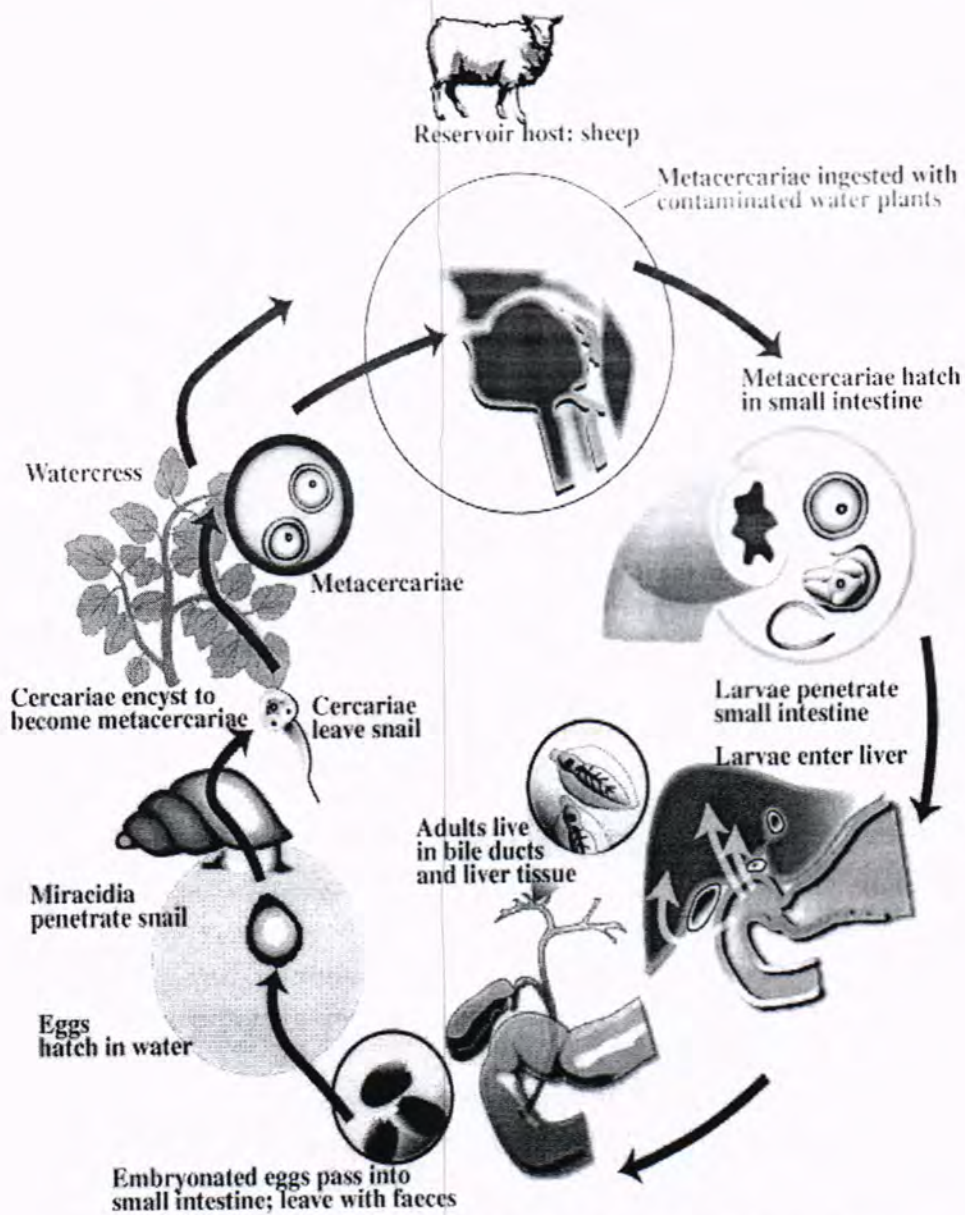


Figure-1: Life-cycle of the liver fluke, *Fasciola hepatica*.

Adult fluke lay eggs that are passed out onto pasture in the faeces. At suitable temperatures, a miracidium develops within the egg, hatches and migrates in thin films of moisture, actively seeking the snail host. Miracidia can only survive for a few hours outside the snail. Within the snail they undergo two further developmental stages, including multiplication, eventually becoming infective cercariae, which emerge from the snail when the temperature and moisture levels are suitable. The cercariae migrate onto wet herbage, encysting as metacercariae, the highly resilient infective stage of the liver fluke. Following ingestion, the young flukes migrate to the liver, through which they tunnel, causing considerable tissue damage. The infection is

patent about 10–12 weeks after the metacercariae are ingested. The whole cycle takes 18-20 weeks, in wet summers, snail populations multiply rapidly and snails are invaded by hatching miracidia from May–July. If wet weather continues, the snails shed massive numbers of cercariae onto pasture during July–October. Conversely, if the climate in May–July is dry or cold, fewer snails appear, fewer fluke eggs hatch and levels of contamination in the autumn are much lower. Clinical fasciolosis resulting from summer infection of snails arises usually from ingestion of large numbers of metacercariae over a short period of time in July–October [2]. Recent reports indicate that fasciolosis is a reemerging highly pathogenic human infection whose epidemiological picture has changed in recent years about 17 million people, most of them are children, are thought to be infected by the liver fluke *F. hepatica*, including human endemics in Europe, Asia, Africa and America [3]. There are two ecological sites which are particularly favourable to fasciolosis development in Babylon.

The first in the south of Babylon with classical ecological conditions [4] and the second in the south west with a microclimate suitable to the development of

the parasitosis [5] [6]. Recently a human case of distomatosis has been reported [7]. The aim of this study to determine the epidemiology of fasciolosis in Babylon. The focal points were upon the frequency of this disease in children and animals and the prevalence of infection of the intermediate host *G. truncatula*.

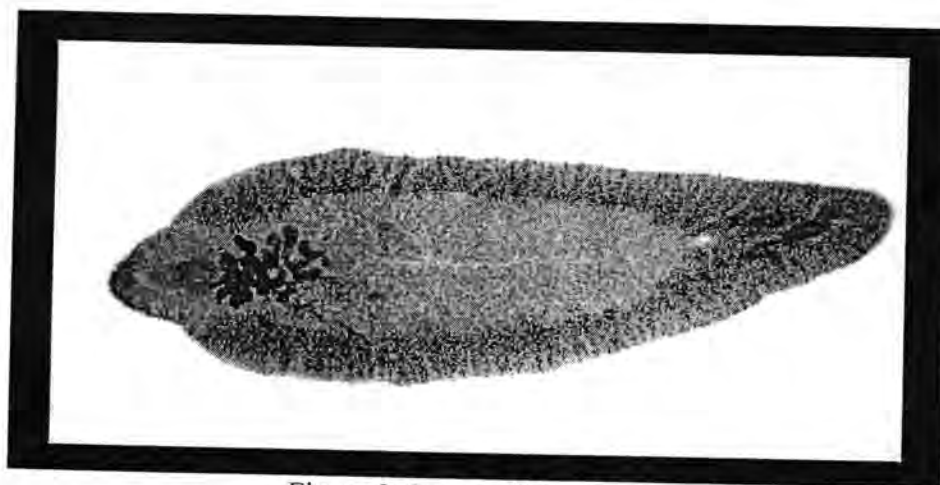


Figure-2: Image of *Fasciola hepatica*.

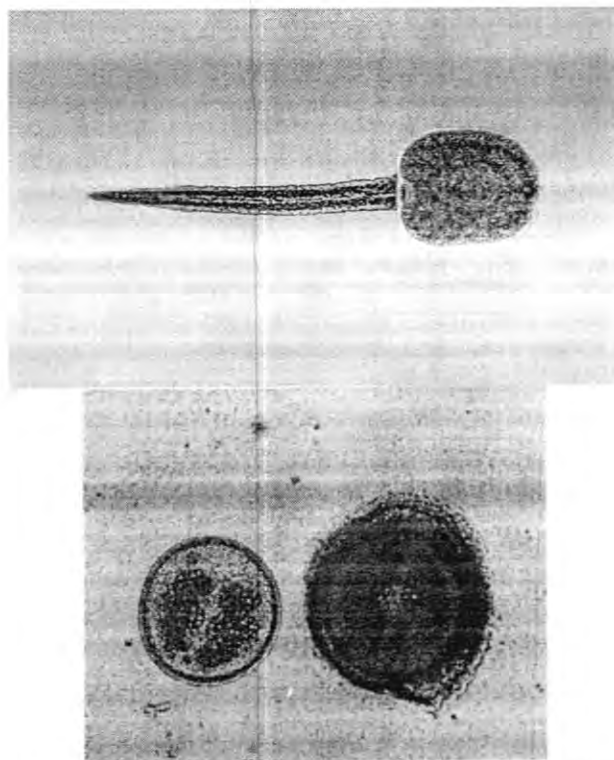


Figure-3: Ceraria of *Fasciola hepatica*. Figure 4: Metacercaria of *Fasciola hepatica*.

### MATERIALS AND METHODS

Venous blood specimens were obtained from all children and animals from July 2010 to June 2011 are centrifuged at 3000xg for 5 min, and the obtained serum specimens were kept in Eppendorf tubes at -20°C. ELISA was used to detect IgG antibodies to *Fasciola hepatica* in the serum specimens.

. Samples our investigations about the importance of animal and children fasciolosis in El Hilla are based on serological analysis using ELISA and electrosyneresis techniques. A total of 30 sera belonging to asymptomatic children were randomly chosen among samples.

. Samples from 53 animals: 14 cattle (all raised in El Hilla city), 20 sheep (nine from El Hilla and 11 from AlMusayib) and 19 goats (all from AlMusayib) were examined to check the presence of fluke infection by taking blood samples. These animals are grazing herbs from these habitats and are living in El Hilla and AlMusayib

Figure 5: Map of Babylon



Snails were collected from habitats1, habitats2 and habitats3 and transported to the laboratory in isothermal conditions. A number of 1,346 snails, whose heights ranging from 3.5 to 5.5 mm, have been dissected and observed by means of a microscope so as to identify *F. hepatica* meracidium, sporocyst and to determine the infection rate.

## RESULTS AND DISCUSSION

The diagnostic of children fasciolasis by serology was positive for two cases among 30 (6.6 %): one case with an age of 1 years ranging from 1 to 3 and another with an age of 4 years ranging from 3 to 5. The serology was negative for the slice age from 5 to 8 years.

The infection rate was 41.5 % for animals. Two cattle among 14 (14.3 %), seven sheep (one from El Hilla and six from AlMusayib) among the 20 (35 %) and 13 goat among the 19 (68.4 %) were infected.

The prevalence of the intermediate host infection was 19.2 % for all molluscs collected. Two infection periods have been observed in each habitat: from September to October and December to April in h1; from October to March and May to June in h2, and from October to January and April to June in h3.



Table-1: Number of samples collected and Percentage of infection in human and animals

Blood samples	Total	Positives	Percentages
Children	30	2	6.6 %
Cattle	14	2	14.3%
Sheep	20	7	35%
Goat	19	13	68.4%

Table-2: Monthly prevalence of intermediate host infection with *F. hepatica* in three populations of *G. truncatula*

Months of study	Habitats1	Habitats2	Habitats3	Total
July	17 (0)	0 (0)	0 (0)	17 (0)
August	11 (0)	0 (0)	0 (0)	11 (0)
September	54 (20.4)	20 (0)	20 (0)	94 (11.7)
October	35 (25)	32 (34)	30 (43)	97 (35)
November	53 (1.8)	39 (28)	46 (67)	138 (31.1)
December	46 (19)	51 (64.7)	44 (45)	141 (43.9)
January	26 (30)	32 (6.2)	29 (48)	87 (27.5)
February	47 (46)	22 (18)	34 (2.9)	103 (26.2)
March	70 (7)	25 (4)	25 (0)	89 (26.9)
April	70 (5)	35 (0)	33 (18)	138 (7.9)
May	39 (2.6)	37 (8.1)	32 (18.7)	108 (9.2)
June	35 (2.8)	50 (14)	38 (13.1)	123 (10.6)
Total	472 (19.3)	543 (13.2)	331 (29)	1,346 (19.2)

The total infection percentage of Children and animals with *F. hepatica* show Significant differences were noticed ( $P \leq 0.05$ ) Table 1.

In our study, the lower rate of 6.6 % in children cases goes in tandem with the rate reported by many researchers in the world: 2 % to 17 % in Egypt [8] 1.8 % in Turkey [9] However human rate of fasciolosis was higher in Mantaro-Valley: 36.3 % in Huertas and 22.7 % in Julcan [10] . Increasing number of infected animals due to the grazing of this animals in contaminated areas with snails that represents the intermediate host for *F. hepatica*. Also there is no controlling for these snails in these areas, In addition to absence of persons knowledge how work with animals [11].

Serological investigations of 53 sera from Hilla city revealed a rate of 35 % in sheep and 68.4 % in goat higher than in cattle (14.3 %).

This could be explained by the fact that cattle were kept in farms and sheep and goats were grazing herbs from habitat with infected snails.

The infection rate of ovine was lower in Algeria (6.4 % in Constantine and 23 % in Jijel) [12]. But the rate was more important in cows in Bolivia (100 %) and in Ethiopia (51.2 %) [13]. usually sheep and cattle are preferential hosts; goats are a less receiver and less parasitized. But in our study goats have a high rate of infection in El Hilla. The high number among this species in the Babylon suggests that they play a local role in the transmission of the parasite.

## REFERENCES

1. Mas-Coma S, Angles R, Esteban JG, Bargues MD, Buchon P, Franken M, Strauss W, The northern Bolivian Altiplano: a region highly endemic for human fasciolosis, *Tropical Medicine and International Health*. 4:454-467.(1999).
2. Moghaddam AS, Massoud J, Mahmoodi M, Mahvi AH, Periago MV, Artigas P; Fuentes M.V., Bargues M.D. & Mascomas. Human and animal fasciolosis in Mazandaran province, Northern Iran. *Parasitology Research*. 94. 61-69. 2004.
3. Hopkins D.R. Homing in on helminths. *American Journal of Tropical Medicine and Hygiene*. 46; 626-634.(1992).
4. Al-Barwary S.E. A survey on liver infections with *F. gigantica* among slaughtered animals in Iraq. *Bull End Dis*. 18; 75-92.(1978). *Iraqi Journal of Veterinary Sciences*, Vol. 22, No. 2, (81-85) 85 2008.
5. Al-Mashhadani H.M. Morphology and ecology of Lymnoid snails of Iraq with special reference to fascioliasis. MSc thesis, College Vet Med University of Baghdad 1970.
6. Altaif. KI. Observation on the incidence and seasonal variation of some helminth eggs and larvae in sheep in Iraq. *Bull End Dis*; 12: 99-109(1970).
7. Sellami H; Elloumi M; Cheikhrouhou F., Makni F., Baklouti S, Ayadi A. *Fasciola hepatica* infestation with joint symptoms. *Joint Bone Spine*. 70; 71-72. (2003).
8. Lotfy W.M. Hillyer G.V. *Fasciola species* in Egypt. *Experimental Pathology and parasitology*. 6, 9-17. (2003).
9. Yilma, J.M. & Mesfin, A. Dry season bovine fasciolosis in northwestern part of Ethiopia. *Revue de Médecine Vétérinaire (Toulouse)*, 151, 493-500 (2000). YILMAZ H. & GODEKMERDAN A. Human fasciolosis in Van province. Turkey. *Acta Tropica*. 92, 161-162. (2004).
10. Raymundo. L.A.; Flores V.M. Terashima A.A., Samalvides F., Miranda E., Tantalean M., Espinoza J.R. Gotuzzo E. Hyperendemicity of human fasciolosis in the Mantaro Valley, Peru: factors for infection with *Fasciola hepatica*. *Revista de Gastroenterología del Peru*, 24, 158-164. (2004).
11. Petalia, T.M. Chronic fascioliasis is the most common clinical syndrome associated with liver fluke infection in sheep and cattle Bellow is a cache of <http://www.Petalia.com.an/templates/storytemplates> (2000).
12. Mekroud A., Benakhla A., Vignoles P., Rondelaud D. & Dreyfuss G. Preliminary studies on the prevalences of natural fasciolosis in

- cattle, sheep and the host snail (*Galba truncatula*) in north-eastern Algeria. *Parasitology Research*. 92, 502-505. (2004).
13. Mas-Coma S., Funatsu I.R. Bargues M.D. *Fasciola hepatica* and lymnaeid snails occurring at very high altitude in South America. *Parasitology*. 123; 115-127. (2001).

## Effect of Phoenix dactylifera Pollen on In Vitro Sperm Activation of Infertile Men

Saad S. AL-Dujaily<sup>1</sup>, Nahla J. AL-Shahery<sup>2</sup>, and Areeg Abbas Zabbon<sup>3</sup>

<sup>1</sup>Institute of Embryo Researches and Infertility Treatment, Al-Nahrain University.

<sup>2</sup>Department of Biology, College of Education/ Ibn AL-Haitham, Baghdad University.

<sup>3</sup>Department of Biology, college of Science, Al- Mustansiriyah University .

Received 23/2/2012 – Accepted 20/6/2012

### الخلاصة

تهدف الدراسة الحالية الى زيادة حركة النطاف البشرية في الزجاج للمرضى للرجال العقيمين باستخدام مستخلص طلع النخيل كمنبه للحركة لتحسين الاوساط عند استخدامها في التقنيات المساعدة على الانجاب ( كعمليات التلقيح الاصطناعي مستقبلا) . شملت الدراسة الحالية السائل المنوي لخمسة وعشرون لرجال عقيمين. وكل عينة سائل منوي قسمت الى جزئين متساويين . الجزء الاول اعتبر السيطرة وتم تنشيطه بالزجاج باستخدام الوسط (Ferticult flashing) في حين عومل الجزء الاخر الذي اعتبر مجموعة الاختبار تم تنشيطه بالزجاج باضافة مستخلص طلع النخيل ( 0.5 ملغم ) للوسط . تم فحص معايير وظائف النطاف الرئيسة قبل وبعد التنشيط في الزجاج باستخدام التقنية الطباقية البسيطة . أظهرت النتائج ان هناك زيادة معنوية عالية ( $P < 0.01$ ) في النسبة المئوية الكلية لنشاط حركة النطاف التقدمية (A+B+C) و درجة نشاط النطاف التقدمية (A) وتحسن معنوي ملحوظ ( $P < 0.05$ ) في درجة نشاط النطاف التقدمية (B) باستخدام وسط طلع النخيل مقارنة بوسط السيطرة بعد 10 و 30 دقيقة حضانة . يمكن الاستنتاج من نتائج الدراسة الحالية بان اضافة 20% من مستخلص طلع النخيل للوسط الزرعي المنشط للنطف في الزجاج أدى الى تحسن في درجة نشاط النطاف .

### ABSTRACT

The objective of this study is to improve sperm motility *in vitro* of infertile men by using *Phoenix dactylifera* Pollen extract ( *P. dactylifera* pollen) as motility stimulant substances that can improve assisted reproductive technologies (such as artificial insemination) in future. Semen was collected from 25 infertile men who involved in this current study. Each semen sample was divided into two portions. One part was considered as a control and *in vitro* activated by using culture medium only. The other portion was considered as treated portion and *in vitro* activated by adding *P. dactylifera* pollen extract (0.5mg) to the culture media. Certain sperm function parameters were examined before and following *in vitro* activation using simple layer technique. The results revealed highly significant increment ( $P < 0.01$ ) in the percentage of total sperm motility grades (A+B+C) and progressive sperm motility grade (A) with a significant improvement ( $P < 0.05$ ) in the percentage of progressive sperm motility grade (B) when using *P. dactylifera* pollen medium in comparison with control medium after 10 and 30 minutes incubation . It is concluded from the results of the present study that adding the 20% *P. dactylifera* pollen extract to the culture medium of the *in vitro* sperm activation leads to an improvement in the sperm motility.

### INTRODUCTION

Pollen grains carry the male genetic material, by a variety of means, for gamogenesis in the plant kingdom. Pollen applications in the rites, and its uses in traditional and herbal medicine, have been recorded throughout history. They have been used in the treatment of sexual incapacity and weaknesses in the Arab World[1]. Suspension of *P.*



*dactylifera* pollen is herbal mixture that is widely used as a folk remedy for curing male infertility in traditional medicine [2]. The male flowers of date palm are also eaten directly by people as a fresh vegetable to enhance fertility [3]. The effect of *P. dactylifera* pollen on sperm parameters and reproductive system of adult male rats was studied and the results indicated that the consumption of *P. dactylifera* pollen suspensions improved the sperm count, motility, morphology and DNA quality with a concomitant increase in the weights of testis and epididymis [4]. Other report is indicating that *P. dactylifera* contain estradiol and flavonoid components that have positive effects on the sperm quality [5]. It has long been believed that date increase the sexual ability in man [3]. Phytochemical studies of *P. dactylifera* pollen grains revealed the presence of steroidal saponin glycoside [6]. In another study the results showed that date extract caused a significant increase in sperm cell concentration (total count) and motility, on other hand *P. dactylifera* pollen extract decreases sperm cell count but increases the percentage of motile sperm [7]. Furthermore, administration of the pollen grains extract caused a decrease in epididymal sperm with tail abnormalities that would interfere with sperm motility and the highest dose retained normal epididymal sperm number. These findings suggested the preventive role of pollen grains against the chemotherapeutic-induced infertility in males [8].

## MATERIALS AND METHODS

Semen samples from 25 infertile men were obtained during their attendance to IVF Institute of Embryo Research and Infertility treatment, University of Al-Nahrain. The mean ages of patients was  $39 \pm 0.96$  years with a rang of 25 to 59 years. The sample of seminal fluid were collected after 3 to 5 days of abstinence directly into a clean, dry and sterile disposable Petri-dishes by masturbation in a room near the laboratory [9]. After liquefaction time, analysis of semen samples before and after swim up preparation *in vitro* were done to determine the sperm count and sperm motility percentage, At least 200 spermatozoa in five different microscopic fields were evaluated from each sample. The specimens was examined in details by macroscopic and microscopic examinations using standardization of WHO [9].

### Preparation of *P. dactylifera* pollen extract

The method for preparation of *P. dactylifera* pollen extract was aqueous method, in which, 1000gm of *P. dactylifera* pollen in granular powder moistened with boiling water and percolated until the *P. dactylifera* pollen was exhausted, filtrated and evaporated until black pillar mass having a characteristic of sweet taste powder was prepared.

The *P. dactylifera* pollen extract was stored in well closed container protected from light and moisture described by Al-Ahliya Flavors and Fragrances Co. Ltd. (IRAQ).

#### **Preparation of *P. dactylifera* pollen for *in vitro* sperm activation**

The concentration of *P. dactylifera* pollen working solution was prepared by adding 0.5 mg of *P. dactylifera* pollen extract to (10ml) of phosphate buffer solution in plastic test tube contained broad spectrum antibiotic (Ampicillin 0.004 gm) to prevent bacterial growth. The media used for activation contained 20% of *P. dactylifera* pollen working solution by adding 2ml of *P. dactylifera* pollen working solution to (8ml) of FertiCult flushing media. The solution was filtered using Millipore 0.45  $\mu$ M and have been fixed at pH 7.4-7.8 at 25 °C.

#### **Experimental design**

Each semen sample was divided into two portions. One part was considered as a control and *in vitro* activated by using culture medium only. The other portion was considered as treated portion and *in vitro* activated by adding *P. dactylifera* pollen (0.5mg) to the culture media. Certain sperm function parameters were examined before and following *in vitro* activation using simple layer technique. Then incubated at 37 °C for 10 and 30 minute . A drop 10 $\mu$ l taken from the top layer was aspirated by pipette to be examined under 40X-objective. The effect of prepared media on sperm parameter were studied.

**Statistical Analysis:** The data were expressed as mean  $\pm$  SE . Analysis of variance (ANOVA) test and least significant test (LST) were used to detect the significance between the variables .

## **RESULTS AND DISCUSSION**

The present study has investigated the positive effect of adding *P. dactylifera* pollen extract to culture medium by *in vitro* direct activation technique on certain sperm function parameters following 10 and 30 minutes ( table.1) . However, The mean of sperm concentration in before activation portion has been highly significant ( $P<0.001$ ) elevation compared to both control and treated portions. While the total sperm motility (A+B+C) and progressive sperm motility grade A and B were highly significant ( $P<0.001$ ) decrease in before activation portions compared with both control and treated portions after 10, 30 minutes . On other hand, a significant ( $P<0.05$ ) increase have been demonstrated in the percentages of sperm motility grade C in before activation compared with samples activated with *P. dactylifera* pollen extract, while no significant ( $P>0.05$ ) difference was observed in control semen

sample when compared with results before activation. This finding may have resulted from the activation technique when only the sperm with active motility have swim-up to the upper layer of the medium [10]. In addition to the contains of culture medium that used for activation select only intact sperm to swim up to the upper surface of the medium.

The data have revealed that the addition of *P. dactylifera* pollen extract to sperm activation medium caused significant ( $P<0.05$ ) improvement in the mean of sperm concentration, total sperm motility (A+B+C) and progressive sperm motility grade A and B compared with control portions through the incubation for 10, 30 minutes. Furthermore, the addition of *P. dactylifera* pollen extract to sperm activation medium caused a significant ( $P<0.05$ ) reduction in the percentages of sperm motility grade C in treated portion compared with the results of control portions. This is probably due to the fact that *P. dactylifera* pollen contain concentrations of phytochemicals and nutrients and are rich in carotenoids, flavonoids and phytosterols [11]. Moreover, they are good source of protein, amino acids, vitamins, dietary fiber, fatty acids, enzymes, hormones and minerals [12].

*In vitro* activation with *P. dactylifera* pollen extract increase the percentage of sperm motility. The constituent of *P. dactylifera* pollen (i.e. phytoestrogens) may sustain this observation. It is well known that the sperm express estrogen receptors, adding *P. dactylifera* pollen leading to increase the influx of  $Ca^{2+}$  and in turn increase cAMP, which has shown to be a very important factor in sperm motility percent and grade activity [13]. In addition *P. dactylifera* pollen mainly contains cholesterol, rutin, carotenoids, as estrone which is known to exhibit gonadotrophin activity in the rat [14]. Furthermore, *P. dactylifera* pollen contain proteins, vitamins (E, A, folic acid and others) mineral such as potassium, magnesium, calcium, manganese and iron [12], all of these substances stimulate sperm motility and the grade activity of forward movement. *In vivo* observation found that administration of the pollens extract for male mice caused a decrease in epididymal sperm with tail abnormalities that would interfere with sperm motility, and the highest dose retained normal epididymal sperm number [8]. These findings suggest the preventive role of the pollen grains against the chemotherapeutic-induced infertility in males. In another study [7] the results show that *P. dactylifera* pollen extract decreases sperm cell count but increases the percentage of motile sperm in male guinea pig. Oral administration of *P. dactylifera* pollen suspension at doses of 120 and 240 mg/kg body weight improved the sperm count, morphology and DNA quality with a concomitant increase in the weights of testis and epididymis [4]. In another study, it has been looked into the antioxidant and hypolipidemic effects of pollen extracts

(cernitins) on male rabbits and Wister rats. They demonstrated the reduction of malondialdehyd (MDA), total cholesterol, and triglyceride content under the influence of cernitins, indicating their antioxidant properties [15]. Also, Al-Shagrawi [16] showed that the existence of some flavonoids, such as quercetin, rutin and  $\beta$ -amirin in the pollen grains, plays a role in preventing the peroxidation of fatty acid in the body. In several studies a close relationship between pollen antioxidant bioactivity and phenolic compounds has been reported [17,18,19]. Carotenoids such as beta-carotene and lycopene also form an important component of the antioxidant defense [20]. Beta-carotenes protect the plasma membrane against lipid peroxidation [21]. Nass-Arden *et al.*, [22] concluded that lipid peroxidation activity has a major role in loss of sperm motility during time of incubation. Other results reported that rutin and quercetine have been recognized to act against apoptosis (programmed cell death) [23]. Therefore, *P. dactylifera* pollen may be protect the sperm against apoptosis leading to increase the percentage of normal sperm form.

*In vitro* studies showed that vitamins E and C are major chain-breaking antioxidants in sperm membranes and appears to have a dose dependent protective effect [24] and this may be the role of *P. dactylifera* pollen when added through activation program *in vitro*. It is concluded from the results of the present study that adding the 20% *P. dactylifera* pollen to the culture medium of the *in vitro* sperm activation leads to an improvement in the sperm motility *in vitro*.



Table-1: The effect of *P. dactylifera* pollen on sperm motility of infertile men following *in vitro* activation .

Certain sperm Characters	Before activation	Incubation time	<i>In vitro</i> activation	
			After activation controls	After activation treated
Sperm concentration ( $10^6$ sperm/ml)	44.6 $\pm$ 4.3	10 min	7.2 $\pm$ 1.9	10.8 $\pm$ 1.7
		30 min	12.7 $\pm$ 2.3	16.5 $\pm$ 3.2
Total sperm motility (%) (A+B+C)	44.1 $\pm$ 5.2	10 min	77.0 $\pm$ 3.0	84.8 $\pm$ 1.6+
		30 min	79.0 $\pm$ 2.4	86.0 $\pm$ 2.4+
Sperm motility grade (A) %	9.2 $\pm$ 0.89	10 min	33.1 $\pm$ 6.5	50.7 $\pm$ 4.2+
		30 min	36.0 $\pm$ 4.9	49.5 $\pm$ 5.2+
Sperm motility grade (B) %	20.1 $\pm$ 2.6	10 min	26.1 $\pm$ 2.9	30.5 $\pm$ 2.9++
		30 min	29.5 $\pm$ 5.5	34.0 $\pm$ 4.5 ++
Sperm motility grade (C) %	20.0 $\pm$ 2.5	10 min	18.2 $\pm$ 3.2	15.6 $\pm$ 3.1 ++
		30 min	19.4 $\pm$ 1.7	16.9 $\pm$ 2.6 ++

Values are mean  $\pm$  SEM.

No. of Samples per portion = 20.

\*P&lt;0.001 Highly Significance between before and after activation of control and treated portions .

\*\* P&lt;0.05 Significance between before and after activation of control and treated portions .

\*\*\* P&lt;0.05 Significance between before and after activation of treated portions .

+ P&lt;0.001 Highly significance between treated portion and control portion.

++ P&lt;0.05 Significantly different between treated portion and control portion .

## REFERENCE

- [1] El-Desoky G.E., Ragab A.A., Ismail S.A. & Kamal A.E.. Effect of palm pollen grains (*Phoenix dactylifera* ) on sex hormones proteins, lipids and liver functions. J. Agri. Sci. Mansoura Univ.; 20: 4249-4268. (1995).
- Zargari A.. Medical plant . Univ. Tehran press.; 3: 33-40. (1999).
- Mirheydar H. Plant sciences. Islamic culture press. Tehran ; 106-107. (1992).
- Bahmanpour T. , Talaei Z. , Vojdani M. R. , Panjehahahin A. , Poostpasand, S. & Zareei M. G. Effect of phoenix dactylifera pollen on sperm parameters and reproduction system of adult male rats . Iran J. Med. Sci.; 31(4) : 208-212. (2006).
- Kostyuk V.A., Potapovich A.L. & Strigunova E.N. Experimental evidence that flavonoid metal complexes may act as mimics of superoxide dismutase. Arch. Biochem. Biophys. 428 : 204-208 . (2004).
- Kikuchi N. & Miki T. The separation of date sterols by liquid chromatography. Mikrochimica Acta.;2: 89-96. (1978).
- Omar M.M.; Shanawany A.A.; Iamail A. & Mohsen M.K. The effect of palm pollen grains and date extracts on the

- spermatogenic activity of male guinea pigs. Arch. Biochem. Biophys.; 4: 433-435. (1989).
8. Al-Kharage E. & Rokaya A. Protective effect of *Phoenix dactylifera* (date palm) against cisplatin-induced genotoxicity. Food Sci. & Technol.; 1: 148-331. (1982).
  9. WHO. Laboratory Manual for Examination of Human Semen and Sperm-Cervical Mucus Interaction . (4<sup>th</sup> ed) . Press, UK.1999.p45.
  10. Al-Dujaily S.S., Al-Janabi A.S. & Nori M. Effect of *Glycyrrhiza* extract on *in vitro* sperm activation of asthenospermic patients. J. Babylon Univ.; 11: 477-483. (2006).
  11. Broadhursts C.L. Bee products: medicine from the hive. Nutr. Sci. News.; 4: 366-368. (1999).
  12. Alferez M.J. & Campos M.S. Beneficial effect of pollen and/or propolis on the metabolism of iron, calcium, phosphorus and magnesium in rats with nutritional ferropenic anemia. J. Agri. Food Chem.;48:5715-5722. (2000).
  13. Hees R.D. , Bunick D. & Lee K.H. A role for oestrogens in the male reproductive system. Natu.; 390:509-512. (1997).
  14. Dostal L.A., Faber C.K. & Zandee J. Sperm motion parameters in vas deferens and cauda epididymal rat sperm. Reprod. Toxicol.; 10:231-235. (1996).
  15. Wojcicki J., Samochowice L. , Kadlubowskam O. & Kownacka A.B. Study on the antioxidant properties of pollen extract. Archimmunol.; 35 : 725-729. (1987).
  16. Al-Shagrawi R.A. Enzyme activities, lipid fractions, and fatty acid composition in male rats fed palm pollen grains. Res. Bult.;79: 5-18. (1998).
  17. Campos M.G., Webby R.F., Markam K.R. , Mitchell K.A. & Cunha D.A. Age-Induced diminution of free radical scavenging capacity in bee pollens and the contribution of consistent flavonoids. J. Agr. & Food Chem.; 51(3): 742-745. (2003).
  18. Leja M. , Mareczek A., Wyzgolik G., Kiepacz-Baniak J. & Czekonska K. Antioxidative properties of bee pollen in selected plant species. Food Chem.; 100 (1): 237-240. (2007).
  19. Le-Blanca B., Davis O., Boue S., Delucca, A. & Deebya, T. Antioxidant activity of sonoran desert bee pollen. Food Chem.; 55 (1): 1010-1016 . (2009).
  20. Gupta N.P. & Kumar R. Lycopene therapy in idiopathic male infertility a preliminary report. Int. Urol. Nephrol. 34: 369-372. (2002).

21. Agarwal S. & Rao A.V. Tomato lycopene and its role in human health and chronic diseases. *Can. Med. Assoc. J.*; 163:739 -744. (2000).
22. Nass-Arden L. & Breitbart H. Modulation of mammalian sperm motility by quercetin. *Molecular Reproduction and Development.*; 25: 369–373. (1990).
23. Khan N. Afaq F. & Mikhtar H. Apoptosis by dietary factors : the suicidal solution of delaying cancer growth . *Carcino.*; 28:233-239. (2006).
24. Agarwal A. ; Prabakarna S.A. & Said T. Prevention of Oxidative Stress Injury to Sperm. *J. Androl.*; 26(6): 327-330. (2005).

## Detection of *Chlamydia trachomatis* Using polymerase chain reaction (PCR)

Shatha T. Ahmed

Baghdad University / Science collage for women/ Biology Department.

Received 22/4/2012 – Accepted 20/6/2012

### الخلاصة

تعد *Chlamydia trachomatis* واحدة من أكثر أنواع البكتيريا انتشارا والمسببة للأمراض المنقطة جنسيا ، لذا فإنها تشكل مشكلة صحية عامة وخطيرة ، يعتمد تشخيص الإصابة بهذه البكتيريا على عزلها في وسط زرع نسيجي والذي يتطلب مالا يقل عن 48-72 ساعة .  
ان الهدف من الدراسة هو الكشف عن بكتريا *Chlamydia trachomatis* باستخدام تقنية التفاعل التضاعفي لسلسلة الدنا (PCR) ، لانه يعد طريقة حساسة ومتخصصة للكشف عن كمية صغيرة من الحمض النووي البكتيري في العينات السريرية .  
للفترة الممتدة من شهر أيار لغاية كانون الأول 2008 ، تم فحص 147 امرأة كانت منهم 100 من المراجعات لقسم الامراض النسائية لمركز صحة المرأة في مستشفى العلوية للولادة في بغداد و 47 من المراجعات لمستشفى السامرائي للاخصاب وذلك للتحري عن جين KL2, KL1 البلازميدي لبكتريا *C. trachomatis* باستخدام تقنية PCR وبنتاج تفاعل بحجم (241) قاعدة نيتروجينية ، حيث كشفت هذه التقنية عن وجود البكتيريا في 39 (26.5%) من النساء المصابات . اثبتت نتائج هذه الدراسة بان تقنية PCR هي طريقة كفوءة للكشف عن بكتريا *C. trachomatis* من المسحات المأخوذة من عنق الرحم .

### ABSTRACT

*Chlamydia trachomatis* now is one of the most prevalent bacteria sexually transmissible diseases (STD), and as such, constitutes a serious public health problem. Diagnosis of *Chlamydial* infections is based on isolation of bacteria in tissue culture media that requires at least 48 to 72h.

The aim of this study was the detection of *Chlamydia trachomatis*, using polymerase chain reaction (PCR), because its a sensitive and specific method for detection of small quantity of bacterial DNA in clinical samples.

From May to December 2008, a total of 147 specimens of endocervical swabs were collect from 100 women were attending the Gynecology Departments of Women Health Center at Al-Elwyia Obstetrics Hospital in Baghdad and 47 women attending to Al-Samarrai infertility Hospital were examined by a specific PCR for the *Chlamydia* plasmid (KL1 and KL2) genes with a PCR product of 241bp. The PCR detection revealed that *Chlamydia trachomatis* in 39(26.5%) of the infected women. The results of this study indicate that PCR technique is a useful method for detecting *C. trachomatis* taken from endocervical area.

Key words: *Chlamydia trachomatis* , PCR, STD

### INTRODUCTION

*C. trachomatis* is one of the most common sexually transmitted pathogens of humans, with an estimated 90 million chlamydial infections are detected annually worldwide [1]. Most chlamydial infections are asymptomatic both in men and women. However, if not treated properly, it can lead to severe sequelae in women, such as pelvic inflammatory disease, ectopic pregnancy, and tubal infertility [2]. Taking in account that chlamydiae are sensitive to antibiotics, it is



crucial to have an accurate method for the diagnosis of infections. Detecting chlamydial genital infection and preventing transmission and spread of this infection to the upper reproductive tract are challenges for both clinicians and laboratory workers [3]. *Chlamydia trachomatis* has 15 serovars (A- K, L1, L2 L3 and Ba). The growth of serovars D to K seems restricted to epithelial columnar and transitional cells, while serovars L1, L2 and L3 cause systemic disease (lymphogranuloma venereum - LGV). The location of the infection determines the nature of the clinical disease [4]. Diagnosis of *C. trachomatis* infection is frequently based on bacterial isolation in tissue culture media. This method requires careful specimen collection and stringent transport condition and requires at least 48 to 72 h to be performed [5]. Molecular genetics techniques are useful for the identification of microorganisms that are difficult to cultivate, such as *C. trachomatis*, and for those that grow slowly [6]. Polymerase chain reaction (PCR) has recently been introduced for detection of *C. trachomatis* and studies have reported its superior sensitivity in comparison with culture [7,8] enzyme - linked immunosorbent assay [6,9] or direct florescent-conjugated antibody (DFA) staining [10]. Information regarding incidence and prevalence of laboratory confirmed *C. trachomatis* infection of the genital tract in Iraq is limited to a few studies because of lack of proper laboratory facilities. Though PCR technique has been successfully used in clinical specimens elsewhere. In view of the sensitivity and broad applicability, as there have been no previous PCR studies of *C. trachomatis* infection in Iraq, in this PCR testing was used for detecting *C. trachomatis* from endocervical samples. Attempted to set up, a PCR based method to detect the *C. trachomatis* infection among the women population using individual single cervical swab samples.

## MATERIALS AND METHODS

**Specimens:** Endocervical swab samples were obtained from 147 women from May to December 2008, out them 100 women were attending the Gynaecology Departments of Women Health Center at Al-Elwyia Obstetrics Hospital in Baghdad and the rest 47 women were attending to Al-Samarrai infertility Hospital.

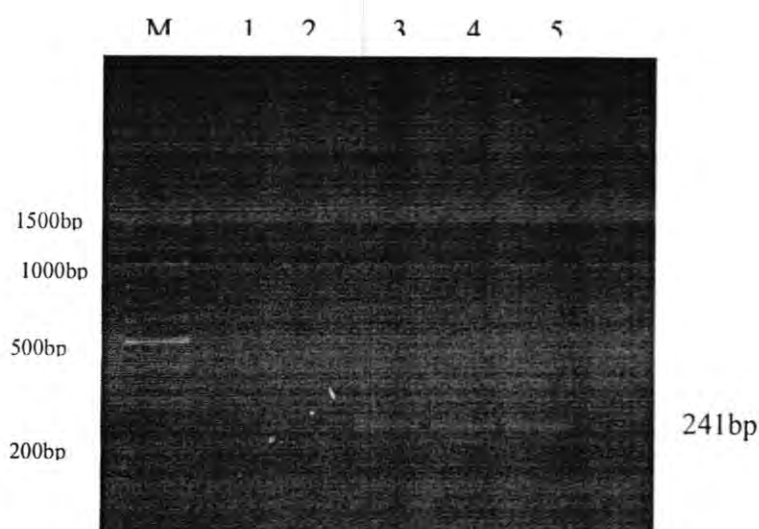
**Preparation the samples for PCR.** In the present study, each clinical specimens was suspended in 1 ml phosphate buffered saline and vortexed for one minute to release the material from swab. The swab was removed and the suspension centrifuged for five minutes at 10,000 rpm/min to pellet cells. After removing the supernatant by aspiration, the cells were resuspended in 400 µl TE buffer (10 mM Tris-HCl, 1 mM EDTA ) with non-ionic detergent Triton X 100 1% and proteinase K (200 µg/ml). Cell suspension was incubated at 55°C for one hour, then

heated to 95°C for ten minutes to inactivate the proteinase K[11].**Primers:** One pair of oligonucleotide primers specific for a region of the *C. trachomatis* gene coding for the 7.5 ORF cryptic plasmid was selected. The sequences from 5' to 3' of these oligonucleotide primers were as follows: The primers KL1-F (5' TCCGGAGCGAGTTACGAAGA 3'); KL2 R(5'AATCAATGCCCCGGGATTGGT 3') were used to amplify 241 bp fragment of chlamydial plasmids (KL1 and KL2) [11,12].

**PCR mixture and amplification** For PCR, Thermocycler (Thermo, USA) PCR reagents from promega, U.S.A. with GoTaq DNA polymerase were used. The mixture of final volum ( 50µl) for each sample contained 0.5µM each primer(forward & reverse); 200µM each dNTPs; 1X PCR buffer pH 8.3; 2.5 mM MgCl<sub>2</sub>; and 1.5 units of Taq DNA polymerase and 9ul of sample DNA was vortexed and subjected to 40 cycles of amplification. Each cycle was composed of 95°C for 5 minute for DNA pre denaturation and sequential incubations of 94°C for 1 minute for denaturation, 55°C for 1 minute for annealing primer to these templates, and 72°C for 2 minutes for DNA chain extension. At the end of 40 cycles, samples were kept for another 7 minutes at 72°C for completion of extension of DNA chain. **Amplified product detection:** Visualisation of amplified product was carried out by agarose gel electrophoresis. A 10µl of post-PCR mixture was subjected to electrophoresis on 2% agarose gel in presence of ethidium bromide. A DNA ladder (100bp) was also run simultaneously to confirm size of the amplified product.

## RESULTS AND DISCUSSIONS

DNA was extracted from all 147 collected endocervical swab specimens, PCR amplification using these DNA samples showed that, of the 147 samples, 39(26.5 %) produced the specific 241bp DNA fragment (Figure.1), 25 of 100 sample from cervicitis women and 14 of 47 sample from infertile women.



**Fig. -1:** Detection of *C. trachomatis* from cervical specimens by PCR (cryptic plasmid primers). 2% agarose gel ,70 volt for 1 hour . Lane M, DNA size markers 100bp(promega, USA); lane 1 and 2, negative patients for *C. trachomatis*; lane 3 - 5 positive patients for *C. trachomatis* ,and lane 6 , negative control.

Culture was earlier considered the gold standard, but PCR studies suggest that the sensitivity of the culture even is as low as 75% to 85%. It is universally accepted that culture can no longer serve as a reference method in the evaluation of diagnostic tests for *C. trachomatis*. [13].

Recently, tests based on the amplification of nucleic acids have been developed as alternatives to conventional methods for the diagnosis of sexually transmitted diseases, such as culture, Direct Immuno Fluorescence and Enzyme Immuno Assay. So far PCR and Ligase Chain Reaction (LCR) are the two most frequently used DNA-based methods [14,15,16 ,17]. The cryptic plasmid have several regions of highly conserved nucleotide sequences, which have been used for primer selection.[11,12,14,18,19 ,20] In the present study, these primer pairs also identified the 241 sequence of KL1&KL2 gene of *C. trachomatis* infection present in individual cervical swab sample. PCR was carried out for 40 cycles, so that any sample with low number of *C. trachomatis* genome could be optimally amplified for visualisation. Present observation demonstrates that *C. trachomatis* can be detected by this PCR-based method, from cervical swabs in properly collected samples using an appropriate cycle number. It offers hope for more accurate diagnosis, which would lead to a better control of this infection and to a better prevention of pelvic inflammatory disease, ectopic pregnancies and tubal infertility. *Chlamydia trachomatis* is a highly prevalent bacteria in many regions, and it seriously affects public

health; therefore it needs effective epidemiological control, starting with an adequate method for correct and effective diagnosis.

There are several studies that determined the frequency of *C. trachomatis* in women with cervicitis. A study in Iran determined the prevalence of 15% by using PCR [21]. In Manaus-AM, Brazil in endocervical smear of sexually active women is 20.7% [11]. Another study In Papua New Guinea is 26% [17]. Another study in Senegal showed that prevalence of *C. trachomatis* in Dakar commercial sex workers is 29% [22]. Although it is consistent with result of current study (26.5%), the high-risk behavior of that study population can explain such a high prevalence of *C. trachomatis* genital infection.

The sharp worldwide increase in the incidence of PID during the past two decades has led to secondary infertility and ectopic pregnancy. *Chlamydia* PID is the most important preventable cause of infertility and adverse pregnancy outcomes. The proportion of tubal factors infertility among all infertility cases ranges from less than 40% in developed countries to up to 85% in developing countries [23]. Punnonen *et al.*, 1979 [24] published the first study linking past Chlamydia infection and tubal factor infertility. Paavonen and Eggert-Kruse, 1999 [25] reported that, based on the available evidence, approximately 4% develop chronic pelvic pain 3% infertility, and 2% adverse pregnancy outcomes.

Watson *et al.* [26] reported that Screening women for lower genital tract infection with *Chlamydia trachomatis* is important in the prevention of pelvic inflammatory disease, ectopic pregnancy and infertility they also demonstrated that nucleic acid amplification techniques are superior to other methods for detecting asymptomatic chlamydial infection in a young and sexually active population. The test most often used to detect this sexually transmitted infection, result of this study revealed that 14 (35.5%) infertile women. For this reason screening women for prevention of pelvic inflammatory disease, ectopic pregnancy and infertility is necessary in Iraq.

**Conclusions** In summary, nucleic acid amplification methods, such as PCR, are significantly sensitive and should therefore be used in preference to other tests for the detection of genital *C. trachomatis* infection.

## REFERENCES

- 1 Gerbase, A.C. Rowley, J.T. and Mertens, T.T. (1998). Global epidemiology of sexually transmitted diseases. *Lancet*, 351(suppl.III), S2-S4.
- 2 Marrazzo JM, Stamm F (1998): New approaches to the diagnosis, treatment and prevention of chlamydial infection. *Curr Top Clin*



- Infect Dis* 18: 37-59.
- 3 Barnes, RC. (1989). Laboratory diagnosis of human chlamydial infections. *Clin Microbiol Rev*; 2: 119-136.
  - 4 Dutilh, B. Bebear, C. Rodriguez, P.Vekris, A. Bonnet,J. Garret,M.(1989). Specific amplification of a DNA Sequence common to all *Chlamydia trachomatis* serovars using the PCR. *Res Microbiol*, 140: 7-16.
  - 5 Crotchfelt, K.A. Welesh,L.E. Debonville,D. Rosenstrauss,M. Quinn,T.C.(1997). Detection of *Neisseria gonorrhoeae* and *Chlamydia trachomatis* in genitourinary specimens from men and women by a coamplification PCR assay. *J Clin Microbiol*, 35 (6): 1536-40.
  - 6 Piémont Y., Jaulhac B. (1995): Use of molecular methods for bacteriology diagnosis. *Ann Dermatol Venereol* 122:206-12.
  - 7 Osewaarde JM, Rieffe M, Rozenberg-Arska M, *et al.* (1992): Development and clinical evaluation of polymerase chain reaction tests for detection of *Chlamydia trachomatis*. *J Clin Microbiol*; 30: 2122-2128.
  - 8 Jolly, A.M. Orr, P.H., Hammond, G. Yong, T.K. (1995). Risk factors for infection in women undergoing testing for *Chlamydia trachomatis* and *Neisseria gonorrhoeae* in Manitoba, Canada. *Sex Transm Dis*; 22(5):289-95.
  - 9 Amal Hussein Salman, (2007). The role of some microbial infections and immune activation in pregnancy loss. Ph.D.Thesis,Al-Mustansiriya University.
  - 10 Comanducci, M. Ricci,S. Cevenini,R.. Ratti,G. (1990):Diversity of the *Chlamydia trachomatis* common plasmid in biovars with different pathogenicity Plasmid23 (2):149-54.
  - 11 Santos,C. Teixeira, and F. Vicente, A. (2003). Detection of *Chlamydia trachomatis* in Endocervical Smears of Sexually Active Women in Manaus-AM, Brazil, by PCR. *Brazilian Journal of Infectious Diseases*; 7:91-95.
  - 12 Mahony, J. B. Jang, D. Chong, S. Luinstra, K. Sellors, J. Tyndal,M. and Chernesky, M.(1997).Detection of *Chlamydia trachomatis*, *Neisseria gonorrhoeae*, *Ureaplasma urealyticum*, and *Mycoplasma genitalium* in First-void Urine Specimens by Multiplex Polymerase Chain Reaction Molecular Diagnosis,2: 161-168.
  - 13 Puolakkainen M, Hiltunen Back E, Reunala T, Suhonen S, Lahteenmaki P, Lehtinen M, Paavonen J. (1998): Comparison of performances of two commercially available tests, a PCR assay and a LCR test, in detection of urogenital *Chlamydia trachomatis* infection. *J Clin Microbiol*, 36 (6): 1489-93.

- 14 Mahony, J. B. Luinstra, K. I. Tyndall, M. Sellors, J. W. Krepel, J. and Chernesky, M. (1995). Multiplex PCR for detection of *Chlamydia trachomatis* and *Neisseria gonorrhoeae* in genitourinary specimens. *J. Clin. Microbiol.* 33: 3049–3053.
- 15 Jayanti,M-P. UM, D., Anurupa, M. (2001).Use of polymerase chain reaction (PCR) for detection of *Chlamydia trachomatis* infection in cervical swab samples. *Indian Journa of Dermatology, Venereology and Leprology.* 167:246-250.
- 16 Garland, S. M. Tabrizi, S.N. Chen,S. Byambaa, C. and Davaajav ,K. (2001). Prevalence of sexually transmitted infections (*Neisseria gonorrhoeae*,*Chlamydia trachomatis*, *Trichomonas vaginalis* and human papillomavirus) in female attendees of a sexually transmitted diseases clinic in Ulaanbaatar, Mongolia *Infect Dis Obstet Gynecol* ;9:143–146.
- 17 Mgone, C. S. MD, MMed, Lupiwa, T.,Yeka,W.(2002): High Prevalence of *Neisseria gonorrhoeae* and Multiple Sexually Transmitted Diseases Among Rural Women in the Eastern Highlands Province of Papua New Guinea, Detected by Polymerase Chain Reaction. *Sexually Transmitted Diseases* .29:775-779.
- 18 Mahony, J. B. Luinstra, .K. E. Waner.J. McNab,G. Hobranzska, H. Gregson, D.Sellors, J. W. and Chernesky,M.(1994).Interlaboratory Agreement Study of a Double Set of PCR Plasmid Primers for Detection of *Chlamydia trachomatis* in a Variety of Genitourinary Specimens *J. Clin. Microbiology*, 32: 87-91.
- 19 Cribb, P. Scapini, J. P. Serra, E.(2002). O ne-tube Nested Polymerase Chain Reaction for Detection of *Chlamydia trachomatis* *Mem Inst Oswaldo Cruz, Rio de Janeiro*: 97(6): 897-900.
- 20 Golshani, M. Eslami, G. Ghobadloo, Sh. M. Fallah, F. Goudarzi,H. Rahbar,A.A S. Faya, F. (2007). Detection of *Chlamydia trachomatis*, *Mycoplasma hominis* and *Ureaplasma urealyticum* by Multiplex PCR in Semen Sample of Infertile Men *Iranian J Publ Health*,. 36: 50-57.
- 21 Fallah, F. Kazemi, B. Goudarzi, H Badam,i. N. Doostdar,F. Ehteda, A. Naseri, M Pourakbari ,B and Ghazi, M.(2005).Detection of *Chlamydia trachomatis* from Urine Specimens by PCR in Women with Cervicitis. *Iranian J. Publ. Health*, , 34 20-26.
- 22 Sturm-Ramirez, K. Brumblay, H. Diop ,K. Aissatou Gueye-Ndiaye, Sankale, J.L. Thior, I. *et al.* (2007).Molecular epidemiology of genital *Chlamydia trachomatis* infection in high-risk women in senegal West Africa. *J Clin Microbiol*, 38 (1): 138-145.
- 23 World Health Organization (1987). Inferction, pregnancies, and infertility perspectives on prevention.*Fertil.Steril.* 47,964-968.

- 24 Punnonen, R., Terho, P., Nikkanen, V. *et al.* (1979): Chlamydial serology in infertile women by immunofluorescence. *Fertil. Steril.* 31:656-659.
- 25 Paavonen, J. & Eggert-Kruse, W. (1999): *Chlamydia trachomatis*: impact on human reproduction. *Human Reproduction Update.* 5:433-447.
- 26 Watson, E. J., Ian Russell, A. T., Paavonen, J. *et al.* (2002). The accuracy and efficacy of screening tests for *Chlamydia trachomatis*: a systematic review. *J. Med. Microbiol* 51 1021-1031.

## Autoimmune Haemolytic Anemia Associated With Some Diseases

Amany Mohammed Jasim and Safa A. Fadil  
College of Medical & Health Technology, Baghdad

Received 24/4/2012 – Accepted 20/6/2012

### الخلاصة

استمرت الدراسة الحالية للفترة مابين تموز ولغاية تشرين الثاني 2011 ، حيث تضمنت جمع اثنا وسبعون عينة دم حيث كانت اعمار المرضى مابين 16-70 سنة ، اثنان واربعون عينة منها كانت لمرضى مصابين بفقر الدم الحاد (16 منهم ذكور و26 اناث) اضافة الى انهم يشكون من امراض اخرى ( اللوكيميا المزمنة النخاعية واللويميا المزمنة اللمفاوية واللويميا اللمفاوية الحادة والسرطان اللمفاوي غير الهوجكن والهوجكن اللمفاوي اضافة الى الروماتيزم الالاثوي وجمعت 30 عينة اخرى من اشخاص غير مصابين بفقر الدم ( 10 منهم ذكور و20 اناث ) كمجاميع سيطرة لهذه الدراسة .  
تم عمل مسحات للدم المحيطي اضافة الى فحص التلزن المباشر (فحص الكومب ) لكل عينات الدراسة ( المرضى ومجاميع السيطرة) ، اضافة الى فحص الانتشار المناعي الشعاعي للمرضى الذين تبين اصابهم بمرض فقر الدم التحللي المناعي الذاتي .  
ولقد تم التوصل من خلال هذه الدراسة الى انه لا توجد فروق معنوية بين اعمار المصابين بالمرض موضوع الدراسة عندما قورنت بمجموعة السيطرة في حين اظهرت الدراسة ان الاناث المرضى كانت لديهم حساسية اكثر للاصابة بالمرض من الذكور  
وتبين من خلال هذه الدراسة ان العامل الريصي الموجب لكافة مجاميع الدم للمرضى كان اكثر حساسية للمرض من العامل الريصي السالب ولوحظ ايضا ان صنف دم نوع B اعطى حساسية اعلى للمرض (33.33%) من صنف دم O (28.57%) وصنف دم AB (21.43%) و A (16.67%) .  
ايضا اعطت جملة المتمم نوع C3,C4 تكرارا اعلى (95.80%) بين المرضى المصابين بفقر الدم لتحللي الذاتي عند مقارنتها بالمعادلات الطبيعية لمنظمة الصحة العالمية عند استخدام فحص الانتشار المناعي  
ولقد اظهرت نتائج فحص مسحات الدم المحيطي للمرضى موضوع الدراسة وجود خلايا غير طبيعية باعداد كبيرة ككريات الدم الحمراء الكروية والشبكية اضافة الى تلزن غير طبيعي لكريات الدم الحمراء وتكون شكل الرولكس ان استخدام فحص الانتشار المناعي الشعاعي في هذه الدراسة مكن من معرفة الخصائص السيرولوجية لدماء المرضى المصابين بفقر الدم التحللي الذاتي مع الاخذ بنظر الاعتبار اصناف الاجسام المناعية الذاتية وجملة المتممة .

### ABSTRACT

The present study, extended from July 2011 to November 2011, a total of seventy two samples were collected from individuals their ages ranged from 16-70 years forty two was anaemic patients (16 males and 26 females) with chronic myelocytic leukemia (CML), acute lymphoblastic leukemia (ALL), chronic Lymphocytic leukemia (CLL), Hodgkin lymphoma (HL), non-Hodgkin lymphoma (NHL) and rheumatoid arthritis (RA).

Other thirty samples were collected from non anaemic individuals as control group (10 males and females). All samples were tested by anti-human globulin (Coomb's test), Preparation of blood film and Radial Immunodiffusion (RID).

It was observed that female more susceptible than male to the Auto immunhemolytic anemia (AIHA), no significant differences were noticed in the ages of AIHA patients compared with the control group. AIHA who gave positive coombs test (DAT), CML anemic patients had a higher AIHA percentage (47.62%), while HL patients had the lower percentage (4.76%). the incidence of +ve RH blood grouping of anemic patients with AIHA presented in this study was more susceptible to AIHA than -ve RH anemic patients. The distribution of blood grouping system was shown that blood group B (33.33%) was more susceptible to the AIHA than other groups. The results of precipitation reaction of IgG, IgM, IgA class and C3, C4 using immnodiffusion techniques. It was observed that the mean



result of C3 had a highly result of precipitation reaction among anemic patients with AIHA according to the normal averages of WHO (2003)

It also documented that autoimmune hemolytic anemia was strongly associated with increased risk of CLL among anemic patients studied.

---

## INTRODUCTION

Hemolytic anemia is a condition of red blood cells destruction in which increased erythrocyte production is insufficient to keep up with accelerated RBC destruction, thus producing anemia[1].

It classified according to the mode of onset either inherited or acquire. Acquired hemolytic anemia may be classified as Alloimmune, drug induced autoimmune and other agents [2].

Autoimmune hemolytic anemia is characterized by increased red cell destruction and/ or decreased red corpuscles survival due to autoantibodies directed against self-antigens on red corpuscles [3]

Autoimmune hemolytic anemia is classified to warm or cold hemolytic anemia based on clinical symptoms and on the optimal temperature [4]

The pathogenicity of AIHA due to deletion of self-reactive T-and B-lymphocytes clones during their maturation in the central lymphoid organs (the thymus for T cells and bone marrow for B cells [5].

Some people with AIHA may have no symptoms, other people developing symptoms like skin pale, weakness, chronic fatigue, shortness of breath dizziness, headache and rapid heartbeat [6].

Secondary AIHA are associated with some diseases including Chronic myeloid leukemia, Chronic lymphocytic leukemia, Acute lymphocytic leukemia, Non- Hodgkin lymphoma, Hodgkin lymphoma, Rheumatoid arthritis, systemic lupus erythematosus and viral infections[7].

Several factors including quantity and class of autoantibodies, complement activation affect in the ability of autoantibodies to provoke hemolysis, drugs and toxins may cause intravascular hemolysis through the formation of heinz bodies resulting in damaged membranes thus destroying RBCs.[8]

The appropriate therapy of AIHA is dependent on the correct diagnosis and classification of this family of hemolytic disorders. Corticosteroid are standard, followed by consideration of splenectomy in complicated cases [9].

## MATERIALS AND METHODS

The present study, extended from July 2011 to November 2011, a total of seventy two samples were collected from individuals their ages ranged from 16- 70 years selected from Ebn AL-Balady hospital,

Baghdad Teaching Laboratories and National Centre for Research and Treatment of Hematology at Al- Mustansiriyah University Hospitals.

**Preparation of patient's samples:**

Five ml of peripheral venous blood sample were taken from forty two anaemic patients with CML, CLL, ALL, NHL, HL and RA( $HB \leq 8$ ), none of these patients had received any treatment including blood transfusion during a period of three months, three ml were taken for Coomb's test and preparing blood film, sera were collected from the remaining blood sample for immunodiffusion technique. Thirty venous blood samples were collected from non anaemic individuals as control group

**1. Anti-human globulin (Coomb's test)**

**Direct antiglobulin test (tube method)**

This procedure was also carried out to anemic and non anemic patients according to [10].

**2-Radial Immunodiffusion (RID)**

This procedure was carried out for anemic patients only to study a detailed serological characterization of autoantibodies of AIHA patients according to [11]

**Statistical analysis of data**

Parametric data were statistically analyzed using percentage and Fischer Exact Probability test at significant level  $P < 0.05$  according to [12]

## **RESULTS AND DISCUSSION**

Table(1) showed the distribution of studied patients with AIHA and control group by age and gender. It was observed that female were more susceptible than male to the AIHA. There was a significant increase in percentage of female than male patients at  $P < 0.05$  using Fischer Exact Probability test. No significant differences were noticed in the ages of AIHA patients compared with the control group (AIHA patients age mean  $\pm$  SE  $42.88 \pm 2.55$ , control group age mean  $\pm$  SE  $34.57 \pm 2.8$ ) using t-student.



**Table-1:** Distribution of studied patients with AIHA and control group by age and gender.

Characteristics	Value age mean $\pm$ SE
Age(years) AIHA patients	42.88 $\pm$ 2.55
Age(years) control group	34.57 $\pm$ 2.8
Female %	(61.9%)
Male %	(38.1%)

Figure(1) showed the number and percentage of anemic patients with AIHA who gave positive coombs test( DAT ),CML anemic patients had higher AIHA percentage ( 47.62%) compared with other patients group, while HL patients had the lower percentage (4.76%) among all anemic patients studied.

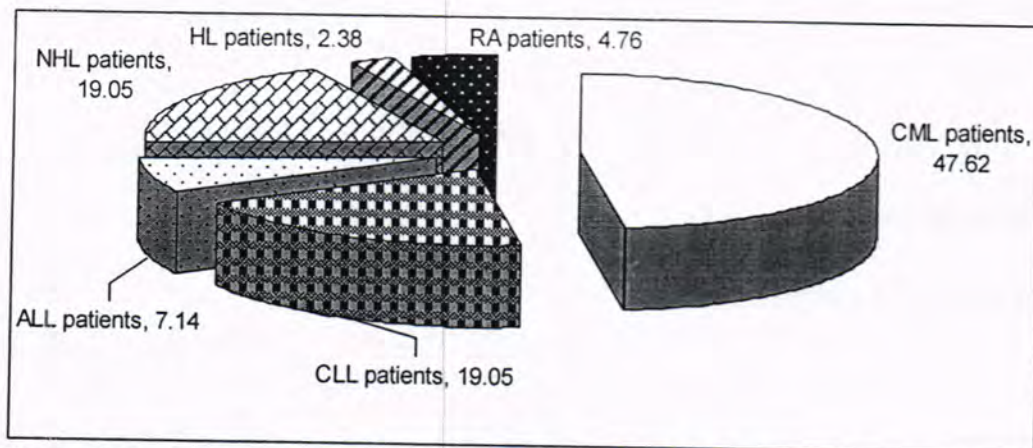


Figure-1: Number and percentage of anemic patients with AIHA positive DAT coombs test

The most common laboratory findings associated with AIHA are found in figure (2,3,4 ) which represented by presence of spherocytes, and reticulocytes on the peripheral blood smear(fig.2,3) which reflect the immune mediated destruction of the erythrocyte, abnormalities of RBCs and rouleaux formation was also observed (fig.4) suggestive hemolytic process.

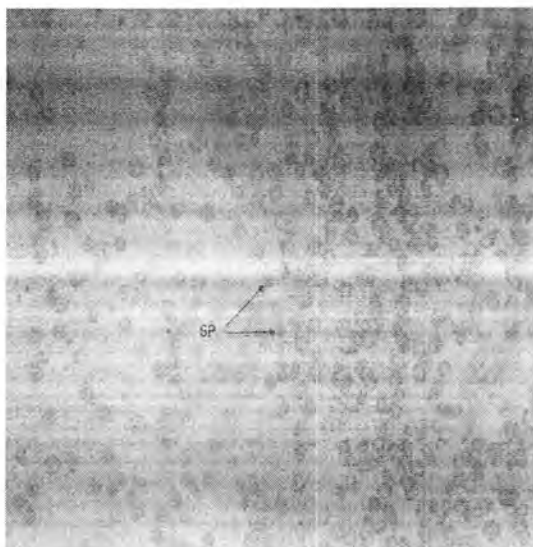


Figure-2:lood smear of patients with ALL showing numerous spherocytes (Leishman stain x 40) sp: spherocytes

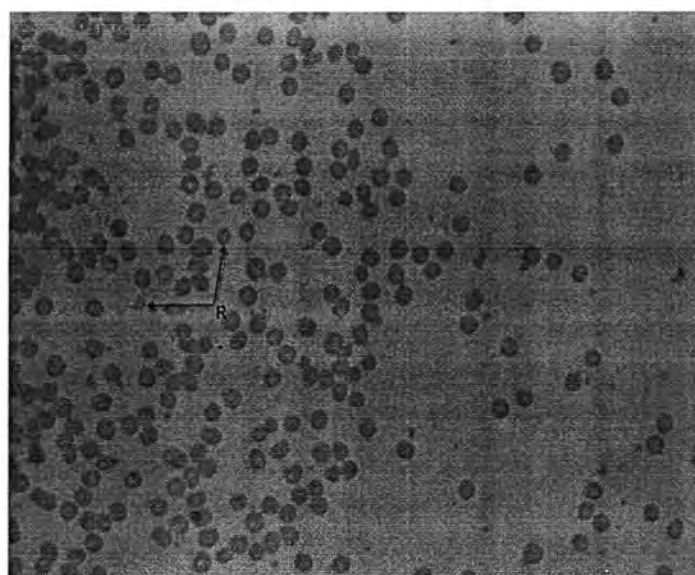


Figure-3:lood smear of patients with CML showing numerous reticulocytes (Leishman stain x 40) R: reticulocytes



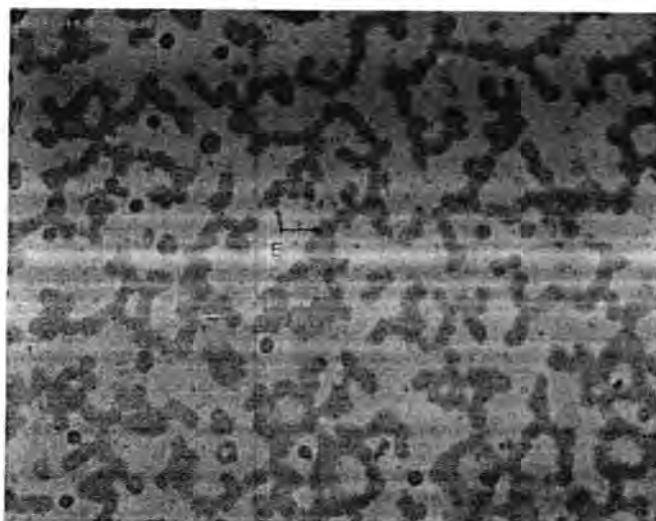


Figure-4: blood smear of patients with NHL showing rouleaux formation (Leishman stain x 40) RO: Rouleaux

The distribution of blood grouping system and Rh among anemic patients with AIHA was shown in Table (2). It was observed that blood group B (33.33%) followed by O (28.57%) was more susceptible to the AIHA than AB (21.43%) and A blood group (16.67%)

Table-2: Distribution of blood grouping system and RH among anemic patients with AIHA included in the work.

Blood group system	No. %	Blood group and RH	No.	%
Blood group B	14 33.33a	Blood group B+ve	11	26.19a
		Blood group B-ve	3	7.14c
Blood group O	12 28.57a	Blood group O+ve	9	21.43a
		Blood group O-ve	3	7.14c
Blood group AB	9 21.43b	Blood group AB+ve	7	16.67b
		Blood group AB-ve	2	4.76c
Blood group A	7 16.67b	Blood group A+ve	6	14.29b
		Blood group A-ve	1	2.38c
Total	42 100	Total	42	100

a, b, c Insignificant difference between similar litter using Fischer Exact Probability test at  $P < 0.01$

Table-3:showed the mean results of precipitation reaction of IgG, IgM, IgA class and C3,C4 using immunodiffusion techniques. It was observed that the mean result of C3 had a highly result of precipitation reaction among anemic patients with AIHA according to the normal averages of WHO (2003)

Characteristics	IgG mg/dl N=39	IgM mg/dl N=41	IgA mg/dl N= 39	C3 mg/dl N= 34	C4 mg/dl N= 34
Mean	1107.41	112.51	196.71	614.21	36.81
± SD	± 381.81	± 56.10	± 81.57	± 2196.81	± 14.02
Normal( WHO)	710-1520	40-250	90-310	91-156	20-50

AIHA is a disease that causes decreased red cells survival due to abnormality of immune system to recognizing self-antigen and autoantibodies are made against RBCs antigen [13]. The present study found that the disease was not associated with age. Females most susceptible to the disease than males. This as may be due to stimulation of cells divisions by both estrogen and androgen hormones in females and elevated levels of these hormones may lead to abnormal cell growth such as autoimmune disease ,ovarian cysts and lymphoproliferative disorders [14]

The present study had excluded all the patient samples who underwent blood transfusion processes to avoid a delayed transfusion reaction that may occur after 2-14 days blood transfusion and patients who has received chemical drugs and taken doses of radiation one months ago. Chemotherapy and radiation often also cause anemia, drugs could bind non specifically on the RBCs membrane of these patients that radiation formation of autoantibodies causing extravascular hemolysis destruction[15].

The present study demonstrated that autoimmune hemolytic anemia was strongly associated with increased risk of CLL. This finding agreed with the results of previous epidemiological study by [16]

[17] documented that warm AIHA are responsible for 70% of lymphoproliferative disorder such as CLL, NHL and HL [14]. Also noted strong associations between autoimmune hemolytic anemia and lymphoid neoplasms, even when a 5-year period before lymphoma diagnosis was excluded, suggesting that other mechanisms could be involved.

[18]documented that warm antibody hemolytic anemia is an autoimmune disorder characterized by the premature destruction of health red blood cells by autoantibodies. Other study by [19]mentioned that secondary AIHA was associated with viral infections ,chemical agents ,drugs and neoplastic diseases.

It was also shown that +ve RH blood grouping system was more susceptible to AIHA than -ve RH, this may be due to more specificity

reactive of autoantibodies against well defined RBCs antigens of +ve RH blood grouping system [19].

Microscopic finding of blood smears in present study showed numerous typical spherocytes and reticulocytes which provided a good indicator to hemolytic anemia. A defect in the surface membrane (the outer covering) of RBCs causes them to have a sphere, or ball-like, shape. These RBCs have life span that's shorter than normal [20].

[21] mentioned that the major cause of numerous spherocytes is warm-antibody hemolytic anemia in which the spleen removes small portions of the red cell membrane from cells coated with IgG destruction antibodies, erythrocyte then emerges from the spleen as a smaller cells.

[22] indicated that spherocytes are not as flexible as normal RBCs, and will be singled-out for destruction in the red pulp of the spleen as well as other portions of the reticuloendothelial system. The RBCs trapped in the spleen cause the spleen to enlarge, leading to the splenomegaly often seen in these patients.

The use of Immunodiffusion techniques could help to study the serological characterization of patients with AIHA with regard to autoantibodies class and complement fractions. Demonstration of the antigenic serum components in patients with AIHA seemed to be associated with autoantibodies classes and complement fraction [23].

The present study revealed that several samples studied had the precipitation reactions either IgG or IgM and IgA and fixed complement, this was due to degree of hemolysis depending on characteristics of the bound antibodies (specificity, quantity and the ability to fix complement as well as the target antigen (density, expression and patients age [24].

Our study showed that patients who had only C3 were in higher number among studied samples, fixing of complement caused intravascular hemolysis. As RBCs are warmed in the central organs, the bound immunoglobulines may be lost, leaving only bound C<sub>3</sub> [24].

Reticuloendothelial cells also have receptors for complement factor present can potentiate the extravascular hemolysis [17].

Very few studies in Iraq on the hematological and serological evaluation of AIHA and other associated diseases were done therefore, more studies are requested to study the clinical evidences and the laboratory findings of such diseases.

## REFERENCES

1. UthanA:Lectures of Diploma students of American Board of Pathology .<http://web2.ladfw.net/uthane/index.html>. (2005)
2. McKenzie, S.B. (2000). Clinical laboratory hematology. Upper Saddl River, USA.(1):304-308.Abbas,A.K. Diseases of immunity.7<sup>th</sup>ed.Philadelphia.Elsevier. Saunders. pp. 223-225(2005).
3. Duffy, T.P. Autoimmune hemolytic anemia and paroxysmal nocturnal hemoglobinuria In: Simon, T .; Dike, W.; Snyder, E; Towel, C. and Strauss , R. (eds) Rossi's principles of transfusion medicine . Lippincott Williams and Wilkins, Philadelphia. 345-366(2002).
4. Oliff, I.A. and Compton, C.C. weekly clinico pathological exercises . N. Eng. J. Med. 2: 342(2000)
5. Abbas,A.K. Diseases of immunity 7<sup>th</sup>ed. Philadelphia. Elsevier. Saunders. pp. 223-225(2005).
6. Trape , G.; Fianchi, L. and Lai, M. Rituximab chimeric anti-CD 20 monoclonal antibody treatment for refractory hemolytic anemia in patients with lymph proliferative disorders. Hematol. 1: 223-224 (2003).
7. Vacca, A.; Felli, M. and Palermo, R. "Notice 3 and pre- TCR interaction unveils distinct NF- Kappa B pathways in T- cell development and leukemia .Embo.2:1000-1008(2006).
8. Byrd, J .; Kitada, S. and Flinn, T.W. The mechanism of tumor cell clearance by rituximab in vivo in patients with B. chronic lymphocytic leukemia: Evidence of activation and apoptosis induction. 2: 1038-1043(2002)
9. Das,S.S.; Nityanand, S.and Chaudhary, R. Clinical and serologica characterization of autoimmune hemolytic anemia in a tertiary care hospital in North India.Ann.Hematol. 88(3):731(2009).
- 10.Flynn, J.C. Essential in immunoheamatology. W. B. Sounders. USA.PP445(1998).
- 11.Palmer, D.A. and Wood, R. Immunology.Dept. of Health Education and Welfare, Publication. Center of disease control, Atlanta.6: 72-8102(1972).
- 12.SPSS 14, Statistical Package for Social Science, SPSS for windows Release 14.0.0, 12 June," Standard Version, Copyright SPSS Inc., 1989-2006.SPSS Inc.( 2006).
- 13.Gehrs, B. C.and Friedberg, R.C. Autoimmune hemolytic anemia Amer. J. Hematol. 69: 258- 271.(2002).
- 14.Anderson, L.A.; Gadall, S.; Morton, L.M.; Pfeiffer, R.; Warren L. Berndt, S.; Ricker, W.; Parson, R. and Engels, A. (2009). Dopulation- based study of autoimmune conditions and the risk of specific lymphoid malignancies Inter. J. cancer. 125: 398-405.



15. Tkachuk, D.S.; Hirschmann, J.V. and McArther, J. R. Atlas of clinical hematology. W.B. Saunder .USA. 9:79(2002).
16. Hauswirth, A.; Skrabs, C.; Shutzinger, C. Geiger, A. and lechner, K. Autoimmune hemolytic anemia's, Evans' syndromes, and pure red cell aplasia in non-Hodgkin lymphomas. *Leuk.* 48:1139-49(2007).
17. Bradly, C.; Gehrs, S. and Richard, F. Autoimmune hemolytic anemia. *Amer .J. Hematol.* 69:258-271.(2002).
18. Naithani, R.; Agarwal, N.; Mahapatra, M .; Pate, H.; Kumar, R. and Choudhary, V. (2006). Autoimmune hemolytic anemia in India. *Ann. Hematol.* 88: 727-732.
19. Garratty, G. Immune hemolytic anemia associated with negative routine serology. *Simen. Hematol.* 4:156-164.(2005).
20. Wheeler, C.A.; Calhoun ,L. and Blackball, D . Warm reactive autoantibodies :clinical and serological correaction *Amer.. J. Clin. Pathol* 3:680-685.
21. Wegrzyn, A.; King, K.; Shirey, R.; Chen, A. ; McDonough, C. and Lederman, H. Fatal warm autoimmune hemolytic anemia resulting from IgM. Autoagglutinins in an infant with severe combined immunodeficiency. *J. Pediatr. Hematol. Oncol.* 23(4): 250-2.(2001).
22. Mohammed Mhtmt: file : // c:/ Document and settings / my Document/ warm autoimmune hemolytic anemia.p 2-3(2011) ..
23. Stroncek, D. F.; Njoroge, J.M.; Doctor, J. L.; Chitds, R.w. and Miller, J. A preliminary comparison of flow cytometry and tube agglutination assays in detecting red blood cell associated C3. *Transfuse. Med.* Vol. 2:p.35-41(2003).
24. Nielsen, C. H.; Fischer, E. M. and Leslies, R.G. the role complement in the acquired immune response. *Immunol.* 12:4-12(2000).

## The Extraction and Purification Of Gallic Acid from the Pomegranate Rind

Entessar H.A. Al-Mosawe and Iman I. Al- Saadi

Biotechnology Division, Applied Sciences Department/ University of Technology,Iraq-Baghdad.

Received 16/5/2012 – Accepted 20/6/2012

### الخلاصة

هدفت هذه الدراسة الى استخلاص وتنقية حامض الكالليك من قشور الرمان المزروع في العراق. واستعمل كروماتوغرافي الطبقة الرقيقة لعزل المركب من مستخلص الكحول الايثيلي (40%) من قشور الرمان باستخدام نظام متكون من التولوين: ايثيل استيت: حامض الفورميك بحجم 3: 3.5: 0.5 حجم/حجم. وقد اجريت الفحوصات للتأكد من نقاوة حامض الكالليك والتي شملت تقدير الحركة النسبية بواسطة TLC واختبار الاشعة الحمراء والكشف بالمطياف الضوئي لمعرفة منحنى اقصى امتصاص وطريقة تحليل كروماتوغرافيا السائل عالي الكفاءة مع المقارنة بالمادة القياسية لجميع الاختبارات.

### ABSTRACT

The study aimed to extract and purify of gallic acid from rind of pomegranate cultivated in Iraq and to investigate the chemical composition of the pomegranate peel this study the original procedure is described for the extraction and purification of gallic acid.

Gallic acid was extracted by ethanol / water (40:60) and identified in the chromatography method ( GA in the FT-IR ,UV spectra and HPLC) and then compared the result with the standard test to determin the isolated compound .

Keywords: *Punica granatum*, rind , Gallic Acid.

### INTRODUCTION

Pomegranate belongs to punicaceae family. *Punica granatum* (Punicaceae), commonly called pomegranate, recently described as nature's power fruit , is a plant used in folkloric medicine for the treatment of various diseases [1,2]. The Babylonians regarded the seeds of Pomegranate as an agent resurrection, the Persians as conferring invincibility on the battlefield and ancient Chinese it used the bright red juice was mythopoetically regarded as a "soul concentrate", The rind of Pomegranate homologous to human blood and capable of conferring on a person longevity or even bearing multiple hydroxyl groups that predominate in immortality [3]. Fruits are one of the oldest forms of food known to man.. According to Qur'an, the fruits like grapes, olive and pomegranate are heavenly fruits of God. The people in ancient times regarded fruits to be endowed with magic or divine properties. The pomegranate is an ancient fruit that has not changed much throughout the history of man. It was found in the Indus Valley so early that there is a word in Sanskrit for pomegranate. The pomegranate is also significant in Jewish, Christian and Muslim traditions [4].The

pomegranate is native of Iran and Afghanistan, known in ancient Egypt [5].

Pomegranate has strong antioxidant and anti-inflammatory properties. Recent studies have demonstrated its anti-cancer activity in several human cancers [6]. In addition, pomegranate peel extract with an abundance of flavonoids and tannins has been shown to have a high antioxidant activity [7]. Antimicrobial drug resistance in human bacterial pathogens is a worldwide issue and as a consequence, effective treatment and control of such organisms remain an important challenge. Bacterial resistance has appeared for every major class of antibiotic [8]. The major class of pomegranate phytochemicals is the polyphenols (phenolic rings bearing multiple hydroxyl groups) that predominate (flavonols, flavanols and anthocyanins), condensed in the fruit. Pomegranate polyphenols include flavonoidstannins (proanthocyanidins) and hydrolysable tannins (ellagitannins and gallotannins). Hydrolyzable tannins (HTs) are found in the peels (rind, husk, or pericarp), membranes and piths of the fruit [9]. HTs are predominant polyphenols found in pomegranate juice and account for 92% of its antioxidant activity. Constituents Pomegranate pericarp (Peel, rind) Phenolic punicalagins; gallic acid and other fatty acids; catechin, EGCG; quercetin, rutin and other flavonols; flavones, flavonones; anthocyanidins [10].

Gallic acid is a trihydroxybenzoic acid, a type of phenolic acid, a type of organic acid, also known as 3,4,5-trihydroxybenzoic acid, found in gallnuts, sumac, witch hazel, tea leaves, oak bark, and other plants [11]. The chemical formula is  $C_6H_2(OH)_3COOH$  (fig.1). Gallic acid is found both free and as part of tannins. Salts and esters of gallic acid are termed 'gallates'. Despite its name, it does not contain gallium.

Gallic acid is commonly used in the pharmaceutical industry [12]. Gallic acid can also be used as a starting material in the synthesis of the psychedelic alkaloid mescaline [14].

Gallic acid seems to have anti-fungal and anti-viral properties. Gallic acid acts as an antioxidant and helps to protect human cells against oxidative damage. Gallic acid was found to show cytotoxicity against cancer cells, without harming healthy cells. Gallic acid is used as a remote astringent in cases of internal haemorrhage. Gallic acid is also used to treat albuminuria and diabetes [15].

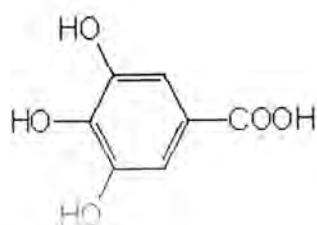


Figure-1: Chemical structure of gallic acid

This study we aimed to extract and purification Gallic acid from rind of pomegranate to use it in biological and chemical tests as a standard compound.

## MATERIAL AND METHODS

### Plant materials

The rind of pomegranate was collected and washed with water to remove any impurities and then dried at room temperature 25°C without light. The samples were put in a grinder to transfer them to powder.

### Extracting solvents:

We weighed 100g of powder and put it in a round bottom flask with solution containing ethanol : water with ratio 40:60. The flask was heated in a water bath at 60°C for 60 min. The solution was then filtered to obtain crude (stock solution) [15].

### Purification of crude:

The crude was distilled to get 1/3rd of the solution using the Soxhlet apparatus at 70°C for 3hrs. Ethanol was recovered to concentrate crude extraction and then the solution was kept overnight at room temperature 25°C to precipitate. The solution and the obtained particles were dried in the oven overnight at 60°C [15]. Water was added in the Soxhlet apparatus, and allowed to evaporate at lower temperature.

### GALLIC ACID TEST:

To detect Gallic acid we take extract (1 ml of ethanol extract) mixed with 10 ml of distilled water and filtered. Ferric chloride reagent (3 drops) was added to the filtrate. A blue-black or green precipitate confirmed the presence of gallic.

### Identification procedure

**Thin layered chromatography (TLC):** the dried methanol extraction was redissolved in 1ml methanol then applied by micropipette on silica gel plate as a continuous straight line with a width range (2-4) mm wide. Plates were inserted into a saturated TLC chamber containing Toluene: ethyl



acetate : formic acid system 3:3.5:0.5 as a mobile phase put two spots sample and standard (fig 2)[16].

**HPLC:** *The yield of extracted from pomegranate peel was gallic acid can be improved by using:*

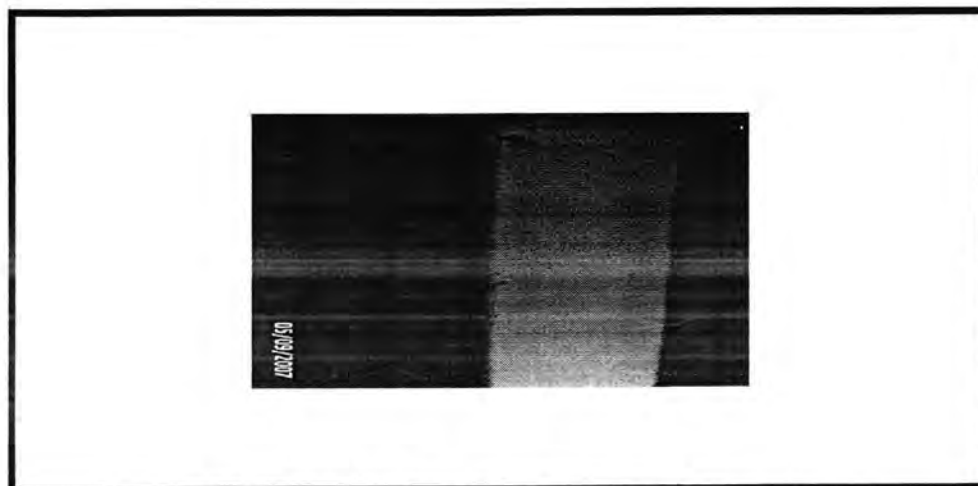
The separation and identification of gallic acid was performed by HPLC using Jasco's Binary Type High Performance Liquid Chromatography; comprising two PU-1550 pumps with 20 $\mu$ l loop and a Jasco multi wavelength detector MD-1510. A Cosmosil C<sub>18</sub> column (150mm x 4.6mm, 5 $\mu$ m particle) was used for the analysis. The mobile phase was a mixture of ethyl acetate: ethanol: water (1:5:4, v/v/v) delivered at a flow rate of 1.0 mL min<sup>-1</sup>. Peak of Gallic Acid in sample was identified by comparison with retention time of standard Gallic Acid [16]. Separation and identification of Gallic Acid in sample extract was performed by HPLC using Cosmosil C<sub>18</sub> column (150mm x 4.6mm, 5 $\mu$ m particle) and mobile phase a mixture of ethyl acetate: ethanol: water (1:5:4, v/v/v), a well resolved separate peak of Gallic Acid was identified at retention time of 3.496 min. which was found to be comparable with the retention time of standard (Figs. 3,4 ).

**FT-IR :** to detect functional groups in resveratrol structure and to be compared with the standard chart. Resveratrol was reported to contain many functional benzene ring, hydroxyl groups and the C=C double bond compared with standard (figures. 5,6)[16].

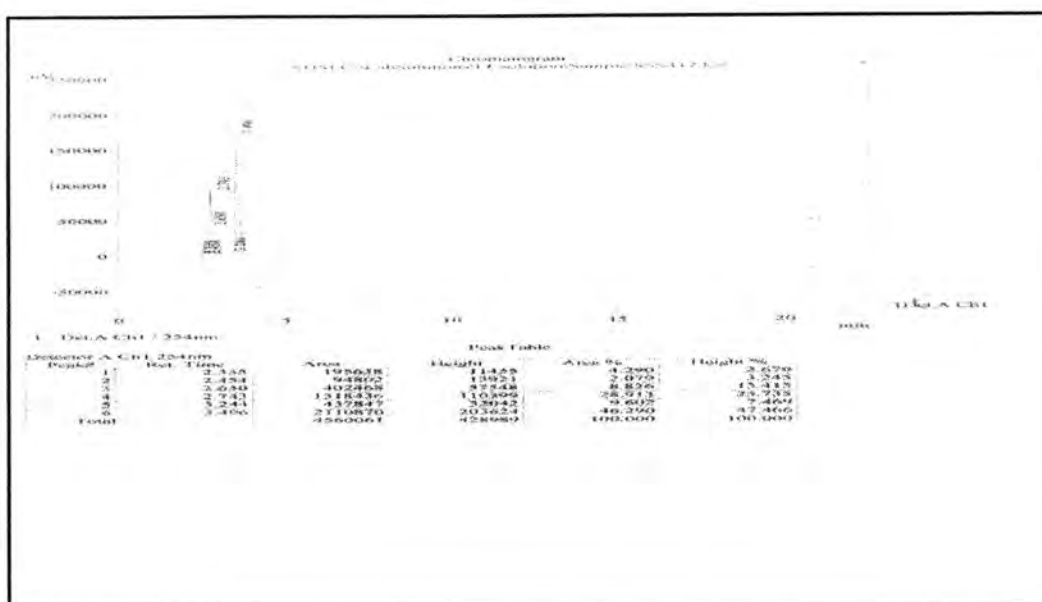
**UV absorption :** show intense purple fluorescence in UV light that was appear in the  $\lambda$  max at 366 with an inflection at 500 that compared with standard (figures. 7,8) .

## RESULTS AND DISCUSSION

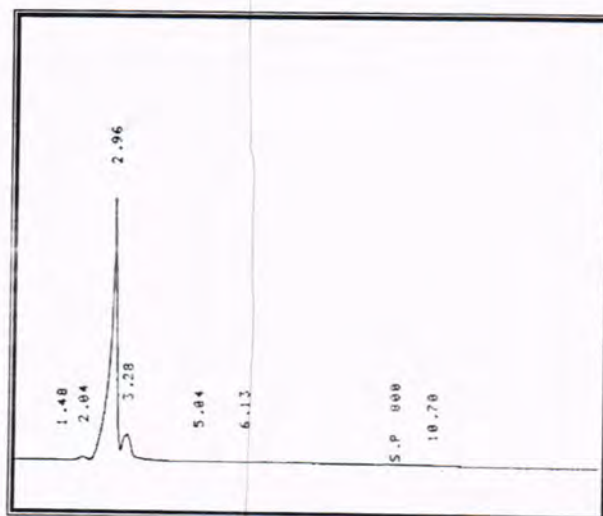
In the TLC obtained one zone were clearly visible: R<sub>f</sub> - 0.9 which compared with R<sub>f</sub> of Gallic acid standred (fig. 2,3).Some R<sub>f</sub> values in the TBA system were identical to luteolin mentioned in literature, and even more in Toluene-atheyl acetate- formic acid system 3:3.5:0.5 due to polarity difference. Bearing in mind the limitations of the identification of substances by the chromatographic method.



Figures-2: TLC of gallic acid A-standard B-sample



Figuer-3: HPLC spectra of gallic acid sample



Figuer-4: HPLC spectra of gallic acid standard

FT-IR Spectral Analysis: The FT-IR analysis fig (5,6) of the were further tested by UV fig(7,8) and and IR spectroscopy methods for identification samples was done and the functional groups associated were determined (table 2).the FT –IR spectrum presence of

Table-2: functional groups in FT –IR spectrum

Major absorption bands	$\nu$ : 3414, 3377, 1716, 1616, 1512, 1454, 1226 $\text{cm}^{-1}$ (KBr)
------------------------	---

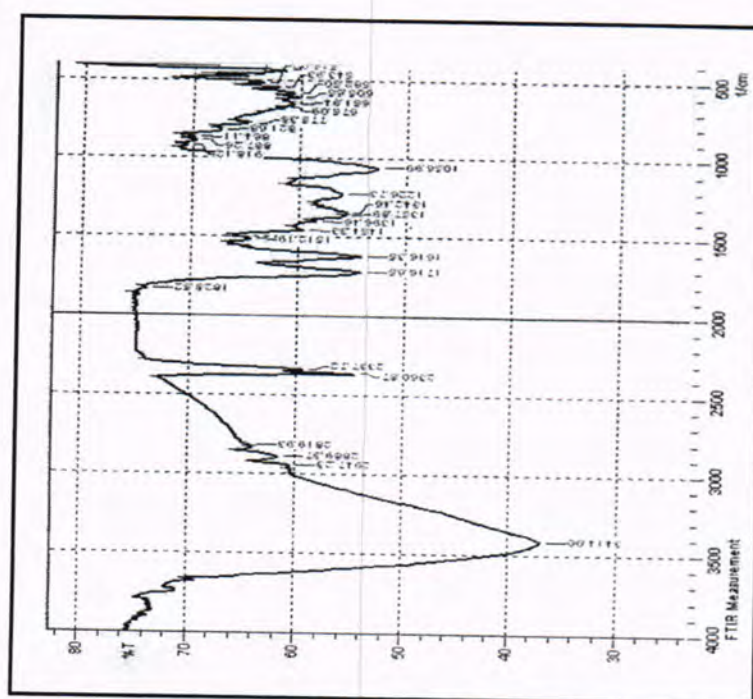


Figure-5: FT-IR spectra of gallic acid sample

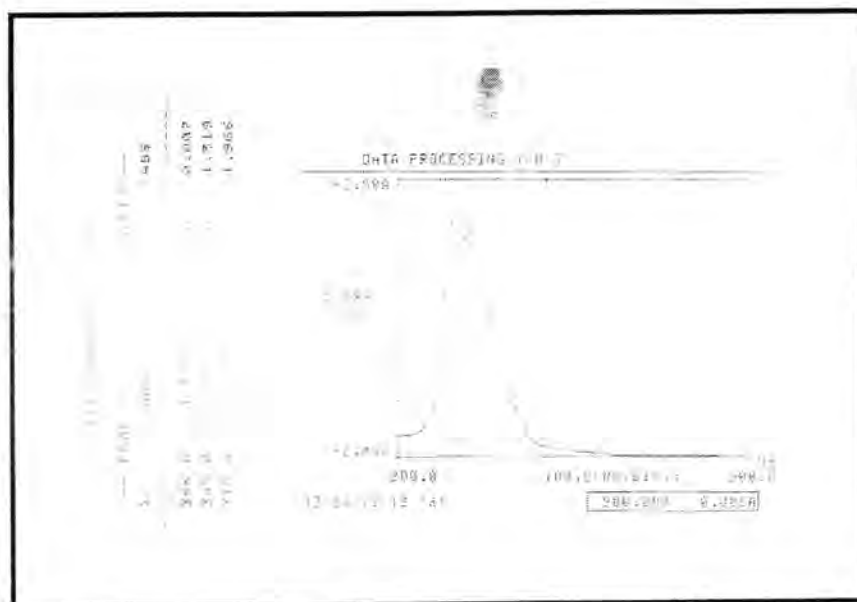


Figure-6: UV. spectra of gallic acid sample

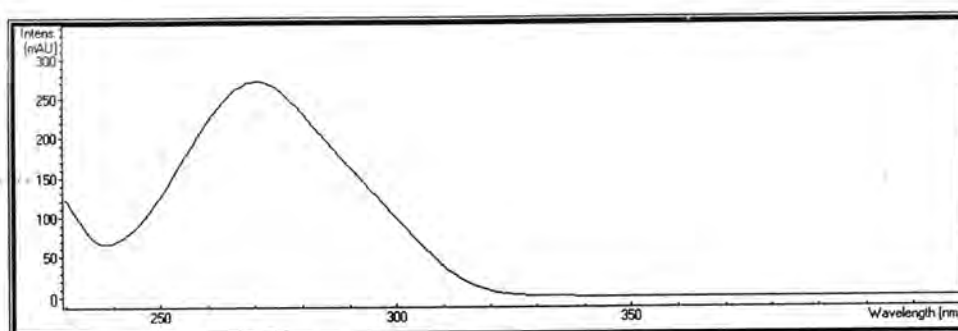


Figure-7: UV. spectra of Gallic acid standard

Peaks of GALLIC ACID in sample was identified by comparsion with IR-standar GALLIC ACID .Determination of gallic acid Uv analysis was performed on a uv – visible spectrophotometer 220, 271 nm (ethanol).

## REFERENCES

1. Abdel MAE. Antioxidant activities of *Punica granatum* (pomegranate) peel extract on brain of rats. J. Nutrition, in July:23-33 (2011).
2. Ajaikumar KB, Asheef M, Babu BH, Padikkala J. The inhibition of gastric mucosal injury by *Punica granatum* L.(pomegranate) methanolic extract. J. Ethnopharmacol., 96: 171-176.(2005).
3. Bakhru, H.K.. Foods That Heal: The Natural Way to Good Health.(book)(2009).



4. Madihassan, S. Outline of the beginnings alchemy and its antecedents. American J. Chines,12:25. (1984).
5. Navindra Seeram, P., N. Risa Schulmann and D. Heber,. Pomegranates: Ancient Roots to D. Heber, 2006. Pomegranates: Ancient Roots t Modern Medicine. CRC. Press. Boca Raton, FL, USA.( 2006).
6. Adhami VM, Mukhtar H. Anti-oxidants from green tea and pomegranate for chemoprevention of prostate cancer. Mol. Biotechnol., 37: 52-57. (2007).
7. Abdel MAE, Dkhil MA, Al-Quraishy. Studies on the effect of pomegranate (*Punica granatum*) juice and peel on liver and kidney in adult male rats. Mol. Biotechnol.,June . (2011)
8. Lambert PA. Bacterial resistance to antibiotics: Modified target sites. Adv. Drug Deliv. Rev., 57: 1471-1485(2005).
9. Wu, X., G. Cao and R.L. Prior,. Absorption andmetabolism of anthocyanins in elderly women afterconsumption of elderberry or blueberry. J. Nutrition. 132: 1865., (2002).
10. Passamonti, S., U. Vrhovsek, A. Vanzo andF. Mattivi, . The stomach as a site for anthocyanins absorption from food, FEBS Letters544(1): 210-213.(2003).
11. LD Reynolds and NG Wilson, "Scribes and Scholars" 3rd Ed. Oxford: pp193-4 (1991).
12. S. M. Fiuza. "Phenolic acid derivatives with potential anticancer properties- a structure-activity relationship study. Part 1: Methyl, propyl and octyl esters of caffeic and gallic acids".(2004).
13. Tsao, Makepeace. "A New Synthesis Of Mescaline". Journal of the American Chemical Society 73 (11): 5495-5496. (1951)
14. H.and Ekrami,E:wool dyeing with extracted dye from pomegranate (punica Granatum) peel .world Applied science journal,8(11):1387-1389 . (2010)
15. Sawant L, Prabhakar B, Pandita N. Quantitative HPLC analysis of Ascorbic Acid and Gallic Acid in *Phyllanthus Emblica*. J. Anal. Bioanal Techniques; 1: 111. (2010).
16. Hafsa D., Pradnya J. P., Development of RP-HPLC method for qualitative analysis of active ingredient (Gallic acid) from Stem Bark of *Dendrophthoe falcate* Linn., International Journal of Pharmaceutical Sciences and Drug Research,; 3(2): 146-149.( 2011)

## Study the effect of Insulin Resistance on visfatin, Total Anti oxidant Capacity and other Anti oxidants in Females with Chronic renal Failure [Stage 3]

Atheer Awad Mehde

Department of Acceptable Analysis, Health and Medical Technical College, Baghdad, Iraq.

E-mail: [atheerawad@yahoo.com](mailto:atheerawad@yahoo.com)

Received 14/2/2012 – Accepted 20/6/2012

### الخلاصة

ينتج الفشل الكلوي المزمن (CRF) عن انخفاض دائم وتدرجي عادة في وظائف الكلى، إلى درجة كافية تؤدي إلى التأثير على أنظمة أخرى في الجسم. وبعد الفاسقتين (Visfatin) نوع من adipocytokines التي ولدت الكثير من الاهتمام في الأونة الأخيرة. إن الزيادة الشديدة في مقاومة الانسولين والتي قد تترافق مع انخفاض مستوى معدل الترشيح الكلبي ومع ذلك، هناك بيانات قليلة عن العلاقة بين Visfatin، ومقاومة الانسولين مع إجمالي مضادات الأكسدة (TAC) ومضادات للتأكد أخرى في الفشل الكلوي المزمن (CRF) [المرحلة 3] وهذا ما تهدف إليه الدراسة الحالية. تم قياس معدل الترشيح الكلبي (GFR) عند 50 مريضة من المصابات بالفشل الكلوي المزمن [المرحلة 3] إضافة لذلك الفحوص المختبرية لوظائف الكلى (اليوريا والكرياتينين)، نسبة الهيموكلوبين، مستوى الكلوكرز الصيامي، الألبومين، الكالسيوم، الفوسفات اللاعضوي، البروتين الكلبي، حامض اليورك، البوتاسيوم، الصوديوم إضافة إلى قياس إجمالي مضادات الأكسدة (TAC) وMDA وفيتامين E وفيتامين C وقد تضمنت الدراسة الحالية قياس visfatin والانسولين ومقاومة الانسولين (HOMA) في أمصال المصابات بالفشل الكلوي المزمن ومقارنتها بمجموعة الضبط المكونة من 25 امرأة من الأصحاء اللواتي راجعن المستشفى لغرض إجراء فحوصات عامة. لوحظ وجود تغييرات معنوية في مستوى الهيموكلوبين، مستوى الكلوكرز الصيامي، معدل الترشيح الكلبي (GFR) اليوريا والكرياتينين، الكالسيوم، البوتاسيوم، حامض اليورك، MDA، TAC، فيتامين E، فيتامين C، عند المصابات بالفشل الكلوي مقارنة بمجموعة الضبط. أظهرت الدراسة زيادة معنوية في مستوى visfatin، الانسولين ومقاومة الانسولين (HOMA) ( $P < 0.001$ ) عند المصابات بالمرض. لقد أشارت الدراسة إلى وجود علاقة طردية بين visfatin و GFR ( $r = 0.59$ ,  $p < 0.01$ ) وكذلك مع Hb ( $r = 0.60$ ,  $p < 0.05$ ) ومع الانسولين ( $r = 0.43$ ,  $p < 0.05$ ) إضافة إلى علاقته مع HOMA ( $r = 0.57$ ,  $p < 0.05$ ) عند مجموعة الضبط. إن مستويات visfatin، الانسولين ومقاومة الانسولين (HOMA) إضافة إلى MDA/TAC ratio ربما تلعب دورا مهما في تطور مضاعفات المرض عند المصابات بالفشل الكلوي المزمن. على حد علمنا لم تشر الدراسات السابقة إلى ذلك. قد تكون نتائج هذه الدراسة مفيدة في الدراسات السريرية والتي تهدف لمتابعة أنظمة مضادات الأكسدة ودورها في التسبب في الفشل الكلوي المزمن.

### ABSTRACT

Chronic Renal Failure (CRF) is the state which results from a permanent and usually progressive reduction in renal function, in a sufficient degree to have adverse consequences on other systems. Visfatin is novel adipocytokine that have recently generated much interest. A greater degree of insulin resistance may predispose to renal injury by worsening renal hemodynamics through the elevation of glomerular filtration fraction. However, there are sparse data on the relationship between Visfatin, insulin resistance with Total Anti oxidant Capacity and other Anti oxidants in chronic renal failure (CRF) [Stage 3]. The glomerular filtration rate (GFR) has been measured in 50 patients with CRF using haemodialysis method. Laboratory investigations including Hemoglobin, fasting serum glucose, serum urea, creatinine, S. potassium, S. Sodium, S. calcium, S. Phosphorus, and Uric acid, in addition to serum total antioxidant capacity (TAC), malondialdehyde (MDA), vitamin C, vitamin E, Visfatin, insulin and insulin resistance [HOMA] had been

measured in female with CRF. Blood samples were obtained from the patients and twenty five healthy individuals who came to the hospital for health checkup. Hemoglobin, fasting serum glucose, Serum urea, S. creatinine, GFR, S. calcium, S. potassium, S. uric acid, TAC, MDA, vitamin C, vitamin E and MDA/TAC ratio showed a significant difference between the female with CRF and control group. Visfatin, insulin and insulin resistance [HOMA] significantly increased [ $p < 0.001$ ] in patients group. There was a positive correlation in Visfatin [ng/ml] with GFR, Hb, insulin, and HOMA. In this study a different significant association was observed between Visfatin, insulin and Homostasis model assessment [HOMA] with TAC, MDA, vitamin C, vitamin E and MDA/TAC ratio in the CRF patients when compared to control group. In conclusion Visfatin, insulin, HOMA and MDA/TAC ratio levels may play an important role in complication of disease in patients. As our knowledge, these results in the present study are shown the first time. The study may be useful in designing clinical studies that target utilizing antioxidant systems to provide protective pathways on the pathogenesis of chronic renal failure.

**Keywords:** Insulin resistance, Total Anti oxidant Capacity, Anti oxidants, MDA/TAC ratio, glomerular filtration rate, Chronic kidney disease

## INTRODUCTION

Chronic kidney disease (CKD) is characterized by progressive deterioration of kidney function, which develops eventually into a terminal stage of chronic renal failure (CRF) [1]. During the last few years, an international consensus has emerged categorizing CRF into five stages according to the glomerular filtration rate (GFR) and presence of signs of kidney damage: stage 1: GFR  $> 90$  ml/min and signs of kidney damage, stage 2: GFR = 60-89 ml/min and signs of kidney damage, stage 3: GFR = 30-59 ml/min, stage 4: GFR = 15-29 ml/min, and stage 5: GFR  $< 15$  ml/min [2]. Chronic Renal Failure is associated with many kinds of metabolic changes caused by the kidney disease and also attributable to dialysis treatment. Phenomena such as accumulation or deficit of various substances and dysregulation of metabolic pathways combine in the pathogenesis of these changes [3]. In the process of accumulation, decreased urinary excretion plays a crucial role and leads to retention of metabolites in the organism (e.g. creatinine, urea, electrolytes, water). The increased formation of metabolites through catabolic processes and alternative metabolic pathways also exerts an influence. Regular dialysis treatment partly decreases this accumulation, but cannot avert the overall deficit [1]. The CRF leads to many complications over a period of time. The most common include cardiovascular, cerebrovascular and peripheral vascular diseases. Deaths due to cardiovascular complications are 4-20 fold higher in CRF patients than any other cause in general population. [4]

Chronic Renal Failure is associated with insulin resistance [5,6] which plays an important role in the pathogenesis of cardiovascular

diseases. Insulin resistance is a risk factor of metabolic syndrome [7]. Insulin resistance is primarily detectable when the GFR is below 50 ml/min. Reduced insulin-mediated non oxidative glucose disposal is the most evident defect of glucose metabolism, but impairments of glucose oxidation, the defective suppression of endogenous glucose production, and abnormal insulin secretion also contribute to uremic glucose intolerance [8]. Accumulating nitrogenous uremic toxins seem to be the dominant cause of a specific defect in insulin action, and identification of these toxins is progressing, particularly in the field of carbamoylated amino acids[1,8].

Oxidative stress due to overproduction of reactive oxygen species and impairment in antioxidant defense mechanisms have been suggested as possible factors contributing to the pathogenesis of atherosclerosis in patients with CRF. Total antioxidant capacity is a parameter characteristics activities of antioxidant status of the body and reflect the oxidative stress imposed on the organism [9]. There is growing interest in the role of free radical damage in the vascular disease, neurodegenerative disease and aging. Oxidative stress occurs in a cellular system when the production of free radical moieties exceeds the antioxidant capacity of that system[10]. Furthermore an increase in oxidative stress is considered an important pathogenic mechanism in the development of various complications like cardio vascular, cerebrovascular and peripheral vascular disease[11]. During this process poly unsaturated fatty acid present in cell membrane are oxidized in vivo to form MDA. This lipid peroxidation product can structurally alter major bio molecules[12].

Visfatin have been linked to diabetes mellitus [13,14], metabolic syndrome [15,16], atherosclerosis [16, 17] as well as some anthropometric parameters [16,18] in non dialyzed populations. However, there is little information about visfatin [19,20] in patients treated with hemodialysis. Fukuhara et al. [21] demonstrated insulin-mimetic effects of visfatin in several animal models of insulin resistance and obesity and reported that visfatin binds to and activates the insulin receptor and they have speculated that its activity as an insulin mimetic might explain its metabolic effects. This interaction between visfatin and insulin receptor was retracted later by Fukuhara's group [22]. Similarly, in renal disease, some investigators have reported higher [19] and other lower [16] plasma visfatin concentrations compared to control groups or the normal range provided by a reagent' producer. Therefore, the aim of the study was to evaluate the relation of Visfatin and HOMA to Total Anti oxidant Capacity and other Anti oxidants parameters in Females with CRF [Stage 3].



## MATERIALS AND METHODS

Fifty female patients , in the age group of 30-50 admitted with clinically diagnosed CRF [Stage 3] in Medical City –Kidney Transplant Center, Iraq were taken for the study. It had been excluded cases with acute renal failure, kidney transplanted patients, patients on antioxidant. A group of 25 healthy subjects were used for comparison of oxidative stress and cardiovascular status. About 5ml of venous blood was drawn under aseptic precautions in a sterile tube from selected subjects after a period of overnight fasting of 12 hr, and serum was separated by centrifugation(at 2500 round/min for 10 min) and stored at -20C.

The fasting serum glucose, urea, creatinine, Uric acid, S. calcium, S. Phosphorus, S. potassium, S. Sodium, and Hemoglobin were measured by spectrophotometric methods supplied by Giesse Diagnostic. Total antioxidant capacity(TAC) in serum samples was carried out according to Rice -Evans and Miller[23]. Plasma Malondialdehyde(MDA) was determined according to the modified method of Satoh[30]. Ascorbic acid levels were estimated by the method of Tietz [24]. vitamin E levels were determined according to a modified of Hashim and Schuttringer[25]. The serum, insulin, Visfatin were measured by Enzyme Linked Immunosorbent Assay (ELISA) (Biovender Laboratory Medicine, Brno,Czech Republic).

The glomerular filtration rate[GFR] can be estimated using prediction equations that take into account the serum creatinine level and some or all of specific variables (age, sex, race, body size) [26,27] The modification of Diet in Renal Disease (MDRD) study equation was used to estimate the GFR and as follow[28]: $GFR (ml/min/1.73 m^2) = 186 \times (Serum\ creatinine)^{-1.154} \times (Age)^{-0.203} \times (0.742\text{ if female}) \times (1.210\text{ if black})$ .

A Homeostasis Model Assessment (HOMA) was used to evaluate insulin resistance [29].The values for a patient can be calculated from the fasting concentrations of insulin and glucose using the following formula:  $\text{fasting serum insulin } (\mu U/ml) \times \text{fasting plasma glucose } (mmol/L)/22.5$  [29].

MDA/TAC ratio was calculated as an index of oxidative stress[30]. All statistical analysis in the study was performed using SPSS version 17.0 for Windows (Statistical Package for Social Science, Inc., Chicago, IL, USA). Values were expressed as mean  $\pm$  SD. Student t test was used to find out the significance level and the Pearson correlation study was used to find the association between the biochemical parameters.

## RESULTS AND DISCUSSION

Descriptive data of patients and control group are shown in table 1. Visfatin ,Fasting serum glucose , insulin and HOMA were significantly elevated in patients compared to control [ $P<0.001$  ]. Average value of urea ,creatinine concentrations were  $110.80\pm30.19$  mg/dl,  $5.53\pm2.09$ mg/dl respectively for patients, while they were  $30.00\pm4.77$ mg/dl ,  $0.92\pm0.70$  mg/dl respectively for control group . Hemoglobin concentration were  $9.42\pm1.99$ gm/dl for patients, in compared to  $12.84\pm 0.87$  for control. The mean GFR was  $39.43\pm6.10$ ml/min/ $1.73m^2$  as shown in table 1. There were no significant differences [ $P>0.05$ ]in S. Sodium and S. Phosphorus when compared to the control group as shown in table 1. Calcium level was decreased significantly [ $P<0.01$  ] in patient group when compared to control.

Table-1: The mean and standard deviation of B. urea,S creatinine, GFR , sodium, potassium, calcium, phosphorous ,Hb, Visfatin ,Fasting serum glucose , insulin and HOMA patients group[Stage 3] and control group.

Characteristic	Patients mean $\pm$ SD	Control mean $\pm$ SD	PValue
Urea [mg/dl/]	110.80 $\pm$ 30.19	30.00 $\pm$ 4.77	<0.001
Creatinine[mg/dl/]	5.53 $\pm$ 2.09	0.92 $\pm$ 0.70	<0.001
GFR[ml/min/ $1.73m^2$ ]	39.43 $\pm$ 6.10	86.34 $\pm$ 5.99	<0.001
S. Sodium [mEq/L]	139.66 $\pm$ 7.71	137.84 $\pm$ 2.15	>0.05
S. Potassium[mEq/L]	4.55 $\pm$ 0.98	4.05 $\pm$ 0.39	<0.05
S. Calcium[mg/dl/]	8.21 $\pm$ 0.79	9.67 $\pm$ 0.65	<0.01
S. Phosphorus[mg/dl/]	3.22 $\pm$ 0.63	2.81 $\pm$ 0.44	>0.05
Hb [gm/dl]	9.42 $\pm$ 1.99	12.84 $\pm$ 0.87	<0.001
Fasting serum glucose[mg/dl/]	153.64 $\pm$ 17.48	95.75 $\pm$ 10.48	<0.001
Insulin[ $\mu$ U/ml]	18.58 $\pm$ 4.34	8.08 $\pm$ 0.73	<0.001
HOMA	4.44 $\pm$ 1.86	1.51 $\pm$ 0.14	<0.001
Visfatin [ ng/ml]	42.98 $\pm$ 6.66	29.88 $\pm$ 3.55	<0.001

Table 2 shows the comparative analysis of serum Total antioxidant capacity, MDA,uric acid, Vitamin E, Vitamin C and MDA/TAC ratio between control and patients with CRF. When compared the result to control, patients with CRF showed significant increase in the in the TAC, MDA,uric acid and MDA/TAC ratio, while Vitamin E, Vitamin C significantly decreased .

Table-2 : Comparison of Different Parameters Related to Antioxidant Parameters in Control and Study Groups in [CRF, stage 3]

Characteristic	Patients mean±SD	Control mean±SD	PValue
TAC [μmol/L]	545.80±68.18	433.80±29.98	<0.001
MDA [μ mol/L]	4.10±0.52	1.39±0.22	<0.001
Uric acid [mg/dl/]	4.85±0.95	4.20±0.54	<0.05
Vitamin E [mg/dl]	1.09±0.13	1.42±0.32	<0.001
Vitamin C [mg/dl]	0.83±0.17	1.62±0.34	<0.001
MDA/TAC ratio	0.008±0.003	0.003±0.0005	<0.01

Table 3 shows the different correlation between visfatin concentrations and other biochemical factors in the CRF patients.

Table-3: Results of correlation analyses of fasting visfatin concentrations in the CRF patients (*n* = 50)

Characteristic	Visfatin [ ng/ml]	
	Correlation coefficient <i>r</i>	<i>P</i> -value
Urea [mg/dl/]	0.08	NS
Creatinine[mg/dl/]	0.06	NS
GFR[ml/min/1.73m <sup>2</sup> ]	0.59	<0.01*
S. Sodium [mEq/L]	0.10	NS
S. Potassium[mEq/L]	-0.25	NS
S. Calcium[mg/dl/]	0.09	NS
S. Phosphorus[mg/dl/]	0.08	NS
Hb [gm/dl]	0.42	<0.05*
Fasting serum glucose[mg/dl/]	0.23	NS
Insulin[μU/ml]	0.57	<0.05*
HOMA	0.60	<0.05*

NS, not significant; \*, significant.

There were a different correlations between visfatin ,insulin and HOMA with antioxidants in sera of patients with CRF as shown in table 4, while there were no significant correlations in control group



Table-4: correlations between Visfatin ,insulin and HOMA with antioxidants in CRF patients

Characteristic	Visfatin [ ng/ml]		Insulin[ $\mu$ U/ml]		HOMA	
	r	p	r	p	r	p
TAC [ $\mu$ mol/L]	0.55	0.01	0.53	0.01	0.64	0.01
MDA [ $\mu$ mol/L]	0.67	0.01	0.75	0.001	0.68	0.01
Uric acid [mg/dl]	0.49	0.05	0.66	0.05	0.58	0.05
Vitamin E [mg/dl]	-0.37	NS	-0.44	0.05	-0.65	0.05
Vitamin C [mg/dl]	-0.68	0.01	-0.79	0.001	-0.86	0.01
MDA/TAC ratio	0.65	0.01	0.70	0.01	0.68	0.01

Correlation coefficient ,r ; P-value ,P

In the present study, there were an agreement with the results obtained by Axelsson et al. [19] that found a higher mean level of visfatin in CRF patients than in the control group .The differences in serum visfatin level in CRF patients, shown in the available literature [20], may be attributable to the different methods of investigation [31]. In patients with chronic renal failure, elevated visfatin levels predict increased mortality [19], most often caused by cardiovascular events [32]. Patients with arteriosclerosis show increased visfatin concentrations [33]. A previous study found association between hyper visfatinaemia and endothelial dysfunction in CRF [34].Other study didn't find any association between visfatin and IR in non-diabetics, newly diagnosed, untreated type 2 diabetic and diabetics treated with insulin or oral hypoglycemic agents [35-37]. The current study have found a positive correlation between visfatin and insulin concentration as well as correlation between visfatin and HOMA in patients with CRF . In agreement with the hypothesis that visfatin could play a role in the regulation of insulin sensitivity [20], Another study suggest that secretion of visfatin may be stimulated not only by endogenous but also by exogenous insulin, and modulated by many factors more expressed in diabetic patients (e.g., hypoxia) [38].

Several studies have clearly shown that the sensitivity to the action of insulin with respect to glucose metabolism is markedly impaired in CRF[39].Mechanisms may contribute to insulin resistance in CRF including defects at post receptor level of insulin action in muscle, adipose, and liver tissues. The defects are primarily localized to glucose uptake and metabolism by these insulin-sensitive tissues[40].Significantly impaired insulin sensitivity is present early in the course of CRF[41].However, in early CRF patients, factors other than impaired kidney function, such as dyslipidemia and adverse effects of medications are likely to cause or contribute to insulin resistance[41].



MDA is a lipid peroxidation product which is formed during oxidation process of polyunsaturated fatty acids by reactive oxygen species [42]. MDA is the sensitive marker of lipid peroxidation. MDA level is significantly elevated in hemodialysis patients when compared to conservatively managed patients. This is in accordance with study of C.M Loughrey et al [43], A. Marjani [44] and Talia Weinstein et al [45]. Although hemodialysis leads to improvement of several biochemical parameters like creatinine, urea levels and plasma lipid patterns, but it can cause harmful atherogenic effects. The increase in lipid peroxidation resulting from hemodialysis could be provoked by bio incompatibility of dialysis membrane. When cells come in contact with the dialyzer membrane leads to sensitization of cell membrane components leading to complement activation which cause formation of other reactive oxygen species which will initiate peroxidation of polyunsaturated fatty acids [44].

As a result of free radical production the Vitamin E is converted into  $\alpha$ -tocopheroxyl free radical. The  $\alpha$ -tocopheroxyl free radical does not possess antioxidant properties and even trigger the process of lipid peroxidation. Vitamin C is a substance responsible for the regeneration of the  $\alpha$ -tocopheroxyl free radical back to tocopherol a continuous supply of Vitamin C into the arterial blood line during dialysis. As demonstrated by most studies patients on dialysis do not show Vitamin E deficiency and Vitamin E levels don't decline during dialysis [46]. Vitamin C deficiency is frequent in the dialysis population by contrast and dialysis associated with significant losses of Vitamin C [47]. Single Vitamin C infusion resulting in maintaining its levels at values comparable to pre dialysis levels. The potent antioxidant activity of Vitamin C maintains cellular GSH conserve the integrity of biomembranes and reduce leakage of cytosolic lactic dehydrogenase in liver. Moreover, it may diminish primary DNA damage of cells [48].

In the current study TAC level increased significantly [ $p < 0.001$ ] in patients when compared to control. These results agree with the other study that findings associating significantly increasing serum TAC levels with progression of chronic renal failure and this elevated TAC levels were strongly correlated to both serum creatinine and uric acid levels [49]. However, lipid peroxidation was not associated with TAC. Because of these facts, authors concluded that increased TAC was related to uric acid accumulation (uremia) resulted from chronic renal failure. In 37 chronic renal failure patients endothelial vasodilatation was positively associated with serum total antioxidant capacity and negatively correlated with lipid peroxidation markers [50]. Total antioxidant capacity summarizes the overall activity of antioxidants and antioxidant enzymes [51]. The co operation between different

antioxidant pathways provides greater protection against attack by ROS, compared to any single compound. Thus the overall antioxidant capacity may give more relevant biological information compared to that obtained by the measurement of individual biomarkers [52].

The correlation between insulin and HOMA with anti oxidants in table 4 may be due to that both hyperglycaemia and insulin resistance are accompanied by reduced insulin action[53,54]. Hyperglycaemia and insulin resistance may also be accompanied by oxidative stress [55,56]. Ceriello hypothesized a model that oxidative stress represents the common pathway through which hyperglycaemia and insulin induce a depressed insulin action[57]. This point of view is supported by studies with antioxidants, which are able to improve the concentration of insulin [58].

A significant positive correlation were seen between serum Visfatin, insulin, HOMA and MDA/TAC ratio. This shows that increase in Visfatin,insulin,HOMA level causes increase in the oxidative stress. MDA/TAC ratio was identified as an ideal marker to assess the oxidative stress [59].These results as our knowledge are a novel markers to evaluate the complication in the CRF patients . The severity of CRF complications is may be correlated with the oxidative stress status of the patients and level of Visfatin,insulin,HOMA, which may leads to the pathogenesis of CVD in patients with CRF.

### CONCLUSION

Enhanced oxidative stress with increased Visfatin ,insulin, and HOMA levels in the patients with chronic renal failure may accelerate the process of atherosclerosis resulting in cardio vascular complications. Hence attention should be paid not only to already accelerated atherogenicity in chronic renal failure but also to the supplementation of antioxidants level and relationship with Visfatin level , insulin resistance.

## REFERENCES

1. R. Cibulka, J. Racek, Metabolic Disorders in Patients with Chronic Kidney Failure, *Physiol. Res.* 2007, 56: 697-705.
2. Levey AS, Eckardt KU, Tsukamoto Y, Levin A, Coresh J, Rossert J, Zeeuw D, Hostetter TH, Lameire N, Eknoyan G: Definition and classification of chronic kidney disease: a position statement from Kidney Disease: Improving Global Outcomes (KDIGO). *Kidney Int* 2005, 67: 2089-2100.
3. Cibulka R, Racek J, Vesela E: The importance of L-carnitine in patients with chronic renal failure treated with hemodialysis (in Czech). *Vnitr Lek*, 2005,51: 1108-1113.
4. Oda H, Keane WF. Lipid abnormalities in end stage renal disease. *Nephrol Dial Transplant* 1998; 13 (Suppl 1): 45-49
5. Kato Y, Hayashi M, Ohno Y, Suzawa T, Sasaki T, Saruta T: Mild renal dysfunction is associated with insulin resistance in chronic glomerulonephritis. *Clin Nephrol* 2000,54: 366-373.
6. Chen J, Muntner P, Hamm LL, Fonesca V, Batuman V, Whelton PK, HE J: Insulin resistance and risk of chronic kidney disease in nondiabetic US adults. *J Am Soc Nephrol*.2003, 14: 469-477.
7. Tuttle KR: Renal manifestations of the metabolic syndrome. *Nephrol Dial Transplant*,2005 20: 861-864.
8. Rigalleau V, GIN H: Carbohydrate metabolism in uremia. *Curr Opin Clin Nutr Metab Care*,2005, 8: 463-469.
9. Bartoz G .Total antioxidant capacity. *Adv. Clin.Chem.*, (2003). 37: 219-292.
10. Halliwell B. Free radicals, antioxidants and human diseases curicity, cause or consequence. *Lancet*, (1994), 344(8924): 721-724
11. Noirie, Nakao A, Uchidna K , Tsukahara H,Ohno M, Fujita T, Brodsky S, GoligorskyMS; Oxidative and Nitrosative stress in acute renal ischemia. *Am J Physiol*,2001, 281: F948-F957.
12. Daschner M ,Lenhartz H, Botticher D,Schaefer F, Wollschlager M , Mehls O et al. Influence of dialysis on plasma lipid peroxidation products and antioxidant levels. *Kidney Int*;1996,50:1268-1272.
13. Arner P Visfatin—a true or false trail to type 2 diabetes mellitus. *J Clin Endocrinol Metab* 2006,91:1:28–30.
14. Katakami N, Matsuhisa M, Kaneto H . Decreased endogenous secretory advanced glycation end product receptor in type 1 diabetic patients. *Diabetes Care* ,2005,28:2716–2721.
15. Filippatos TD, Derdemezis CS, Kiortisis DN et al . Increased plasma levels of visfatin/pre-B cell colony enhancing factor in obese and overweight patients with metabolic syndrome. *J Endocrinol Invest*,2007, 30:4:323–326

16. Koyama H, Shoji T, Yokoyama H et al . Plasma level of endogenous secretory RAGE is associated with components of the metabolic syndrome and atherosclerosis. *Arterioscler Thromb Vasc Biol*,2005, 25:2587–2593.
17. Takebayashi K, Suetsugu M, Wakabayashi S et al . Association between plasma visfatin and vascular endothelial function in patients with type 2 diabetes mellitus. *Metabolism* 2007,56:4:451–458.
18. Beltowski J Apelin and visfatin: unique “beneficial” adipokines upregulated in obesity? *Med Sci Monit*,2006, 12:6:112–119
19. Axelsson J, Witasp A, Carrero JJ et al Circulating levels of visfatin/pre-B-cell colony-enhancing factor 1 in relation to genotype, GFR, body composition, and survival in patients with CKD. *Am J Kidney Dis* ,2007,49:2:237–244.
20. Nu'sken KD, Petrasch M, Raut M et al . Reduced plasma visfatin in end-stage renal disease is associated with reduced body fat mass and elevated serum insulin. *2007 Exp Clin Endocrinol Diabetes* 115.
21. Fukuhara A, Matsuda M, Nishizawa M et al Visfatin: a protein secreted by visceral fat that mimics the effects of insulin. *Science*, 2005, 307:426–430.
22. Fukuhara A, Matsuda M, Nishizawa M et al . Retraction. *Science*,2007, 318:565.
23. Rice -Evans C, Miller NJ., Total antioxidant status in sera and body fluids . In: *Methods in Enzymology*. New York: Academic Press 1994 : 279–293.
24. Tietz, N W (1986). “In; Text book of clinical chemistry, Edited by N W Tietz, W B Saunders company, Philadelphia, London, Toronto”, pp.960-962.
25. Hashim S.A.; Schuttringer G.R., Rapid determination of tocopherol in macro- and microquantities of plasma, results obtained in various nutrition and metabolic studies. *Am. J. Clin. Nutr.*, 1966, 19:2 : 137-145.
26. Levey A.S., Bosch J.P., Lewis J.B., Greene T., Rogers N. & Roth D., A more accurate method to estimate glomerular filtration rate from serum creatinine : a new prediction equation. *Ann. Int. Med.* , 1999, 130:6:461-470.
27. Manjunath G, Darnak M.J & Levey A.S., Estimating the glomerular filtration rate. Dos and don'ts for assessing kidney function. *Postgrad. Med.* 2001,110:6:55-62.
28. Johnson C.A., Levey A.S., Coresh J., Levin A., Lau J. & Eknoyan G, Clinical practice guidelines for chronic kidney disease in adults: part I. definition, disease stages, evaluation, treatment, and risk factors. *American Family Physician.* , 2004,70:5.



29. Matthews DR, Hosker JP, Rudenski AS, Naylor BA, Treacher DF, Turner RC: Homeostasis model assessment: Insulin resistance and  $\beta$ -cell function from fasting plasma glucose and insulin concentration in man. *Diabetologia* , 1985,28: 412–419,.
30. Suresh D R1. Senthilkumaran Annam and Hamsaveena. Age related changes in:Total antioxidant capacity ratio-A novel marker of oxidative stress . *International Journal of Pharma and Bio science*,2010, VI(2) .
31. Nusken KD, Nusken E, Petrasch M et al . Preanalytical influences on the measurement of visfatin byenzyme immuno assay. *Clin Chim Acta*,2007, 382:154–156
32. de Mutsert R, Grootendorst DC, Axelsson J et al. NECOSAD Study Group. Excess mortality due to interaction between proteinenergy wasting, inflammation and cardiovascular disease in chronic dialysis patients. *Nephrol Dial Transplant* ,2008; 23: 2957– 2964
33. Zhong M, TanHW, Gong HP et al. Increased serum visfatin in patients with metabolic syndrome and carotid atherosclerosis. *Clin Endocrinol (Oxf)* 2008; 69: 878–884.
34. Yilmaz MI, Saglam M, Carrero JJ et al. Serum visfatin concentration and endothelial dysfunction in chronic kidney disease. *Nephrol Dial Transplant* 2008; 23: 959–965
35. Kenji O, Kiminori Y, Nozomu K et al . Circulating visfatin level is correlated with inflammation, but not with insulin resistance. *Clin Endocrinol (Oxf)*,2007, 67:5:796–800
36. Dogru T, Sonmez A, Tesci I et al . Plasma visfatin levels in patients with newly diagnosed and untreated type 2 diabetes mellitus and impaired glucose tolerance. *Diabetes Res Clin Pract*2006, 76:1:24–29
37. Chen MP, Chung FM, Chang DM et al . Elevated plasma level of visfatin/pre-B cell enhancing factor in patients with type 2 diabetes mellitus. *J Clin Endocrinol Metab*,2006, 91:295–299.
38. Bae SK, Halestrap AP . Hypoxia induction of human visfatin gene is directly mediated by hypoxia-inducible factor-1. *FEBS Lett*,2006, 580:4105–4113.
39. DeFronzo RA, Tobin JD, Rowe JW, Andres R. Glucose intolerance in uremia: Quantification of pancreatic beta cell sensitivity to glucose and tissue sensitivity to insulin. *J Clin Invest*, 1978,62: 425-35.
40. Mak RH, DeFronzo RA. Glucose and insulin metabolism in uremia. *Nephron*, 1992, 61: 377-82
41. . Stenvinkel P, Ottosson-Seeberger A, Alvestrand A. Renal hemodynamics and sodium handing in moderate renal insufficiency: The role of insulin resistant and dyslipidemia. *J Am Soc Nephrol*,1995, 5: 1751-60

42. Halliwell B, Gutteridge JMC (Eds): Free radicals in Biology and Medicine, 3rd Oxford University Press, 1999, 936 p.
43. Laughrey CM, Young IS, Lightbody JH, McMaster D, McNamee PT, Trimble ER. Oxidative stress in hemo-dialysis Q J Med ,1994, 87: 679-683.
44. Marjani A. Clinical effect of hemodialysis on plasma lipid peroxidation and erythrocyte antioxidant enzyme activities in Gorgan (South East of Caspian Sea). Ind J Nephrol 2005, 15: 214-217.
45. Weinstein T, Chagnac A, Korzets A, Boaz M, Ori Y, Herman M et al. Hemolysis in hemodialysis patients : evidence for impaired defense mechanisms against oxidative stress. Nephrol Dial Transplant ,2000,15: 883-887
46. Hegbrant J, Hult V. and Begsson V . Vitamin C and E as antioxidants in hemdialysis patients. Int. J.Artif. Organs., 1999, 22: 69-73.
47. Boham V, Tthroke K, Scacider S, Sperschneider H, Stein G and Bistsch R . Vitamin C status of patients with chronic renal failure,dialysis patient and patients after renal transplantation. Int. J. Vitamin Nutr. Res., 1997, 67:4: 262-266.
48. Benkovic V, OrsolicN, Knezevic AH, Ramic S, Dikic D, Basic I and Kopjar N .Evaluation of the radioprotective effects of propolis and flavonoids in gamma-irradiated mice: the alkaline comet assay study.Bid. Pharm. Bull., 2008. 31:1: 167-172.
49. Sofic E, Rustembegovic A, Kroyer G, Cao G. Serum antioxidant capacity in neurological, psychiatric, renal diseases and cardiomyopathy. J Neur Transm.,2002 109:711-719.
50. Annuk M, Zilmer M, Lind L, Linde T and Fellström B. Oxidative stress and endothelial function in chronic renal failure. J Am Soc Nephrol., 2001, 12:2747-2752,
51. Psotova J.,J. Zahalkova.J. Hrbac.V.Simanek and J.J.Bartek. Determination of total antioxidant capacity (TAC) in plasma by cyclic voltammetry . Biomed.Pap.,2001,145:81-83.
52. Malliaraki,N.,D. Mpliamplias,M.Kampa,K.Perakis,A.N Margioris and E .Castanas .Total and corrected antioxidative capacity in haemodialysis patients.BMC. Nephrol,20034:1471-2369.
53. De Fronzo RA , BonadonnaRC and Ferrannini DR : Pathogenesis of NIDDM: A Balanced Overview Diabetes Care 1992; 15: 318.368.
54. Zierath JR, Krook A, Wallberg-Henriksson H. Insulin action and insulin resistance in human skeletal muscle. [In Process Citation]. Diabetologia 2000; 43: 821-835.
55. Ceriello A. Acute hyperglycaemia and oxidative stress generation. Diabet Med 1997;14:S45-S49

56. Ceriello A, Pirisi M: Is oxidative stress the missing link between insulin resistance and atherosclerosis? *Diabetologia* 1995; 38: 1484-1485.
57. Ceriello A: "Oxidative Stress and Glycemic Regulation." *Metabolism* 2000; 49 (Suppl. 1): 27-29.
58. Paolisso G, D'Amore A, Giugliano D, Ceriello A, Varricchio M, D'Onofrio F. Pharmacologic doses of vitamin E improve insulin action in healthy subjects and non-insulin-dependent diabetic patients. *Am J Clin Nutr.* 1993;57:5:650-656.
59. Suresh D R1. Senthilkumaran Annam and Hamsaveena. Age related changes in:Total antioxidant capacity ratio-A novel marker of oxidative stress . *International Journal of Pharma and Bio science*,2010, V1(2) .



## Synthesis Of Some Pyranopyrazoles-6-One Derivatives By Microwave Method

Redha I,H,AL-Bayati, Fouad .M, Saed and Wassan B, Ali  
Department of Chemistry, College of Sciences,AL- Mustansiriya University

Received 12/4/2012 – Accepted 20/6/2012

### الخلاصة

في هذا البحث تم تحضير بعض مشتقات البايرونوبايرزول بطريقة المايكروويف بالإضافة الى الطريقة الاعتيادية. حيث تم تحضير المركبات (1-5) عن طريق تسخين مشتقات الهيدرازين مع الاثيل اسيتو اسيتيت في حمام زيتي ثم اعيد تحضير المركبات السابقة باستخدام تقنية المايكروويف. بينما تم تحضير قواعد شيف (8,9,10,11) عن طريق تفاعل المركبات (6,7) مع الالديهيدات الاروماتية بطريقة التصعيد ثم اعيد تحضير المركبات السابقة ايضا بطريقة المايكروويف. اما المركبات (12,13) فقد تم تحضيرها عن طريق تفاعل المركب (2) مع الاثيل ايزوثايوسيانات ونفثيل ايزوسيانات بطريقة التصعيد وكذلك اعيد تحضير المركبات الاخيرة بتقنية المايكروويف ايضا. تم تشخيص المركبات المحضرة باستخدام بعض الطرائق الطيفية، الأشعة فوق البنفسجية والمرئية، الأشعة تحت الحمراء، ومطيافية الرنين النووي المغناطيسي.

### ABSTRACT

In this work, pyranopyrazoles derivatives have been synthesized Under conventional and microwave conditions. The compounds (1-5) were prepared by heating hydrazine derivatives with ethyl acetoacetate and then repeated the reaction by microwave technique. While the Schiff bases (8-11) were synthesized by the condensation of compounds (6,7) with aromatic aldehydes and then repeated the reaction by microwave technique. Treatment of compound (2) with naphthylisocyanate or ethylisothiocyanate to give derivatives (12-13) and then repeated the reaction by microwave technique. The structure of the synthesized compounds were deduced by using some spectroscopic methods, UV –Visible ,FT-IR and NMR.

### INTRODUCTION

The Pyranopyrazoles derivatives are widely used as organic intermediates and well known for their biological activity.[1] Pyranopyrazoles exhibit useful biological properties such as cytotoxic [2], antibacterial [3] and molluscicidal [4] . Microwave irradiation of organic reactions has rapidly gained popularity as it accelerates the reaction towards a variety of synthetic transformations. Chemical transformations that took hours or even days to complete can now be accomplished in minutes. Microwave energy offers numerous benefits for performing synthesis such as increased reaction rates, enhanced yields and cleaner chemistries[5]. Schiff bases are used as substrates in the preparation of a number of industrial and biologically active compounds via ring closure, cycloaddition and replacement reactions[6]. Moreover, Schiff bases derived from various heterocycles have been reported to possess cytotoxic[7], anticonvulsant [8], antiproliferative [9], antimicrobial activity [10].



## MATERIALS AND METHODS

Melting points were determined on Gallenkamp(MFB-600) melting point apparatus and are uncorrected. The IR spectra of the compounds were recorded on ashimadzu FT-IR-3800 spectrometer as KBr disk. The UV spectra were performed on Cintra-5-Gbes scientific equipment . The  $^1\text{H}$ -NMR spectra(solvent DMSO- $d_6$  ) were recorded on Bruker 400 MHz spectrophotometer using TMS as internal standard.

### Synthesis of compounds (1-5):[11]

**Conventional method** :prepared from ethylacetoacetate and hydrazine derivatives according to reference (11).

**Microwave method** : A mixture of hydrazine derivative (0.0025 mole ) and redistilled ethyl acetoacetate (0.65gm,0.005 mole) were taken in a small beaker and mixed thoroughly. The mixture was then irradiated under microwave oven for (5-6) min at 850 W. Upon the completion of the reaction, the reaction mixture was then allowed to stand at room temperatures. The solid product obtained was washed with water and then filtered, dried and recrystallized from suitable solvent.

### Synthesis of compound (6) :

Potassium hydroxide (1.68gm., 0.03 mole) was dissolved in absolute ethanol (30 ml) .The solution was cooled in an ice bath and compound 2 (3.28gm., 0.02 mole) was added with stirring .then carbon disulfide (2.28gm., 0.03 mole) was added in small portions with constant stirring. The reaction mixture was agitated continuously for 5 hour at room temperature. After that hydrazine hydrate (1.5gm., 0.03 mole )was added and then refluxed for 2 hour. The mixture was neutralized with dilute HCL and the precipitated solid was collected by filtration, dried and recrystallized from ethanol. (Table 1)

**Synthesis of compound (7):** Iron powder (4 gm) was added portion wise to a mixture of compound 3 (2.85gm., 0.01 mole), concentrated hydrochloric acid (15 ml) and ethanol (10 ml). The reaction mixture was refluxed for 6 hour, cooled; the precipitate formed was filtered off, washed with water, dried and recrystallized from DMF.(Table 1)

### Synthesis of compounds (8-11)

**Conventional method:** To a solution of compounds (6,7) (0.001 mole) in (20 ml) of absolute ethanol, the appropriate aromatic aldehyde (0.001 mole) was added with 3-4 drops of glacial acetic acid. The

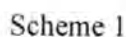
mixture was refluxed for 6 hours, cooled then the solid formed was filtered and recrystallized from appropriate solvent. Table (1)

**Microwave method:** Compounds that contain  $\text{NH}_2$  group (6-7) (0.001 mole) was dissolved in a little mount of ethanol and (0.001 mole) of appropriate aromatic aldehyde was dissolve in a little mount of ethanol with 1-2 drops of glacial acetic acid . Then the well-stirred mixture was irradiated under microwave oven for (6-8) min at 850 W. Upon completion of the reaction, the reaction mixture was then allowed to stand at room temperatures. The solid product obtained was recrystallized from suitable solvent.

#### Synthesis of compounds (8-11)

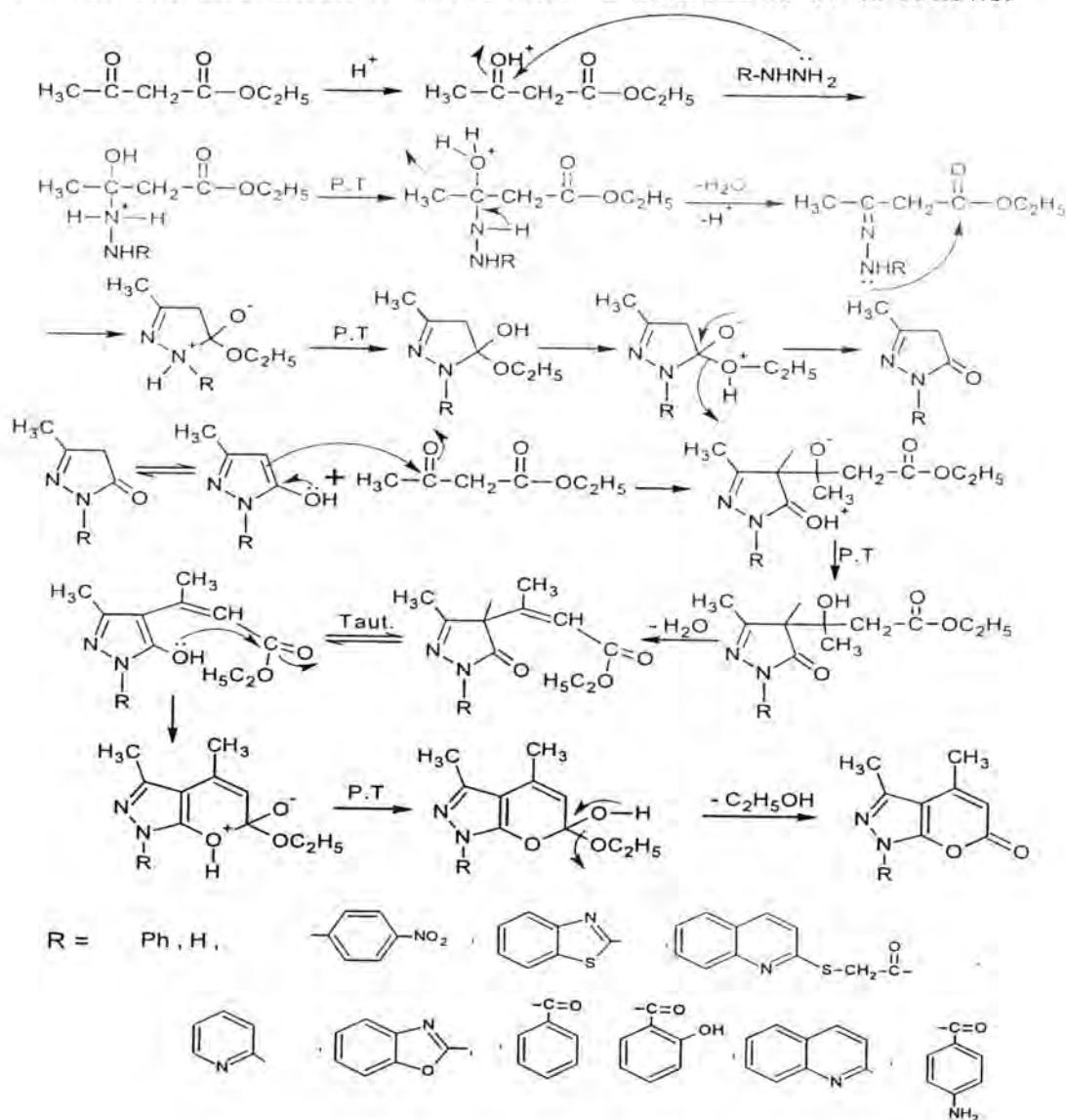
**Conventional method:** A mixture of compound 2 (0.01 mole) and ethylisothiocyanate or naphthylisocyanate (0.01 mole) was dissolved in DMF (20 mL) in a round bottom flask and two to three drops of morpholine was added as a catalyst. Then the well-stirred mixture was refluxed for 6-8 hours. The reaction mixture was then allowed to stand at room temperatures. After that the mixture was poured in ice-cold water. The resulting solid product was filtered, dried, and recrystallized from appropriate solvent.

**Microwave method [12] :** A mixture of compound 2 (0.49 gm., 0.003 mole) and alkyl thiocyanate or aryl isocyanate (0.003 mole) in a 10 ml DMF was taken in an Erlenmeyer flask. In the reaction mixture 2-3 drops of morpholine was add as a catalyst. The mixture was irradiated under microwave for 5.00 min at 850 W. The resulting solid was filtered, dried and recrystallized from benzene.



Pyranopyrazoles derivatives were synthesized by microwave irradiation in addition to conventional method. microwave irradiation is known to allow a striking reduction in reaction times, good yields and cleaner reaction than the purely thermal procedures. The compounds (1-5) were synthesized by the reaction of one mole of hydrazine

derivatives with two moles of ethyl acetoacetate in microwave oven for 5 min. The mechanism of the reaction is believed to be as follows:



The structure of the synthesized compound (1) has been characterized and identified by UV., FTIR and NMR spectrum. The FTIR shows an absorption band at (1755) due to the stretching vibration of (C=O) lacton, (1608) due to the stretching vibration of C=N, and 3070 for C-H aromatic. The  $^1H$ NMR of compound (1) show: 7.4-7.8(m, Ar-H), 5.7(s, 1H, Ar-H), 2.4(s, 6H, CH<sub>3</sub>). Schiff's bases (8-11) have been synthesized by the reaction of compounds (6, 7) with the appropriate aromatic aldehydes and few drops of glacial acetic acid (GAA) in microwave oven. The structure of the synthesized compound (8) has been characterized and identified by UV., FTIR and  $^1H$  NMR spectrum. The FTIR shows an absorption band at (1699) due to the stretching



vibration of C=O, (1618) due to the stretching vibration of C=N, and a band at 3180 for N-H. The  $^1\text{H}$  NMR of compound (8) showed: 8(s,1H,N=CH), 6.8-7.3(m,Ar-H), 5.7(s,1H,Ar-H), 3.7(s,6H,OCH<sub>3</sub>), 2.4(s,6H,CH<sub>3</sub>), 2(s,1H,NH). The FTIR spectrum of compound (11) showed the disappearance of the absorption bands for NH<sub>2</sub> and appearance of new absorption band at 1630 due to the stretching vibration of new CH=N, and two bands at 1355,1530 for  $\nu$  NO<sub>2</sub>. The  $^1\text{H}$  NMR of compound (11) showed: 9.1(s,1H,N=CH),7.3- 8.2(8H,Ar-H),6.6(s,1H,Ar-H),2.5(s,6H,CH<sub>3</sub>). The two last compounds were synthesized by reaction of equimolar quantities of the compound 2 with ethylisothiocyanate or naphthylisocyanate in microwave oven for 5 min. The FTIR spectra of compound 12 showed the appearance absorption bands for NH (3269  $\text{cm}^{-1}$ ), absorption band at (1701  $\text{cm}^{-1}$ ) due to the carbonyl group of lactone , appearance of new absorption bands of C=O of the amide at (1633  $\text{cm}^{-1}$ ). The  $^1\text{H}$ NMR spectrum of compound 13 showed the following data:6.09(s,1H,Ar- H), 4.1(m,2H,CH<sub>2</sub>CH<sub>3</sub>), 2.7 (s,3H,CH<sub>3</sub>),2.6 (s,3H,CH<sub>3</sub>),2.2(m,1H,NHCH<sub>2</sub>)1.2(t,3H, CH<sub>2</sub>CH<sub>3</sub>).

Table-1:physical properties of the synthesized compounds(1-13)

Comp.No.	Conventional Method		Microwave Method		M.P° C	Recryst.solvent
	Time (hrs)	Yield %	Time (min)	Yield %		
1	1	85	5	88	140-142	Ethanol
2	1	90	6	92	243-245	Ethanol
3	1	81	6	89	180-182	Ethanol
4	1	77	6	82	171-173	Ethanol
5	1	72	6	82	130-132	Ethanol
6	7	77	-	-	176-178	Ethanol
7	6	70	-	-	300 dec	DMF
8	6	66	6	70	128-131	Ethanol
9	6	70	8	76	163-165	Ethanol:water 1:1
10	6	80	7	89	246-248	Ethanol
11	6	72	8	79	197-200	Ethanol
12	8	68	5	74	171-173	Dioxane
13	8	71	5	80	100-102	Benzene

Table-2:UV and IR spectral data for compound (1-7)

Comp.No	UV Ethanol	Characteristic bands of FT-IR (cm <sup>-1</sup> ,KBr)					
	$\lambda$ max nm	C=O	C=C	C-Har	C-Hal	C=N	Others
1	246 306	1755	1491- 1548	3070	2922- 2987	1608	-
2	221 300	1703	1454- 1577	3088	2827- 2980	1604	$\nu$ N-H 3217
3	255 300	1750	1445-1555	3070	2976	1606	$\nu$ NO <sub>2</sub> 1340-1519
4	225 360	1715	1450- 1555	3065	2875- 2975	1610	$\nu$ C=O amid 1668( $\nu$ NH <sub>2</sub> ) 3300-3400
5	220 338	1705	1490- 1566	1055	2899- 2978	1606 1633	$\nu$ NO <sub>2</sub> 1348, 1521
6	256 338	1701	1440- 1512	3088	2985	1604	$\nu$ (NHNH <sub>2</sub> ) 3201-3317 $\nu$ C=S 1234
7	267 307	1735	1496- 1575	3078	2858- 2968	1606	$\nu$ (NH <sub>2</sub> ) 3250

Table-3:UV and IR spectral data for Schiff base compounds (8-11)

Comp.No	UV Ethanol	Characteristic bands of FT-IR (cm <sup>-1</sup> ,KBr)					
	$\lambda$ max nm	C=O	C=C	C-Har	C-Hal	C=N	Others
8	215 342	1699	1471-1587	3080	2978	1618	$\nu$ N-H 3180
9	210 330	1697	1411-1518	3080	2926	1602	$\nu$ N-H 3228 $\nu$ O-H 3414
10	202 325	1740	1490-1560	3067	2899	1630	$\nu$ NO <sub>2</sub> 1355-1530
11	243 338	1718	1450-1555	3060	2945	1610	-

Table-4:UV and IR spectral data for compound (12-13)

Comp. No	UV Ethanol	Characteristic bands of FT-IR (cm <sup>-1</sup> ,KBr)					
	$\lambda$ max nm	C=O	C=C	C-Har	C-Hal	C=N	Others
12	220 344	1701 1633	1448-1556	3053	2860- 2926	1610	$\nu$ N-H 3269
13	237 315	1703	1490-1580	3080	2933- 2985	1606	$\nu$ N-H 3195 $\nu$ C=S 1320

## REFERENCES

1. Topno N.S, Kumaravel K, M. kannan, Vasuki G., and R. Krishna,(6-amino-3,4-dimethyl-4-phenyl-2H,4H-Pyrano[2,3]Pyrazole-5-carbonitrile), Acta. Cryst.Sect E, 67,1-10,( 2011).

2. Kostakis IK, Magiatis P, Pouli N, Marakos P, Skaltsounis AL, Pratsinis H, Léonce S, Pierré A,( synthesis, and antiproliferative activity of some new pyrazole-fused amino derivatives of the pyranoxanthenone, pyranothioxanthenone, and pyranoacridone ring systems: a new class of cytotoxic agents.), *J Med Chem.* ,45, (12):2599-6093,(2002).
3. EL-Tamany E.H, EL-Shahed F.A and Mohamed B.H, (Synthesis and biological activity of some pyrazole derivatives), *J. Serb. Chem. Soc.* , 64(1) 9-18 (1999)
4. F. M. Abdelrazek, P. Metz, O. Kataeva, A. Jäger, S. F. El-Mahrouky,( Synthesis and Molluscicidal Activity of New Chromene and Pyrano[2,3-c]pyrazole Derivative),*Arch. Pharm. Chem. Life Sci.* , 340, 543-548,(2007).
5. Alexandre F.R, Berecibal A, and Besson T, ( Microwave-assisted Niementowski reaction. Back to the roots),*Teta.Lett.* ,43,3911-3913 , (2002).
6. Karia, F.D.; Parsania, P.H. (Synthesis, biological and thermal properties of schiff bases of bisphenol-C). *Asian J. Chem.* ,1999, 11, 991-995.
7. Tarafder, M.T.; Kasbollah, A.; Saravan, N.; Crouse, K.A.; Ali, A.M.; Tin, O.K. S (methyldithiocarbamate and its schiff bases: Evaluation of bondings and biological properties). *J. Biochem. Mol. Biol. Biophys.* 2002, 6, 85-91.
8. Küçükgülzel, İ.; Küçükgülzel, Ş.G.; Rollas, S.; Ötük-Sarıış, G.; Özdemir, O.; Bayrak, İ.; Altuğ, T.; Stables, J.P. (3- (Arylalkylthio)-4-alkyl/aryl-5-(4-aminophenyl)-4H-1,2,4-triazole derivatives and their anticonvulsant activity. *Farmaco.*, 59, 893-901, (2004).
9. Vicini, P.; Geronikaki, A.; Incerti, M.; Busonera, B.; Poni, G.; Kabras, C.A.; Colla, P.L. (Synthesis and biological evaluation of benzo[d]isothiazole, benzothiazole and thiazole Schiff bases). *Bioorg. Med. Chem.*, 11, 4785-4789, (2003).
10. Kahveci, B.; Bekircan, O.; Karaoglu, SA. (Synthesis and antimicrobial activity of some 3-alkyl-4- (arylmethyleneamino)-4,5-dihydro-1H-1,2,4-triazol-5-ones). *Indian J. Chem.*, 44B, 2614- 2617, (2005).
11. Redha I,H,AL-Bayati, Foad .M, Saed and Wassan B,Ali, (Synthesis of New Pyrano Pyrazole Derivatives), *Al-Mustansiriya J.Sci*,22,(2011)
12. Bharat Parashar, Sudhir Bhardwaj, Shard Sharma, G.D.Gupta, V.K.Sharma andP.B. Punjabi, (Comparative Conventional and Microwave assisted synthesis of some pyrazoline derivatives and their antimicrobial activity), *J. Chem.Pharm. Res*, 2, 33-40,(2010).



## Synthesis of new pyrazole derivatives derived from 4-hydroxy coumarin and evaluation of their biological activity

Redha I. H. Al-Bayati<sup>1</sup>, Ammar A.R. Kubba<sup>2</sup> and Mahdi H. Radi<sup>3</sup>

<sup>1,3</sup>Dept. of Chemistry, College of Science, Al-Mustansiriyah University

<sup>2</sup>Dept. of Pharmaceutical Chemistry, College of Pharmacy, University of Baghdad,

E.mail: kubbaammar1963@gmail.com

Received 4/4/2012 – Accepted 20/6/2012

### الخلاصة

في هذا البحث، تم تحضير مشتقات جديدة للكومارين من 4-هيدروكسي كومارين كمادة اساس، باستعمال الاسيتيل كلورايد و البيريدين كوسط قاعدي، ولتكوين 3- اسيتيل-4-هيدروكسي كومارين 2. ان متابعة واتمام التفاعل الكيماوي قد تمت بتكوين قواعد شف-3-7، من خلال معاملة المركب 2 ومشتقات الهيدرازين بوجود المذيب الايثانول المطلق. ومن ثم تم غلق قواعد شف-3-7 بوجود قطرات من حامض الكبريتيك المركز، كعامل مساعد، ليعطي مشتقات البايرازول 8-12. ان المركبات المصنعة قد تم الكشف عنها والتعرف على تركيبها الكيماوي باستعمال التحليل الطيفي للأشعة تحت الحمراء والتحليل الدقيق للعناصر. وكذلك تم اختبار الفعالية البيولوجية لبعض منها كمضادات للبكتريا والفطريات. ان مركبات الكومارين والتي تحتوي على قواعد شف وحلقات البايرازول الغير متجانسة 3,4,5,7 و 9, 12 على التوالي، قد اظهرت فعالية مضادة وجيدة ضد البكتريا الموجبة غرام وكذلك فعالية معتدلة ضد البكتريا السلبية غرام ( الاشريكية القولونية- جرثومة الامعاء الغليظة). المركب 3 كان من اكثر المركبات فعالية ضد فطريات المهبل " كانديدا البيكانس". لقد اظهرت نتائج فحص مضادات المكروبات، ان المركب 12 كان من اكثر المركبات التي لها تأثير فعال جدا ومقاوم للبكتريا السلبية غرام -المسببة لالامراض- الزائفة الزنجارية (عصية القيقح الازرق).

### ABSTRACT

In this work new coumarin derivatives were synthesized, from 4-hydroxy coumarin as a starting material, by its reaction with acetyl chloride, using pyridine as a base to form 3-acetyl-4-hydroxy coumarin 2. Then the reaction was followed up by the formation of schiff bases 3-7, through the treatment of 2 and hydrazine derivatives in boiling absolute ethanol. Pyrazole derivatives 8-12 were finally synthesized by ring closure reaction of schiff bases in the presence of few drops of concentrated sulfuric acid as a catalyst. The newly synthesized compounds were confirmed by FT-IR-spectra and CHN-analysis, and they showed good agreement with the proposed structures. Also the biological activity of some of the test compounds were investigated *in vitro*, against some bacterial and fungal microorganisms.

Coumarin containing schiff bases and pyrazole derivatives: 3,4,5,7 and 9, 12 respectively, exhibited good antimicrobial activity against Gram (+) bacteria and a reasonable antibacterial activity against Gram (-) *E.coli*.

Compound 3 demonstrated the maximum antifungal activity against *C.albicans*.

Compound 12 was the most potent against the resistant pathogenic bacteria, *Pseudomonas aeruginosa*.

### INTRODUCTION

Coumarin derivatives possess a wide spectra of biological activities<sup>1-5</sup>, including anticoagulant, anti-inflammatory, antimicrobial and vasodilator, etc. Also, its well documented that heterocyclic rings like, pyrazol,



pyrazolin-5-ones, 4-thiazolidines and 1,3,4-oxadiazoles display pronounced antioxidant<sup>6-8</sup> and anti neoplastic activity<sup>9-12</sup>.

The pyrazole ring is prominent structural motif found in different pharmaceutically active compounds. This is due to ease preparation and the

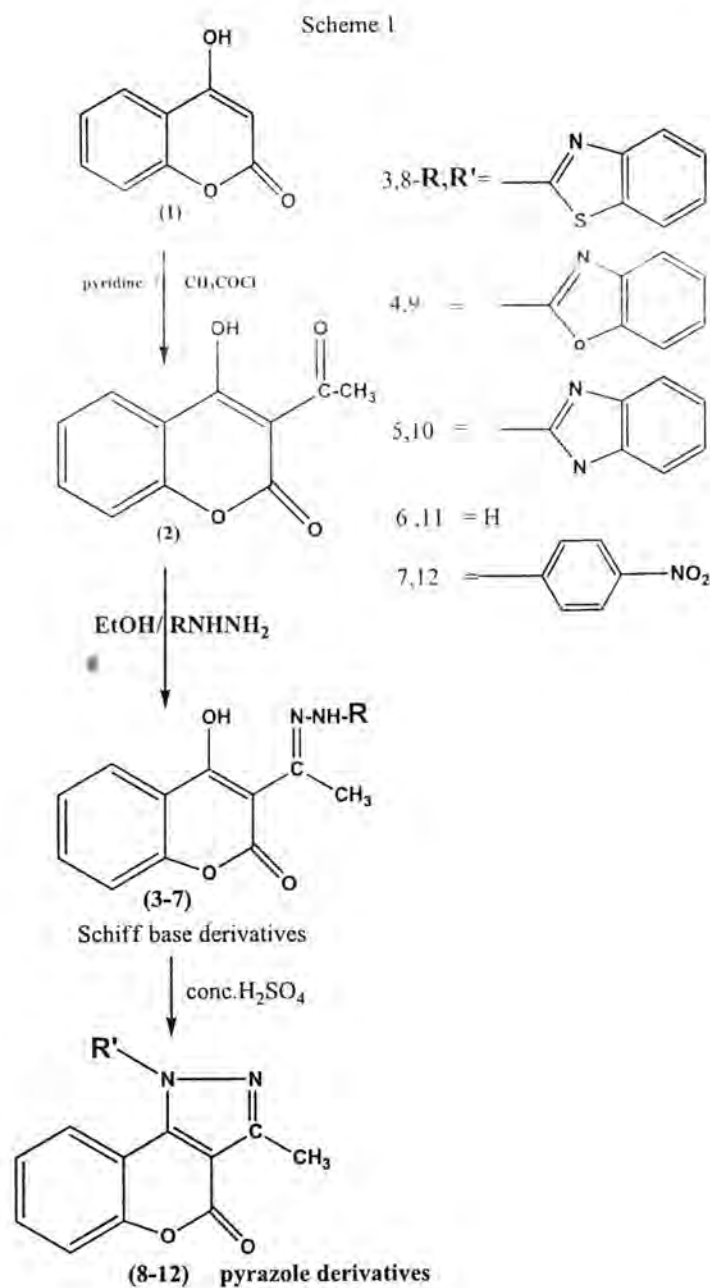
pyrazole based derivatives have been regarded as anxiolytic<sup>13</sup>, GABA receptor antagonists and insecticides<sup>14</sup>, anti-inflammatory and antimicrobial agents<sup>15</sup>, and growth inhibition activity<sup>16</sup>

In view this considerable importance of the coumarins and heterocycles mentioned above, the present work is aimed to design and synthesis of new heterocyclic pyrazole derivatives bearing coumarin nucleus, in order to have biologically more potent compounds.

Results and discussion:

The coumarin derivatives are important as biologically active compounds, and these compounds possess a wide range of biological and pharmaceutical activities.

For the synthesis of new coumarin derivatives, the following reaction sequences depicted in Scheme 1.



3-acetyl-4-hydroxy coumarin 2 was obtained by reaction of 4-hydroxy coumarin 1 with acetyl chloride in dry pyridine for 48h., in a good yield (table 2).

The chemical structure of compound 2 was confirmed from its spectral data.

In the I.R spectrum of compound 2, the lactone carbonyl stretching frequency( $C=O$ ), was observed at  $1732\text{ cm}^{-1}$ , and the appearance of

ketonic carbonyl stretching at position 3 of 4-hydroxy coumarin nucleus, at  $1674\text{ cm}^{-1}$

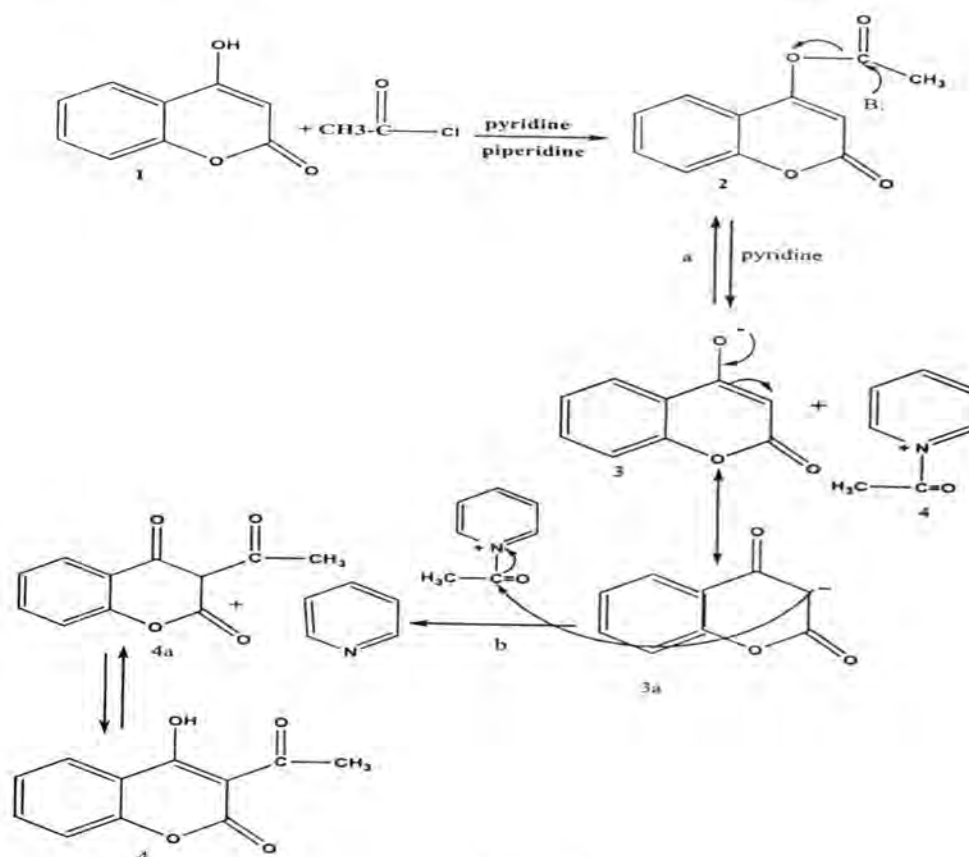
In addition to that, the consideration of the following bands:  $3087\text{ cm}^{-1}$ , represent the (C-H) aromatic stretching,  $2933\text{ cm}^{-1}$  aliphatic (C-H) stretching, and  $1610, 1545\text{ cm}^{-1}$  respectively, the (C=C) stretching.

It's worth mentioning, that the reaction between-4-hydroxy coumarin 1 and acetyl chloride, afforded 3-acetyl-4-hydroxy coumarin 2, (see scheme 2)<sup>17</sup>.

Acetyl chloride reacts irreversibly with 4-hydroxy coumarin I in the presence of pyridine and piperidine to yield 4-acetoxy coumarin 2.

A nucleophilic attack of pyridine on the ester group reversibly cleaves this compound to give the anion of 4-acetoxy coumarin 3, and the acetyl pyridinium cation 4.

This latter moiety further reacts with different resonance form of 4-hydroxy coumarin anion 3a to yield after enolization, 3-acetyl-4-hydroxy coumarin, (Scheme 2).



Scheme 2

Reaction of compound 2, (scheme 1) with hydrazine derivatives in boiling absolute ethanol, afforded the Schiff bases 3-7.

The I.R spectra of the above compounds, illustrate the disappearance of ketonic carbonyl in compound 2 (Scheme 1), and the appearance of the new absorptions at (1610-1602)  $\text{cm}^{-1}$  which indicate the presence of azomethan group ( $\text{C}=\text{N}$ ).

The NH-group is also displayed at 3439 -3150  $\text{cm}^{-1}$ . The I.R data of these compounds are shown in table 1.

Beside that, compounds 8-12, represent different pyrazole derivatives linked to coumarin nucleus, these derivatives were confirmed by the disappearance of NH-bands clearly, in compounds 8,9,10 and 12 respectively (table 1).

Moreover, elemental microanalysis showed good agreement with proposed chemical structures for compounds 3-7 and 8-12.

Table-1: I.R ( $\nu$ ,  $\text{cm}^{-1}$ ) spectral data for the synthesized compounds.

Compd No.	C=O	C-H aromatic	C-H aliphatic	C=C aromatic	C=N	others
2	1732	3087	2933	1610 1545	—	C=O, ketone 1674
3	1696	3071	2920 2872	1494	1610	NH-3439
4	1664	3063	2992 2880	1562 1544	1602	NH- 3150
5	1728	3069	2976 2926	1548 1510	1612	NH- 3157,3115
6	1695	3063	2924	1558 1460	1608	NH- 3286,3196
7	1676	3066	2980	1498	1602	NH-3271, NO <sub>2</sub> -1323
8	1710	3056	2956 2897	1545 1496	1610	—
9	1732	3072	2922 2852	1548 1496	1612	—
10	1732	3066	2926 2852	1543 1494	1610	—
11	1708	3043	2926 2882	1566 1533	1608	NH-3159
12	1741	3078	2928 2854	1514 1443	1556	NO <sub>2</sub> -1325

## MATERIALS AND METHODS

### General

All chemicals used in this work were supplied either by Sigma-Aldrich or Fluka and used without further purification. The FT-IR spectra were recorded in the (4000-400)  $\text{cm}^{-1}$  on KBr disk, using Shimadzu FT-IR-8300 spectrophotometer.



Elemental microanalysis for C,H,N were performed on PerkinElmer elemental analyzer.

Melting points were determined in open capillary tubes on a Gallenkamp M.F.B. 600.010F melting point apparatus, and are uncorrected.

**Synthesis of 3-acetyl-4-hydroxy coumarin (2):**

A solution of 4-hydroxy coumarin 1 (2.4 g, 0.015 mole) in dry pyridine (30) ml and few drops of piperidine was added, then cooled to 0 -5°C. The acetyl chloride (2g, 0.025mol) added drop wise addition, and the mixture stirred for 48h.

The dark -red reaction mixture was then poured into ice-water, and the mixture brought up to pH 1-2 using 2M HCl.

The precipitate was filtered, and washed out thoroughly with cold distilled water to give compound 2.

Physical properties of this compound are shown in table (2).

**Synthesis of schiff bases (3-7):**

**General procedure:**

A mixture of 3-acetyl-4-hydroxycoumarin 2, (0.0015) mole in absolute ethanol (25) ml, and hydrazine derivatives (0.0015) mole was added drop wise. The mixture was refluxed for 4h.

The mixture was cooled and the precipitate was collected by filtration.

The physiochemical properties of compounds (3-7) are shown in table 2.

**Synthesis of pyrazole derivatives (8-12):**

**General procedure:**

A suspension of schiff base (3-7), (0.0015) mole in glacial acetic acid (15) ml was treated with few drops of conc. H<sub>2</sub>SO<sub>4</sub>, and then heated for 2h. under reflux.

After cooling the mixture, was poured into ice-water, stirred until crystallization was complete, the precipitate was collected by filtration, washed with cold water and then dried.

Table- 2: physical properties of the new synthesized compounds

Compd. No.	m.p C°	yield%	Color	Recryst.solvent
2	132-134	82	dark yellow	Ethanol/water
3	140-142	80	orange	Ethanol/water
4	220-222	80	yellow	Ethanol/water
5	206-208	87	yellow	Ethanol/water
6	162-164	91	yellow	Ethanol/water
7	218-220	90	orange	Ethanol/water
8	124-126	50	yellow	Ethanol
9	108-110	58	red	Ethanol
10	135(dec.)	52	brown	Ethanol
11	228-230	79	yellow	Ethanol
12	165 (dec.)	80	yellow	Ethanol

#### Preliminary antimicrobial assay:

The antimicrobial activity of the new synthesized compounds ,schiff bases 3,4,5and 7, and pyrazole derivatives 9,12 was determined by using well-plate method.

The antimicrobial assay was carried out against 24h. cultures of representative *Gram (+) and Gram(-) bacteria* : *Staph aureus*, *Bacillus subtilis*, *Pseudomonas aeruginosa*, *Escherchia coli*, using agar media, The fungi used is *Candida albicans*.

The absolute ethanol was used as a solvent for the test compounds.

The minimum inhibitory concentrations (MIC values), of these newly synthesized compounds were also determined using two dilution concentrations 100mg/ml and 50mg/ml.

Ethanol was used as a control and the antibacterial activities were presented as a zone of inhibition for each test compound (see table 3).

Table-3:

Minimum inhibitory concentrations (MIC) of the new synthesized compounds.

Compd.	Bacteria	Conc.100mg/ml	Conc.50mg/ml	Control Abs.ethanol
3	<i>Staph aureus</i>	20	18	0
	<i>Bacillus subtilis</i>	23	20	0
	<i>Pseudomonas aeruginosa</i>	10	10	10
	<i>E.coli</i>	19	19	0
	<i>C.albicans</i>	35		0
4	<i>Staph aureus</i>	22	Not tested	0
	<i>Bacillus subtilis</i>	20		0
	<i>Pseudomonas aeruginosa</i>	15		12
	<i>E.coli</i>	25		0
	<i>C.albicans</i>	37		12
5	<i>Staph aureus</i>	18	Not tested	10
	<i>Bacillus subtilis</i>	18		0
	<i>Pseudomonas aeruginosa</i>	15		10
	<i>E.coli</i>	20		10
	<i>C.albicans</i>	42		10
7	<i>Staph aureus</i>	30	Not tested	0
	<i>Bacillus subtilis</i>	22		0
	<i>Pseudomonas aeruginosa</i>	21		15
	<i>E.coli</i>	22		0
	<i>C.albicans</i>	28		10
9	<i>Staph aureus</i>	20	Not tested	0
	<i>Bacillus subtilis</i>	20		0
	<i>Pseudomonas aeruginosa</i>	0		10
	<i>E.coli</i>	10		0
	<i>C.albicans</i>	35		10
12	<i>Staph aureus</i>		20	0
	<i>Bacillus subtilis</i>		40	0
	<i>Pseudomonas aeruginosa</i>		23	0
	<i>E.coli</i>		11	0
	<i>C.albicans</i>		32	10

### Acknowledgments

The anti microbial activity was kindly done by Dr. Rehab S. Ramadan and lect.assist., Rana K.Naem, university of Al-Nahrain-college of science-department of Biotechnology ,they are gratefully appreciated for their assistance.

### REFERENCES

1. C. A. Kontogiorgis and D. J. Hadjipavlou-Litina, Synthesis and biological evaluation of novel coumarin derivatives with a 7-azomethine linkage, *Bioorg. Med. Chem. Lett.*, 14, 611–614 (2004).
2. M. Ghate, D. Manohar, V. Kulkarni, R. Shobha and S. Y. Kattimani, Synthesis of vanillin ethers from 4-(bromomethyl) coumarins as anti-inflammatory agents, *Eur. J. Med. Chem.*, 38, 297–302 (2003)
3. D. N. Nicolaides, K. C. Fylaktakidou, K. E. Litinas and D. Hadjipavlou-Litina, Synthesis and biological evaluation of several coumarin-4-carboxamidoxime and 3-(coumarin-4-yl)-1,2,4-oxadiazole derivatives, *Eur. J. Med. Chem.*, 33, 715–724 (1998).
4. Christos A. Kontogiorgis and Dimitra J. Hadjipavlou-Litina, Synthesis and anti-inflammatory activity of coumarin derivatives, *J. Med. Chem.*, 48 (20), 6400–6408 (2005)
5. Kayser O, Kobodziei H., Antibacterial activity of some coumarins: structural requirements for biological activity, *Planta Med.*, 63(6), 508-510 (1997)
6. T. S. Jeong, K. S. Kim, J. R. Kim, K. H. Cho, S. Lee and W. S. Lee, Novel 3,5-diaryl pyrazolines and pyrazole as low-density lipoprotein (LDL) oxidation inhibitors, *Bioorg. Med. Chem. Lett.*, 14, 2719–2723 (2004)
7. T. Saibara, K. Toda, A. Wakatsuki, Y. Ogawa, M. Ono and S. Onishi, Protective effect of 3-methyl-1-phenyl-2-pyrazolin-5-one, a free radical scavenger, on acute toxicity of paraquat in mice, *Toxicol. Lett.*, 143, 51–54 (2003)
8. M. H. Shih and F. Y. Ke, Synthesis and evaluation of antioxidant activity of sydnonyl substituted thiazolidinone and thiazoline derivatives, *Bioorg. Med. Chem.*, 12, 4633–4643 (2004)
9. R. Lin, G. Chiu, Y. Yu, P. J. Connolly, S. Li, Y. Lu, M. Adams, A. R. Fuentes-Pesquera, S. L. Emanuel and L. M. Greenberger, Design, synthesis, and evaluation of 3,4-disubstituted pyrazole analogues as anti-tumor CDK inhibitors, *Bioorg. Med. Chem. Lett.*, 17, 4557–4561 (2007)
10. Y. Kakiuchi, N. Sasaki, M. Satoh-Masuoka, H. Murofushi and K. Murakami-Murofushi, A novel pyrazolone, 4,4-dichloro-1-(2,4-dichlorophenyl)-3-methyl-5-pyrazolone, as a potent catalytic inhibitor of human telomerase, *Biochem. Biophys. Res. Commun.*, 320, 1351–1358 (2004)



11. V. P. M. Rahman, S. Mukhtar, W. H. Ansari and G. Lemiere, Synthesis, stereochemistry and biological activity of some novel long alkyl chain substituted thiazolidin-4-ones and thiazan-4-one from 10-undecenoic acid hydrazide, *Eur. J. Med. Chem.*, 40, 173–184
12. S. Rollas, N. Gulerman and H. Erdeniz, Synthesis and antimicrobial activity of some new hydrazones of 4-fluorobenzoic acid hydrazide and 3-acetyl-2,5-disubstituted-1,3,4-oxadiazolines, *Farmaco.*, 2002, 57, 171–174 ((2005).
13. Geronikaki, A.; Babaev, E.; Dearden, J.; Dehaen, W.; Filimonov, D.; Galaeva, I.; Krajneva, V.; Lagunin, A.; Macaev, F.; Molodavkin, G.; Poroikov, V.; Pogrebnoi, S.; Saloutin, V.; Stepanchikova, A.; Stingaci, E.; Tkach, N.; Vladg, L.; Voronina, T. Design, synthesis, computational and biological evaluation of new anxiolytics. *Bioorg. Med. Chem.*, 12, 6559–6568 (2004)
14. Sammelson, R.E.; Caboni, P.; Durkin, K.A.; Casida J.E. GABA receptor antagonists and insecticides: common structural features of 4-alkyl-1-phenylpyrazoles and 4-alkyl-1-phenyltrioxabicyclooctanes. *Bioorg. Med. Chem.*, 12, 3345–3355(2004).
15. Bekhit, A.; Abdel-Aziem, T. Design, synthesis and biological evaluation of some pyrazole derivatives as anti-inflammatory-antimicrobial agents. *Bioorg. Med. Chem.*, 12, 1935–1945 (2004).
16. Debeljak, Z.; Škrbo, A.; Jasprica, I.; Mornar, A.; Plečko, V.; Banjanac, M.; Medić-Sarić, M. QSAR study of antimicrobial activity of some 3-nitrocoumarins and related compound. *J. Chem. Inf. Model.*, 47, 918–926(2007).
17. Hugh R. Eisenauer and Karl P. Link, Studies on 4-hydroxycoumarins. XIII. The mechanism for the reaction of 4-hydroxycoumarin with aliphatic acid chlorides, *J. Am. Chem. Soc.*, 75 (9), 2046–2049(1953)

### Preparation Of New 2-Imino-hexahydro-1,3-Thiazepine Derivatives

Hamed Jassim Jaffar and Ahmed Qassim Abdul-Hussein

Al-Mustansiriya University / College of Science / Department of Chemistry

Received 5/4/2012 – Accepted 20/6/2012

## الخلاصة

حضرت مشتقات جديدة لـ 2-imino-hexahydro-1,3-thiazepine من تكاتف مشتقات الثايورييا مع 4,4-ثنائي يروموبوتان لتكوين الحلقة السباعية بوجود هيدريد الصوديوم . واستخدمت هاليدات الحوامض الكربوكسيلية والامينات الاولية كمواد اولية مناسبة لتحضير (33) مشتق الثايورييا . وتم تشخيص المركبات المحضرة باستخدام الطرق الطيفية مثل ( $^1\text{H-NMR}$ , FTIR).

## ABSTRACT

A new 2-imino-hexahydro-1,3-thiazepine derivatives were synthesized from cyclo condensation of thiourea derivatives with 1,4- dibromobutane in presence of NaH as reducing agent . Acid chlorides were used with primary amine as convenient starting materials for synthesis of (33) thiourea derivatives . The synthesized compounds were characterized by different spectroscopic methods (FTIR, <sup>1</sup>H-NMR).

**Key words :** 1,3-thiazepines , thiourea derivatives , primary amine , sodium hydride , acid chlorides

## INTRODUCTION

Heterocyclic compounds include many biochemical material essential to life such as nucleic acid , and many of them are naturally occurring pigments , vitamins , and antibiotics. However , synthetic heterocyclic compounds are widely use as medicaments , pesticides , and plastics[1] . Thiazepines are heterocyclic compounds possessing N and S atoms in it is seven member ring. The different types of this class brought a considerable interst because of their biological activity as inhibitors of HIV-1 integrate , antitumor , antibiotics , enzyme inhibitors , muscle relaxants , sedatives and hypnotics[2-4]. The 1,3-thiazepine derivatives are of considerable interest due to their biological activity[5-8]. A novel pyrrolo[2,1-b][1,3]benzo thiazepines have been prepared and they demonstrate activity as anti-psychotic agents with serotonin and dopamine antagonist properties[9]. The 1,3-thiazepine ring system is present in omapatrilat drug , which it is in the late stage of approval . It inhibits the activity of angiotensin converting enzyme (ACE) , that causes blood vessels to constrict , leading to lower blood pressure. The drug inhibits the enzyme known as neutral endopeptidase(NEP),causes the relaxation of blood vessels[10,11]. Thiazepine derivatives of different types [(1,3),(1,4) and (1,5)] were prepared by various methods .Such as the preparation of methylene-bis-

benzofurano[1,5]benzothiazepine[12], and 3-(2-substitutedphenyl)-4-(3-pyridine)-2,3-dihydro-[1,5]benzothiazepine[13].

The preparation of [1,4] type derivatives are widely reported[14-16], such as the preparation of some novel pyrido[3,2-f][1,4]thiazepines[17] and pyrazolo[3,4-e][1,4]thiazepine[18]. The 1,3-thiazepine ring system have constructed by various synthetic routes[19,20]. An excellent yield of ethyl- 2-amino-7-methyl-4-oxo-4,5,6,7-tetrahydro-1,3-thiazepine-5-carboxylate was prepared from the cyclocondensation of thiourea derivative that, derived from the reaction of diethylallylmalonate with thiourea. Also the preparation of 2-amino derivatives of 7-methyl-4-oxo-4,5,6,7-tetrahydro-1,3-thiazepine-5-carboxylic acid ester from the cyclocondensation of 1-alkyl-3-pent-4-enoyl-thiourea with bromine. The thiourea derivatives may be obtained from the reaction of 4-amino-butanol with isothiocyanate. In acidic solution resulted in formation of 4-substituted (methyl, benzyl and propyl) imino-4,5,6,7-tetrahydro-1,3-thiazepine[8,9]. The reaction of 4-bromobutyl isothiocyanate with aromatic amines may be regarded as a general method for preparation of 2-arylimino-1,3-thiazepine derivatives[21]. The 1,3-thiazepine ring system could be formed from the condensation of thiourea derivatives with 1,4-dibromobutane. Tricycloderivatives of 1,3-thiazepine were obtained by this route[20].

### MATERIALS AND METHODS

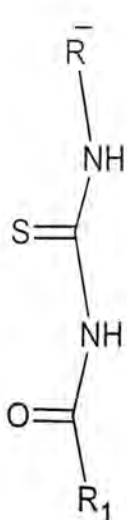
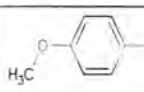
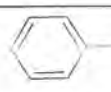
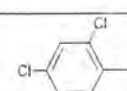
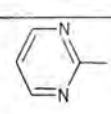

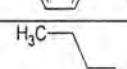
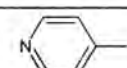
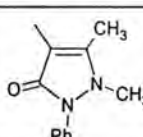
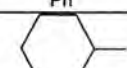
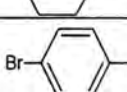
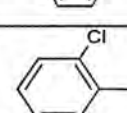
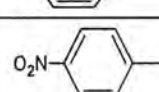
Acid chlorides, sodium hydride, potassium thiocyanate and primary amines were purchased from Sigma-Aldrichs. Silica gel were supplied by merck company. Melting points were determined at SMP30 type melting point apparatus (Stuart, Germany) and are uncorrected. FTIR (KBr disc) spectra were recorded on a shimadzu FTIR 8400S spectrophotometer between 4000-400 $\text{cm}^{-1}$ .  $^1\text{H-NMR}$  spectra were recorded on a Bruker DMX500 NMR spectrometer operating at 400MHz at Al-alby university, Jordon. The chemical shift values are expressed in ppm relative to TMS as an internal standard. TLC plates was used for analysis, and they made from silica gel F<sub>254</sub>, 0.25thickness coated on aluminum sheets (20cm $\times$ 20cm).

#### **General method for the preparation of thiourea derivatives (T<sub>1</sub>-T<sub>33</sub>)[22]**

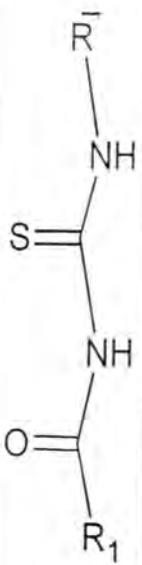


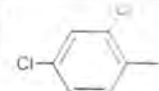
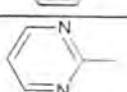
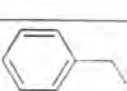
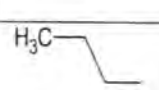
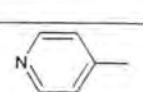
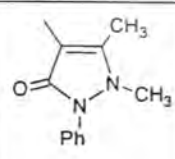

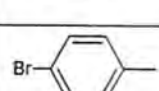
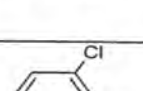
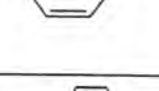
The acid chloride (0.025mol) was dissolved in acetone (20ml) and added gradually with continuous stirring to a solution of potassium thiocyanate (0.025mol) in acetone (20ml). The reactants were heated by reflux for half an hour with stirring. A solution of primary amine (0.025mol) in acetone (20ml) was added gradually at room temperature. The reactants were left to stir at room temperature for two hours. The product was acidify with HCl (100ml, 0.1N), and the resulted precipitate was filtered, off washed with distilled water. The precipitate was

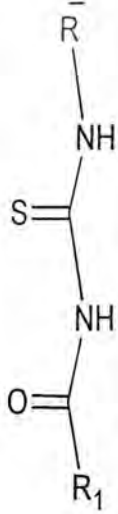
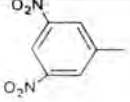
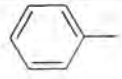
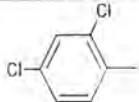
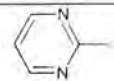
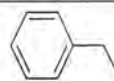
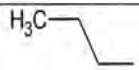
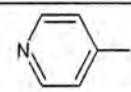
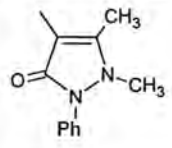

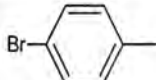
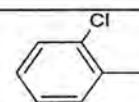
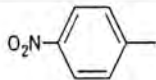
crystallized from mixture of chloroform-ethanol (2:1). The physical properties of the prepared compounds are in table (1).

Table-1: Physical properties of the prepared thiourea derivatives.

Comp No.	Compounds structure	R <sub>1</sub>	R'	melting point C°	color	product (%)
T <sub>1</sub>				120-121	White	75
T <sub>2</sub>		=		165-166	Gray	62.5
T <sub>3</sub>		=		183-185	Yellow	61
T <sub>4</sub>		=		122-123	Yellow	73
T <sub>5</sub>		=		72-73	Light Yellow	70
T <sub>6</sub>		=		155-156	White	87.5
T <sub>7</sub>		=		174-176	Light Yellow	69.4
T <sub>8</sub>		=		95-97	Yellow	61.5
T <sub>9</sub>		=		193-194	White	97.3
T <sub>10</sub>		=		163-164	White	77.6
T <sub>11</sub>		=		181-182	Yellow	83.7



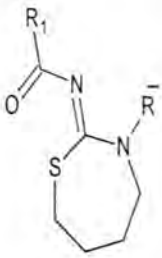
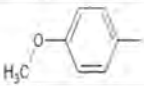
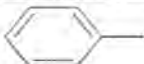
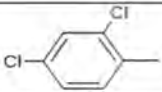
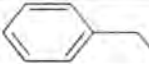


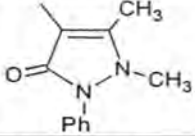

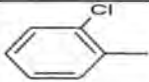
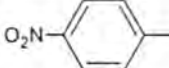
Comp No.	Compounds structure	R <sub>1</sub>	R'	Melting point C°	Color	product (%)
T <sub>12</sub>				131-132	Light green	79
T <sub>13</sub>		=		175-176	Gray	86.9
T <sub>14</sub>		=		201-203	Yellow	64.8
T <sub>15</sub>		=		94-96	Dark yellow	65.2
T <sub>16</sub>		=		167-169	Light Yellow	68.7
T <sub>17</sub>		=		154-156	Yellow	81
T <sub>18</sub>		=		110-112	Yellow	94
T <sub>19</sub>		=		135-137	Dark yellow	60.8
T <sub>20</sub>		=		174-175	Light Yellow	98
T <sub>21</sub>		=		166-168	White	92.5
T <sub>22</sub>		=		191-193	Yellow	95.3

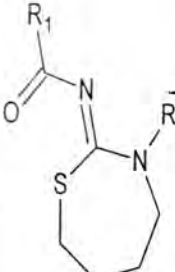

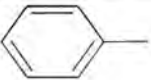
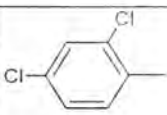
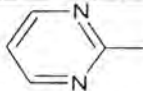

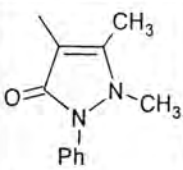

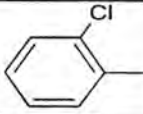
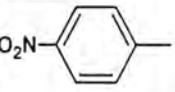
Comp No.	Compounds structure	R <sub>1</sub>	R'	Melting pointC°	color	product (%)
T <sub>21</sub>				144-146	green	75
T <sub>22</sub>		=		196-198	Light Yellow	60
T <sub>23</sub>		=		163-165	Light Yellow	93.4
T <sub>26</sub>		=		166-167	Light Yellow	94.8
T <sub>27</sub>		=		151-152	Yellow	87.5
T <sub>28</sub>		=		202-203	white	91.6
T <sub>29</sub>		=		230-232	white	63
T <sub>30</sub>		=		110-111	Nutty	65.2
T <sub>31</sub>		=		111-113	white	72
T <sub>32</sub>		=		199-201	Yellow	67.3
T <sub>33</sub>		=		140-142	Yellow	78

### General methods for the preparation of thiazepine (Z<sub>1</sub>-Z<sub>26</sub>)[23]

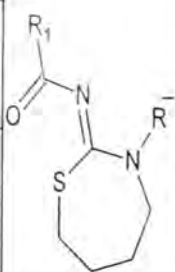
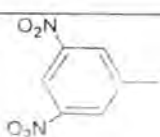

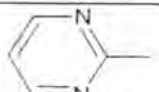
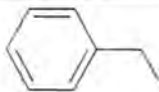
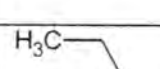
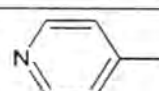
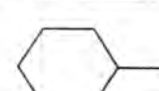

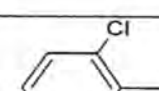
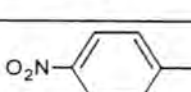
Sodium hydride NaH dispersion (60%) in mineral oil (supplied by aldrich) ,(0.003mol) was added to a solution of thiourea derivatives (T<sub>1</sub>-

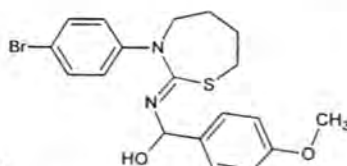
T<sub>33</sub>) (0.003mol) in anhydrous DMF (30ml) with a contineons stirring at room temperature. At the end of hydrogen liberation untile hydrogen bobbles was cessed , the 1,4-dibromobutane (0.0045mol) was added during a 15 minutes. The reactants were left to stir for 6 hours at room temperature. The solvent (DMF) was evaporated under reduced pressure to gave a crude solid product which was purified by crystallization from tetrahydro furan. Physical properties of the prepared compounds in table (2)

Comp No.	Compounds structure	R <sub>1</sub>	R <sup>+</sup>	Meltig pointC°	color	product (%)
Z <sub>1</sub>				143-145	Yellow	56.3
Z <sub>2</sub>		=		227-229	white	43
Z <sub>3</sub>		=		154-156	white	55
Z <sub>4</sub>		=		148-150	Yellow	48.2
Z <sub>5</sub>		=		213-213.5	white	59.3
Z <sub>6</sub>		=		203-205	Light Yellow	51.9
Z <sub>7</sub>		=		170-172	Yellow	61.4
Z <sub>8</sub>		=		195-196	white	46.5
Z <sub>9</sub>		=		186-187	Dark yellow	51.7

Comp No.	Compounds structure	R <sub>1</sub>	R'	Melting pointC°	color	product (%)
Z <sub>10</sub>				75-76	Yellow	52.5
Z <sub>11</sub>		=		232-234	white	60.8
Z <sub>12</sub>		=		91-93	Orange	45
Z <sub>13</sub>		=		175-177	Light Yellow	59
Z <sub>14</sub>		=		211-213	Yellow	53
Z <sub>15</sub>		=		173-174	white	62
Z <sub>16</sub>		=		83-84	Yellow	58.6
Z <sub>17</sub>		=		140-142	Yellow	53.4



Comp No.	Compounds structure	R <sub>1</sub>	R'	Meltig pointC°	color	(%) product
Z <sub>18</sub>				150-152	Light Yellow	47.6
Z <sub>19</sub>		=		133-134	Orange	60.8
Z <sub>20</sub>		=		128-129	Yellow	55.6
Z <sub>21</sub>		=		165-166	Light Yellow	54.1
Z <sub>22</sub>		=		152-154	Light nutty	60
Z <sub>23</sub>		=		103-104	Light nutty	48
Z <sub>24</sub>		=		145-146	Nutty	50.7
Z <sub>25</sub>		=		122-123	Yellow	46.4
Z <sub>26</sub>		=		153-155	Orange	56.6



#### Preparation of thiazepine (Z<sub>27</sub>)

Sodium hydride NaH dispersion (60%) in mineral oil (0.009mol) (3folds excess) was added to the solution of thiourea (0.003mol) in anhydrous DMF (30ml), (dried by sodium sulphate) with continuous stirring at room temperature. After liberation of hydrogen, the 1,4-

dibromobutane (0.0045mol) was added gradually with stirring through 15 min. The reactants were left to stir overnight. The solvent (DMF) was removed under reduced pressure and the resulted yellow solid was crystallized from chloroform. The physical properties of the product is in table (3).

Table-3: physical properties of thiazepine ( $Z_{27}$ ).

R.F	Melting point C°	color	Product (%)
0.81	298-300	Light Yellow	62

#### Preparation of thiazepine ( $Z_7$ )

Calcium hydride  $CaH_2$  (added to the proper amount of mineral oil) (0.009mol) (3folds excess) was added to the solution of thiourea (0.003mol) in anhydrous DMF (dried by sodium sulphate) , (30ml) with continuous stirring at room temperature. After liberation of hydrogen the 1,4-dibromobutane (0.0045mol) was added gradually with stirring through 15 min. The reactants were left to stir overnight. The solvent (DMF) was removed under reduced pressure and the resulted yellow solid was crystallized from tetrahydrofuran. The physical properties of the product is in indential to these in table (2)

#### Preparation of thiazepine ( $Z_{22}$ )

The above compound was prepared using the same general procedure for preparation of thiazepines except that the reaction mixture, resulted from the addition of 1,4-dibromobutane to the reduced thiourea, was heated by reflux for two hours. After removal of the solvent and crystallization of the resulted residue. The yield of the product increased to 67.5% .

#### Antimicrobial activity test

The well-diffusion agar technique[12] was followed to measure the antimicrobial activity of same prepared thiazepines on three types of bacteria , *Staphylococcus aureus* , *Pseudomonas aeruginosa* , and *Escherichia coli*. The cefotaxime was used as a standard antibiotic. The solvent used for the tested compounds and the standard was DMF. The inhibition zone was measured in mm for four concentrations in ppm (5000,10000,20000 and 30000). The result are in table (4).

Table 4: Antimicrobial activity of some 1,3-thiazepines derivatives.

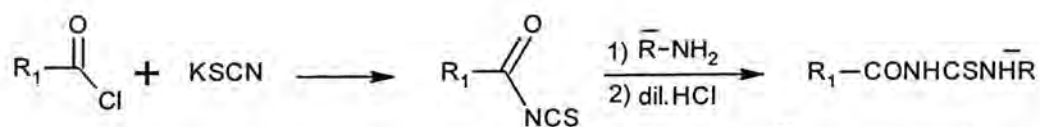
## RESULTS AND DISCUSSION

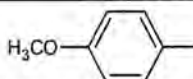

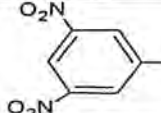
In this work we have prepared (33) new thioureas starting from the acid chloride of aromatic carboxylic acids. The aromatic rings of the acids

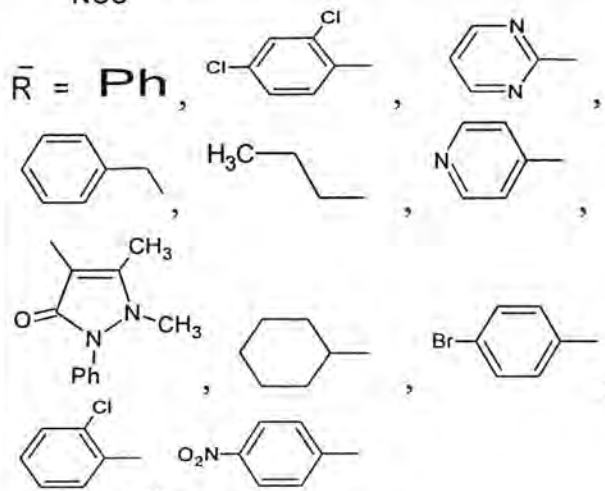
Zone of Inhibition												
Comp. No.	E.Coli				S.aureus				Pseudo. aeruginosa			
	30000 ppm	20000 ppm	10000 ppm	5000 ppm	30000 ppm	20000 ppm	10000 ppm	5000 ppm	30000 ppm	20000 ppm	10000 ppm	5000 ppm
Z <sub>1</sub>	0.9	0.8	0.6	0.6	—	—	—	—	1.45	1.15	1.1	1.1
Z <sub>4</sub>	0.55	0.6	0.8	0.8	—	—	—	—	0.9	1	1	1
Z <sub>12</sub>	0.9	0.9	0.9	1	0.95	0.75	0.65	—	0.95	1.4	1.4	1.45
Z <sub>16</sub>	0.7	0.7	0.7	0.9	—	—	—	—	1.4	1.1	1.6	1.5
Z <sub>22</sub>	0.75	0.9	0.75	0.8	1.45	1.4	1.25	1	0.8	0.59	1.05	1.25
Z <sub>23</sub>	0.8	1.1	0.9	0.9	1.6	1.5	1.4	0.95	1.2	1.55	1.1	1.55
Cefotaxime	1.9	1.7	1.65	0.9	3.25	3.25	2.75	2.65	3.3	3.3	3	2.55

one substituted with 4-methoxy, 4-chloro and 3,5-dinitro groups. The nucleophilic substitution reaction of potassium thiocyanate on the acid chloride gave isothiocyanate derivatives which was elaborated to thioureas by a nucleophilic reaction with different primary amines[22]. The primary amines used in this work are aliphatic and aromatic amines.

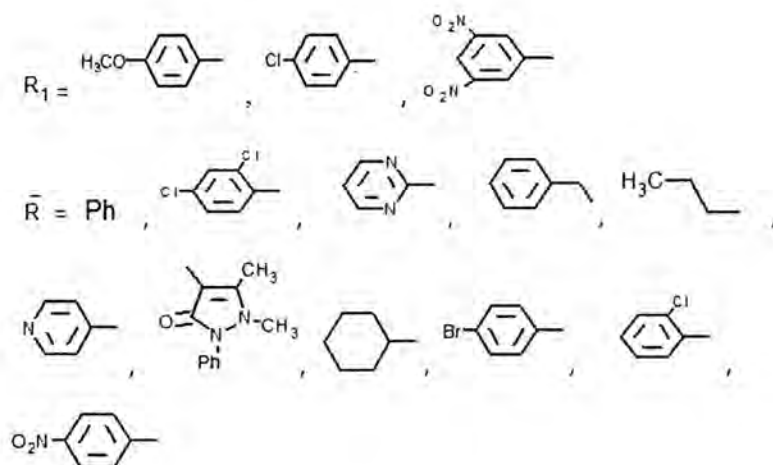
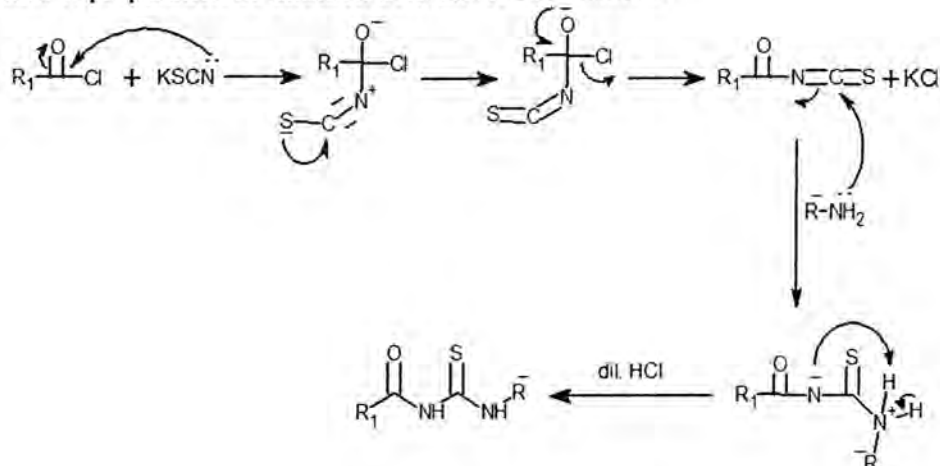
The reaction is summerised in schem (1).



Comp.No.	R <sub>1</sub>
T <sub>11</sub> -T <sub>11</sub>	
T <sub>12</sub> -T <sub>22</sub>	
T <sub>23</sub> -T <sub>33</sub>	



Scheme 1: preparation of thiourea derivatives Mechanisim

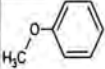
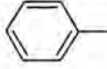
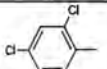
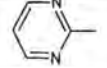
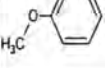
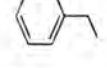
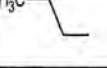
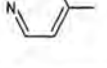
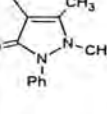
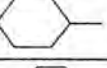
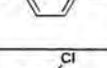



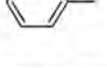
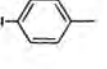
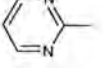
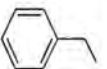


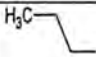
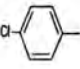
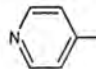
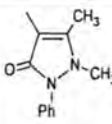
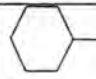
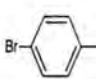
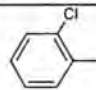
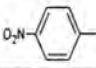
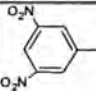
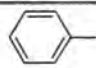
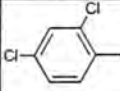
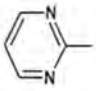

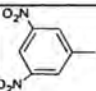
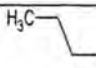


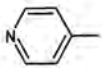
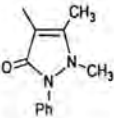

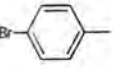
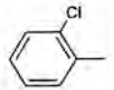
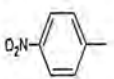
The structure of thiourea derivatives were characterized by using FTIR and  $^1\text{H-NMR}$ [24,25]. The characteristic bands observed in infrared spectra of these derivatives are the stretching vibration of carbonyl group of the amides ( $\text{C=O}$ ) which was noted at ( $1631\text{-}1710\text{cm}^{-1}$ ) and the band for stretching vibration of ( $\text{N-H}$ ) at ( $3101\text{-}3410\text{cm}^{-1}$ ). In some of the prepared derivative ( $\text{T}_1\text{-T}_{33}$ ) the two ( $\text{N-H}$ ) bands were strongly overlapped and appeared approtimatley at the same region. This may be due to the equivalent effects of the substituents on two nitrogen atoms. The carbon sulfur double bond stretching vibration ( $\text{C=S}$ ) appeared in the region ( $1122\text{-}1230\text{cm}^{-1}$ ).

The values of important and characteristic absorp bands of each prepared compounds are listed in table (5).

Table-5: characteristic bands in IR spectra of thiourea derivative

Comp No.	R <sub>1</sub>	R'	$\nu(\text{C=O})$ $\text{cm}^{-1}$	$\nu(\text{N-H})$ $\text{cm}^{-1}$	$\nu(\text{C=S})$ $\text{cm}^{-1}$	$\nu(\text{C=C})\text{Ar}$ $\text{cm}^{-1}$	$\nu(\text{C-H})\text{Ar}$ $\text{cm}^{-1}$	$\nu(\text{C-H})\text{Alph}$ $\text{cm}^{-1}$	$\nu(\text{Others})$ $\text{cm}^{-1}$
T <sub>1</sub>			1662	3292	1149	1599, 1498	3014	2976	—
T <sub>2</sub>	=		1666	3244	1161	1589, 1537	3084	2987, 2839	$\nu(\text{C-Cl})$ 686
T <sub>3</sub>	=		1710	3167	1168	1577, 1506	3095	2968, 2843	$\nu(\text{C=N})$ 1599
T <sub>4</sub>			1664	3410, 3192	1166	1600, 1496	3059	2933, 2839	—
T <sub>5</sub>	=		1654	3340	1182	1606, 1514	3047	2966, 2841	—
T <sub>6</sub>	=		1666	3277	1174	1600, 1500	3047	2947, 2847	$\nu(\text{C=N})$ 1600
T <sub>7</sub>	=		1664	3363	1157	1539, 1500	3028	2916, 2806	$\nu(\text{C=O})$ 1664
T <sub>8</sub>	=		1647	3248	1153	1602, 1454	3030	2852	—
T <sub>9</sub>	=		1664	3377	1174	1593, 1496	3020	2976, 2839	$\nu(\text{C-Br})$ 599
T <sub>10</sub>	=		1674	3267	1172	1608, 1471	3005	2962, 2833	$\nu(\text{C-Cl})$ 720
T <sub>11</sub>	=		1666	3298	1174	1606, 1498	3076	2970, 2839	$\nu(\text{C-NO}_2)$ 1572, 1329
T <sub>12</sub>			1662	3269	1149	1600, 1485	3036	—	$\nu(\text{C-Cl})$ 717
T <sub>13</sub>	=		1674	3300	1149	1585, 1487	3095	—	$\nu(\text{C-Cl})$ 725
T <sub>14</sub>	=		1712	3174	1165	1570, 1489	3000	—	748 $\nu(\text{C-Cl})$ $\nu(\text{C=N})$ 1590
T <sub>15</sub>	=		1639	3313	1155	1597, 1485	3080	2931, 2806	$\nu(\text{C-Cl})$ 711

T <sub>16</sub>	=		1660	3369	1178	1574, 1487	3078	2775	$\nu(\text{C-Cl})$ 725
T <sub>17</sub>			1674	3333, 3261	1122	1554, 1487	3036	—	$\nu(\text{C-Cl})$ 750 $\nu(\text{C=N})$ 1587
T <sub>18</sub>	=		1654	3311, 3147	1178	1550, 1496	3088	2939	$\nu(\text{C-Cl})$ 700 $\nu(\text{C=O})$ 1642
T <sub>19</sub>	=		1654	3169	1159	1597, 1446	3020	2933, 2854	$\nu(\text{C-Cl})$ 680
T <sub>20</sub>	=		1660	3338	1143	1599, 1483	3001	—	$\nu(\text{C-Cl})$ 752 $\nu(\text{C-Br})$ 648
T <sub>21</sub>	=		1678	3273, 3113	1159	1585, 1475	3032	—	$\nu(\text{C-Cl})$ 727
T <sub>22</sub>	=		1683	3286, 3115	1155	1597, 1514	3020	—	$\nu(\text{C-Cl})$ 758 $\nu(\text{C-NO}_2)$ 1550, 1323
T <sub>23</sub>			1660	3207	1209	1595, 1458	3014	—	$\nu(\text{C-NO}_2)$ 1535, 1342
T <sub>24</sub>	=		1640	3291	1180	1597, 1471	3001	—	$\nu(\text{C-NO}_2)$ 1543, 1350 $\nu(\text{C-Cl})$ 727
T <sub>25</sub>	=		1685	3335	1230	1575, 1460	3099	—	$\nu(\text{C-NO}_2)$ 1541, 1348 $\nu(\text{C=N})$ 1622
T <sub>26</sub>	=		1653	3271	1219	1537, 1458	3099	2968, 2881	$\nu(\text{C-NO}_2)$ 1537, 1348
T <sub>27</sub>			1705	3101	1195	1552, 1464	3076	2958, 2816	$\nu(\text{C-NO}_2)$ 1539, 1350

T <sub>28</sub>	=		1676	3331	3331	1539, 1450	3095	—	$\nu(\text{C-NO}_2)$ 1539,1348 $\nu(\text{C=N})$ 1624
T <sub>29</sub>	=		1675	3295	1190	1523, 1446	3028	2868	$\nu(\text{C-NO}_2)$ 1523,1346 $\nu(\text{C=O})$ 1647
T <sub>30</sub>	=		1633	3107	1186	1610, 1454	3000	2864, 2750	$\nu(\text{C-NO}_2)$ 1537,1342
T <sub>31</sub>	=		1705	3101	1184	1543, 1483	3059	—	$\nu(\text{C-NO}_2)$ 1543,1342 $\nu(\text{C-Br})$ 638
T <sub>32</sub>	=		1705	3191	1178	1545, 1469	3005	—	$\nu(\text{C-NO}_2)$ 1545,1348 $\nu(\text{C-Cl})$ 725
T <sub>33</sub>	=		1631	3362, 3219	1180	1593, 1475	3078	—	$\nu(\text{C-NO}_2)$ 1493,1300

The <sup>1</sup>H-NMR of some prepared thiourea derivatives (T<sub>2</sub>, T<sub>9</sub>, T<sub>14</sub>, T<sub>20</sub>, T<sub>25</sub>, T<sub>27</sub>) are recorded:

For compound T<sub>2</sub>:  $\delta$  3.3ppm(3H,s, OCH<sub>3</sub>),  $\delta$  7.3-8.8ppm(7H,m,aromatics),  $\delta$  12.1ppm(1H,s,R<sub>2</sub>-NH),  $\delta$  13.5ppm(1H,s,R<sub>1</sub>CONH).

The compound T<sub>9</sub>:  $\delta$  3.85ppm(3H,s, OCH<sub>3</sub>),  $\delta$  7-8ppm(8H,m,aromatics),  $\delta$  11.4ppm(1H,s, R<sub>2</sub>-NH),  $\delta$  12.6ppm(1H,s, R<sub>1</sub>CONH).

The compound T<sub>14</sub>:  $\delta$  7.2-8.7ppm(7H,m, aromatics),  $\delta$  11.8ppm(1H,s, R<sub>2</sub>NH),  $\delta$  13.1ppm(1H,s, R<sub>1</sub>CONH).

The compound T<sub>20</sub>:  $\delta$  7.6-7.9ppm(8H,m, aromatics),  $\delta$  11.7ppm(1H,s,R<sub>2</sub>NH),  $\delta$  12.4ppm(1H,s, R<sub>2</sub>CONH).

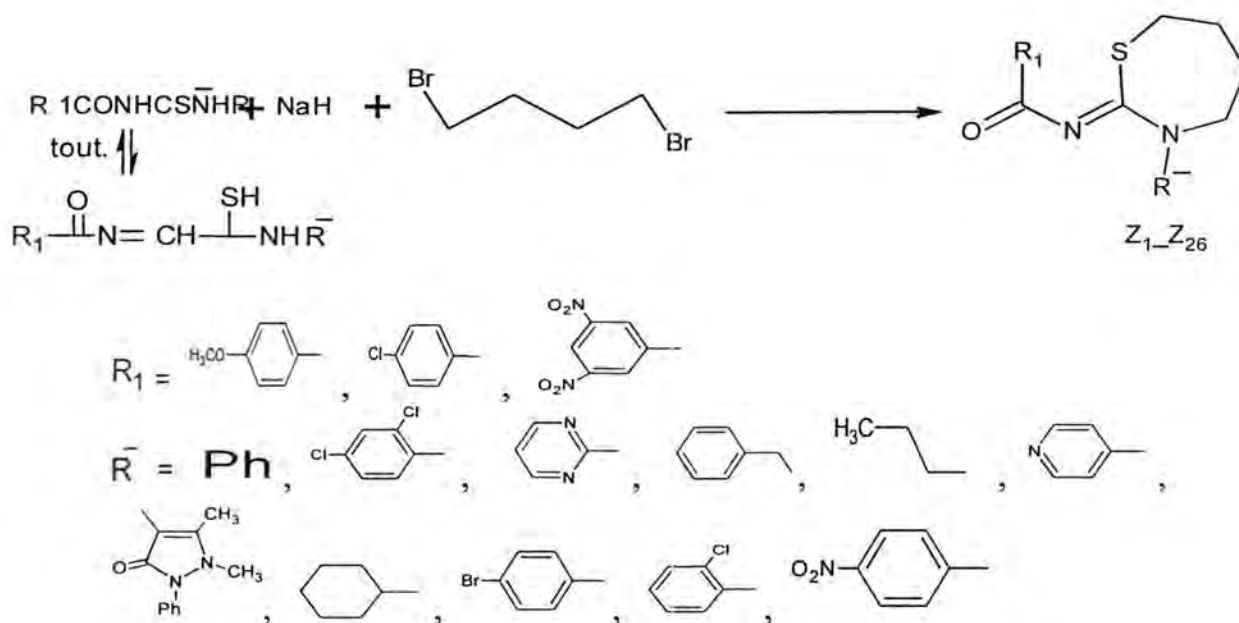
The compound T<sub>25</sub>:  $\delta$  6.2ppm(1H,s, R<sub>2</sub>NH),  $\delta$  6.6ppm(1H,s, R<sub>1</sub>CONH),  $\delta$  6.5ppm(1H,t, H5, Pyrimidine),  $\delta$  8.8ppm(2H,d, H4 and H6, Pyrimidine),  $\delta$  9ppm(3H,s,H3,H4,H6, dinitrophenyl).



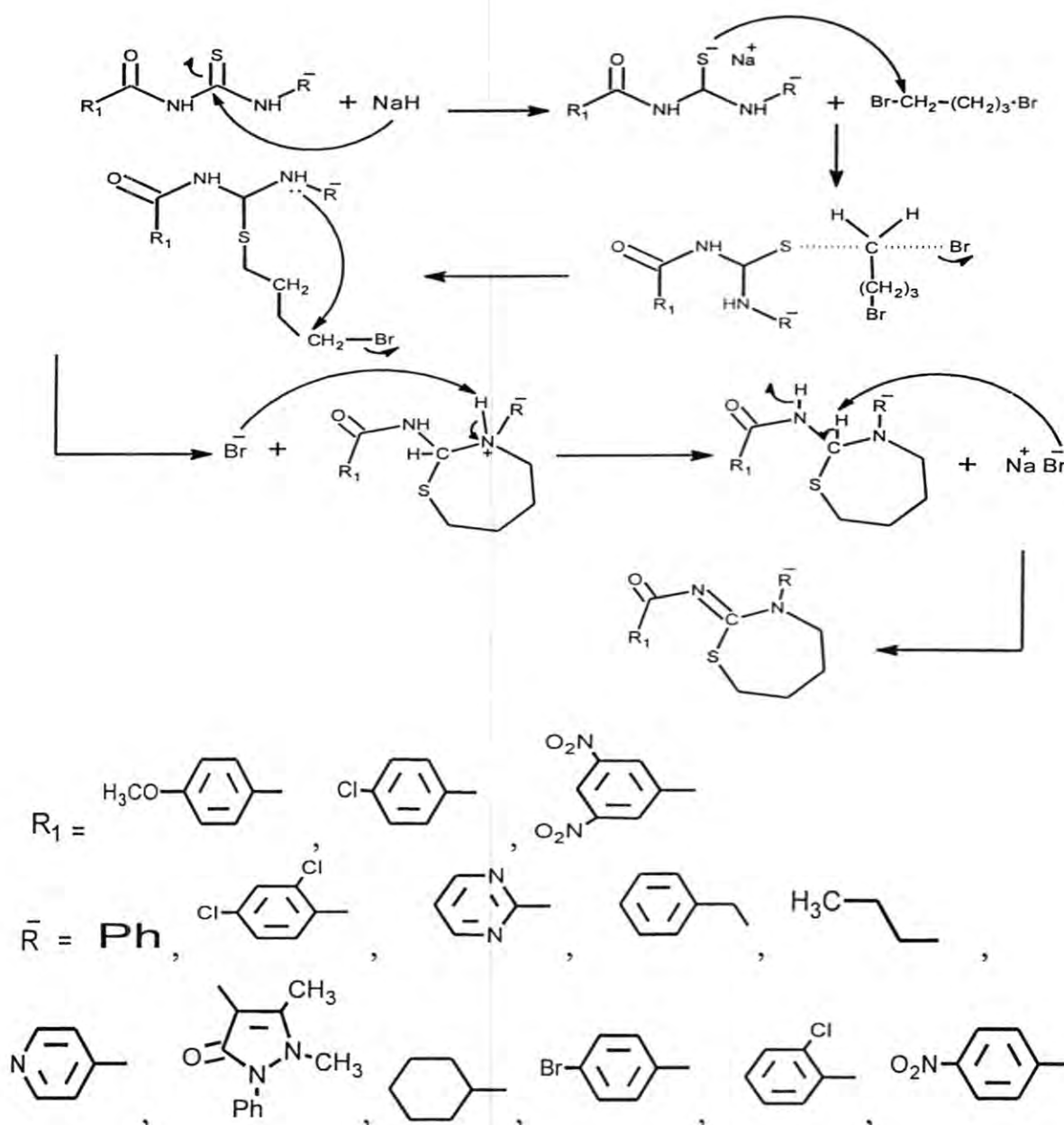
The compound  $T_{27}$  :  $\delta$  0.9ppm(3H,t, CH<sub>3</sub>),  $\delta$  1.6ppm(2H,m,CH<sub>3</sub>CH<sub>2</sub>),  $\delta$  2.8ppm(2H,q,CSNHCH<sub>2</sub>),  $\delta$  8.2ppm(1H,S, R<sub>2</sub>NH),  $\delta$  8.5ppm(1H,S,R<sub>1</sub>CONH),  $\delta$  8.8ppm(3H,S,H<sub>2</sub>,H<sub>4</sub>,H<sub>6</sub>, 3,5-dinitrophenyl).

The (N-H) signals for all recorded compounds ( $T_2, T_9, T_{14}, T_{20}, T_{25}, T_{27}$ ) were disappeared from the spectra on addition of D<sub>2</sub>O (exchange with D). This confirmed their position and therefore the formation of thiourea derivatives.

The prepared 1,3-thiazepine derivatives were resulted from two nucleophilic condensation between two compounds to which lead to the formation of 1,3-thiazepine seven member ring[23]. The reduction of thiourea derivatives using sodium hydride. The resulted thiourea derivative nucleophil attacks the 1,4-dibromobutane at the carbon 1 associated with the liberation of HBr. A second nucleophilic reaction takes place by nitrogen atom, that originated from the primary amine, at the second end of the bromobutane resulted in the formation of seven membered ring of 1,3-thiazepine. The resulted thiazepines are bearing aroylimino group at position 2. The 1,3-thiazepines derivatives ( $Z_1-Z_{26}$ ) are resulted from thiourea prepared from three different aroylhalides with aliphatic and aromatic primary amines. Therefore, the seven member ring essentially substituted at the nitrogen with variation of aliphatic and aromatic groups. In addition to that, the resulted rings are attached to a different aroylimino groups at position 2. The prepared derivatives were identified and their structures were elucidated using chromatographic and spectroscopic methods[24,25]. The reaction is summerised in scheme (2)

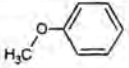
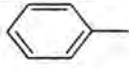
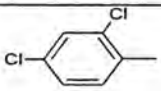
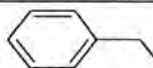
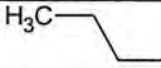
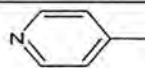
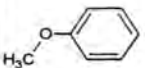
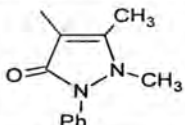
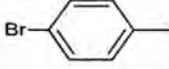
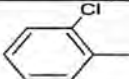
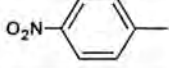

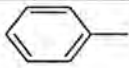
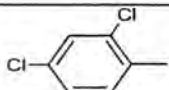
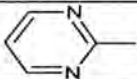
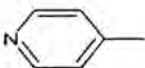


Scheme 2: preparation of 1,3-thiazepine derivatives Mechanisim

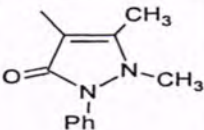

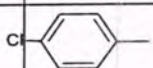
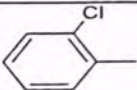
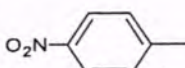
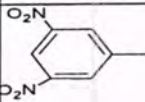
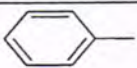
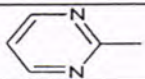
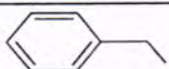

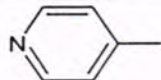
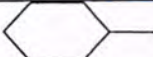
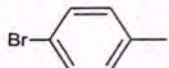
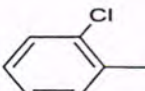
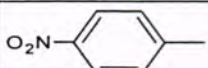


The first characteristic band of the prepared compounds (C=N) which it is stretching vibration appeared between  $(1575-1681\text{cm}^{-1})$ . The stretching vibration of amide carbonyl groups were at  $(1644-1728\text{cm}^{-1})$ . Disappearance of (N-H) stretching vibration indicates the consumption of thiourea derivative. The values of important and characteristic band absorption of each prepared compounds are listed in table (6).

Table- 6: characteristic bands in IR spectra of 1,3-thiazepine derivatives

Comp. No.	R <sub>1</sub>	R'	$\nu(\text{C}=\text{N})$ $\text{cm}^{-1}$	$\nu(\text{C}=\text{O})$ $\text{cm}^{-1}$	$\nu(\text{C}=\text{C})$ Ar $\text{cm}^{-1}$	$\nu(\text{C}-\text{H})$ Ar $\text{cm}^{-1}$	$\nu(\text{C}-\text{H})$ Alph $\text{cm}^{-1}$	$\nu(\text{Others})$ $\text{cm}^{-1}$
Z <sub>1</sub>			1654	1699	1599, 1473	3068	2926	—
Z <sub>2</sub>	=		1681	1708	1599, 1479	3088	2968, 2845	$\nu(\text{C}-\text{Cl})$ 759
Z <sub>3</sub>	=		1637	1693	1604, 1477	3020	2937, 2841	—
Z <sub>4</sub>	=		1589	1644	1556, 1464	3061	2968, 2874	—
Z <sub>5</sub>	=		1608	1683	1573, 1452	3000	2922, 2850	$\nu(\text{C}=\text{N})$ 1573
Z <sub>6</sub>			1643	1666	1602, 1465	3072	2931, 2839	$\nu(\text{C}=\text{O})$ 1695
Z <sub>7</sub>	=		1660	1699	1595, 1481	3064	2968, 2839	$\nu(\text{C}-\text{Br})$ 603
Z <sub>8</sub>	=		1674	1707	1589, 1481	3066	2980, 2841	$\nu(\text{C}-\text{Cl})$ 734
Z <sub>9</sub>	=		1670	1699	1602, 1435	3080	2972, 2939	$\nu(\text{C}-\text{NO}_2)$ 1556, 1338
Z <sub>10</sub>			1637	1687	1600, 1462	3049	2964, 2779	$\nu(\text{C}-\text{Cl})$ 754
Z <sub>11</sub>	=		1589	1701	1541, 1477	3138	2928, 2858	$\nu(\text{C}-\text{Cl})$ 752
Z <sub>12</sub>	=		1602	1668	1579, 1487	3043	2989, 2943	$\nu(\text{C}-\text{Cl})$ 759
Z <sub>13</sub>	=		1608	1689	1515, 1456	3082	2968, 2858	$\nu(\text{C}-\text{Cl})$ 744 $\nu(\text{C}=\text{N})$ 1575



Z <sub>14</sub>	=		1643	1697	1581, 1465	3097	2982, 2841	$\nu(\text{C-Cl})$ 756 $\nu(\text{C=O})$ 1664
Z <sub>15</sub>	=		1672	1701	1591, 1475	3093	2970	$\nu(\text{C-Cl})$ 763 $\nu(\text{C-Br})$ 624
Z <sub>16</sub>			1597	1703	1545, 1487	3080	2931, 2858	$\nu(\text{C-Cl})$ 746
Z <sub>17</sub>	=		1616	1668	1593, 1450	3086	2928	$\nu(\text{C-Cl})$ 750 $\nu(\text{C-NO}_2)$ 1504, 1332
Z <sub>18</sub>			1626	1724	1545, 1462	3091	2964, 2895	$\nu(\text{C-NO}_2)$ 1545, 1350
Z <sub>19</sub>	=		1629	1728	1545, 1456	3086	2943	$\nu(\text{C-NO}_2)$ 1545, 1350
Z <sub>20</sub>	=		1626	1726	1546, 1464	3088	2966	$\nu(\text{C-NO}_2)$ 1546, 1350
Z <sub>21</sub>	=		1626	1722	1545, 1462	3091	2966	$\nu(\text{C-NO}_2)$ 1545, 1352
Z <sub>22</sub>	=		1658	1724	1595, 1462	3091	2964, 2940	$\nu(\text{C-NO}_2)$ 1545, 1352 $\nu(\text{C=N})$ 1626
Z <sub>23</sub>	=		1626	1726	1546, 1452	3000	2933, 2858	$\nu(\text{C-NO}_2)$ 1500, 1348
Z <sub>24</sub>	=		1626	1724	1545, 1462	3091	2964, 2920	$\nu(\text{C-NO}_2)$ 1545, 1350 $\nu(\text{C-Br})$ 606
Z <sub>25</sub>	=		1622	1724	1543, 1456	3090	2943, 2920	$\nu(\text{C-NO}_2)$ 1543, 1350 $\nu(\text{C-Cl})$ 712
Z <sub>26</sub>	=		1604	1653	1519, 1465	3109	2976, 2858	$\nu(\text{C-NO}_2)$ 1519, 1296

The  $^1\text{H-NMR}$  of four of the prepared 1,3-thiazepine derivatives ( $Z_7, Z_{13}, Z_{19}, Z_{21}$ ) were recorded. The spectra confirmed the formation of the compounds and helped the elucidation of their structures.

For compound ( $Z_7$ ):  $\delta$  1.2-1.8ppm(4H,m, -CH<sub>2</sub>CH<sub>2</sub>- ,C5+C6 in cyclic),  $\delta$  2.8-3ppm(2H,t,N-CH<sub>2</sub> cyclic),  $\delta$  3.6ppm(2H,t, S-CH<sub>2</sub> cyclic),  $\delta$  6.9-8ppm(8H,m, aromatic).

The compound ( $Z_{13}$ ):  $\delta$  0.9-2.1ppm(4H,m,-CH<sub>2</sub>CH<sub>2</sub>- ,C5+C6 in cyclic),  $\delta$  3.6ppm(2H,t, N-CH<sub>2</sub> cyclic),  $\delta$  3.7ppm(2H,t,S-CH<sub>2</sub> cyclic),  $\delta$  7.6-7.9ppm(8H,m, aromatic).

The compound ( $Z_{19}$ ):  $\delta$  1.7-1.9ppm(4H,m, -CH<sub>2</sub>CH<sub>2</sub>- ,C5+C6 in cyclic),  $\delta$  3.4-3.6ppm(2H,t, N-CH<sub>2</sub> cyclic),  $\delta$  4.1-4.4ppm(2H,t, S-CH<sub>2</sub> cyclic),  $\delta$  7.1-9ppm(8H,m, aromatic).

The compound ( $Z_{21}$ ):  $\delta$  0.8ppm(3H,t,CH<sub>3</sub>),  $\delta$  1.2-1.9ppm(6H,m,-CH<sub>2</sub>CH<sub>2</sub>- C5+C6 in cyclic and CH<sub>3</sub>CH<sub>2</sub>-),  $\delta$  2.7ppm(2H,t, N-CH<sub>2</sub> out cyclic),  $\delta$  2.9-3.2ppm(2H,t, N-CH<sub>2</sub> cyclic),  $\delta$  4.4ppm(2H,t,S-CH<sub>2</sub> cyclic),  $\delta$  8.9-9ppm(3H,m, aromatic).

A preliminary study to improve some of reaction condition and other parameters finished the following conclusion:

1- The use of an excess of sodium hydride (at least two folds) resulted in the reduction of the carbonyl group in the thiazepine derivative as in the preparation of ( $Z_{27}$ ).

Table -7: shows the absorption spectral packs of the compound ( $Z_{27}$ ).

Comp. No.	$\nu(\text{C=N})$ $\text{cm}^{-1}$	$\nu(\text{O-H})$ $\text{cm}^{-1}$	$\nu(\text{C=C})$ Ar $\text{cm}^{-1}$	$\nu(\text{C-H})$ Ar $\text{cm}^{-1}$	$\nu(\text{C-H})$ Alph $\text{cm}^{-1}$	$\nu(\text{Otheres})$ $\text{cm}^{-1}$
$Z_{27}$	1595	3446	1554, 1460	3074	2928, 2852	$\nu(\text{C-Br})$ 615

2- The use of different reducing agent such as calcium hydride, which was added to mineral oil in other to obtain a desparation of the hydride on the surface of the oil. The outcome of such change resulted of a low conversion of thiourea derivative to 1,3-thiazepine derivative. This might be due to the limited capacity of calcium hydride as a reducing agent. However, the use of an excess of calcium hydride (three folds) resulted in a complete conversion to the desired compounds ( $Z_7$ ).

3-After the completion of 1,4-dibromobutane addition, the reactants were heated by reflux in DMF for two hours. After elaboration of the product the yield was increased by about 10% . TLC, m.p. and IR analysis confirmed such changes in the structure of the previous product.

The preliminary antimicrobial evalution of some of the synthesized 1,3-thiazepine derivatives was carried out . Using three types of bacteria was , staphylococcus aureus, Pseudomonusaeruginosa, EscherichiaColi. The cefotaxime used as a standard antibiotic. The resules of this

evaluation are listed in table (5). The tested compounds ( $Z_1$ ,  $Z_4$ ,  $Z_{16}$ ) demonstrated a moderate inhibition activity against *Pseudomonas aeruginosa* and *E. coli*. However, it showed no activity against *S. aureus* in the range of concentration used in this work and the compound ( $Z_{16}$ ) was the most significant. The compounds ( $Z_{12}$ ,  $Z_{22}$ ,  $Z_{23}$ ) showed some activity against the three bacteria except compound ( $Z_{12}$ ) in the concentration (5000ppm) which did not demonstrate activity against *S. aureus*. However, All the compounds under study show a variable activity against the used bacteria and it needs a further study by expanding the scope of the tested bacteria and fungi. In addition to that, the rest of the prepared compounds need to be evaluated in order to assist their activity and thereafter their importance.

### REFERENCES

1. Natori S., Ikekaw N and Suzuki M, Advance in natural products chemistry, Kodansha scientific books, Tokyo, Japan, (1981).
2. Neamati N., Turpin J.A., Winslow H.E., Christensen J.I., Williamson K., Orr A., Rice W.J., Pommier Y., Garofalo A., Brizzi A., Campiani J., Fiorini I and Nacci V.E., Thiazolothiazepine Inhibitors of HIV-1 Integrase, *J. Med. chem.*, 42, 3334 (1999).
3. Garofalo A., Balconi G., Botta M., Corelli F., Dincalci M., Fabrizi G., Fiorini I., Lamba A and Nacci V., Eur. Evidence for a structural motif in toxins and interleukin-2 that may be responsible for binding to endothelial cells and initiating vascular leak syndrome, *J. Med. chem.*, 28, 213 (1993).
4. Grunewald J.L., Dahanukar H.V., Ching V and Criscione K.R., Synthesis of 2-substituted 1-benzyl-2,3,4,5-tetrahydro-1-benzothiazepines by palladium catalysis. Observation of a competitive  $\beta$ -hydride elimination pathway, *J. Med. chem.*, 39, 3539 (1996).
5. Strobel H., Bohn H., Klingler O., Schindler U., Schoenafinger K., Zoller G., Bioreactors in Tissue Engineering: From Basic Research to Automated Product Manufacturing, *Eur. pat. Ep*, 1966, 718, 294.
6. Shinji Y., Hidekazu O., Karekiyo W., Multigene expression vectors for the biosynthesis of products via multienzyme biological pathways, *Eur. Pat. Ep.*, (1996), 40, 717.
7. Shah S.K., Grant S.K., Maccoss M., Shankaran K., Qi H., Guthikonda., Compositions and Methods for Inhibiting Expression of the PCSK9 Gene, *R.N.PCT Int. Wo.*, (1996), 9614, 842.
8. Rongione J., Brown R., Dwight R., *Synthesis of new 1,3-Thiazepine derivatives*, *U.S.*, (2001), 300, 503.



9. Compiani G.,Nacci V.,Bechelli S.,Clani S.M.,Carofalu A.,Fiorini I.,Wikstrom H.,  
Deboer,P.,Liao,Y.,Tepper,P.G.,Cagnotto,A.,Mennini,T. Synthesis of benzothiazepines (review), *J.Med.chem.*,(1998),41,3763.
10. Robl J.A.,Sun C.Q.,Stevenson J.,Ryono D.E.,Simpkins L.M.,Cimarusti M.P., Dejneka T.,Slusarchyk W.A.,Chao S.,Stratton L.,Misra R.N.,Bednarz M.S.,Asaad M.M.,Cheung H.S.,Abboaoffei B.E.,Smith P.L.,Mathers P.D.,Fox M.,Schaeffer T.R., Seymour A.A.,Trippodo N.C., Dual metalloprotease inhibitors .4. utilization of thiazepines and thiazines as constrained peptidomimetic surrogates in mercaptoacyl dipeptides,*J.Med.chem.*,(1997),40,1570.
11. Delancy N.G.,Barrish J.C.,Neubeck R.,Natarajan S.,Cohen M.,Rovnyak G.C., Huber G.,Murugesan N.,Girotra R.,Sieber-McMmaster E.,Robl J.A.,Assad M., Cheung H.S.,Bird J.E.,Waldron T.,Petrillo and E.W.,*Bioorg. Synthesis of new 1,3-thiazepine derivatives*,*Med.chem.Leth.*,(1994),4,1783.
12. Cherkupally S.R.,Gurralla P.R.,Adki N and Avula S., Synthesis and biological study of novel methylene-bis-benzofuranyl-[1,5]-benzothiazepines,Cherkupally etal.;*Org.Comm.*,(2008),11,84.
13. Kaur H and Kumar A.,*International J.of pharma. And Biosci.*, synthesis and evaluation of some newbenzothiazepinylpyridine derivatives as anticonvulsant agents.,( 2010),1,1.
14. Zask A., Kaplan J.,Du X.M.,Ewan G.M.,Sandanyaka V.,Eudy N.,Levin J.,Jin G.,Xu J., Cummons T.,Barone D.,A-Kaloustian S and Skotnicki J.,Synthesis and SAR of diazepine and thiazepine TACE and MMP inhibitors,*Bioorg.Med.chem.Lett.*, (2005),15,1641.
15. Mahale J.D.,Kumar A.,Singh D.,Ramaswamy V.A and Waghmode S.,A green process for the preparation of 11-{4-[2-(2-hydroxyethoxy)ethyl]-1-piperazinyl} dibenzo[b,f][1,4]thiazepine,*J.Serb.chem.soc.*,(2008),73,385.
16. Calvo L.A.,G-Ortega A.,Marcos R.,Perez M and Sanudo M.C.,Synthesis of 2,3,4,7-tetrahydro[1,4]thiazepines from thiazolidines and  $\beta$ -enaminonitriles. *Tetrahedron.*,( 2008),64,3691.
17. Faty R.F.,Youssef M.M and Youssef A.M.S.,Microwave assisted synthesis and unusual coupling of some novel pyrido[3,2-f][1,4]thiazepines.*Molecules.*,(2011), 16,4549.
18. Elmaati T.M.A and El-Taweel K.M.I.,Routes to pyrazolo[3,4-e][1,4]thiazepine, pyrazolo[1,5-a]pyrimidine and pyrazole derivatives.*J.chin.chem.soc.*,(2003),50,413.
19. Ambartsumova R.F.,Levkovich J.M.,Milgrom G.E and Abdullaev N.D., Synthesis and spectral properties of 2-iminohexahydro-1,3-thiazepines. *Chemistry of heterocyclic compounds*.(1997),33,112.



20. Struga M., Kossakowski J., Mirosław B., Koziol A.E and Zimniak A., Synthesis of new 1,3-thiazepine derivatives. *J. Heterocyclic chem.*, (2009), 46, 298.
21. Levkovich M.J., Abdullaev N.D and Ambartsumova R.F.T., Inoue, 1,3-Thiazepines. 5. Study of 2-Phenyl(benzyl)imino-hexahydro-1,3-thiazepines and Their Derivatives by  $^{13}\text{C}$  Spectroscopy, *Heterocycles*. (2002), 38, 612.
22. Hakan A., Nizami D., Gulay B., Cemal K.O and Cevdet A., Antimicrobial activity of some thiourea derivatives and their nickel and copper complexes. *Molecules*, (2009), 14, 519.
23. Struga M., Kossakowski J., Mirosław B., Koziol A and Zimniak A., *Synthesis of new 1,3-Thiazepine derivatives*. *J. Heterocyclic chem.*, (2009), 46, 298.
24. Dudley H., Williams and Ian F., Spectroscopic methods in organic chemistry, 3<sup>rd</sup>. ed. MC Graw-Hill Book company (uk), (1980), 304.
25. Robert M., Silverstein., Francis X., Webster., David J and Kiemle., Spectrometric identification of organic compounds, 7<sup>th</sup>. ed. John Wiley and sons, USA., (2005), 512.

## Study of Some *Mirabilis jalapa* L. Leaves Components and Effect of Their Extracts on Growth of Pathogenic bacteria

Mustafa Taha Mohammed

Department Of Chemistry, College Of Science, Al-Mustansiriyah University, Baghdad, Iraq.

Tahabiochem@Yahoo.Com,

Received 14/3/2012 – Accepted 20/6/2012

### الخلاصة

شملت الدراسة معرفة المكونات الكيميائية الفعالة الموجودة في أوراق نبات لالة عباس *Mirabilis jalapa* إذ أظهرت الدراسة أن محلولي المستخلصين المائي والكحولي يحتويان على مجموعة من المركبات الكلايوسيدية والعفصية والفينولية والراتنجات والقلويدات والبروتينات بينما لا تحتوي على الصابونيات والفلافونيدات .

اثبت التحليل الدقيق للعناصر المعدنية لأوراق النبات احتواءها على تراكيز من K و Na و Fe وهي 161.2, 19, 18.7 µg/ml , على التوالي ، وكميات من Zn و Ca وهي 14.2, 12 µg/ml وكميات على Cd , Cu و Pb وهي 0.8, 0.3, 0.1 µg/ml . وعلى التوالي، وعدم احتوائها على Cr. كما درس تأثير المستخلصات المائية والكحولية على أنواع مختلفة من البكتريا إذ لوحظ أن التركيز 0.5 ملغم /مل تأثيراً فعالاً تجاه تثبيط نمو بكتريا *Proteus mirabilis* و *E.coli* و *Staphylococcus aureus* خاصة تجاه المستخلص الكحولي .

### ABSTRACT

The chemical components of the *Mirabilis jalapa* L. leaves in the watery and alcoholic extracts were identified .The results showed that the extract contain : glycosides ,tannins ,phenolic compounds , resins ,alkaloids and proteins ,while the saponins and flavonoids were not found.

The results also showed that there were concentrations of the following trace elements in the leaves K , Na , Fe with 161.2 ,19 ,18.7 µg/ml , respectively and concentrations of Zn ,Ca with 14.2 , 12 µg/ml respectively , concentrations Cd ,Cu, Pb with 0.8 ,0.3,0.1 µg/ml respectively ,and Cr were not found.

The effects of these extracts on growth of different bacteria were studied, has been found that 0.5 mg/ml concentration was effective inhibitor of growth of *Staphylococcus aureus* , *E.coli* and *Proteus mirabilis* .

### INTRODUCTION

*Mirabilis jalapa* Linn (Nyctaginaceae), known as four o'clock, maravilla, belle de nuit, buenas tardes, Dondiego de noche, jalap, noche buena,[1,2] *Mirabilis jalapa* L. is widely used to treat dysentery, diarrhea, muscular pain, and abdominal colics in different countries [3-5] and its extract has antibacterial, antiviral, and antifungal functions [6-8]. In China, *Mirabilis jalapa* L. is widely distributed and commonly used with its root, and has been used as traditional Chinese medicine and ethnic drug to treat diabetes [9,10], constipation [11], genitourinary system disorders and injuries [12].Several constituents of the *Mirabilis jalapa* plant have been isolated from the root and aerial part, including some rotenoids (mirabijalones A-D, boeravinones C and F), an isoquinoline derivate [13], as well as terpenoids, steroids, phenolic compounds, stigmasterol, p-sitosterol, p-sitosterol- p-D-glucoside, ursolic acid, mirabalisoic acid, mirabalisol, trigonellin and an antiviral

protein [14]. Furthermore, *Mirabilis jalapa* extracts have also been reported to have biological activities (antibacterial, antiviral, antifungal, protein synthesis inhibition) by many research groups [15], though few studies have been performed on muscular activity [16]. It is difficult to correlate the biological effects with the traditional use of this plant, because common people employ this medicinal plant for many different illnesses, as spasmogenic or spasmodic drug between others, with apparently opposite effects as purgative or for treating dysentery. That contradictory use given at *Mirabilis jalapa* could be due to a lot of bioactive elements this plant contains (as trigonellin, a purgative and p-sitosterol- p-D-glucoside, some rotenoids and other compounds reported as antispasmodics), their irregular distribution in the enter plant and to differences in the traditional extraction processes.

The aim of this study the watery and alcoholic extracts for *Mirabilis jalapa* leaves posses *in vitro* antibacterial activity because of its content (glycosides, tannins, proteins, various phenolic compounds, alkaloids, trace elements), however if plant leaves extracts are to be used for food preservation or medical purposes.

## MATERIALS AND METHODS

### Collection and treatment of samples:

The leaves of *Mirabilis jalapa* were collected from the north of Baghdad, Iraq. The leaves were transported to the laboratory, washed, cleaned with filter paper or soft clothes to remove all traces of dust and insects, then dried in shade 25-30°C for one week, with continuous overturn to prevent mould. weighed, ground in a mortar and pestle, placed in airtight bottles and stored in dessicator to be used for extraction [17].

### Preparation of extracts:

#### a) Watery extract:

Air dried leaves 50 g were suspended in one liter of distilled water and left for 24 hrs at 35°C with continuous stirring in shaking incubator. Then the mixture was filtered by filter paper, the filtrate was centrifuged for 10 min. at 2500 rpm, and the extract evaporated to dryness at 40°C in the incubator for 24 hrs.

#### b) Alcoholic extract:

Prepared as in watery extract described above, but with using 70% ethanol alcohol instead of water to give alcoholic extract powder [18-21].

### Determination of Ash content:

Dried leaves 2 g were taken and heated at 900°C for 20 min. in muffle furnace until the material converted to white powder, after its cooling the percentage of ash content was determined [22].

### Chemical detection of the plant components:

The chemical components of the prepared watery and alcoholic extract were detected: glycosides, alkaloids, saponins, phenolic compounds, tannins, resins, flavonoids (20-22) and proteins [23].

### Determination of trace element levels:

Dried leaves 3 g were taken and mixed with 8 ml of concentrated nitric acid and 2 ml of 60% perchloric acid in a conical flask, the mixture was kept for 24hrs covered with watch glass. After that it was left for 6hrs at sand bath at 80°C, until the digestive material converted to white powder. Deionized water 8 ml were added to this powder, and the trace elements were determined [22] by (Shimadzu AA-670, Flame Atomic Absorption Spectrophotometer).

### The biological activity:

The biological activity against various bacterial species was determined by using wells-diffusion method. From gram negative bacteria, *E.coli* and *Proteus mirabilis* was chosen, while *Staphylococcus aureus* was used as gram positive bacteria. These isolates were obtained from department of Biology /College of Science /Al-Mustansiriyah University. The concentrations for both extracts were 0.1 , 0.5, 1 mg/ml [20,21].

### Inhibition of hyaluronidase:

Hyaluronidase inhibition activity was determined turbidimetrically by the method of Kass *et al.* [24] by using 0.01 mg/ml enzyme mixed with 250 µg/ml from the extracts with inhibition time 45 min. and the percentage of inhibition was calculated according to this equation [25]:

$$\% \text{inhibition} = \frac{\text{Activity of control} - \text{Activity in the presence of Extract}}{\text{Activity of control}} \times 100$$

### Assay system :

- 1- 100µl of hyase ( serum) was made up to 900 µl with 0.1 M acetate buffer (pH 3.7 containing 0.15 M NaCl), then incubated for 15 min at 37 °C.
- 2- After preincubation .the assay was commenced by added HA (100µl) to each tube and incubated for 45 min. all incubations were carried out in triplicate.
- 3- Other tube was prepared for the initial HA in sample , contained (100 µl ) of substrate and the volume was made up to 900 µl with acetate buffer pH 3.7 and a 100µl of serum sample was then added after 45 min of incubations time with a total volume of 1ml.



- 4- The blank which was contained 100µl of enzymes were prepared and the volume was made up to 1ml with acetate buffer , but in the case of serum sample the contained only 1ml acetate buffer pH 3.7 .
- 5- Reaction were terminated by the addition of 2ml of Cetrimide (CTAB) (25% w/v) in 2% (w/v) NaOH solution (stop reaction)and produced the turbidity.

## RESULTS AND DISCUSSION

The results showed that Ash content for the *Mirabilis jalapa* leaves is 34 %. The qualitative chemical analyses of the watery and alcoholic extracts are represented in Table.1, Which shown that leaves contents are (glycosides, proteins, tannins, resins and various phenolic compounds) Our results similar with other studies (26), alkaloids are obtained in alcoholic extract only, while the saponins and flavonoids are not found.

Table-1: Chemical components analysis for watery and alcoholic extracts of *Mirabilis jalapa* leaves.

components	Reagents	Note	Result Watery extract	Result Alcoholic extract
Glycosides	Iodine test	Blue ppt.	Ve+	Ve-
	Molish test	Violet ring	Ve+	Ve +
	Benedict test	Orange ppt.	Ve+	+Ve
Proteins	Folin-Ciocalteu reagent	Blue color	Ve+	Ve+
Saponins	Fast stirring	No Dense foam for long time	Ve -	Ve-
	Mercuric Chloride	No White ppt.	Ve -	Ve-
Phenolic compounds	Aqueous%1 Ferric chloride	Green ppt.	Ve+	Ve+
Tannins	Aqueous%1	Green ppt.	Ve+	Ve+
	Ferric chloride	Preface yellow	Ve+	Ve+
	Lead acetate%1	ppt.		
Resins	Ethanol + Boiling + D.w.	turbidity	Ve+	Ve+
Flavonoids	aqueous%1	No Green ppt.	Ve-	Ve-
	Ferric chloride Ethanol hydroxide alcohol	No Yellow ppt.	Ve-	Ve-
Alkaloids	Mayer's reagent	No white ppt.	Ve-	Ve+
	Wagner reagent	Brown ppt.	Ve-	+Ve
	Picric acid	Yellow ppt.	Ve-	Ve+

The concentrations of trace elements in *Mirabilis jalapa* leaves are represented in Table.2 .which shows , concentrations of (K , Na , Fe) with (161.2 , 19 , 18.7) µg/ml , respectively and concentrations of (Zn ,Ca) with (14.2 ,12) µg/ml , respectively , concentrations (Cd , Cu , Pb ) with (0.8 , 0.3, 0.1) µg/ml and (Cr) were not founds .

Table-2: The concentration of trace elements content of *Mirabilis jalapa* leaves.

Trace elements	symbol	Concentration( $\mu\text{g/ml}$ )
Potassium	K	161.2
Sodium	Na	19
Iron	Fe	18.7
Calcium	Ca	12
Zinc	Zn	14.2
Cadmium	Cd	0.8
Chromium	Cr	Nil
Lead	Pb	0.1
Copper	Cu	0.3

The effect of these extracts on different microorganisms were studied and compared between them. In addition to that the results seen in Table 3 show that the concentrations 0.5 , 1 mg/ml exhibit very effective inhibition towards tested bacteria , *P. mirabilis* and *E.coli* and *S. aureus* , specially for the alcoholic extract , while less inhibition effects were seen for the same concentrations when the watery extract was used. In general , when the both extracts were tested against the intended bacteria they were no activity at concentration of 0.1 mg/ml .

Table-3: The effect of watery and alcoholic extracts of *Mirabilis jalapa* represented by inhibition zone (mm) on different bacteria species.

<i>Bacterial species</i>	<i>mg/ml (Alcoholic extract)</i>			<i>mg/ml ( Watery extract )</i>		
	0.1	0.5	1	0.1	0.5	1
<i>S. aureus</i>	-	+	+	-	+	+
<i>E.coli</i>	-	+	++	-	+	+
<i>P. mirabilis</i>	-	++	++	-	++	++

(-) No inhibition zone

(++) Inhibition zone between (4-10) mm .

(+++ ) Inhibition zone more than (10) mm .

This work shows , the two extracts were examined for their effects on hyaluronidase .The percentage of inhibition for watery extract was

7.5% , and 6.25% for Alcoholic extract with respect to control assays run simultaneously .

## CONCLUSION

the present study confirm that the watery and alcoholic extracts for *Mirabilis jalapa* leaves posses *in vitro* antibacterial activity because of its content (glycosides , tannins , ,proteins ,various phenolic compounds ,alkaloids , trace elements) , however if plant leaves extracts are to be used for food preservation or medical purposes ,issues of safety and toxicity will need to be addressed ,and this results will serve as a precursor for further research.

## REFERENCES

1. Encarnaci'on D.R., Virgen M., Ochoa N., "Antimicrobial activity of medicinal plants from Baja California Sur (Mexico)", *Pharmaceutical Biology* 36, 33-43. (1998).
2. Holdsworth D.K., " A preliminary study of medicinal plants of Easter Island, South Pacific", *International Journal of Pharmacognosy* 30, 27-32. (1992).
3. Dimayuga R.,Virgen M., Ochoa N. "Antimicrobial activity of medicinal plants from Baja California Sur (Mexico)," *Pharm Biol*, vol. 36, no. 1, pp. 33-43,(1998).
4. Holdsworth D., "A preliminary study of medicinal plants of Easter Island, South Pacific," *Pharm Biol*, vol. 30, no. 1, pp. 27-32, (1992).
5. Walker C. I. Trevisan G., Rossato M. F. , et al., "Antinociceptive activity of *Mirabilis jalapa* in mice," *J Ethnopharmacol*, vol. 120, no. 2, pp. 169-75, (2008).
6. Kusamba C., Byamana K., Mbuyi W. M. , "Antibacterial activity of *Mirabilis jalapa* seed powder," *J Ethnopharmacol*, vol. 35, no. 2, pp. 197-9, (1991).
7. De Bolle M. F., Osborn R. W., Goderis I. J. et al., "Antimicrobial peptides from *Mirabilis jalapa* and *Amaranthus caudatus*: expression, processing, localization and biological activity in transgenic tobacco," *PlantMolBiol*, vol. 31, no. 5, pp. 993-1008, (1996).
8. Vivanco J. , Querci M. Salazar L. , "Antiviral and antiviroid activity of MAP-containing extracts from *Mirabilis jalapa* roots," *Plant Dis*, vol. 83, no. 12, pp. 1116-1121, (1999).
9. S. A. o. T. C. M. C. M. M. E. Board, Chinese Materia Medica (II). In Shanghai Science and Technology Press: Shanghai,; pp 748-749. (1999).

10. J. N. M. C. compiled, The second volume of Dictionary of Chinese Medicine. In Shanghai People's Publishing House: Shanghai, pp 2370-2371. (1977).
11. Lee S. Xiao C., Pei S. "Ethnobotanical survey of medicinal plants at periodic markets of Honghe Prefecture in Yunnan Province, SW China," *J Ethnopharmacol*, vol. 117, no. 2, pp. 362-77, (2008).
12. Weckerle C. S., Ineichen R., Huber F. K., Yang, Y., "Mao's heritage: medicinal plant knowledge among the Bai in Shaxi, China, at a crossroads between distinct local and common widespread practice," *J Ethnopharmacol*, vol. 123, no. 2, pp. 213-28, (2009).
13. Yi-Fen W., Ji-Jun, C., Yan Y., Yong-Tang Z., Shao-Zong T., Shi-De L., "New rotenoids from roots of *Mirabilis jalapa*," *Helvetica Chimica Acta* 85, 2342-2348, (2002).
14. Wei Y., Yang X.S., Hao X.J., "Studies on chemical constituents from the root of *Mirabilis jalapa*". *China Journal of Chinese Materia Medica* 28, 1151-1152. (2003).
15. Oskay M., Sari D., "Antimicrobial screening of some Turkish medicinal plants". *Pharmaceutical Biology* 45, 176-181. (2007).
16. Cortés A.A.R., Lara Ch.B., Aoki M.K., "Screening and selection of plants by positive pharmacologic effect on jejunum muscular contractility". *Pharmaceutical Biology* 42, 24-29, (2004).
17. Jassim A.M.N., "Study of Some *Cucurbita moschata* Duchesne ex poiret Leaves Components and Effect of Its Extracts on Different Microorganisms and Identification of Some Flavonoids by HPLC", *Al-Mustansiriya J. Sci.*, 21, 101-110 (2010).
18. Al-Bayati R.I.H., Naji, N. A. and Al-Sedah M.M.M., "Study on The Effect of *Capparis Spinosa* Fruits Extracts on Acetylcholinesterase Activity in Human Blood", *Al-Mustansiriya J. Sci.*, 13, 1, 146-131 (2002).
19. Al-Bayati R.I.H., Al-Janabi S.A. and Al-Mudarees M.F., "Hypoglycemic Activity of *Mentha Longifolia* Leaves Composites", *Iraqi Journal of Chemistry*, 27, 1 (2001).
20. Jassim A.M.N., "Study of Some *Eucalyptus Rostrata* Leaves Components and Effect of Its Extract on Different Microorganisms", *Al-Mustansiriya J. Sci.*, 16, 2, 62-71 (2005).
21. Mohammed M.T., "Study of Some *Vinca Rosea l.* (Apocynaceae) Leaves Components and Effect of Its Extract on Different Microorganisms", *Al-Mustansiriya J. Sci.*, 18, 1, 28-36, (2007).
22. الدليمي، نصر حامد، "دراسة مظهرية و فسلجية و خلوية كمؤشر على آلية تحمل نبات الحنطة للجفاف"، أطروحة ماجستير، (1997).
23. Plummer D.T, *An Introduction of Practical Biochemistry*, 2ed, pp. 145-146, McGRAW-HILL Book Co., England, (1978).



24. Kass E. and Seastone C. , "The Role of the Mucoïd Polysaccharide (Hyaluronic Acid ) In the Virulence of Group A Hemolytic Streptococci", J.Exp.Med.,79,1944,319.
25. Jassim A.M.N. , "Inhibition Effects of Flavylum Salt on (Serum, Testicular, Bacterial) Hyaluronidase", Al-Mustansiriya J.Sci.,15,4, ,32-43(2004).
26. Hudec J., Burdova M., Komora L., Macho V., Kogan G., Turianca I., Kochanova R., Lozek O.;Haban M. and Chlebo P.," Antioxidant Capacity Changes and PhenolicProfile of *Echinacea purpurea*, Nettle (*Urtica dioica* L.), and Dandelion (*Taraxacum officinale*) After Application of Polyamine and Phenolic Biosynthesis Regulators, J.Agric.Food Chem.,55, 5689-5696(2007).

## Unifying Technique for Multisource Remote Sensing Images

Firas Abdulrazzaq Hadi And Rawnaq Adil Abdulwahhab  
Ministry Of Science And Technology

Received 3/1/2009 – Accepted 14/11/2010

### الخلاصة

تعرف عملية دمج البيانات على أنها آلية لتوحيد ووضع معلومات سبق وان تم الحصول عليها من متحسسات مختلفة. حيث تهدف البحوث التي تناولت موضوع توحيد صهر البيانات الى تطوير نماذج جديدة وملائمة لدمج مدى واسع ومعقد وغني من البيانات الصورية لمدى واسع ومتنوع من المتحسسات. في هذا البحث، تم تطبيق العديد من التقنيات لغرض تحديث (باعتبار الصورة ذات الدقة الاعلى احدث من الاخرى) وتطوير المعلومات في الصور متعددة الالوان وذات الدقة الواطنة، بالاستفادة من الصور احادية اللون ذات الدقة العالية والاحداث لنفس الموقع.

وقد استخدمت الطرق ادناه في توحيد الصور:

- 1- تقنيات التوحيد القائمة على عمليات التحويل المويجي Wavelet؛ حيث تم توظيف كل من تقنية Haar و Tab3/5 ولعدة مستويات من التحويل. وذلك من خلال استبدال المركبة Low-Low للصورة الواطنة الدقة بنظيرتها من المستوى المقابل لمركبة التحويل Low-Low للصورة عالية الدقة.
  - 2- استخدمت ثلاث طرق للتحويل اللوني لمعالجة حالة الضعف لدقة الصور المتحسنة عن بعد؛ حيث تم استخدام أساليب التحويل اللوني YUV, HLS, Lab لغرض التوحيد، وذلك باستبدال الحزمة اللونية الأكثر فعالية (L-band) العائدة لكل من تحويلات HLS, Lab وكذلك YUV، بمشاهد الدقة العالية والمتمثلة بحزمة Panchromatic لصورة القمر SPOT. بعدها يتم تطبيق طريقة عكس التحويل لاسترجاع الصور المحسنة.
  - 3- تقنية PCA للقيام بعملية التوحيد أو الدمج. وتعد طريقة التحويل هذه هي الطريقة المثلى، أي إنها تؤدي إلى تحقيق أعلى درجة من عدم الترابط Decorrelation حيث إن المستوى الأول من هذا التحويل للصورة ذات الدقة الواطنة تستبدل بالصورة ذات الدقة العالية Panchromatic والمأخوذة من القمر SPOT. ومن ثم تطبيق طريقة PCA العكسية لغرض استرجاع الصورة المحسنة.
- من كل التقنيات السابقة يمكن الاستنتاج عياناً ان تقنية ال PCA هي الأكثر تفوقاً في الحفاظ على المعلومات اللونية وزيادة الدقة المكانية، اما بالنسبة للتحويل اللوني فإن HLS جاءت بنتائج مرضية واكثر قبولاً من التحويلات اللونية الاخرى (YUV و Lab). بينما كانت نتائج طرق التحويل المويجي غير مقبولة عياناً بالرغم من تحسن النواتج عند زيادة عدد المستويات للنوع Tap3/5.

### ABSTRACT

Data fusion is the process of putting together information obtained from many heterogeneous sensors. Data fusion research focus on the development of novel sensor-centric data fusion models appropriate to fusion of disparate range and image data, with complex information.

In this research, many fusion techniques have been used to improve small scale (low resolution) remotely sensed images, and renewing the information by considering that the large scale (high resolution) images are newer than the restored image. The fusion methods used are:

- Fusion techniques based on wavelet transformations; The Haar and the Tap 3/5 wavelet transformations have been adopted and used with several transformation levels.
- Three color transformation methods are, also, used to improve the lower scale remotely sensed scenes; The HLS, Lab, and YUV color transformation algorithms have been adopted for the unification purposes. Inverse color transformation then implemented to reconstruct the enhanced scenes.

- The PCA transformation technique is used to perform the Unification method. This transformation (as indicated at the literature) represents the optimum transformation, in the sense; it is yielding maximum de-correlation.

From all the proceedings techniques, the results subjectively showed that PCA technique is the superior one at each two meanings spatial resolution improving and color information preserving, while in color transform the HLS is the most sufficient and adequate than other transforms (color transforms Lab and YUV). Wavelet transforms has no acceptable results despite Tap3/5 in high level Wavelet transformation shows more beneficent results than Haar Wavelet technique.

---

## 1. INTRODUCTION

Many types of remote sensing images are routinely recorded in digital form and then processed by computers to produce images for interpreters to study. The simplest form of digital image processing employs a micro processor that convert the digital data into a film image with minimal corrections and calibrations. At the other extreme, some dedicated computers systems are employed for sophisticated interactive manipulation of the data to produce images in which specific information has been produced and highlighted [1].

Remote sensing system, particularly those deployed on satellite, provides a repetitive and consistent view of earth that is invaluable to monitoring the earth system and the effects of human activities on the earth.

In remote sensing, rapid developments of new satellites and more advanced sensor systems allow researches to have a wide spectrum of data for the same region of the Earth. The appropriate combination of information from these different sources might produce a product, which contains the information of higher quality and is more reliable for different applications in remote sensing. Such product, otherwise, might be difficult to obtain by other means or be totally unavailable because of different restrictions of the sensors, satellite's orbit, etc. Since the source data in remote sensing are images of the land surface, the combination process is called "*image fusion*". A sketch of image fusion is shown in Fig. (1). As can be seen; the combination produced a scene with better enhanced features.

Another impetus was the Landsat program, which began in 1972 provided worldwide coverage in digital format. In addition the continued development of faster and more powerful computers with software that is suitable for image processing [2].

The ultimate goal of the project in this search is; unifying multispectral, low-resolution and high-resolution remote sensing scenes to improving, enhancing, globalizing and exhibiting faint and un existed features on the oldest low-resolution scenes.

## 2. IMAGE UNIFICATION METHODOLOGIES

In this research, the problem of fusion images of different modulates is investigated, by utilizing different fusion's algorithms. High spatial resolution scenes are combined with enlarged blurred lower resolution "ETM+" images to produce several enhanced bands of "ETM+" images Fig.(1).



Figure-1: Demonstration of image

Since the source data in remote sensing are images of the land surface, the combination process is called "*image fusion*". A sketch of image fusion is shown in Fig. (1). As can be seen; the combination produced a scene with better enhanced features. As we mentioned before, in this research work many data fusion methods have been used, these are:

- Two types of wavelet transformations have been adopted and used to fuse the samples of images, illustrated in Fig. (1); these are *Haar* and *Tab3/5* wavelet transformation algorithms.
- Different color transformation (i.e. HLS, Lab, and YUV) techniques have been adopted and used to unifying samples of different resolution images.
- The PCA transformations have been used to fuse the samples of images, this transformation represents the optimum transformation, in the sense; it is yielding maximum de-correlation.

### 2.1 WAVELET UNIFICATION METHODS

In order to perform the WT fusion, images should be decomposed to a desired level; in this project the 1<sup>st</sup>, 2<sup>nd</sup> and 3<sup>rd</sup> level are adopted, as it has been found yielding best fusion result. The fusion processes involved in this method are illustrated in the block-diagram shown in Fig. (2). For each level, 4 sub-bands, contain the color information, are created. The low-low band of the last level from ETM+ image is replaced by the same sub-band of the PAN image. An inverse WT should then be applied to produce the unified ETM+ scene [3]. The procedures mentioned above should be repeated with each band of the multispectral ETM+ scene. A variety of wavelet transformations have been developed and implemented in wide range of image processing. Among these, we have chose two types which represent; the simplest one (*Haar wavelet*) and the most recent one named (*Tab3/5 wavelet transform*).



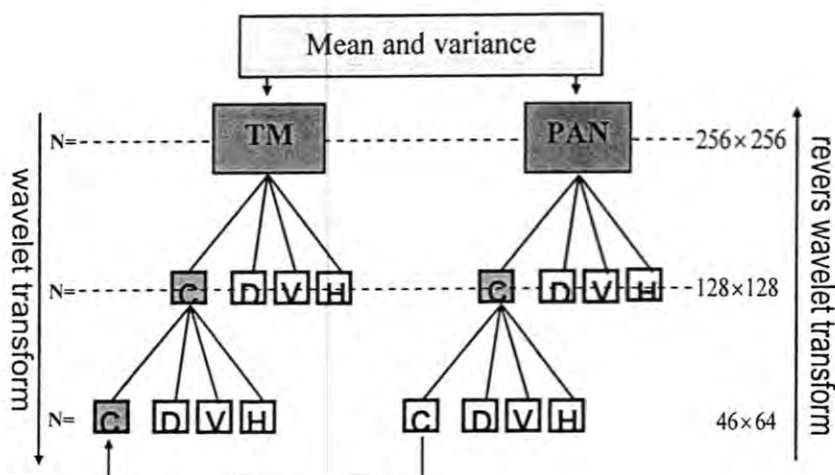


Figure-2: Schematic methodological sequence of the WT fusion method.

#### A. THE HAAR WAVELET TRANSFORM

The *Haar wavelet* is even simpler and mostly common used one. It is often used for educational purposes. It is separable, so it can be used to implement a wavelet transform by first convolving it with the rows and then with the columns [4]. The Haar basis vectors are simply:

$$LOWPASS: \frac{1}{\sqrt{2}} \begin{bmatrix} 1 & 1 \end{bmatrix} \quad , \dots \dots \dots (1) \quad ,$$

$$HIGHPASS: \frac{1}{\sqrt{2}} \begin{bmatrix} 1 & -1 \end{bmatrix} \quad , \dots \dots \dots (2)$$

#### B. BI-ORTHOGONAL TAB3/5 FILTERS

In this transformation, the a sequence of simple filtering operations for which alternately, odd pixel values are updated with a weighted sum of odd pixel values and is rounded to an integer value, and even pixel values are updated with a weighted sum of odd pixel values and also rounded to an integer value. The odd coefficients of the output pixel  $C$  are computed first for all values of  $x$  such that  $-1 \leq 2x+1 \leq W+1$  :

$$C(2x+1) = C_{ext}(2x+1) - \frac{C_{ext}(2x) + C_{ext}(2x+2)}{2} \quad , \dots \dots \dots (3)$$

Where;  $W$  is the original image width.

Then the even coefficients of the output signal  $C$  can now computed from the even values of extended pixel  $C_{ext}$ , and the odd coefficients of pixel  $C$  for all values of  $x$  such that  $-1 \leq 2x+1 \leq W+1$  [5]:

$$C(2x) = C_{ext}(2x) + \frac{C_{ext}(2x-1) + C(2x+1) + 2}{4} \quad , \dots \dots \dots (4)$$

This procedure is applied in both directions (vertical and horizontal) to get the final transformed image [5].

#### 2.2 COLOR SPACE-BASED FUSION

Image fusion based on color transformation is one of the oldest methods for sharpening of multisensor data. In our fusion research we based on three color transformation (HLS, Lab, and YUV).

**A. HLS** Firstly, three components of the original image  $R$ ,  $G$  and  $B$  are transformed into the HLS color space. The transformation is given by the HLS procedure.

RGB → HLS Transformation	
$R_n = \frac{R}{255}, G_n = \frac{G}{255}, B_n = \frac{B}{255}$ $M = \max(R_n, G_n, B_n), m = \min(R_n, G_n, B_n)$ $\Delta = \text{Max} - \text{Min}, L = \frac{M + m}{2}$ <p>if <math>\Delta = 0</math> then, <math>H = 0, S = 0</math> else</p> $S = \begin{cases} \frac{\Delta}{M + m} & \text{if } L < 0.5 \\ \frac{\Delta}{2 - M - m} & \text{otherwise} \end{cases}$	$R' = \frac{\frac{M - R_n}{6} + \frac{\Delta}{2}}{\Delta}, G' = \frac{\frac{M - G_n}{6} + \frac{\Delta}{2}}{\Delta}$ $B' = \frac{\frac{M - B_n}{6} + \frac{\Delta}{2}}{\Delta}$ $H = \begin{cases} B' - G' & \text{if } R_n = M \\ \frac{1}{3} + R' - B' & \text{if } G_n = M \\ \frac{2}{3} + G' - R' & \text{if } B_n = M \end{cases}$ $H = \begin{cases} H + 1 & \text{if } H < 0 \\ H - 1 & \text{if } H > 1 \end{cases} \text{ endif}$

After the transformation, the low-resolution Lightness component  $L$  is replaced by the panchromatic band with higher spatial resolution, The final step is to transform the image back to  $RGB$  color space with the original values of  $H$  and  $S$ :

HLS → RGB Transformation	
<p>If <math>S = 0</math></p> $R = L * 255$ $G = L * 255$ $B = L * 255$ <p>else</p> $i2 = \begin{cases} L(1 + S) & \text{if } L < 0.5 \\ (L + S) - SL & \text{otherwise} \end{cases}$ $i1 = 2L - i2$ $R = 255 \text{ Hue\_2\_RGB}(i1, i2, H + \frac{1}{3})$ $G = 255 \text{ Hue\_2\_RGB}(i1, i2, H)$ $B = 255 \text{ Hue\_2\_RGB}(i1, i2, H - \frac{1}{3})$ <p>endif</p>	<p>Where <math>\text{Hue\_2\_RGB}(v1, v2, H)</math> is a function defined as:</p> <p>if <math>(H &lt; 0)</math> then <math>H = H + 1</math>  elseif <math>(H &gt; 1)</math> then <math>H = H - 1</math></p> $\text{Hue\_2\_RGB} = \begin{cases} v1 + 6H(v2 - v1) & \text{if } H < \frac{1}{6} \\ v2 & \text{if } \frac{1}{6} \leq H < \frac{1}{2} \\ v1 + 6(v2 - v1)(\frac{2}{3} - H) & \text{if } \frac{1}{2} \leq H < \frac{2}{3} \\ v1 & \text{if } H > \frac{2}{3} \end{cases}$

**B. Lab** space fusion done by the following steps:

- First we convert only Multispectral image (excluding PAN image from converting) from RGB to XYZ space by using the formula was shown below and then
- Converting from XYZ to Lab space,
- In Lab space we replace L-band by PAN image then,
- Reversing the transformation upward RGB enhanced image.

RGB → XYZ Transformation Steps	
$R' = \begin{cases} \left( \frac{\frac{R}{255} + 0.055}{1.055} \right)^{2.4} \times 100 & \text{if } \frac{R}{255} > 0.0405 \\ \frac{\frac{R}{255}}{12.92} \times 100 & \text{otherwise} \end{cases}$	$B' = \begin{cases} \left( \frac{\frac{B}{255} + 0.055}{1.055} \right)^{2.4} \times 100 & \text{if } \frac{B}{255} > 0.0405 \\ \frac{\frac{B}{255}}{12.92} \times 100 & \text{otherwise} \end{cases}$
$G' = \begin{cases} \left( \frac{\frac{G}{255} + 0.055}{1.055} \right)^{2.4} \times 100 & \text{if } \frac{G}{255} > 0.0405 \\ \frac{\frac{G}{255}}{12.92} \times 100 & \text{otherwise} \end{cases}$	$X = 0.4124R' + 0.3576G' + 0.1805B'$ $Y = 0.2126R' + 0.7152G' + 0.0722B'$ $Z = 0.0193R' + 0.1192G' + 0.9505B'$

XYZ → Lab Transformation Steps	
$L = 10\sqrt{Y}$ , $a = 17.5\left(\frac{1.02X - Y}{\sqrt{Y}}\right)$ , $b = 7\left(\frac{Y - 0.847Z}{\sqrt{Y}}\right)$	
Lab → XYZ Transformation	
$Y' = \frac{L+16}{116}$ $X' = \frac{a}{500} + Y'$ $Z' = Y' - \frac{b}{200}$ $X' = \begin{cases} X'^3 & \text{if } X'^3 > 0.008856 \\ \frac{X' - \frac{16}{116}}{7.787} & \text{otherwise} \end{cases}$ $Y' = \begin{cases} Y'^3 & \text{if } Y'^3 > 0.008856 \\ \frac{Y' - \frac{16}{116}}{7.787} & \text{otherwise} \end{cases}$	$Z' = \begin{cases} Z'^3 & \text{if } Z'^3 > 0.008856 \\ \frac{Z' - \frac{16}{116}}{7.787} & \text{otherwise} \end{cases}$ $X_{ref} = 95.047$ , $Y_{ref} = 100.000$ , $Z_{ref} = 108.883$ $X = X_{ref} X'$ , $Y = Y_{ref} Y'$ , $Z = Z_{ref} Z'$
XYZ → RGB	
$R' = \frac{X}{100}$ , $Y' = \frac{Y}{100}$ , $Z' = \frac{Z}{100}$ , $X' = \frac{X}{100}$ $R' = 3.2406X' - 1.5372Y' - 0.0415Z'$ $G' = -0.9689X' + 1.1875Y' + 0.0415Z'$ $B' = 0.0557X' - 0.2040Y' + 1.0570Z'$	$R = \begin{cases} (1.055R'^{2.4} - 0.055) \times 255 & \text{if } R' > 0.0031308 \\ 12.92R' \times 255 & \text{otherwise} \end{cases}$ $G = \begin{cases} (1.055G'^{2.4} - 0.055) \times 255 & \text{if } G' > 0.0031308 \\ 12.92G' \times 255 & \text{otherwise} \end{cases}$ $B = \begin{cases} (1.055B'^{2.4} - 0.055) \times 255 & \text{if } B' > 0.0031308 \\ 12.92B' \times 255 & \text{otherwise} \end{cases}$

**C. YUV** space fusion done by converting just multispectral image from RGB to YUV space then replace Y-band by PAN image, then backward the transformation to yield fused image.

RGB → YUV Transformation	YUV → RGB Transformation
$\begin{bmatrix} Y \\ U \\ V \end{bmatrix} = \begin{bmatrix} 0.299 & 0.587 & 0.114 \\ -0.147 & -0.289 & 0.436 \\ 0.615 & -0.515 & -0.100 \end{bmatrix} \begin{bmatrix} R \\ G \\ B \end{bmatrix}$	$\begin{bmatrix} R \\ G \\ B \end{bmatrix} = \begin{bmatrix} 1 & 0.000 & 1.140 \\ 1 & -0.396 & -0.581 \\ 1 & 2.029 & 0.000 \end{bmatrix} \begin{bmatrix} Y \\ U \\ V \end{bmatrix}$

### 2.3 PRINCIPAL COMPONENT ANALYSIS (PCA) FOR IMAGE FUSION

The principal Component Analysis fusion method can be performed by replacing the normalized brightness high resolution scene by the 1<sup>st</sup> PCA (i.e. PCA<sub>1</sub>), and then the inverse PCA transform is implemented as illustrated in the block diagram shown in Fig.(3).



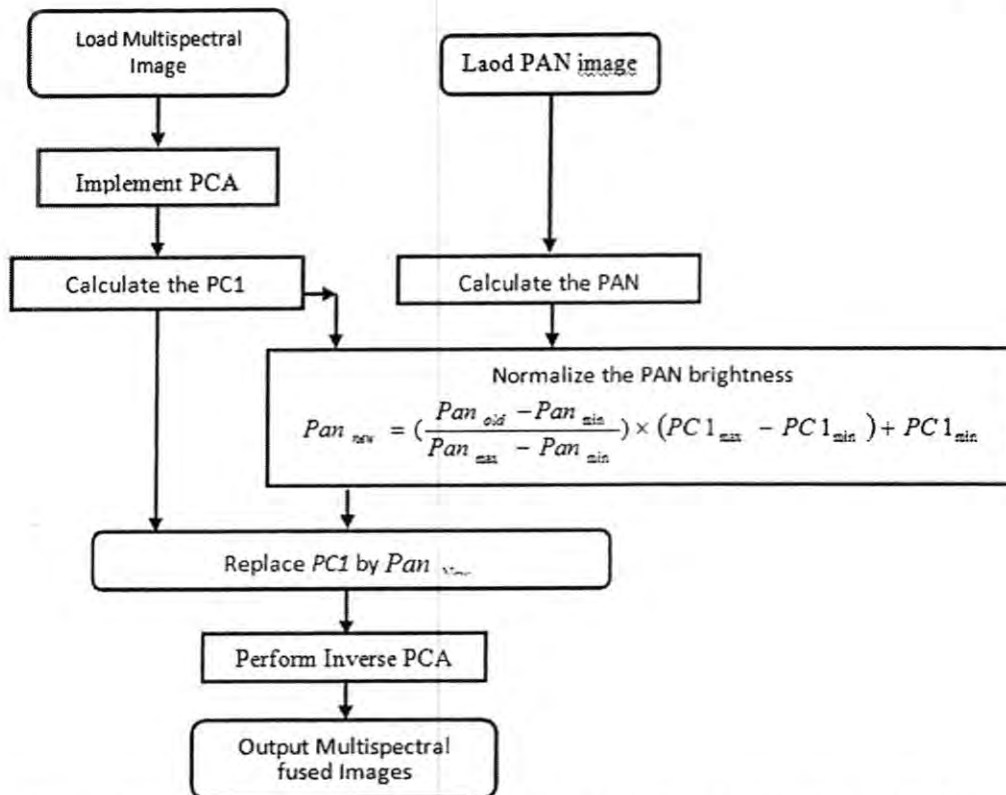


Figure -3: block diagram illustrating the procedures involved in the pca fusion method.

### 3. EXPERIMENTAL RESULTS

The unification results obtained by the fusion algorithms discussed above will be demonstrated and will be compared by displaying them. All algorithms applied on Mousel-City images (ETM+ [(natural colored, bands 1, 2, and 3), 28.5m resolution] image fused with Spot-Panchromatic "PAN" has 10m spatial resolution). The fusion results will be investigated, depending on their qualities (i.e. ascended from the worst to the best); i.e.

- 1) Wavelet Transformation;
- 2) Color Transformation; and

#### 3) Principle Component Analysis Transformation

Two types of wavelet transformations have been adopted and used to fuse the samples of images that illustrated in Fig.(4), These types are **Haar** and **Tap3/5** wavelet transformation algorithms.

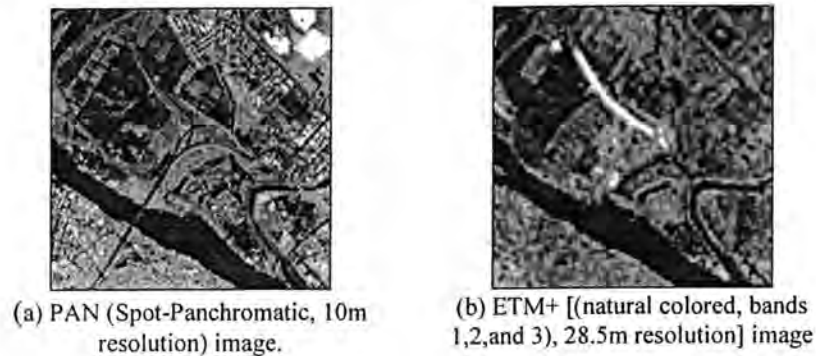


Figure -4:: Samples of Mousel-City images; (a) 256×256 pixels Spot-Panchromatic “PAN”, (b) 256×256 pixels Original natural colored ETM.

### 3.1 THE WAVELET FUSION TECHNIQUES

Two types of wavelet transformations have been adopted and used to fuse the samples of images, illustrated in Fig.(4); These are *Haar* and *Tap3/5* wavelet transformation algorithms.

#### A) The Haar Wavelet Transform Fusion Technique:

This fusion technique has been implemented in different ways, as illustrated in Figs.(5); i.e.

1. Replacing the 1<sup>st</sup> level Low-Low quarter of the ETM+ image by the same transform level Low-Low of the PAN image.
2. Replacing the 2<sup>nd</sup> level Low-Low sub-quarter of the ETM+ image by the same transform level Low-Low of the PAN image.
3. Replacing the 3<sup>rd</sup> level Low-Low sub-quarter of the ETM+ image by the same transform level Low-Low of the PAN image.

#### B) The Tap 3/5 Wavelet Transform Fusion Technique:

This fusion technique has been performed by the same way as that done with Haar method; the demonstrated results are in Figs. (5).

### 3.2 COLOR TRANSFORMATION FUSION TECHNIQUES

Different color transformation (i.e. HLS, Lab, and YUV) techniques have been adopted and used to unifying samples of different resolution images; This fusion technique has been implemented in different ways, as illustrated in Figs.(5) respectively; i.e.

A) *HLS* (Hue-Lightness- Saturation) space fusion can be implemented by replacing L-band (comes from multispectral image) by panchromatic image (PAN); it's done by:

1. Three components of the original image *R*, *G* and *B* are transformed into the HLS color space.
2. Then the low-resolution Lightness component *L* is replaced by the panchromatic band with higher spatial resolution.

3. The final step is to transform the image back to *RGB* color space with the original values of *H* and *S*.

**B) Lab** space fusion done by the following steps:

1. Convert Multispectral image from *RGB* to *XYZ* space by using the formula was shown in chapter three
2. Converting from *XYZ* to *Lab* space,
3. Replace L-band by PAN image then,
4. Reversing the transformation upward *RGB* enhanced image.

**C) YUV** space fusion done by

1. Converting Multispectral image from *RGB* to *YUV* space
2. Replace Y-band by PAN image
3. Then transform back to yield fused image.

### 3.3 THE PCA FUSION TECHNIQUES

PCA transformations have been used to fuse the samples of images; this technique has been implemented in different ways, as illustrated in Fig. (5); i.e.

1. Implement PCA transforms on multispectral image to product PC1, PC2, PC3..,
2. Replace PC1 by PAN image,
3. Inverse PCA transform to obtain fused image.

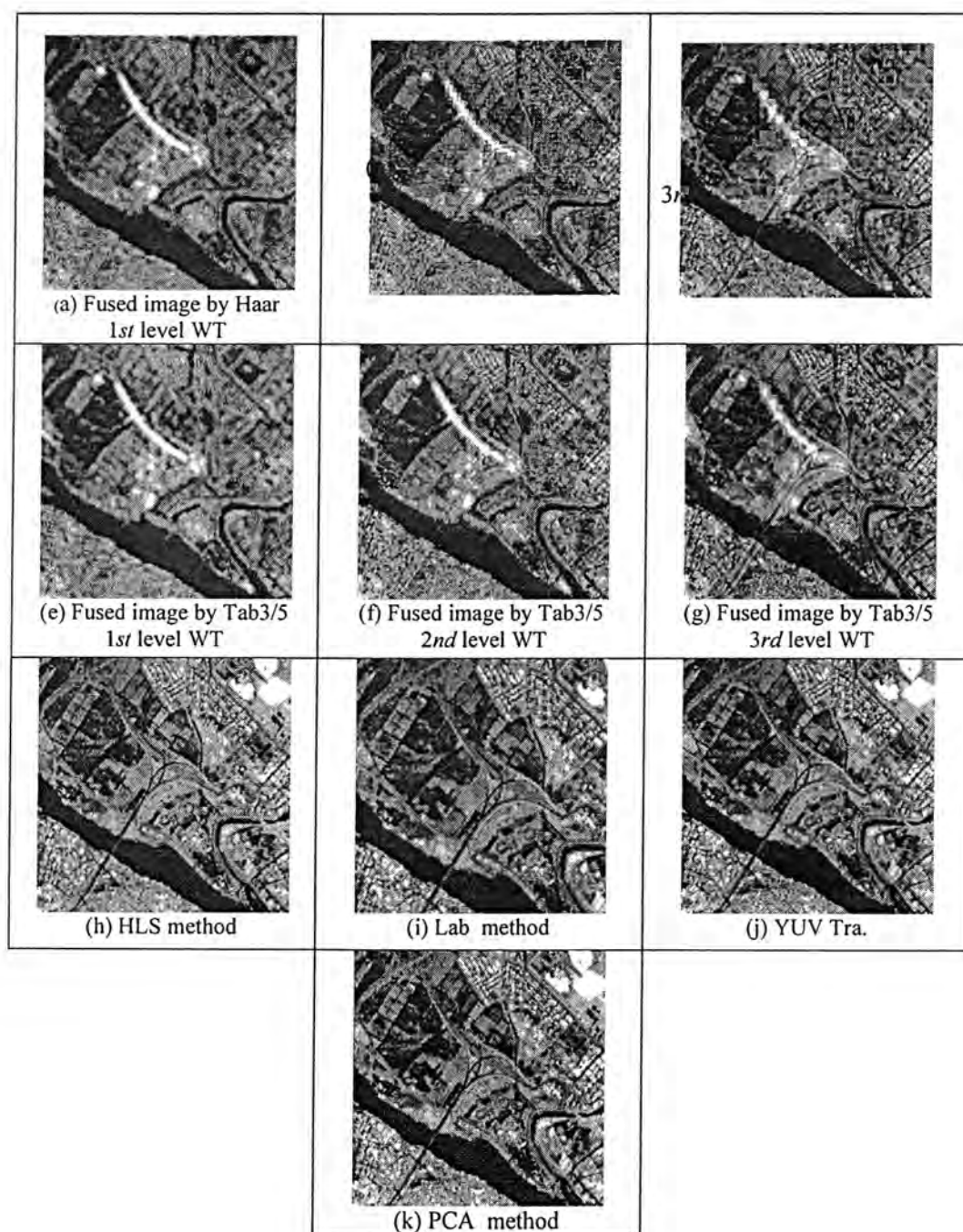


Figure -5: The results of fusion techniques beyond to different fusion ways

#### 4. CONCLUSIONS

The wavelet-Haar transformation was nastier then the Tap 3/5 because the Low-Low sub-band of the Haar holds less image energy (i.e. less image information). This was the same for the 2<sup>nd</sup> and 3<sup>rd</sup> transformation levels. For the 3<sup>rd</sup> transformation level, the Tap 3/5 performed better because most of the high frequency information was preserved at the High-Low, Low-High, and the High-High sub images.



Generally, the color transform fusion techniques are better than the wavelet techniques; this could be interpreted by the amount of energy preserved at the replaced color band than that at the wavelet sub-band. However, the HLS color transformation showed better quality than other color transformation, which means that this transformation produced less correlated information than other transformations; i.e. as the transform produce less correlate information means yield higher compacted image energy in few component.

It was very obvious, that the PCA technique yields a better result than the previously mentioned (color and wavelet transformations). This transformation, as can be seen at the most literature is considered as an optimum because of its de-correlation and its energy compaction.

### REFERENCES

1. Chavez, P. S., Sides, S. C., and Anderson, J. A., "Comparison of three different methods to merge multiresolution and multispectral data: TM & SPOT pan". Photogrammetric Engineering and Remote Sensing, Vol. 57, pp. 295-303,(1991).
2. Floyd F. Sabins, "Remote Sensing a Principle and Interpretation", chevron oil field research company, university of southern California and university of California, Los Angeles 1st Edition (1978).
3. Crawford M. M., Kumar S., Richard M. R., Je and Schwander A.N., "Fusion of Airborne Palarimetric and Interferometric SAR for Classification of Coastal Environments" IEEE Tran.Geosci&Engg .vol.39, No 3, pp.1306-1315 (1991).
4. Li L., and sheng Y., "Improving Spatial Resolution of IR Image by Means of Sensor Fusion", URL, (2000). <http://www.tropin.phy.uiaval.ca/jli>.
5. Garguct. B. J., Girel J. M., Chassery and Pautou G., "The Use of Multi-resolution Analysis and Wavelet Transform for Merging Spot panchromatic and multispectral image Data" Photogrammetric Engineering and Remote Sensing (1996).

## Fitting a Two Parameters of Weibull Distribution Using Goodness of Fit Tests

Rasha Abdul Hussein Ali  
Physical Education College, Baghdad University

Received 15/2/2012 – Accepted 20/6/2012

### الخلاصة

ان اختبار جودة التوفيق يستخدم لتحديد مدى نجاح قيم عينة الملاحظة التي تطابق النموذج المقترح. الاختبار يكون مرتكز على دالة التوزيع الاعتيادية، هذا التوزيع يكون موجود عندما يكون التوزيع الافتراضي كامل ومحدد ومعلمات التوزيع غير معروفة ويجب ان تخمن من بيانات العينة. في هذا البحث بعض النتائج العددية حصلت عليها من خلال دراسة محاكاة للحصول على قيم الحرجة لاختبار كولموجوروف – سميرنوف D، اختبار كرامير وفان ميسس  $W^2$  واختبار اندرسون – دارلينك  $A^2$ . بالنسبة لتوزيع ويبل ذو المعلمات المجهولة، هذه المحاكاة نفذت باستعمال تقنية مونت كارلو للحصول على جدول للقيم الحرجة لهذا الاختبارات. بالإضافة الى التحقق في مقارنة بين قوة كفاءة الاختبار D، اختبار  $W^2$  واختبار  $A^2$  لثلاث توزيعات بديلة.

### ABSTRACT

Goodness of fit test is used to determine how well the observed sample data fits with a proposed model. The test is based on the empirical distribution function, these test statistics are a variable when the hypothesized distribution is completely specified and the parameters of the distribution are unknown and must be estimated from the sample data. In this paper, some numerical results were obtained through a simulation study to obtain critical values of Kolmogorov-Smirnov D test, Cramer-Von Mises  $W^2$  test and Anderson-Darling  $A^2$  test. For weibull distribution with unknown parameters, this simulation was carried out using Monte Carlo techniques to create table of critical values for such tests. Furthermore, the power comparison between D test,  $W^2$  test and  $A^2$  test is investigated for a three alternative distributions.

**Key words:** Goodness-of-fit test, empirical distribution function, critical values, power studies.

### INTRODUCTION

The weibull distribution has been widely used as a model in many areas of application specifically in the studies of failure components and as a model for product life. The two parameters form, the density function is:

$$f(x; \alpha, \beta) = \begin{cases} \alpha\beta x^{\alpha-1} e^{-\beta x^\alpha}, & -\infty < x < \infty \text{ where } \alpha, \beta > 0 \\ 0 & \text{e.w.} \end{cases}$$

Goodness-of-fit tests for the two parameters of weibull distribution have received considerable attentions. Mann and others (1974) [1], Smith and Bain (1976) [2], Stephens (1977) [3], Littell and others (1979) [4], Chandra and others (1981) [5], Tiku and Singh (1981) [6], and Wozniak and Warren (1984) [7] have all discussed aspects of this problem. Mann and others (1974) [1] and Tiku and Singh (1981) [6] proposed a new statistics to test the goodness-of-fit of two parameter weibull distribution, Smith and Bain (1976) [2] proposed a test statistic analogous to the Shapiro-Francis statistics for testing the normality. The



Smith and Bain T statistic was based on the sample correlation between the order statistics of the sample and the expected value of the order statistics under the assumption that the sample comes from two parameter weibull distribution. For complete samples and two levels of censoring, they provided critical values for the samples containing 8, 20, 40, 60, or 80 observations. Stephens (1977) [3] produced tables of the asymptotic critical values of the Anderson-Darling  $A^2$  statistic and the Cramer-von Mises  $w^2$  statistics for various significance levels. Littell and others (1979) [4] compared the Mann, Scheuer, and Fertig S statistic, the Smith and Bain T statistic, the modified Kolmogorov-Smirnov D statistic, the modified Cramer-von Mises  $w^2$  statistic, and modified Anderson-darling  $A^2$  statistics through a series of power studies for sample size  $n = 10$  to 40. They also calculated critical values for the D,  $W^2$ , and  $A^2$  statistics for  $n = 10, 15, \dots, 40$ . Chandra and others (1981) [5] calculated critical values for the Kolmogorov-Simonov D statistic for  $n = 10, 20, 50$ , and infinity for three situations.

### 1. Goodness-of-fit technique

Goodness-of-fit technique means the methods of examining how well a sample of data agree with assumed distribution as its population the important goodness-of-fit techniques are:

1. Tests of chi-square types.
2. Moment ratio techniques.
3. Tests based on correlation.
4. Tests based on empirical distribution function.

Most of these test statistics suffer from serious limitations. In general test of chi-square type have less power due to loss of information caused by grouping. The distribution theory of chi-square statistics is a large sample theory. The higher order moments are usually underestimated and this fact prevents the use of moment ratio techniques and so would be the case with correlation type tests. Several power studies have revealed empirical distribution function (EDF) tests to be more powerful than other tests of fit for wide range of sample sizes [8][3].

We Consider tests of fit based on the empirical distribution function (EDF). The EDF is a step function, calculated from the sample, which estimates the population distribution function. EDF statistics are measures of the discrepancy between the EDF and a given distribution function and are used for testing the fit of the sample to the distribution this may be completely specified or may contain parameters which must be estimated from the sample.

## 2. Empirical distribution function [8]

Suppose a given random sample of size  $n$  is  $X_1, X_2, \dots, X_n$  and let  $X_{(1)} < X_{(2)} < \dots < X_{(n)}$  be the order statistics; and also suppose that the cumulative distribution function of  $X$  is  $F(x)$  and we assume this distribution to be continuous. The empirical distribution function (EDF) is defined as that proportion of the sample having a value less than or equal to  $x$ . [8]

$$F_n(x) = \sum_{i=1}^n f(x_i), \text{ where } f(x_i) = 1/n \text{ for } x_i \leq x, \text{ 0 e.w.}$$

More precisely, the definition is

$$F_n(x) = \begin{cases} 0 & x < X_{(1)} \\ i/n & X_{(i)} < x < X_{(i+1)}; i = 1, 2, \dots, n-1 \\ 1 & X_{(n)} \leq x \end{cases}$$

Thus,  $F_n(x)$  is a step function, calculated from the data; as  $x$  increase it take a step up of height  $1/n$  as each sample observation is reached. For any  $x$ ,  $F_n(x)$  records the population less than or equal to  $x$ , while  $F(x)$  is probability of an observation less than or equal to  $x$   $\{[F(x) = P(X \leq x)]\}$ . We can expect  $F_n(x)$  to estimate  $F(x)$ , and it is in fact a consistent estimator of  $F(x)$ ; as  $x \rightarrow \infty$ ,  $|F_n(x) - F(x)|$  decreases to zero with probability one.

## 3. Empirical distribution function statistics [9]

A statistic measuring the difference between  $F_n(x)$  and  $F(x)$  will be called an empirical distribution function (EDF) statistic. We shall concentrate on several EDF statistics which have attracted most attention. They are based on the vertical differences between  $F_n(x)$  and  $F(x)$ , and are conveniently divided into two classes, "the supremum class" and "the quadratic class". The supremum statistics include Kolmogorov  $D$  and Kuiper  $V$  statistics and quadratic statistics are Cramer-von Mises  $W^2$ , Anderson-Darling  $A^2$  and Watson  $U^2$  statistics.

**3.1 The supremum statistics. [10]** The first two EDF statistics,  $D^+$  and  $D^-$ , are respectively, largest vertical difference when  $F_n(x)$  is greater than  $F(x)$  and the largest vertical difference when  $F_n(x)$  is smaller than  $F(x)$ ; formally,

$$D^+ = \sup_x \{F_n(x) - F(x)\}$$

$$\text{And } D^- = \sup_x \{F(x) - F_n(x)\}$$

The most well-known EDF statistics is  $D$ , introduced by Kolmogorov-Simonov (1933):

$$D = \sup_{-\infty \leq x \leq \infty} |F_n(x) - F(x)| = \max_x (D^+, D^-)$$



**3.2 The quadratic statistics.** [11] A second and wide class of measures of discrepancy which is given by Anderson-Darling (1954) as:

$$W_n^2 = n \int_{-\infty}^{\infty} \{F_n(x) - F(x)\}^2 \Psi(x) dF(x)$$

Where  $\Psi(x)$ ,  $0 \leq x \leq 1$  is a suitable function which gives weights to the squared difference  $\{F_n(x) - F(x)\}^2$  where  $\Psi(x) = 1$  the statistic is Cramer-Von Mises statistic, now usually called  $W^2$ , and when  $\Psi(x) = [\{F_n(x)\}\{1 - F(x)\}]^{-1}$  the statistic is the Anderson-Darling(1954) statistic, called  $A^2$ . A modification of  $W^2$  is the Watson (1961) statistic  $U^2$  defined by:

$$U^2 = n \int_{-\infty}^{\infty} \left\{ F_n(x) - F(x) - \int_{-\infty}^{\infty} [F_n(x) - F(x)] dF(x) \right\}^2 dF(x)$$

Clearly  $U^2 = W^2 - (W)^2$

#### 4. Computing formulas

Form the basic definitions of the supremum statistics and the quadratic statistic given above in section (3) suitable computing formula must be found. To each observation  $x_i$ , on the random variable  $X$ , the Probability Integral Transformation (PIT) is applied to give a new observation  $z_i$  on a random variable  $Z$ . It may be defined as:

$z(x) = \int_{-\infty}^x f(x)dx$ , where  $f(x)$  is the probability density function of the random variable  $X$ .

Let  $Z = F(X)$ ; when  $F(x)$  is the true distribution of  $X$ , the new random variable  $Z$  is uniformly distributed between 0 and 1 [9]. Then  $Z$  has the distribution function  $F^*(z) = z$ ,  $0 \leq z \leq 1$ .

Suppose that a sample  $X_1, X_2, \dots, X_n$  gives the values  $Z_i = F(X_i)$ ,  $i = 1, 2, \dots, n$ , and let  $F_n^*(z)$  be the EDF of the values  $Z_i$ . EDF statistics can now be calculated from a comparison of  $F_n^*(z)$  with the uniform distribution for  $Z$ . It easy to show the values  $z$  and  $x$  related by  $z = F(x)$ , the corresponding vertical difference in the EDF diagrams for  $X$  and  $Z$  are equal; that is,

$$F_n(x) - F(x) = F_n^*(z) - F^*(z) = F_n^*(z) - z$$

Consequently EDF statistics calculated from the EDF of the  $Z_i$  compare with the Uniform distribution will take the same values as if they were calculated from the EDF of the  $x_i$  compare with  $F(x)$ . This leads to the following formulas [9] for calculating EDF statistics from the  $Z$ -values, the formulas involve the  $Z$ -values arranged in ascending order let  $Z_{(1)} < Z_{(2)} < \dots < Z_{(n)}$ . Then, with  $\bar{Z} = \sum_{i=1}^n \frac{Z_i}{n}$ ,

a) The Kolmogorov statistics  $D^+$ ,  $D^-$ ,  $D$ .

$$D^+ = \max_{1 \leq i \leq n} \left\{ \frac{i}{n} - Z_{(i)} \right\}; D^- = \max_{1 \leq i \leq n} \left\{ Z_{(i)} - \frac{(i-1)}{n} \right\}$$

$$D = \max_{1 \leq i \leq n} (D^+, D^-)$$

b) The Cramer-von Mises statistic  $W^2$ .

$$W^2 = \sum_{i=1}^n \left\{ z_i - \frac{2i-1}{2n} \right\}^2 + \frac{1}{12n}$$

c) The Anderson-Darling (1952-1954) statistic  $A^2$ .

$$A^2 = \frac{-(\sum_{i=1}^n (2i-1) \{ \ln z_i + \ln(1 - z_{n+1-i}) \})}{n} - n$$

## 5. The test statistic based on the EDF

Suppose the sample  $x_1, x_2, \dots, x_n$  has been obtained on the random variable  $X$ . We wish to test the null hypothesis is:  $X \sim F(x, \tilde{\theta})$ , i.e.  $H_0$ : a random sample of  $n$   $X$  - values comes from  $X \sim F(x, \tilde{\theta})$  where  $X \sim F(x, \tilde{\theta})$  is a continuous distribution and  $\tilde{\theta}$  is a vector of parameters. When  $\tilde{\theta}$  is fully specified i.e. the parameters are known. Then  $z_{(i)} = F(x_{(i)}; \theta)$  gives a set  $Z_{(i)}$  which, on  $H_0$ , are ordered uniform [9] and equations in section (4,a,b,c) are used to give EDF statistics. On the other hand,  $F(x, \theta)$  may be defined only as a member of a family of distributions, but all or part of the vector  $\tilde{\theta}$  may be known.

When  $\tilde{\theta}$  is known, distribution theory of EDF statistics is well-developed, even for finite samples, and tables are available for some time. When  $\tilde{\theta}$  contains one or more unknown parameters, these parameters may be replaced by estimates, to give  $\hat{\tilde{\theta}}$  as the estimate of  $\tilde{\theta}$ . Then formulas in section (4,a,b,c) may still be used to calculate EDF statistics, with  $Z_i = F(x_{(i)}; \hat{\tilde{\theta}})$ . However, even when  $H_0$  is true, The  $Z_{(i)}$  will now not be an ordered uniform sample, and the distributions of EDF statistics will be very different from those when  $\tilde{\theta}$  is known, they will depend on the distribution tested, the parameters estimated, and the method of estimation, as well as on the sample size. New points should then be used for the appropriate test, even for large samples; otherwise a serious error in significance level will result.

### 5.1 EDF statistics with unknown parameters

The EDF statistic will not depend on true values of unknown parameters, when unknown parameters are estimated by appropriate method. Therefore percentage points for EDF tests depend only on the sample size  $n$ . Since, the exact distributions of EDF statistics are very difficult to find, Monte Carlo studies have been extensively used to find points for finite  $n$ . Fortunately, for the quadratic statistics  $W^2$ ,  $U^2$  and  $A^2$ , asymptotic theory is available; the percentage points of these statistics



for finite  $n$  converge rapidly to the asymptotic points. No asymptotic theory for the statistics,  $D^+$ ,  $D^-$ ,  $D$  and  $V$  except in case  $F(x)$  is continuous and completely specified, the asymptotic points must be estimated.

David and Johnson (1948) [12] showed that if the parameters estimated are parameters of scale or location, and the estimators satisfy certain general conditions, then when one applies the probability integral transformation, the joint distribution of the transformed variables will not depend on the true parameter values.

## 6. EDF test for Weibull distribution

### 6.1 Estimation of unknown parameters

This section is concerned with the MLE of unknown parameters  $\alpha$  and  $\beta$  for weibull distribution which is given by

$$f(x; \alpha, \beta) = \begin{cases} \alpha\beta x^{\alpha-1} e^{-\beta x^\alpha}, & -\infty < x < \infty \text{ where } \alpha, \beta > 0 \\ 0 & \text{e.w.} \end{cases}$$

And whose distribution function takes the form

$$F(x; \alpha, \beta) = 1 - e^{-\beta x^\alpha} \quad 0 < x < \infty$$

When the parameters  $\alpha$  and  $\beta$  are unknown and are estimated from a random sample. Let  $x_1, x_2, \dots, x_n$  be a random sample of size  $n$  from weibull distribution with parameters  $\alpha$  and  $\beta$ .

It is well known that maximum likelihood estimators of  $\alpha$  and  $\beta$  are obtained by solving [13]

$$\frac{\partial}{\partial \alpha} \ln L(\alpha, \beta) = \frac{n}{\alpha} + \sum_{i=1}^n \ln x_i - \hat{\beta} \sum_{i=1}^n x_i^{\hat{\alpha}} \ln x_i = 0 \quad (1)$$

And

$$\frac{\partial}{\partial \beta} \ln L(\alpha, \beta) = \frac{n}{\beta} - \sum_{i=1}^n x_i^{\hat{\alpha}} = 0 \quad (2)$$

Solution for  $\hat{\alpha}$  and  $\hat{\beta}$  cannot be found analytically from the non-linear equations (1) and (2). An approximate solution for  $\hat{\alpha}$  and  $\hat{\beta}$  from equation (1) and (2) can be made iteratively by using Newton-Raphson method for solving non-linear equations as follows:

Let

$$f_1 = f_1(\hat{\alpha}, \hat{\beta}) = \frac{n}{\hat{\alpha}} + \sum_{i=1}^n \ln x_i - \hat{\beta} \sum_{i=1}^n x_i^{\hat{\alpha}} \ln x_i$$

And

$$f_2 = f_2(\hat{\alpha}, \hat{\beta}) = \frac{n}{\hat{\beta}} - \sum_{i=1}^n x_i^{\hat{\alpha}}$$

Suppose that  $(\hat{\alpha}^{(s)}, \hat{\beta}^{(s)})$  represent the approximate solution of  $(\hat{\alpha}, \hat{\beta})$  at stage  $(s)$ . Then the approximate solution at stage  $(s+1)$  for  $(\hat{\alpha}^{(s)}, \hat{\beta}^{(s)})$  is:

$$\hat{\alpha}^{(s+1)} = \hat{\alpha}^{(s)} + \delta_1 \quad (3)$$

$$\hat{\beta}^{(s+1)} = \hat{\beta}^{(s)} + \delta_2$$

(4)

Solving (3) and (4), we get:

$$\hat{\alpha}^{(s+1)} = \hat{\alpha}^{(s)} - \frac{1}{ac - b^2} (cf_1 - bf_2)$$

$$\hat{\beta}^{(s+1)} = \hat{\beta}^{(s)} - \frac{1}{ac - b^2} (-bf_1 + af_2)$$

Let  $y_i = \ln x_i$ ;  $i = 1, 2, \dots, n$  and  $z_{(i)} = F(x_{(i)}; \hat{\alpha}, \hat{\beta})$  where  $x_{(i)}$  is the  $i$ th order statistics.

## 6.2 Calculation of test statistics

A goodness-of-fit test is used to test null hypothesis.

$H_0$ : the random sample  $x_1, x_2, \dots, x_n$  comes from the weibull distribution  $f(x; \alpha, \beta)$  with unknown parameters  $\alpha$  and  $\beta$ .

We will construct on the following main test for goodness-of-fit for the weibull distribution.

1. Modified Kolmogorov-Smirnov statistic  $D$ .

$$D = \sup |F(x_{(i)}; \hat{\alpha}, \hat{\beta}) - F_n(x)| = \sup |(1 - e^{-\beta x^\alpha}) - F_n(x)|$$

Where  $F_n(x) = \sum_{i=1}^n f(x_i)$ ,  $f(x_i) = \frac{1}{n}$  for  $x_i \leq x$ , 0 e. w.

Is the empirical distribution function of the sample.

This is equivalent to  $D = \max(D^+, D^-)$  where  $D^+ = \max_{1 \leq i \leq z_{(i)}} \left\{ \frac{i}{n} - z_{(i)} \right\}$ ,  $D^- = \max_{1 \leq i \leq z_{(i)}} \left\{ z_{(i)} - \frac{(i-1)}{n} \right\}$

Where  $z_{(i)} = F(x_{(i)}; \hat{\alpha}, \hat{\beta})$  and  $x_{(i)}$  is the  $i$ th order statistics.

2. Modified Cramer-Von Mises statistics  $W^2$ .

$$W^2 = n \int_{-\infty}^{\infty} \{F_n(x) - F(x)\}^2 dF(x)$$

Where  $F_n(x) = \sum_{i=1}^n f(x_i)$ . Put  $Z = F(x)$  where

$$Z_n(n) = \begin{cases} 0 & z < Z_i \\ i/n & Z < z < Z_{i+1} \\ 1 & Z_{(n)} \leq z \end{cases} \quad , i=1, 2, \dots, n-1$$

$z_{(0)} = 0$  and  $z_{(n+1)} = 1$ . Then

$$W^2 = n \int_0^1 \{z_n(n) - z\}^2 dz = n \sum_{i=1}^n \int_{z_{(i)}}^{z_{(i+1)}} \left[ \frac{i}{n} - z \right]^2 dz$$



$$\begin{aligned}
&= n/3 \sum_{i=1}^n \left[ \left( z_{(i+1)} - 1/n \right)^3 - \left( z_{(i)} - 1/n \right)^3 \right]^2 \\
&= \sum_{i=1}^n \left\{ z_{(i)} - \frac{2i-1}{2n} \right\}^2 + \frac{1}{12n} \\
&= \sum_{i=1}^n \left\{ 1 - e^{-\beta x^\alpha} - \frac{2i-1}{2n} \right\}^2 + \frac{1}{12n}.
\end{aligned}$$

### 3. Modified Anderson-Darling statistic $A^2$ .

$$\begin{aligned}
A^2 &= n \int_{-\infty}^{\infty} \{F_n(x) - F(x)\}^2 \frac{1}{F(x)(1-F(x))} dF(x) \\
&= n \int_0^1 \{z_n(n) - z\}^2 \frac{1}{z(1-z)} dz \\
&= -n - \frac{1}{n} \sum_{i=1}^n (2i-1) [\ln z_{(i)} + \ln \{1 - z_{(n+1-i)}\}].
\end{aligned}$$

The results of David and Johnson (1948) [12] imply that the distributions of  $D$ ,  $W^2$  and  $A^2$  do not depend upon the values  $\alpha$  and  $\beta$ . Therefore without loss of generality, the distributions of  $D$ ,  $W^2$  and  $A^2$  can be obtained assuming  $\alpha = \frac{1}{2}$  and  $\beta = 1$ . (See [4] for results may be used to arrive at the same conclusion, specific to the Weibull distribution).

## RESULT AND DISCUSSION

The main objective of the research reported here in were two things: first to show the goodness-of-fit test for weibull distribution by using the test  $D$ ,  $W^2$  and  $A^2$  for the sample of size  $n$ , and second to compare between the power functions of test statistics  $D$ ,  $W^2$  and  $A^2$  for several distributions. To calculate the critical values for proposed test statistics for weibull distribution with unknown parameters, by Monte Carlo simulation which is carried out via Mathcad (2001) package [14]. The following steps are used in calculating critical values for the proposed test statistics:

1st step A random sample  $X_1, X_2, \dots, X_n$  from weibull distribution was generated. Firstly a random sample  $Z_1, Z_2, \dots, Z_n$  of  $n$  order statistics from a uniform (0,1) distribution was generated, then the  $i$ th order statistic from the  $W(\alpha, \beta)$  with  $\alpha = \frac{1}{2}$  and  $\beta = 1$  will obtained as follows

$$X_{(i)} = \frac{-1}{\beta} \{\ln(Z_{(i)})\}^{1/\alpha}$$

2nd step This random sample was used to estimate the unknown parameters by method of MLE in section (6.1).

3rd step The resulting maximum likelihood estimator of the unknown parameters is used to determine the hypothesized cumulative distribution function for the weibull distribution.

4th step Selected sample size as  $n = 10(10)100$ . The appropriate test statistics mentioned in section (6.2) was calculated for the given values of  $n$ .

5th step This procedure was repeated 10000 times, thus generating 10000 independent values of the appropriate test statistics. These 10000 values were then ranked, and the values of these test statistics at five significance levels, i.e.,  $\alpha = 0.01, 0.05, 0.10, 0.15$ , and  $0.20$  are calculated.

Table (1) list the critical values for the statistics test  $D$ ,  $W^2$  and  $A^2$ , using Monte Carlo method.

The power of a goodness-of-fit test is defined as the probability that a statistic will lead to the rejection of the null hypothesis,  $H_0$ , when it is false, i.e. when a sample is not from the hypothesized population but an alternative population [1].

To evaluate our results we conducted a power study of the three statistics  $D$ ,  $W^2$  and  $A^2$  using three different distributions.

- The gamma distribution with density  $(\Gamma(t))^{-1}x^{t-1}e^{-x}$  denoted by  $\Gamma(t)$ .
- The exponential distribution with density  $te^{-tx}$  denoted by  $\exp(t)$ .
- The chi-square distribution with density  $\frac{1}{2^{n/2}}\Gamma\left(\frac{n}{2}\right)x^{n/2-1}e^{(-\frac{x}{2})}$  denoted by  $\chi_n^2$ .

We generate 1000 pseudo- random samples of size  $n$  from each of the three alternative distributions considered. We then calculated each of the three test statistics and compared them to its respective critical values from Table (1). In this case we counted the number of rejections of the null hypothesis. We repeated this procedure for sample size  $n=10(10)40$ .

Results of power study are presented in Table (2) which show that the Anderson-Darling  $A^2$  is general has a larger power than (superior to) both the Kolmogorov-Smirnov  $D$ , and Cramer-Von Mises  $W^2$  statistics for the alternatives presented. Neither  $D$  nor  $W^2$  appears to be very powerful across this group of alternative distributions.

## CONCLUSIONS

From the results of the critical points appears to be very good for the range of sample sizes  $n=10(10)100$  at  $\alpha = 0.01, 0.05, 0.10, 0.15$  and  $0.20$  significance levels for the sample sizes. And for  $n=10(10)40$  at significance levels considered the Anderson-Darling  $A^2$  statistic appears to be the best of EDF test statistics for testing the goodness of fit of a two parameter weibull distribution to a set of data because the larger power it displayed in the power studies. The Kolmogorov-Smirnov  $D$  tends to be the least powerful among the three EDF tests considered here. So it may advisable to use the Anderson-Darling  $A^2$  and Cramer-Von Mises  $W^2$  test statistics for testing the two parameter weibull distribution.

Table-1: Two weibull critical values for  $D$ ,  $W^2$  and  $A^2$  when  $n=10(10)100$ .

Sample size $n$	Test statistics	Significance levels				
		0.01	0.05	0.1	0.15	0.2
10	$D$	0.3109	0.2903	0.2785	0.2561	0.1955
	$A^2$	0.9522	0.7536	0.6437	0.2411	0.2001
	$W^2$	0.2361	0.2102	0.1995	0.1813	0.1651
20	$D$	0.3162	0.2982	0.2791	0.2565	0.1958
	$A^2$	0.9529	0.7539	0.6439	0.2423	0.2016
	$W^2$	0.2369	0.2116	0.1999	0.1815	0.1659
30	$D$	0.3241	0.2992	0.2798	0.2569	0.1962
	$A^2$	0.9532	0.7545	0.6449	0.2429	0.2025
	$W^2$	0.2372	0.212	0.2009	0.1822	0.1662
40	$D$	0.3295	0.3002	0.2802	0.2572	0.1965
	$A^2$	0.9534	0.7566	0.6452	0.2433	0.2028
	$W^2$	0.2377	0.2139	0.2015	0.1839	0.1666
50	$D$	0.3309	0.3012	0.2818	0.2575	0.1973
	$A^2$	0.9537	0.7583	0.6461	0.2441	0.2030
	$W^2$	0.2381	0.2141	0.2025	0.1845	0.1672
60	$D$	0.3322	0.304	0.2823	0.2577	0.1979
	$A^2$	0.9544	0.7591	0.6465	0.2448	0.2041
	$W^2$	0.2385	0.2149	0.2027	0.1849	0.1677
70	$D$	0.3354	0.3085	0.2829	0.2581	0.1980
	$A^2$	0.9548	0.7592	0.6478	0.2461	0.2059
	$W^2$	0.2395	0.2156	0.2031	0.1853	0.1683
80	$D$	0.3398	0.3102	0.2831	0.2592	0.1986
	$A^2$	0.9551	0.7631	0.6489	0.2465	0.2092
	$W^2$	0.2401	0.2159	0.2039	0.1861	0.1691
90	$D$	0.4115	0.3129	0.2836	0.2594	0.1991
	$A^2$	0.9552	0.7635	0.6501	0.2481	0.2067
	$W^2$	0.2422	0.2166	0.2045	0.1874	0.1695
100	$D$	0.4191	0.3153	0.2842	0.2600	0.1995
	$A^2$	0.9556	0.7642	0.6514	0.2486	0.2078
	$W^2$	0.2429	0.2173	0.2048	0.1881	0.1702



Table -2: powers of tests for weibull distribution when  $n=10(10)40$ .

Sample size n	Significance levels	Alternatives								
		Gamma			lognormal			Chi square		
		D	W <sup>2</sup>	A <sup>2</sup>	D	W <sup>2</sup>	A <sup>2</sup>	D	W <sup>2</sup>	A <sup>2</sup>
10	0.01	0.0032	0.0059	0.0098	0.0532	0.1029	0.1145	0.1129	0.1436	0.1762
	0.05	0.0048	0.0063	0.0113	0.0984	0.1031	0.1248	0.1162	0.1411	0.1791
	0.10	0.0106	0.0098	0.0120	0.1321	0.1096	0.1298	0.1134	0.1598	0.1856
	0.15	0.0123	0.0105	0.0131	0.1329	0.1124	0.1301	0.1193	0.1564	0.2002
	0.20	0.0114	0.0109	0.0139	0.1351	0.1225	0.1331	0.1209	0.1613	0.2141
20	0.01	0.0164	0.0550	0.1889	0.2109	0.1983	0.2832	0.0138	0.0197	0.0241
	0.05	0.0654	0.0875	0.0932	0.2110	0.2110	0.2902	0.0154	0.0229	0.0276
	0.10	0.1277	0.1951	0.1248	0.2134	0.2156	0.3021	0.0162	0.0239	0.0293
	0.15	0.1468	0.1932	0.2301	0.2198	0.2163	0.3109	0.0164	0.347	0.0351
	0.20	0.1766	0.2009	0.2998	0.2264	0.285	0.3507	0.0175	0.0399	0.0342
30	0.01	0.0150	0.0183	0.0225	0.1196	0.1880	0.2847	0.0072	0.0105	0.0125
	0.05	0.0764	0.0894	0.0869	0.1459	0.1941	0.2932	0.0088	0.0125	0.0131
	0.10	0.1310	0.1520	0.1437	0.1481	0.1880	0.3012	0.0109	0.0143	0.0149
	0.15	0.1895	0.2026	0.2082	0.1554	0.1941	0.3103	0.0127	0.0147	0.0166
	0.20	0.2403	0.2513	0.2799	0.1594	0.2141	0.3219	0.0131	0.0158	0.0177
40	0.01	0.0111	0.0132	0.0215	0.1200	0.1751	0.3197	0.0193	0.0225	0.0199
	0.05	0.0138	0.0164	0.0237	0.1491	0.1932	0.3243	0.0208	0.0236	0.0241
	0.10	0.0142	0.0185	0.0296	0.1625	0.2281	0.3276	0.0211	0.0315	0.337
	0.15	0.0159	0.0191	0.0361	0.1931	0.2531	0.3599	0.0319	0.0377	0.0424
	0.20	0.0221	0.0239	0.0399	0.2175	0.3019	0.3861	0.0337	0.0389	0.0451

## REFERENCES

1. Mann, N. R., Schafer, R. E. and Singpurwalla, N. D. (1974). *"Methods for statistical analysis of reliability and life data"*. John Wiley & Sons.
2. Smith, R.M.; Bain, L.J. (1976). *"Correlation type goodness-of-fit statistics with censored sampling"*. Communications in Statistics, Part A-Theory and Methods. 5:119-132.
3. Stephens, M.A. (1977). "Goodness-of-fit for the logistic distribution". Biometrika, 64, 585-588.
4. Littell, R. D.; McClave, J. R.; and Offen, W. W. (1979). "Goodness-of-fit tests for two parameters Weibull distribution or extreme-value distribution with unknown parameters". Communications in Statistics. Part B-Simulation and Computation. 8:257-269.
5. Chandra, M.; Singpurwalla, N.D.; Stephens, M.A. (1981). *"Kolmogorov statistics for tests of fit for the extreme-value and Weibull distribution"*. Journal of the American Statistics Association. 76: 729-731.
6. Tiku, M.L.; Singh, M. (1981). "Testing the two parameter Weibull distribution". Communications in Statistics, Part A-Theory and Methods. 10:907-917.



7. Wozniak, P.J.; Warren, W.G. (1984). "*Goodness of fit for the two-parameter Weibull distribution*". Presented at the American Statistical Association National Meeting, Philadelphia, PA.
8. Stephens, M. A. "*EDF statistics for goodness-of-fit and some comparisons*". J. Am. Statist Assoc. 69, 730-737(1974).
9. D'Agostino, R.B. and Stephens, M. A. "*Goodness of fit techniques*". Marcel Dekker, New York(1986).
10. Kolmogorov, A. N. "Sulla determinazione empirica di una legge di distribuzione". 1<sup>st</sup>. Ital. Attuari, 83-91(1933).
11. Anderson, T. W. and Darling, D. A. "*A test of goodness of fit*". J. Am. Stat. Assoc. 49:765-769(1954).
12. David, F. N.; Johnson, N. L. "*The probability integral transformation when parameters are estimated from the sample*". Biometrika. 35:182-190(1948).
13. Ahmed, S. A. "*Estimation of parameters for weibull distribution with application by using Monte Carlo simulation*". M. Sc. Thesis, Dept. of Math. & Comp. Applications, Al-Nahrain University(2008).
14. Mathcad professional. (1986-2000). Mathsoft, Inc(2001).

## Investigation of Reciprocity of Energy Loss in Gases and Solid Materials

Baida Mohsen Ahmed

College of Science, Department of physics, Al-Mustanseria University

Received 9/4/2012 – Accepted 20/6/2012

### الخلاصة

الهدف من الانعكاسية هو حدوث عملية التغير في التصادمات الغير مرنة بين الايون والذرة وحدث تغير في شحنة القذائف مع الهدف. حيث تم تطبيق فقدان الطاقة للمقطع العرضي عند السرعة الواطئة والعالية وتحقيق الانعكاسية والشحنة المؤثرة لمواد مختلفة مثل (Kr,Ar,Si,Ge,Bi,Ni)، تم استخدام صيغة Lindhard (1961) and Firsove (1957) ومن ثم تطبيق معادلة H.Paul (2009) للتحقق من النتائج نظريا. حصلنا على نتائج جيدة تتفق مع نتائج SRIM في الانعكاسية.

### ABSTRACT

The principle of reciprocity, is the invariance of the inelastic excitation in ion-atom collisions against interchange of projectile and target. The energy loss has been applied to the electronic stopping cross section at low- and high velocity. The present work investigates the reciprocity and effective charge on different material, involving (Kr,Ar,Si,Ge,Bi,Ni) are projectile ions or as target material, using Lindhard (1961) and Firsove (1957) model, and apply equation of H.paul (2009) to find and to check theoretically, the reciprocity in metal, semiconductors and gases theoretically. We got good result in reciprocity agreement with SRIM result.

### INTRODUCTION

The energy loss and the range of ions in matter are of interest in many disciplines of science such as radiation physics, radiation damage, material analysis by ion beams, ion implantation, semiconductor technology, and metallurgy. Especially, ion implantation profiles are frequently used to determine the surface properties of materials modified by the implantation process.[1]

The stopping of charged particles in matter is characterized primarily by the mean energy loss per path length or stopping force  $dE/dx$ .

Reciprocity denotes the fact that the electronic energy loss of two colliding atoms is independent of the frame of reference. In other words, the cross section for a given excitation is the same. The principle of reciprocity invariance of elastic excitation in ion-atom collision against interchange of projectile and target.[1]

The next stop to be considered is effective nuclear charge.

Generally the effective charge is the charge left by the valence electrons after you have taken into account the number of shielding electrons that surround the nucleus.[2] Effective charge important to evaluate because describe the electronic properties of semiconductors, ionization potentials, and energy gaps.[3]

## Theories

### Firsov model

Firsov consider an ion with a speed  $v$  below the Bohr velocity  $v_b$ , colliding with a target atom at rest. Firsov view such an event is indicated as: [4]

- At any instant of time there exists a surface, the 'Firsov surface', which defines the respective domains of the collision partners.
- This surface is thought to be placed so that the normal component of the electric field vanishes everywhere.
- Electrons passing from the target domain to the projectile domain are taken as captured and hence transfer a momentum  $-mv$  to the projectile, thus causing it to slow down.
- The cross section for momentum transfer is determined by the electron flux from the target to the projectile domain.

Firsov expression is found for the electronic energy loss is given by

$$T_e(\rho) = m \int \frac{dR}{dt} \cdot R \int ds \frac{1}{4} n(r) v_e(r) \dots \dots \dots (1)$$

where  $R(t)$  denotes the trajectory of the projectile, is an integration Firsov surface;  $n(r)$  is the electron density;  $v_e(r)$  is the average electron speed. The factor  $1/4$  originates in the assumption, Firsove model condition is  $0.02 < v/v_b < 0.5$ .

After integration over the impact parameter  $\rho$  we obtain the stopping cross section:

$$S_e = \int_0^\infty 2\pi\rho d\rho T_e(\rho) = \frac{4\pi^2}{3} m v \int_0^\infty r^4 dr n(r) v_e(r) \dots \dots \dots (2)$$

With some functions which may depend on Thomas-fermi relation, the stopping cross section reduce to

$$S_e = C \hbar Z^{4/3} a v \dots \dots \dots (3)$$

$C=20.4$  is the integral constant.

$Z$ = atomic number.

$a$ = screening radius.

$v$ =velocity of incident ion.

### Lindhard-Scharff

Firsove Model is study the stopping slow ions on target, where assumed the projectile capturing by target electrons. Lindhard-Scharff operates with elastic collisions between ion and atom of target and inelastic collisions between ion and target electrons. Two models leading to know material properties such as density and velocity distribution. The key quantity in such a description is the transport cross section  $\delta(v)$ .

$$d(\nu) = d(\nu, \theta)(1 - \cos\theta) \dots \dots \dots (4)$$

$d(\nu, \theta)$  : cross section as a function to velocity and scattering angle,  $\theta$  is the scattering angle of electron.

The stopping of Fermi-Dirac velocity distribution is:

$$S_e(\nu, \nu_f) = m \nu \nu_f d(\nu_f) \dots \dots \dots (5)$$

$\nu_f$  = Fermi speed

Tomas Fermi assumption the energy loss in a collision at impact parameter  $\rho$

$$T_e(\nu, \rho) = \int_{-\infty}^{\infty} dx n(x, \rho) s(\nu, \nu_f) \dots \dots \dots (6)$$

By integrating eq (6) and use some factors, find the lindhard-scharff formula.

$$S_e = \xi 8\pi \frac{z_1 z_2}{(z_1^{2/3} + z_2^{2/3})^{3/2}} a \cdot \hbar \nu \dots \dots \dots (7)$$

$\xi = Z_1^{1/6}$ ,  $\hbar = h/2\pi$ ,  $\nu$  = velocity of ion,

Lindhard-Scharff condition  $\nu \ll Z_1^{2/3} \nu_o$ .

Use Paul's equation experimental stopping cross sections to investigation theoretically eqs.(3) and (7) under condition

$$0 \leq \nu \leq 0.5 Z_1^{2/3} \nu_o \dots [1]$$

$$R = \frac{S(z_1 \rightarrow z_2) - S(z_2 \rightarrow z_1)}{S(z_1 \rightarrow z_2) + S(z_2 \rightarrow z_1)} \dots \dots \dots (8)$$

### Charge-exchange effects of cross sections

Charge exchange is important parameter, the charge-exchange cross section which involves the electron capture and loss processes. Three different charge transfer processes have been proposed to understand electronic exchange mechanisms for ions moving in condensed matter[5].

- (i) Auger processes, in which an electron is captured ( or lost) by the ion creating an electronic excitation in solid.
- (ii) Resonant processes, which is see by the ion as a time-dependent perturbation.
- (iii) Sell processes, where an inner shell electron of a target atom is captured directly by the moving ions.

When incident ions in solid targets and after pass through some penetrations distance the ions reach to state of charge equilibrium.



There are many methods lead to concept of effective charge, one of this method is energy loss.

Stopping power of atomic number  $Z$  and velocity  $v$  preparation with effective charge according to perturbation theory.[8]

The equation of evaluate effective charge is:

$$Z^* = Z_1 \left( 1 - e^{-0.92v/Z_1^{2/3}} \right) \dots\dots\dots \theta$$

### Band gab in material

In insulating material, all of the electrons are held within the valence band, and no electrons are in the conduction band and free to move around to create currents. In a conducting material, the outer electrons fill the valence band but they also occupy the conduction band, so some electrons are available to move around and create currents. Also, in an insulator, the band gap is large meaning that an electron must gain a lot of energy to move up to the conduction band. In a conductor. A semiconductor is much like an insulator in that its outer electrons fill the valence band but do not occupy the conduction band; however, the band gap is much smaller than in an insulator. Figure (1) appear the energy gab in (Insulator, Semiconductor and Metal) in (0)k this different in energy gab limited the move electron from valance band to contractive band [6]

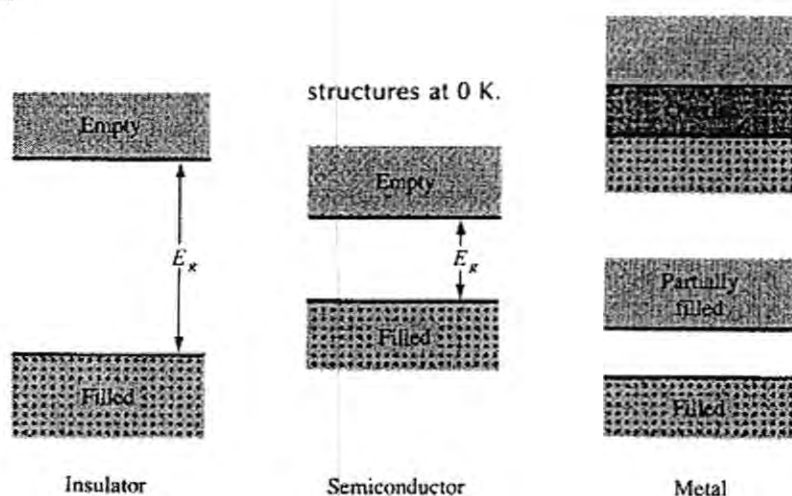


Fig -1:energy band gab in metal,semiconductor and insulator at (0)k[6]

**Implications:  
Reciprocity**

Reciprocity denotes the fact that the electronic energy loss of two colliding atoms is independent of the frame of reference. In other words, the cross section for a given excitation is the same, regardless of whether projectile A with a speed  $v$  hits target B at rest, or projectile B with the same speed  $v$  hits target A at rest.[1]

Sigmund suggested that, as a first estimation, the stopping cross section may be determined from the inverted ion-target system by applying the concept of reciprocity. The principle of reciprocity is based on the invariance of the inelastic excitation in ion-atom collisions against interchange of projectile and target, and is applicable in the low velocity range ( $v \leq v_0$  or  $E \text{ keV/nucleon} \leq 25$ ), where the projectiles are neutral and the probability for electron loss is small. Reciprocity in the stopping cross section can be observed by the symmetric expression for  $Z_1$  and  $Z_2$  in Firsov's theory and in the formula of Lindhard and Scharff. More recently, the binary stopping theory predicts strict reciprocity in the velocity range where the projectile is neutral.[7]

With increasing velocity the equilibrium charge of the projectile will increase, and the difference in the charge versus velocity dependence will increase with increasing difference between  $z_1$  and  $z_2$ .

## RESULTS AND DISCUSSION

Reciprocity does not require the positions of minimum and maximum stopping cross sections to be fixed to specific  $Z$ -values. With increasing velocity, the equilibrium charge of the projectile will increase, and the difference in the charge versus velocity dependence will increase with increasing difference between  $Z_1$  and  $Z_2$ .

Using eqs. (3) and (7) to find reciprocity of stopping atom in different material (gas, metal and semiconductor) depending on Lindhard and Fivsove model and compare with SRIM theory. In All figures see the approximation between two theories Lindhard and Fivsove, In figure (2) obvious difference in curve between (Ar-Kr arrive to  $30 \times 10^3$ ) and (Kr-Ar arrive to  $40 \times 10^3$ ) that is because the atomic number of (Ar=18) less than (kr=36) therefore number of collision when incident (kr on Ar) more than incident (Ar on kr). And see same thing in figures (3,4) between (Ge-Si) and (Bi-Ni ).

When compare between figures ( 2,3,4) The curve of reciprocity appear in metal-metal larger from semiconductors and gasses that because the number of atomic is larger in metal than others., Also fined energy gab in gases and semiconductor large than metal that make the number of collisions in metal is more and the curve in metal arrive to ( $50 \times 10^3$ ) therefore the reciprocity in metal is large. using equation (8) by H.Paul to investigation the reciprocity theoretically, where see its investigation the reciprocity from result obtain it.

The reciprocity investigation more in stopping nuclei that is because the distribution of nuclear. So the results are smaller than Lindhard and Firsov because SRIM dependent Bohr velocity but Lindhard and Firsov dependent Behte velocity

The next thing to be considered effective nuclear charge, electron left the valence band after you have taken energy from incident ions and move conductive band. When electron move change the charge and happens many processes loss and capture until arrive to state of charge equilibrium. From figures see the effective charge preoperational exponential with velocity.

### Gas-gas

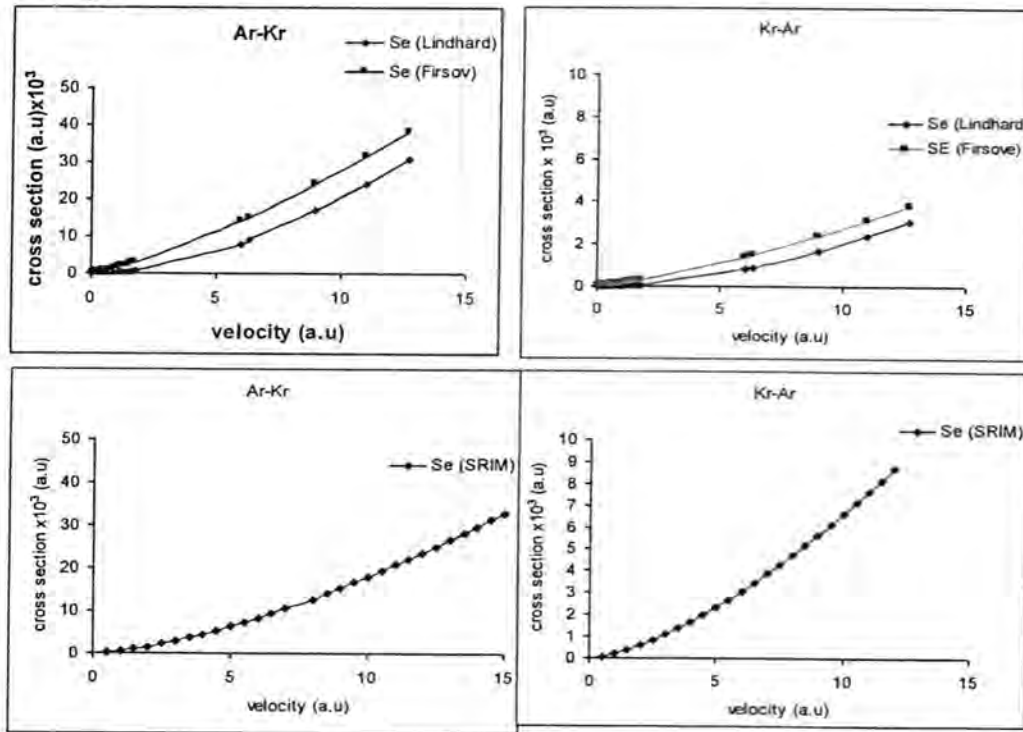


Fig -2:Reciprocity of stopping cross section: Kr in Ar and Ar in Kr (gas-gas),SRIM[9]

By application eq. (8) on (Ar-Kr) at velocity (12.68 a.u)

$$R = \frac{S(z_1 \rightarrow z_2) - S(z_2 \rightarrow z_1)}{S(z_1 \rightarrow z_2) + S(z_2 \rightarrow z_1)}$$

$$\frac{3069.72 - 4066.22}{4066.22 + 3069.72} = -0.1$$

SRIM Reciprocity (Ar-Kr) at velocity (12.681 a.u)

$$R = \frac{9476.901 + 25693.521}{25693.521 - 9476.901}$$

$$= -0.4$$

### semiconductor-semiconductor

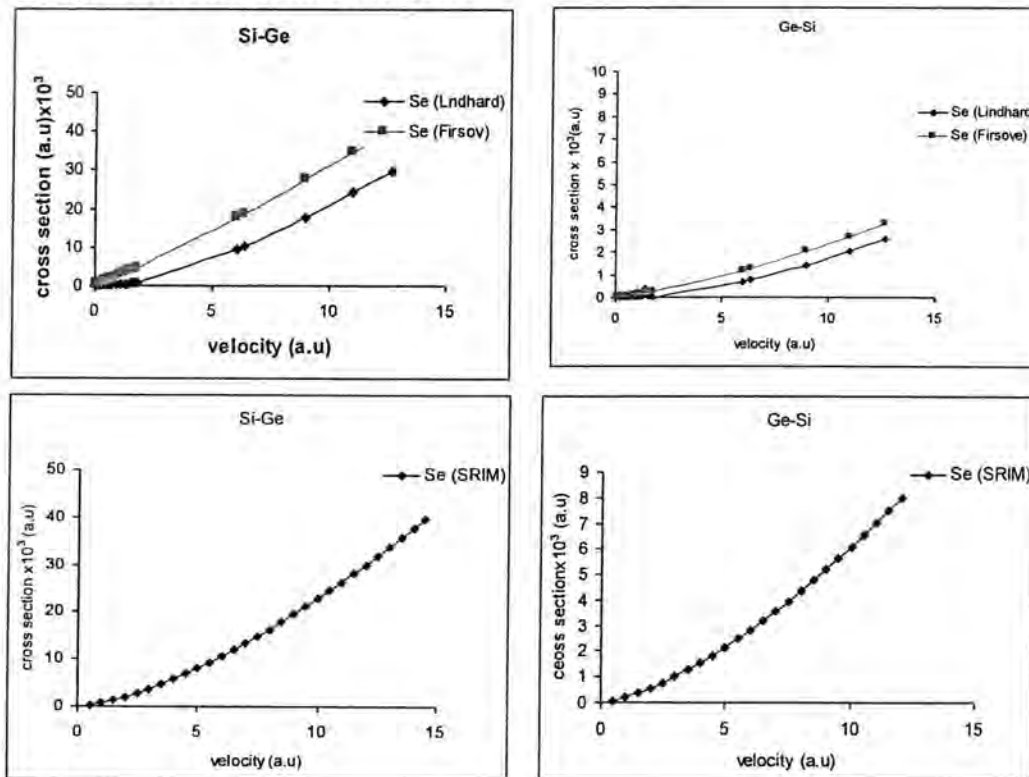


Fig-3:Reciprocity of stopping cross section: Ge in Si and Si in Ge (semi.semi.)

By application eq. (8) on (Si-Ge) at velocity (12.681a.u)

$$R = \frac{S(z_1 \rightarrow z_2) - S(z_2 \rightarrow z_1)}{S(z_1 \rightarrow z_2) + S(z_2 \rightarrow z_1)}$$

$$\frac{2959.58 - 2587.7}{2587.7 + 2959.58} = 0.1$$

SRIM Reciprocity (Si-Ge) at velocity (12.681 a.u )

$$R = \frac{32529.404 - 8689.655}{8689.655 + 32529.404}$$

$$= 0.5$$



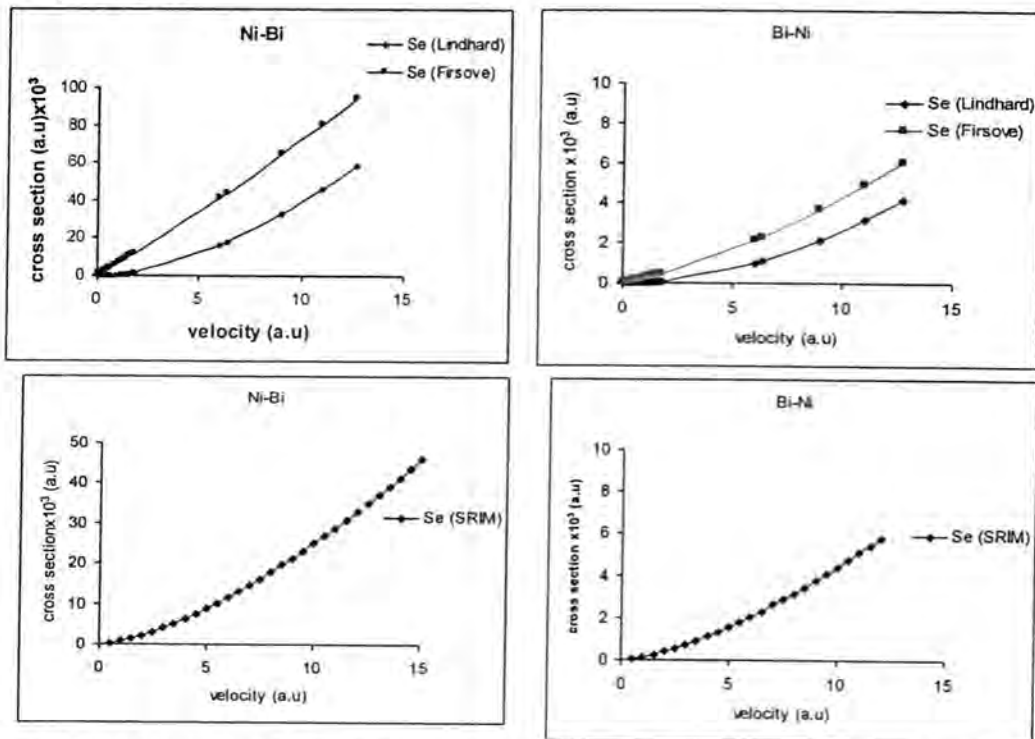
**metal-metal**

Fig-4:Reciprocity of stopping cross section: Bi in Ni and Ni in Bi (metal-metal)

By application eq. (8) on (Bi-Ni) at velocity (12.68 a.u)

$$R = \frac{S(z_1 \rightarrow z_2) - S(z_2 \rightarrow z_1)}{S(z_1 \rightarrow z_2) + S(z_2 \rightarrow z_1)}$$

$$\frac{4148.27 - 5841.29}{5841.29 + 4148.27} = -0.1$$

SRIM Reciprocity (Bi-Ni) at velocity (12.681 a.u)

$$R = \frac{6261.894 - 35737.968}{35737.968 + 6261.894} = -0.7$$

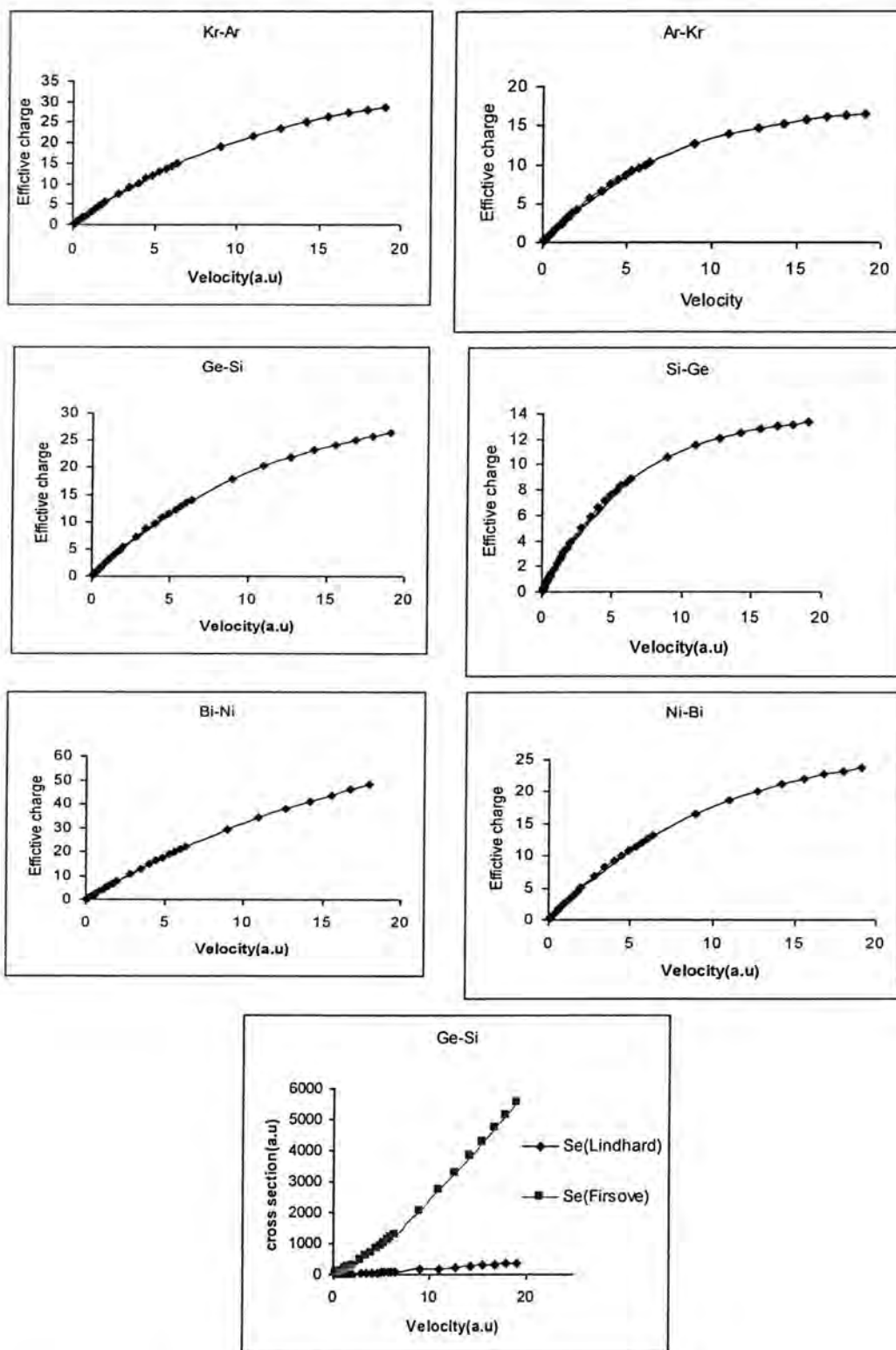


Fig-5:Reciprocity of effective charge: gases, semiconductors and metal

### CONCLUSION

Obvious Firsove dependent Boher velocity to fined the collision between atoms and target and ignores ionization of ion and dependent on neutral collision.

The Results of Theories Lindhard and Firsove agreement with Paul theory of reciprocity. See reciprocity dependent on  $Z_1$ ,  $Z_2$ , and the scatter increases with increasing  $Z$ .

Charge exchange for many stopping cross sections where take place many processes loss and capture until arrive to state of charge equilibrium the effective charge preoperational with velocity.

Dependent SRIM on Bohr velocity to account stopping energy but Lindhard dependent on Bethe velocity, see the reciprocity investigation in low energy in nuclear collision because the distribution of ion in matter more regular.

### REFERENCES

1. V.Kuzmin, P.Sigmund, Exploring reciprocity as a tool in low-energy electronic stopping, Department of Physics and Chemistry, University of Southern Denmark, DK-5230 Odense M, Denmark (2010).
2. P.M.Echenique, Nonlinear stopping power of and electron gas for slow ions, Physical Review A, vol. 33, No.2, (1986).
3. G.J.phys. C: Solid State Phys. 0022-37(2012).
4. P.Sigmund, stopping of slow ions, Department of Physics and Chemistry, University of Southern Denmark, DK-5230 Odense M, Denmark(2000).
5. M.M.Li, A Study of the charge stat approach to the stopping power of MeV B, N and O ions in carbon, Instruments and Methods in Physics Research, No 8, (2004).
6. A. Mason Hndout 11, EE 562 Intro to Solid State Physics .
7. Y.Zhang, K.Sun, Damage profile and ion distribution of slow heavy ions in compounds, Journal of Applied Physics- Volume 105- Issue 10 (2009).
8. A. F. Lifschitz and N. R. Arista, Effective charge and the mean charge of swift ions in solids, PHYSICAL REVIEW A69, 012902 (2004).
9. F.Ziegler, M.D.Ziegler, J.P.Biers, Significant data contributions (SRIM), (2011).



## Study the Design of Dielectric Chirped Mirror

Elham Jasim Mohammad

Al-Mustansiriyah University – Collage of Sciences – Physics Department

Received 5/12/2010 – Accepted 25/5/2011

### الخلاصة

إن توليد نبضات فائقة القصر، وهي تلك النبضات في مرتبة نبضات Femtosecond و Picoseconds تحتوي عناصر بصرية مطلية، ومثال على ذلك: - العاكسات العالية (HR)، مرايا الخرج الضوئي (OC) وطلاءات ضد الانعكاس (AR). هذه العناصر البصرية مستندة على ظاهرة تداخل الضوء. إن التحليل النظري يعتمد على الشكليات العامة لمصفوفة الاستطارة المعروفة التي اشتقت من معادلات ماكسويل. يعتمد أداء الليزر بصورة أساسية على نوعية الطلاءات البصرية. وإن الانعكاسية العالية للعاكسات يجب أن تقترب من القيمة المثالية 100% في الأطوال الموجية العملية لكي يقلل خسائر فجوة الليزر وإن إنتاج الإزدواج لقيم معينة هو لضمان العملية المثالية. هذا البحث تضمن تصميم نظري لمراة الزرققة للحصول على انعكاسية عالية والتشتت على مدى طيفي. استعملت الصيغة التحليلية للانعكاسية، التأخر وتشتت تأخر المجموعة. إن الهدف هو ضغط عرض النبضة لكي تصل إلى تدرج Femtosecond. تعتمد فكرة مرايا الزرققة على أساس مفهوم الحزمة ذات الربع طول موجي كبناء لعاكس عازل عالي الانعكاسية. المواد العازلة  $\text{TiO}_2/\text{SiO}_2$  رتب كحزمة دورية استعملت لتصميم مرايا الزرققة على أساس من مادة Fused Silica. في هذا البحث قدمنا مراة الزرققة بعدة طبقات عازلة مع السيطرة على الانعكاسية والتشتت في مدى طول الموجة 650 – 900nm الذي يعرض الانعكاسية بقيمة أكبر من 99.995%. علاوة على ذلك، يبين تشتت تأخر المجموعة سلوكاً متماثلاً ضمن مدى الطول الموجي.

### ABSTRACT

The generation of ultrashort pulses, that are pulses in the order of picoseconds and femtosecond lasers contains optical coatings as important functional elements, e.g. high reflectors HR, output couplers (OC) and antireflection (AR) coatings. These optical elements are based on the interference phenomenon of light. Their theoretical analysis generally relies on the well-known scattering matrix formalism derived from the Maxwell equations. Laser performance strongly depends on the quality of optical coatings: reflectance of high reflectors should approach the ideal 100% value at the operation wavelengths in order to minimize laser intracavity losses and output coupling has to be set to specific values to ensure optimal operation.

This paper reports a theoretical design of chirped mirror to achieve high reflectivity and dispersion compensation over a broad bandwidth. Analytic expressions for reflectivity, group delay and group delay dispersion are used.

The aim is to compress the limits of pulse duration to reach femtosecond scale. The idea of chirped mirrors is based on the quarter-wave stack concept as a building block of dielectric high reflector.

Dielectric materials  $\text{TiO}_2/\text{SiO}_2$  arranged as a periodic stack have been used to design chirped mirrors using a Fused Silica as a substrate.

In this paper we demonstrate a chirped dielectric multilayer mirror with controlled reflectivity and dispersion in the wavelength range 650–900nm, it exhibits a reflectivity of >99.995%. Furthermore, group delay dispersion shows monotonic behavior within the wavelength range.

**Keyword:** Dielectric Mirror, Chirped Mirror, Group Delay, Group Delay Dispersion, Fresnel reflection, Reflectivity.



## INTRODUCTION

Chirped mirrors, (CM) for dispersion control were proposed and demonstrated in 1994 and since then have found widespread use for broadband dispersion control in ultrafast systems. CM has proved ideal for controlling dispersion inside femtosecond oscillators [1].

This paper is concerned with theoretical study on optoelectronics physics to design dielectric chirped mirrors. A dielectric mirror consists of multiple thin layers of (usually two) different transparent optical materials (thin film coatings). Even if the Fresnel reflection coefficient from a single interface between two materials is rather small (due to a small difference of refractive indices), the reflections from many interfaces can (in a certain wavelength range) constructively interfere to result in a very high overall reflectivity of the device. The simplest and most common design is that of a Bragg mirror, where all optical layer thickness values are just one quarter of the design wavelength. This design leads to the highest possible reflectivity for a given number of layer pairs and given materials. It is also possible to design dichroic mirrors with controlled properties for different wavelengths [2].

The cavity mirrors of a laser are usually dielectric mirrors, because such devices routinely achieve a very high reflectivity of large than 99.9%, and their limited reflection bandwidth can be convenient because it allows to transmit pump light (at a shorter wavelength) through a folding mirror of the cavity. Because of this use, dielectric mirrors are often called laser mirrors. As dielectric mirrors usually provide a high reflectivity at most in a smaller part of the visible spectrum, they often do not look similar to other mirrors as e.g. silver mirrors, with which we are familiar from the household: dielectric mirrors are usually quite transparent to visible light and shine in colors, which depend on the angle of view. It can even be difficult to determine which side of the substrate has got the mirror coating. Dielectric multilayer mirrors can be made on plane as well as on curved surfaces. In the latter case, one obtains focusing or defocusing mirrors [1,3].

## CHIRPED MIRROR (CM)

Although grating and prism pairs are widely used as the compressor schemes, they suffer from high order dispersion. By contrast, chirped mirrors which are dispersive multilayer structures designed by optimizing the initial design are usually used for pulses compression by providing dispersion without much material in the beam path. They can provide the precisely controlled group delay (GD), group delay dispersion (GDD), even higher order dispersion such as third order dispersion (TOD), as well as the high reflectivity in a broadband or ultra-broadband wavelength range. They are key components for

extremely short pulse compression and especially have played a critical role in the development of octave-spanning lasers and the generation of mono-cycle pulses. In 2007, 1.5-octave chirped mirrors (Figure-1) have been proposed and demonstrated, for extra-cavity compression to 3fs pulses (Pervak et al. 2007) [1].

There are always ripples in GDD curves of broadband-chirped mirrors, due to the interference between the reflections from different layers of a multilayer structure. Although the ripples can be minimized by the optimization procedure such as with commercially available software, it is difficult to reduce the ripples to acceptable level when the design of a single chirped mirror has to operate over the wavelength ranges up to an octave spanning or more [4,5].

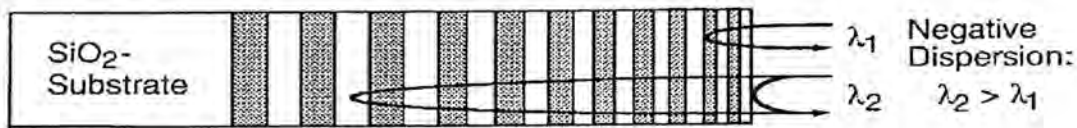


Figure-1: Standard dielectric chirped mirror [6].

Therefore, several other approaches to reduce GDD ripples have been proposed, such as double-chirped mirrors (Kärtner et al. 1997; Matuschek et al. 1998; Kärtner et al. 2001), complementary CM pairs (Pervak et al. 2005; Pervak et al. 2007). By pairing the CMs, the dispersion ripples of CMs are opposite to each other. Thus, the residual ripple of the CM pairs could be very small.

#### CHIRPED MIRRORS PRINCIPLE OF OPERATION

The principle of operation can be understood as follows. Each interface between the two materials contributes a Fresnel reflection ( $f_r$ ) [6]:

$$f_r = (n_h - n_l) / (n_h + n_l) \quad \dots\dots(1)$$

Where  $f_r$  Fresnel reflectivity,  $n_h$  high refractive index and  $n_l$  low refractive index.

The basic idea of chirped mirror designs is that the Bragg wavelength is not constant but varies within the structure, so that light at different wavelengths penetrates to a different extent into the mirror structure and thus experiences a different group delay (see figure-2).



Figure-2 : Operation principle of a chirped mirror [7].

Light with a long wavelength penetrates deeper into the mirror structure and thus experiences a larger group delay. This leads to anomalous



chromatic dispersion [7]. However, a naive design directly based on this idea would not work: it would exhibit strong oscillations of the group delay and even more so of the group delay dispersion. This disturbing effect can to some extent be mitigated by numerical optimization of the layer structure, but this is difficult because the optimization has to be done in a multi-dimensional space (resulting from the large number of layers) where a huge number of local optima exist, most of which do not correspond to satisfactory designs [7].

### CHROMATIC DISPERSION

The chromatic dispersion (CD) of an optical medium is the phenomenon that the phase velocity and group velocity of light propagating in a transparent medium depend on the optical frequency. A related quantitative measure is the group velocity dispersion.

The attribute "chromatic" is used to distinguish this type of dispersion from other types, which are relevant particularly for optical fibers: intermodal dispersion and polarization mode dispersion [8].

Chromatic dispersion is caused by the fact that different spectral components travel at different velocities. In optical fibers, chromatic dispersion arises from two reasons: the wavelength dependence of refractive index that leads to material dispersion and the radial power distribution of different optical frequencies that leads to waveguide dispersion [9].

Chromatic dispersion is a broadening of the input signal as it travels down the length of the fiber. The concept to consider when talking about chromatic dispersion should be optical phase. It is important to mention optical phase before any explanations of CD or group delay because of their mathematical relationship.

Group delay is defined as the first derivative of optical phase with respect to optical frequency. Chromatic dispersion is the second derivative of optical phase with respect to optical frequency. These quantities are represented as follows [10]:

$$CD = \frac{\partial^2 \phi}{\partial \omega^2} \quad \dots (2)$$

Where  $\phi$  = optical phase and  $\omega$  = optical frequency . Chromatic dispersion consists of both material dispersion and waveguide dispersion as illustrated in Figure-3 [11→13].

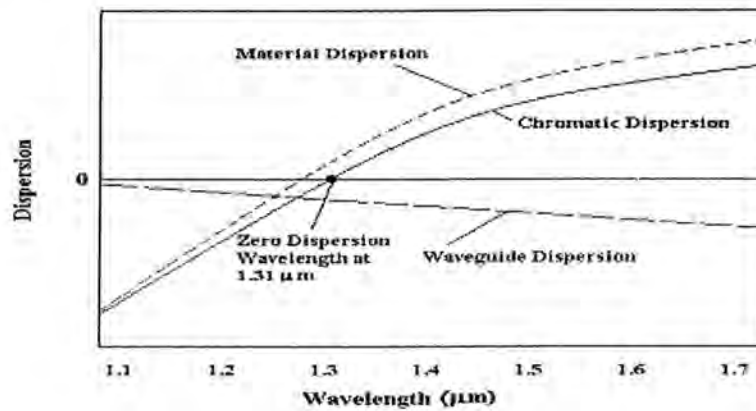


Figure-3: Chromatic dispersion consists of both material dispersion and waveguide dispersion [10].

There are several techniques for measuring chromatic dispersion:

- The pulse delay technique: based on measuring the difference in propagation time (group delay) for pulses with different center wavelengths. This is typically done using hundreds of meters (or even some kilometers) of a fiber. The dispersion is obtained by differentiation of these data.
- The phase shift technique: a light beam with a sinusoidally modulated intensity is sent through a fiber, and the phases of the oscillations of input and output power are compared. The group delay can be calculated from that phase, and the dispersion can be measured by performing the measurement at different wavelengths.
- Dispersion in the resonator of a wavelength-tunable passively mode-locked laser can be measured by monitoring changes in the pulse repetition frequency when the laser wavelength is changed, as this reveals the wavelength-dependent group delay.
- Different types of interferometry (e.g. white-light interferometry or spectral phase interferometry) can be used to measure the phase delay caused by a dispersive component. The dispersion properties can be obtained from this phase by numerical differentiation. The method is normally used for dispersion measurements on dispersive laser mirrors and sometimes for fibers [9].

## GROUP DELAY

The group delay is defined as the negative of the derivative of the phase response with respect to frequency [14,15], GD, also known as "Envelope Delay" [16]. In physics and in particular in optics, the study of waves and digital signal processing, the term group delay has the following meaning:



1- The rate of change of the total phase shift with respect to angular frequency [17- 20]:

$$GD = -\frac{d\phi}{d\omega} \quad \dots\dots(3)$$

Through a device or transmission medium, where  $\phi$  is the total phase shift in radians, and  $\omega$  is the angular frequency in radians per unit time, equal to  $2\pi f$ , where  $f$  is the frequency (hertz if group delay is measured in seconds).

2- In an optical fiber, the transit time required for optical power, traveling at a given mode's group velocity, to travel a given distance.

### GROUP DELAY DISPERSION

Group delay dispersion is a ubiquitous, and often irritating, phenomenon in ultrafast laser labs. When ultrashort pulses propagate through dispersive media, their frequency components emerge at different times due to GDD, causing the resulting pulse to be chirped, stretched and reducing the pulse's peak power. This effect can be compensated by using a *pulse compressor*, which can introduce negative GDD [21]. The standard method for computing the GDD is to compute complex reflection coefficients using the transfer matrix technique and then take successive finite difference over frequency [22]:

$$GDD = -\frac{d^2\phi}{d\omega^2} \quad \dots\dots(4)$$

The effect of group velocity dispersion (GVD) shown in Figure-4. GVD means that the group velocity will be different for different wavelengths in the pulse. Because ultrashort pulses have such large bandwidths, GVD is a bigger issue than for continued wave light [17].

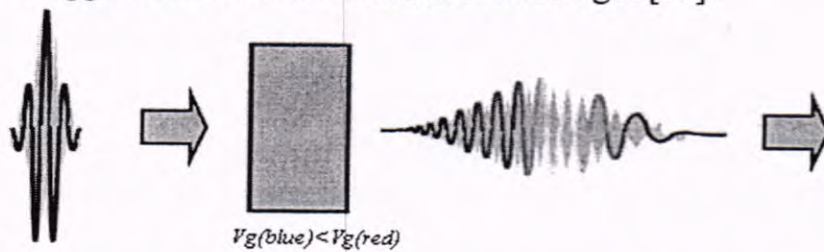


Figure-4: the effect of group velocity dispersion (GVD) [17].

GDD of optical elements is a critical parameter for the generation and control of femtosecond laser pulses. GDD can either increase or decrease then pulse duration by modulating the spectral phase of the femtosecond laser pulses. The effect of GDD becomes more significant as the laser pulse duration gets shorter. Ideally, a femtosecond dielectric mirror should not only have high reflectance but also low dispersion

over a sufficiently broad spectral bandwidth. Recently, dispersion control using a pair of dielectric chirped mirrors, which generate a relatively flat negative GDD over a broad spectral region, made it possible to routinely generate sub-10fs pulses in the near-infrared and visible wavelength regions [23].

### MECHANISM

Dielectric mirrors function based on the interference of light reflected from the different layers of dielectric stack. This is the same principle used in multi-layer anti-reflection coatings, which are dielectric stacks, which have been designed to minimize rather than maximize reflectivity. Simple dielectric mirrors function like one-dimensional photonic crystals, consisting of a stack of layers with a high refractive index interleaved with layers of a low refractive index (see Figure-5).

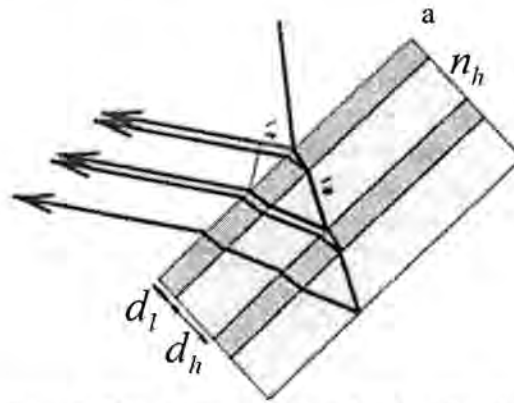


Figure-5: of a dielectric mirror. Thin layers with a high refractive index  $n_h$  are interleaved with thicker layers with a lower refractive index  $n_l$ . The path lengths  $l_A$  and  $l_B$  differ by exactly one wavelength, which leads to constructive interference [3].

The thicknesses of the layers are chosen such that the path-length differences for reflections from different high-index layers are integer multiples of the wavelength for which the mirror is designed. The reflections from the low-index layers have exactly half a wavelength in path length difference, but there is a 180-degree difference in phase shift at a low-to-high index boundary, compared to a high-to-low index boundary, which means that these reflections are also in phase. In the case of a mirror at normal incidence, the layers have a thickness of a quarter wavelength.

The layers are chirped with [4]:

$$d_h = (k/17)^{0.5} \lambda_B / (4\pi n_h) \quad \dots\dots(5)$$

and

$$d_i = (k/17)^{O_{ch}} \lambda_B / (4\pi n_i) \quad \dots(6)$$

Where  $O_{ch}$  are the chirping order and  $n_h$  high refractive index and  $n_l$  low refractive index.

In the design of dielectric mirrors, an optical transfer-matrix method can be used. The most general method of calculating the reflectance  $R$  and the transmittance  $T$  of a multilayer from these quantities is based on a matrix formulation, of the boundary conditions at the film surfaces derived from Maxwell's equations.

The interfaces between the films and the final film and the substrate, can be treated in exactly the same way as the simple boundary. The phase shift experienced as a wave traverses a distance  $d$  normal to the boundary of one film to the next is then given by:

$$\delta = 2\pi N d \cos(\theta) / \lambda \quad (7)$$

where  $N$  denote the complex refractive index and take the form:  $N = n - ik$ , where  $n$  is the real part of the refractive index,  $k$  is known as the extinction coefficient and  $\theta$  is the incident angle.

Dielectric mirrors exhibit retardance as a function of angle of incidence and mirror design [3].

The characteristic optical admittance,  $y$ , is defined as the ratio of the magnetic and electric fields:

$$y = \frac{H}{E} \quad (8)$$

and  $y$  is usually complex. In free space,  $y$  is real and denoted by  $Y = 2.6544 \times 10^{-3} \text{ s}$ .

Since the tangential components of  $E$  and  $H$  are continuous across a boundary, and since there is only a positive going wave in the substrate, a  $2 \times 2$  matrix can be used to express the relationship which connects the tangential components of  $E$  and  $H$  at the incident interface with the tangential components of  $E$  and  $H$  which are transmitted through the final interface. This matrix is known as the characteristic matrix of the thin film [2]:

$$\begin{bmatrix} E_a \\ H_a \end{bmatrix} = \begin{bmatrix} \cos(\delta) & i \sin(\delta) / \eta_i \\ i \eta_i \sin(\delta) & \cos(\delta) \end{bmatrix} \begin{bmatrix} E_b \\ H_b \end{bmatrix} \quad \dots(9)$$

The characteristic optical admittance of a medium is connected with the refractive index by:

$$y = NY \quad \dots(10)$$

Now, the tilted optical admittance  $\eta$  can be defined as:

$$\eta_p = \frac{NY}{\cos(\theta)} \quad \text{for p-polarized} \quad \dots(11)$$

$$\eta_s = NY \cos(\theta) \quad \text{for s-polarized} \quad \dots(12)$$

The input optical admittance of an assembly,  $Y$ , can be defined as  $Y = H/E$ . Hence the above equation can be rewritten as:



$$E_a \begin{bmatrix} 1 \\ Y \end{bmatrix} = \begin{bmatrix} \cos(\delta) & i \sin(\delta) / \eta_1 \\ i \eta_1 \sin(\delta) & \cos(\delta) \end{bmatrix} \begin{bmatrix} 1 \\ \eta_2 \end{bmatrix} E_b \quad \dots\dots(13)$$

This result can be general for  $L$ th layers and written as:

$$\begin{bmatrix} B \\ C \end{bmatrix} = \left\{ \sum_{r=1}^L \begin{bmatrix} \cos(\delta_r) & i \sin(\delta_r) / \eta_r \\ i \eta_r \sin(\delta_r) & \cos(\delta_r) \end{bmatrix} \right\} \begin{bmatrix} 1 \\ \eta_m \end{bmatrix} \quad \dots\dots(14)$$

Where:  $\delta_r = \frac{2\pi N_r \cos(\theta_r)}{\lambda}$  and where  $\eta_m$  is the substrate admittance. This expression is of prime importance in optical thin film work and forms the basis of almost all calculation. The order of multiplication is important. If  $L$  is the layer next to the substrate the order is:

$$\begin{bmatrix} B \\ C \end{bmatrix} = [M_1][M_2] \dots [M_L] \begin{bmatrix} 1 \\ \eta_m \end{bmatrix} \quad \dots\dots(15)$$

The reflectance is given by [5]:

$$R = \left( \frac{\eta_0 B - C}{\eta_0 B + C} \right) \left( \frac{\eta_0 B - C}{\eta_0 B + C} \right)^* \quad \dots\dots(16)$$

### DATA ANALYSIS ALGORITHM

The current implementation is done by using MATLAB language with can be described by the next step:

- 1- Input all constants.
- 2- Calculate  $\theta$  at each interface using Snell's law.
- 3- Calculate each layer thickness using equations 5 and 6.
- 4- Calculate each optical admittance  $\eta$  using equations 11 and 12.
- 5- Calculate  $\delta$  using equation 7.
- 6- Calculate each layer characteristic matrix using equation 14.
- 7- Calculate reflectivity using equation 16.
- 8- Calculate GD and GDD using equations 3 and 4.
- 9- End.

### SIMULATION RESULTS

The calculation that has been carried out by using the program of MATLAB (a high performance language that integrates computing, visualization and programming in an easy to use environment where problems and solutions are expressed in familiar mathematical notation).

The chirping mirror with chirping both high and low refractive index layers are investigated. In our case, the structure of chirped mirror design consists of 35 layers, with  $n_h = 2.2505$ ,  $n_l = 1.4716$ , similar to the refractive indices of TiO<sub>2</sub> and SiO<sub>2</sub>, which results in a Fresnel reflectivity  $r = 0.209$ . The Bragg wavelength  $\lambda_B = 800nm$  in the rang



650–900nm. A mirror consisting of 35 layers and in the wavelength range 650–900nm for normal incidence of light from the air.

For visible region, the most common coating materials is titanium dioxide TiO<sub>2</sub>. For infrared region the silicon dioxide SiO<sub>2</sub> is a good low index materials.

Figures-6 shows the relationship between the reflective index and the wavelength for (the Fused silica substrate, TiO<sub>2</sub> material and SiO<sub>2</sub> material). This determines the dispersion properties of the structure. Figures-7 shows the characteristics of (GD, GDD, GD&CGG and Reflectivity) as a function of wavelength, where the group delay in Figure-7-a is nearly constant over a bandwidth of about 690-830nm. While Figure-7-b shows the dependence GDD on the optical wavelength. It is clearly seen that the decrease of the oscillation in GDD in the rang wavelength from 6670-740nm.

Figure-7-c shows the relationship between the GD&GDD with the optical wavelength it is clearly seen the decrease of the oscillation in GD and GDD as a function of wavelength, i.e. the group delay and group delay dispersion has low oscillation. Figure-7-d that has a high reflectance in the range 650–900nm at design wavelength 800nm when the distribution reflectors consist of alternating periodic quarter wavelength stack of low and high refractive index. These stacks have a peak in the reflectivity at 800nm. The properties of dielectric optical materials, which used in this paper, are shown in table-1.

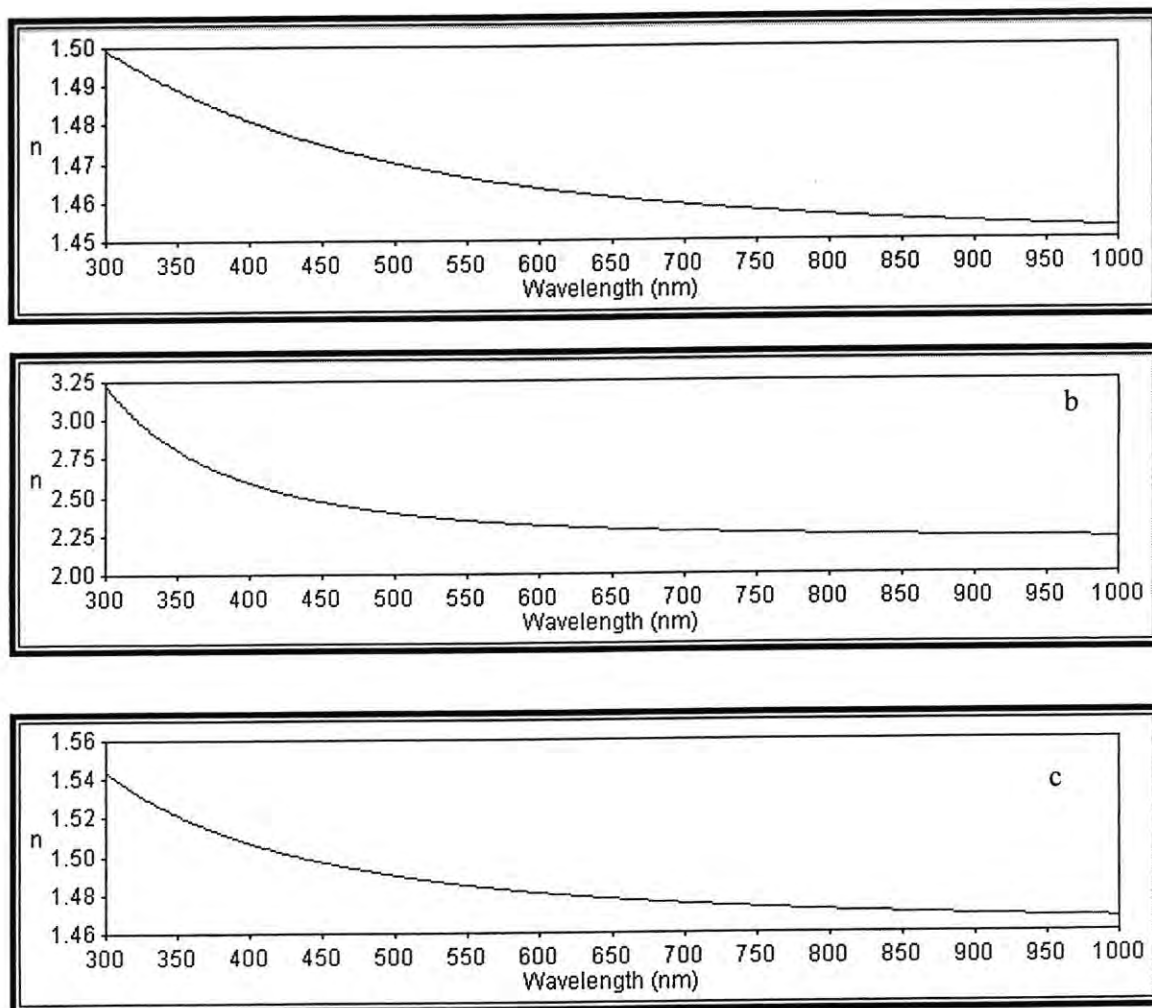
The chirped dielectric multilayer mirror with controlled reflectivity and dispersion in the wavelength range 650–900nm. It exhibits a reflectivity of >99.995%. Furthermore, group delay dispersion shows monotonic behavior within wavelength range.

## CONCLUSION

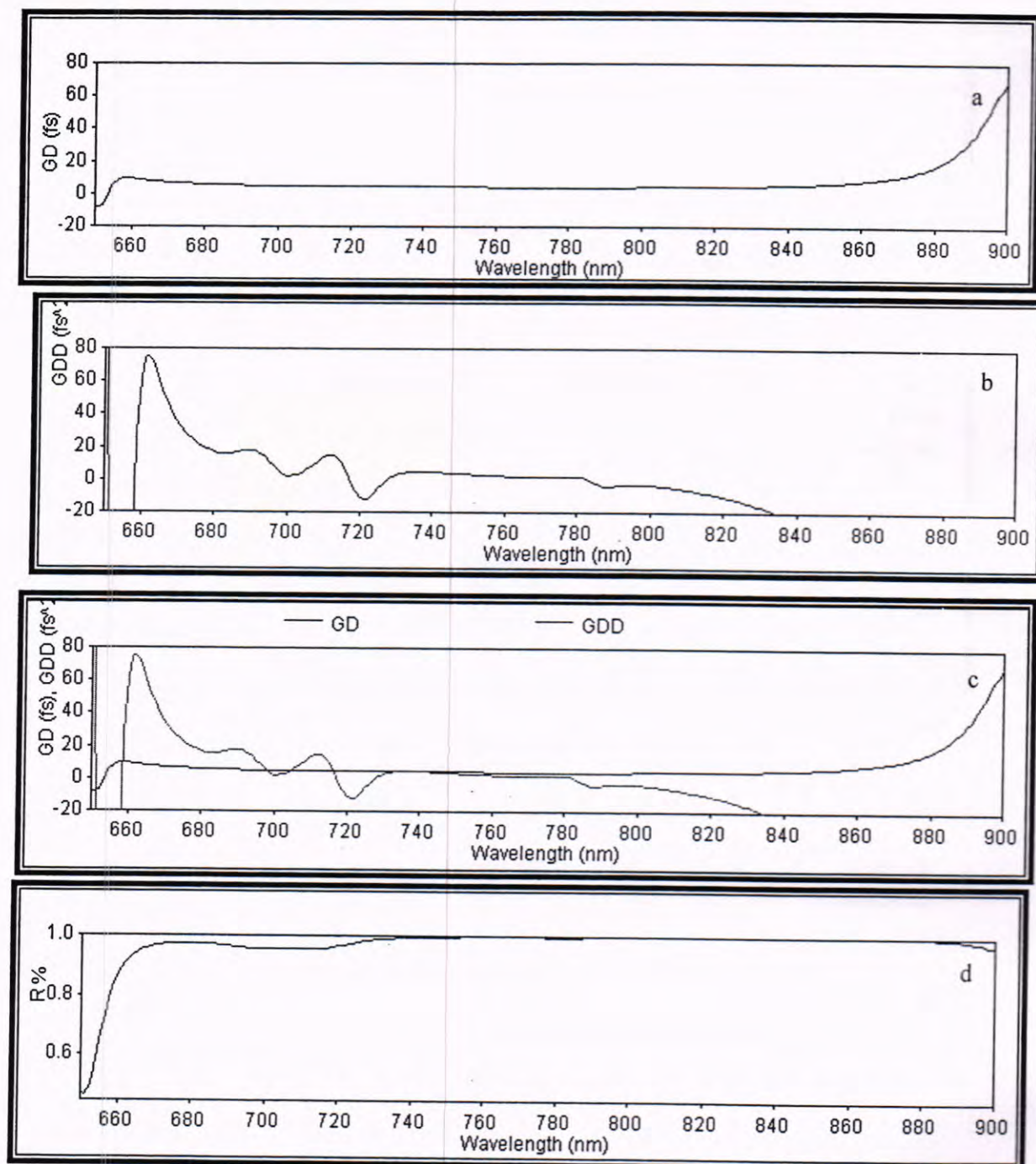
In view of the simulation results presented in this study, the main contributions of this research can be summarized below:

In the case of high reflectors, a combination of materials with the highest refractive-index ratios  $n_h/n_l$  is usually preferred since the higher the ratio, the higher the theoretical reflectance and bandwidth of standard quarter wave stacks. Among its competitors, the TiO<sub>2</sub>/SiO<sub>2</sub> pair has the highest ratio. The results in relatively high density optical coatings of the TiO<sub>2</sub>/SiO<sub>2</sub> material pairs with low absorption and scattering losses.

Tow materials  $\text{SiO}_2/\text{Ta}_2\text{O}_5$  have been used to design chirped mirrors with a flat GD over bandwidth of 690-830nm and the reflectivity was found to be greater than 99.995%. Therefore, chirped mirror is a good device for generating pulse duration down to  $10\text{fs}^2$ .



Figures-6: The relationship between the refractive index and the wavelength for (a- Substrate, b- TiO<sub>2</sub> material c- SiO<sub>2</sub> material).



Figures-7: The relationship between the optical wavelength and (a- GD. b- GDD. c- GD with GDD. d- Reflectivity).

Table-1: Properties of Dielectric Optical Materials in the Wavelength Range 650 – 900nm.

Materials Name	Materials Symbol	Materials Index of Refraction	Optical Region	Method of Deposition
Titanium Dioxide	TiO <sub>2</sub>	2.2505	Visible	Electron beam evaporation/ Sputtering
Silicon Dioxide	SiO <sub>2</sub>	1.4716	Infrared	Electron beam evaporation/ Sputtering

## REFERENCES

- 1-Pervak V., Naumov S., Krausz F. and Apolonski A.; "Chirped Mirrors with Low Dispersion Ripple", *OSA, Vol. 15, No. 21, Pag. 13768-13772, (2007).*
- 2- Ya-Ping Li , " Investigation of Chirped-Cavity Dispersion Compensator Filter", Ph.D. Theses, Optics and Photonics, (2007).
- 3- Apfel J. H., "Phase retardance of periodic multilayer mirrors", *Applied Optics* 21, 733-738 (1982).
- 4- Lysak V. V., Sukhoivanov I. A. and Petrov S. I.; "Group Delay Investigation of N-Order Chirping Mirrors", *Institute of Semiconductor Physics, National Academy of Sciences of Ukraine, Vol. 4, No. 4, Pag. 389-390, (2001).*
- 5- Matuschek N., Franz X. Kärtner, and Ursula Keller, " Theory of Double-Chirped Mirrors", *IEEE Journal of Selected Topics in Quantum Electronics*, Vol. 4, No. 2, Pag. 197, (1998).
- 6- Bishnu Pal, "Frontiers in Guided Wave Optics and Optoelectronics", ISBN 978-953-7619-82-4, Pag. 674, China, (2010).
- 7- Kärtner F. X., Matuschek N., Schibli T. and Keller U., "Design and fabrication of double-chirped mirrors", *Optics Letters*, Vol. 22, No. 11, (1997).
- 8- Rüdiger Paschotta, " Chirped Mirrors ", *Encyclopedia of Laser Physics and Technology*, (2008).
- 9- Rüdiger Paschotta, " Chromatic Dispersion ", *Encyclopedia of Laser Physics and Technology*, (2010).
- 10- "Introduction to Chromatic Dispersion" *Technologies Optical Component DNA*, page 1, (2001).
- 11- Rüdiger Paschotta, "Waveguide Dispersion", *Encyclopedia of Laser Physics and Technology*, (2010).
- 12- Elisabet X. P., "Design, Fabrication and Characterization of Porous Silicon Multilayer Optical Devices", *University Rovira I Virgili*, ISBN: 978-84-691-0362-3/DL: Pag. 86, (2007).
- 13- Alexander P., "Slow light photonic crystal line-defect waveguides", *Technischen Universität Hamburg-Harburg zur Erlangung des*



- akademischen Grades Doktor der Naturwissenschaften genehmigte Dissertation, (2008).
- 14- Adobe PDF-View as html, "Definition of Group Delay":(2008)  
www.dsprelated.com/blogimages/AndorBariska/NGD/ngdblog.pdf.
  - 15- Microwave Encyclopedia, "Group Delay", (2010).
  - 16- Itzhak . and Senior M., "Suggestion for a new Formula to Calculate Group-Delay from Frequency Domain Measurements".
  - 17- Steinmeyer G., " Pulse generation and dispersion compensation", BIPM comb workshop, Max-Born-Institute for Nonlinear Optics and Short Time Spectroscopy, Berlin, Germany, (2003).
  - 18- Masao K., Toshihiro . and Kazuhiko S., "Negative Group Delay and Superluminal Propagation: an Electronic Circuit Approach", IEEE Journal of Selected Topics in Quantum Electronics, Vol. 9, No. 1, (2003).
  - 19- Woodley J. F. and Mojahedi M., "Negative Group Velocity and Group Delay in Left-Handed Media", American Physical Society, 2004.
  - 20- Al-Tayar G. H., "Design Study on Chirped Mirror"; Ph.D thesis, University of Technology, Department of Applied Science, Laser and Optoelectronic, (2009).
  - 21- Selcuk A., Xun G., Mark K. and Trebion, " Extremely simple single-prism ultrashort-pulse compressor ", Optics Express, Vol. 14, No. 21, Pag. 10101, (2006).
  - 22- Jonathan R. B., Christian J. and Franz X. K., "Efficient Analytic Computation of Group Delay Dispersion from Optical Interference Coatings", Optical Society of America, (2004).
  - 23- Imran T., Kyung-Han Hong, Tae Jun Yu and Chang Hee Nam, " Measurement of the group-delay dispersion of femtosecond optics using white-light interferometry", American Institute of Physics, Review of Scientific Instruments, Vol. 75, Pag. 2266-2270, (2004).

## Studies on Physical Properties of $\text{SnO}_2$ : Co Nano-crystalline Thin Films Prepared by Spray Pyrolysis Technique

Ali Jasim AL-Jabiry

Al-Mustansiryah University, College of Science, Department of Physics

E-mail: [spiritjabir@yahoo.com](mailto:spiritjabir@yahoo.com)

Received 6/2/2012 – Accepted 20/6/2012

### الخلاصة

حضرت اغشية القصدير الشفافة المشوبة بالكوبلت ذات الشفافية والتوصيلية العالية على قواعد زجاجية باستخدام تقنية التحلل الكيميائي الحراري (الرش) لمحلول رابع كلوريد القصدير المائي . تمت دراسة الخصائص التركيبية والبصرية للاغشية المحضرة بظروف مختلفة تركيز الشوائب (2%، 4%، 6%) وكانت الاغشية ذات تبلور متعدد وبتركيب بلوري رباعي الاضلاع. من خلال تحليل نتائج فحوصات حيود الاشعة السينية تم التعرف على التبلور والحجم الحبيبي ووضحت النتائج ان الاغشية ذات تبلور جيد وان الحجم الحبيبي يتناقص بزيادة تركيز الشوائب وان بعض الخصائص التركيبية تتغير باضافة الشوائب ولهل اتجاه تفضيلي باتجاه المستوي (101). تمت دراسة طوبوغرافية وخشونة السطح باستخدام مجهر القوة الذرية (AFM) حيث بينت النتائج زيادة الخشونة مع زيادة تركيز الشوائب لغاية (4%). الاغشية لها نفاذية بصرية تزداد بشكل هادي لغاية 80% عند الطول الموجي 800 نانو متر وان النفاذية تم قياسها ، وتم حساب معامل الامتصاص وفجوة الطاقة مع زيادة تركيز شوائب الكوبلت وبينت النتائج ان الاشابة ادت الى نقصان في النفاذية وفجوة الطاقة وزيادة في معامل الامتصاص. ان مدى سمك الاغشية المحضرة كانت بحدود (90 - 123) نانومتر ، بينما مدى الحجم الحبيبي كان بحدود (24 - 60) نانومتر ، والقيم المناظرة لخشونة السطح هي (3.7، 5.8، 9.4 و 6.7) نانومتر على التوالي .

### ABSTRACT

Highly transparent and conductive thin films of  $\text{SnO}_2$  and  $\text{SnO}_2$ : Co have been prepared on glass substrates using spray pyrolysis technique from  $\text{SnCl}_4.5\text{H}_2\text{O}$  precursor . Structural and optical properties were studied under different preparation conditions like doping concentration (2%, 4% and 6%). These prepared films are polycrystalline with a tetragonal crystal structure. The crystallinity and the particle size of the prepared samples were analyzed by X-ray diffraction ( XRD ) spectroscopy, the results indicated that all samples had a good crystallinity, and the particle size of the prepared samples decreased with the increase of Co doping concentrations Some of the structure properties are changed by the addition Co concentrations as dopants. The films are preferentially oriented along the (101) direction. We have got some surface morphology and the roughness measured by Atomic Force Microscopy (AFM), the results show increasing of roughness with doping concentration up to 4wt.%. The films have moderate optical transmission (up to 80% at 800 nm), and the transmittance, absorption coefficient and energy gap were measured and calculated with increasing Co doping concentration, the results show that the doping caused to decreased the transmittance and energy gap while it caused to increase the absorption coefficient.  $\text{SnO}_2$  semiconductor thin film having thickness 90–123 nm and nanocrystallite size 24 - 60 nm is obtained. Similarly, the corresponding values of surface roughness are 3.7, 5.8, 9.4 and 6.72 nm, respectively.

**Keywords:**  $\text{SnO}_2$ , Optical properties, Spray pyrolysis, Atomic Force Microscopy, Co doping .



## INTRODUCTION

Tin oxide has the unique properties of being transparent and at the same time conducting. The conductivity arises from the oxygen deficient sites and the conductivity could be modulated from normal semiconducting to degenerate one by suitably doping the material and manoeuvring the oxygen deficient sites[1]. There are many techniques that have been used to prepare the tin oxide films. Spray pyrolysis is a reliable and cheap method. It is a known technique that is closely related to chemical vapour deposition (CVD). A chemical spray deposition process can be described with six parameters [2]: temperature of the gaseous environment, flow of carrier gas, distance between nozzle-substrate, droplet radius, solution concentration and solution flow. Direct deposition of thin films of SnO<sub>2</sub> at a temperature of 65°C by simple and inexpensive chemical bath deposition (CBD) technique. [3]

In this study, spray pyrolysis technique was adopted to deposit Cobalt doped SnO<sub>2</sub> coatings onto glass substrates. Films thus produced were characterized by measuring optical and structural properties.

Spray pyrolysis is a useful alternative to the traditional methods for obtaining pure and doped SnO<sub>2</sub> thin films, because of its simplicity, low cost and minimal waste production. The spray pyrolysis process allows the coating of large surface and it is easy to include in an industrial production line. This technique is also compatible with mass production systems. With spray pyrolysis, the solution is sprayed directly onto the substrate. A stream of gas, e.g., compressed air, can be used to help the atomization of solution through the nozzle. The properties of the deposited material can be varied and controlled by proper optimization of spraying conditions[4].

## MATERIALS AND METHODS

SnO<sub>2</sub> and SnO<sub>2</sub>: Co thin films were deposited onto glass substrates using spray pyrolysis method with 350 °C substrate temperature. 0.1 M solution of SnCl<sub>4</sub>.5H<sub>2</sub>O precursor diluted in deionized water was used for all the films. For cobalt doping, CoCl<sub>2</sub> was added to starting solution. The SnO<sub>2</sub>: Co ratio in the solution was 0 %, 2 %, 4 % and 6% respectively. The carrier gas (Ar) of 15 l/min. during deposition, solution flow-rate was held constant at 3.5 ml/min, and the ultrasonic nozzle to substrate distance was 25 cm and diameter of nozzle was 0.3 mm. The time of the deposition is 4 sec each 1 min. The film thicknesses were found to be approximately (90, 110, 115 and 123) nm. The Co doped SnO<sub>2</sub> films were deposited by spray pyrolysis technique. Glass substrates were placed at a distance of 30 cm under the baker of

the precursor solution . The glass substrates were ultrasonically cleaned and dried before loading them into the chamber.

Thickness of ZnO thin film is calculated using gravimetric method through weighing the substrate before and after deposition as in relation:

$$t = \Delta m / \rho A \dots\dots\dots(1)$$

Where  $\Delta m$  is the mass difference ( before and after deposition ) ,  $\rho$  is the density and  $A$  is the area of deposited film

The structure analysis of the films were carried out by analyzing the X-ray diffraction pattern obtained via diffractometer (Philips ) with  $\text{CuK}\alpha$  radiation with wavelength (1.5405 Å ). The surface morphology analyzed by using the Scanning Probe Microscope ( CSPM – AA 3000). A double-beam spectrophotometer (Shimadzu UV 160) operating in the UV/VIS regions was used for the optical transmittance measurements. The optical transmittance at normal incidence was recorded in the wavelength range of (300-900) nm.

## RESULTS AND DISCUSSION

Figure 1 shows the X-ray diffraction patterns of the  $\text{SnO}_2$  films deposited at various Co concentrations (0, 2, 4, 6 at wt.%). For all deposited films, major peaks corresponding to the tetragonal  $\text{SnO}_2$  were observed.

The X-ray diffraction patterns of the pure and Co doped thin film deposited at  $350^\circ\text{C}$  are shown in Figure (1) . The peaks were broad, showing that the obtained films were small-sized nanocrystalline  $\text{SnO}_2$ . The average crystalline size of  $\text{SnO}_2$  was estimated from XRD data using Scherrer's equation (1) [5] applied to the most intense 101 diffraction line. A broad size distribution of about 60 nm was found for the undoped film, however, the addition of Co into the precursor decreased the crystalline size and the size distribution became narrower and the line became broadened .

$$D = K\lambda/\beta \cos \theta \dots\dots\dots(2)$$

where  $D$  is the average crystalline size,  $K$  is a constant ( $\sim 1$ ),  $\lambda$  is the wavelength,  $\beta$  is the FWHM of peaks and  $\theta$  is the Bragg angle. The increase in temperature enhances the preferred orientation with an increase in grain size. The increase in substrate temperature may cause decrease of the density of nucleation centers and, under these circumstances, a smaller number of centers start to grow, which results in large grains [6].



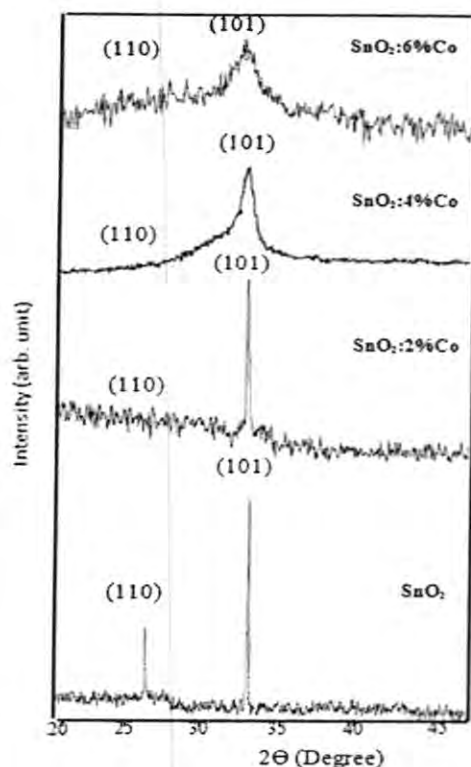


Figure-1: XRD patterns of  $\text{SnO}_2$  films deposited under different Co concentrations.

Figure (2) shows the effect of Co doping concentrations on the average grain size of the prepared  $\text{SnO}_2$  (101) thin films, it is clearly appear that the increasing of Co concentration caused to decreased the average grain size.

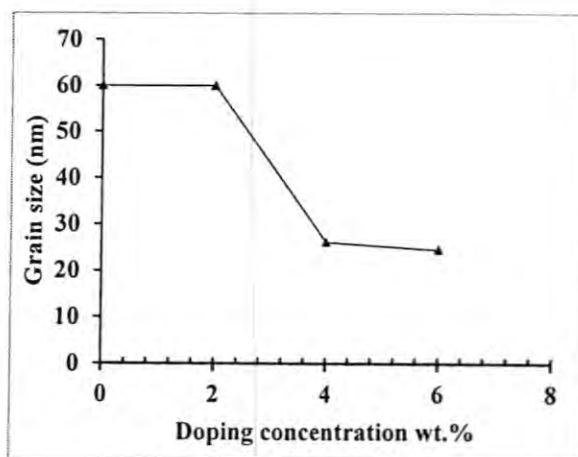


Fig-2: The dependence of Co doping on the grain size of  $\text{SnO}_2$  thin films.

Surface morphology of the films with different Co concentrations was examined by Atomic Force Microscopy (AFM). The 3D images recorded at  $5\ \mu\text{m} \times 5\ \mu\text{m}$  planar in contact mode are depicted in Figure (3).

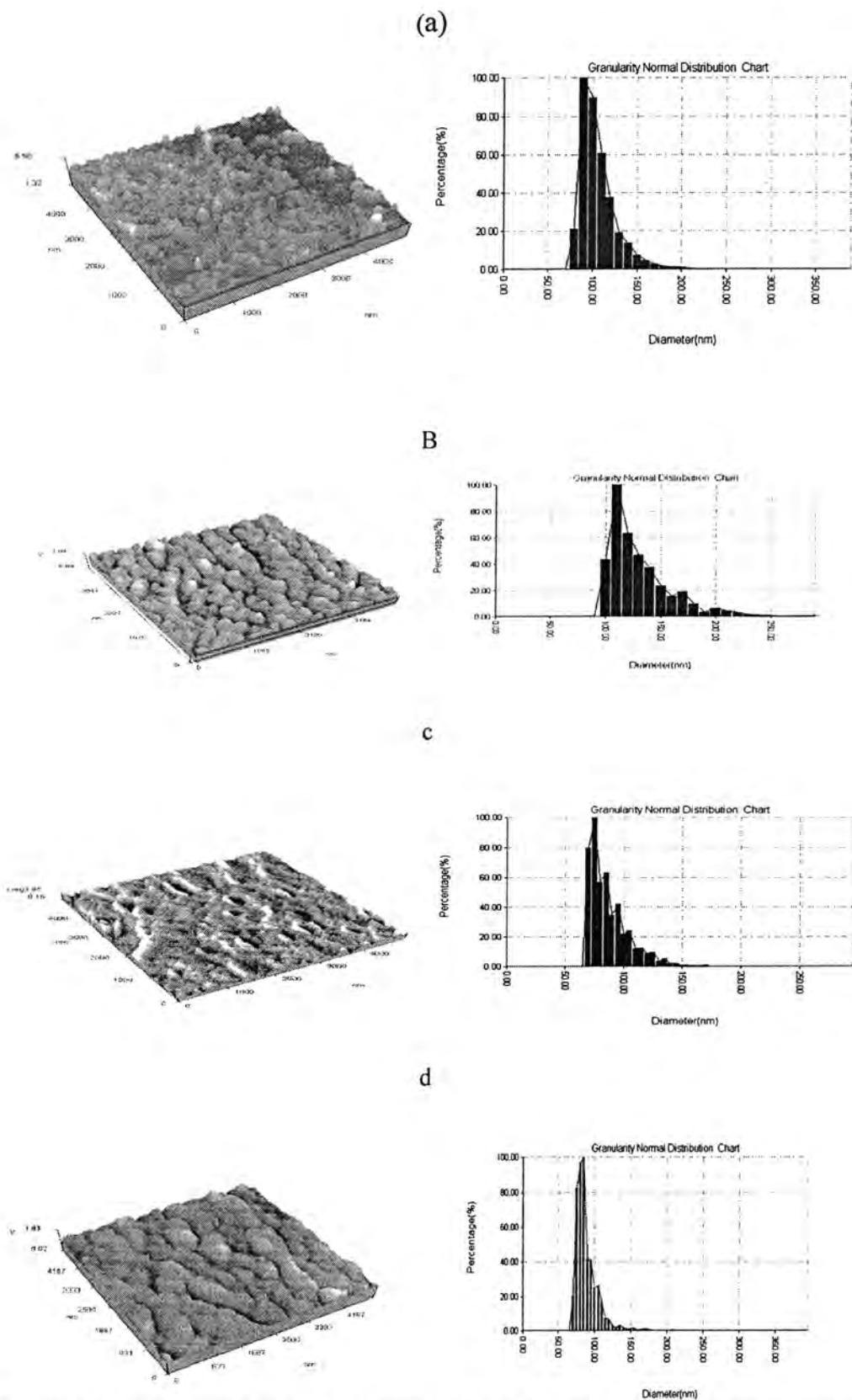


Figure-3: Three-dimensional AFM images of SnO<sub>2</sub> films deposited under different Co concentrations a: 0wt.% b: 2wt.% c: 4wt.% and d: 6wt.%.

Root mean square (RMS) roughness of the films was obtained from the AFM data list, and the results plotted with the doping concentration as in Figure 4. It was clearly seen that the oxide thin films deposited by spray pyrolysis technique showed a nanoscale texture. AFM study reveals that the roughness of the films is dependent on the doping concentration. As shown in the figure, the surface roughness increased with increasing Co concentrations and reached a maximum of 9.45 nm at 4 wt.%. While, it decreased with further increases in concentration (higher than 4 wt.%). These changes may be due to the Co atoms distribution in the tin dioxide structure.

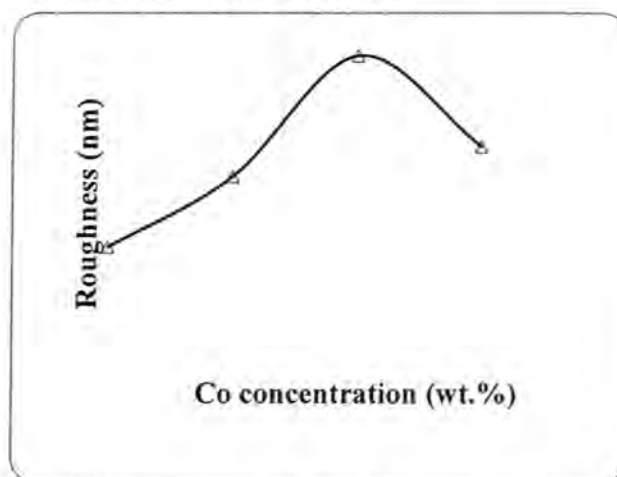


Fig-4: The RMS roughness of the Co doped SnO<sub>2</sub> thin films with doping concentrations.

The transmittance (T) of the deposited thin films was measured and determined in the ultraviolet, visible, and near infrared regions of the electromagnetic spectrum. Optical constants; absorption coefficient and energy gap were deduced using relations depending on the transmittance measurements, the details will be explained in the next paragraphs. The fundamental absorption, which corresponds to electron excitation from the valence band to conduction band was used to determine the nature and value of the optical energy band gap.

Figure (5) shows the wavelength dependence on optical transmittance of SnO<sub>2</sub>:Co thin films deposited with various doping concentrations. The transmittance of all samples was more than 65% up to 80% in the whole visible-light region (*i.e.*, above 400 nm).

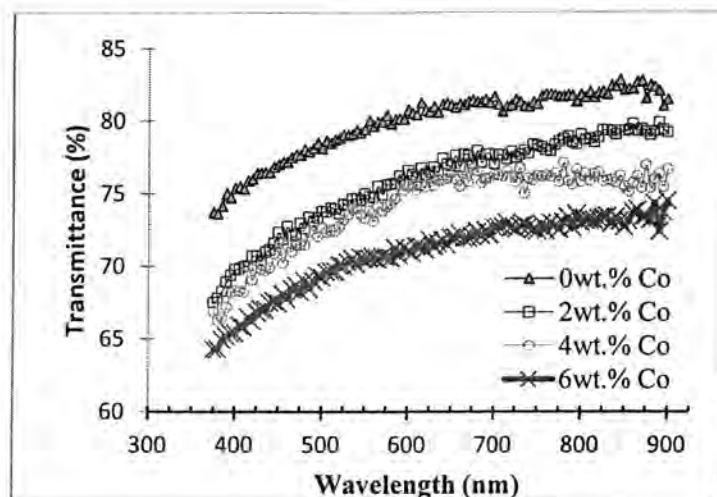


Fig.-5: The transmittance of the pure and Co doped  $\text{SnO}_2$  thin films

In order to obtain the band gap, the absorption coefficient ( $\alpha$ ) was calculated from the transmission data by using the following relation [7],

$$\alpha = -\ln T / t \dots\dots\dots(3)$$

where  $t$  is the film thickness and  $T$  is the transmittance.

Figure (6) shows the absorption coefficient versus wavelength for different Co doping concentrations. In general the absorption coefficient decreases with the wavelength increase while it will be increased especially for doping concentrations greater than 4wt.%.

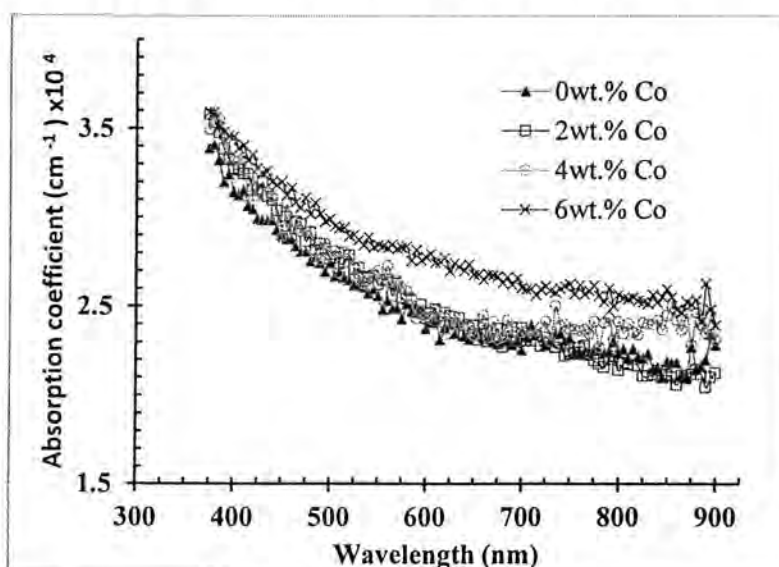


Fig-6: The absorption coefficient of pure and Co doped  $\text{SnO}_2$  thin films.



The band gaps of these films were calculated from fig 6 & fig.7 using the formula [8]:

$$\alpha h\nu = A (h\nu - E_g)^n \quad \dots\dots\dots(4)$$

where  $\alpha$  = Absorption coefficient

$h$  = Planck's constant

$\nu$  = Frequency of incident light

$E_g$  = Band gap of the material

$m$  = Factor governing the direct/ indirect, etc. transitions of the electrons from

the valence band to the conduction band.

where  $h\nu$  is the photon energy and  $E_g$  is the optical band gap which could be calculated from  $(\alpha h\nu)^2$  versus  $h\nu$  plot. For direct allowed transition  $n = 2$ , indirect allowed transition  $n = 1/2$ .

To determine the possible transitions,  $(\alpha h\nu)^{1/n}$  versus  $(h\nu)$  was plotted. The corresponding band gap energies were obtained from extrapolating the straight portion of the graphs on the  $h\nu$  axis at

$$(\alpha h\nu)^{1/n} = 0$$

The plot of  $(\alpha h\nu)^2$  against  $h\nu$  is shown in Figure (7). By extrapolating the linear part of the plot to  $\alpha = 0$ , the optical band gap of 3.77 eV was estimated for pure SnO<sub>2</sub> film. While the optical band gap increases with increasing the Co concentration up to 3.85 eV.

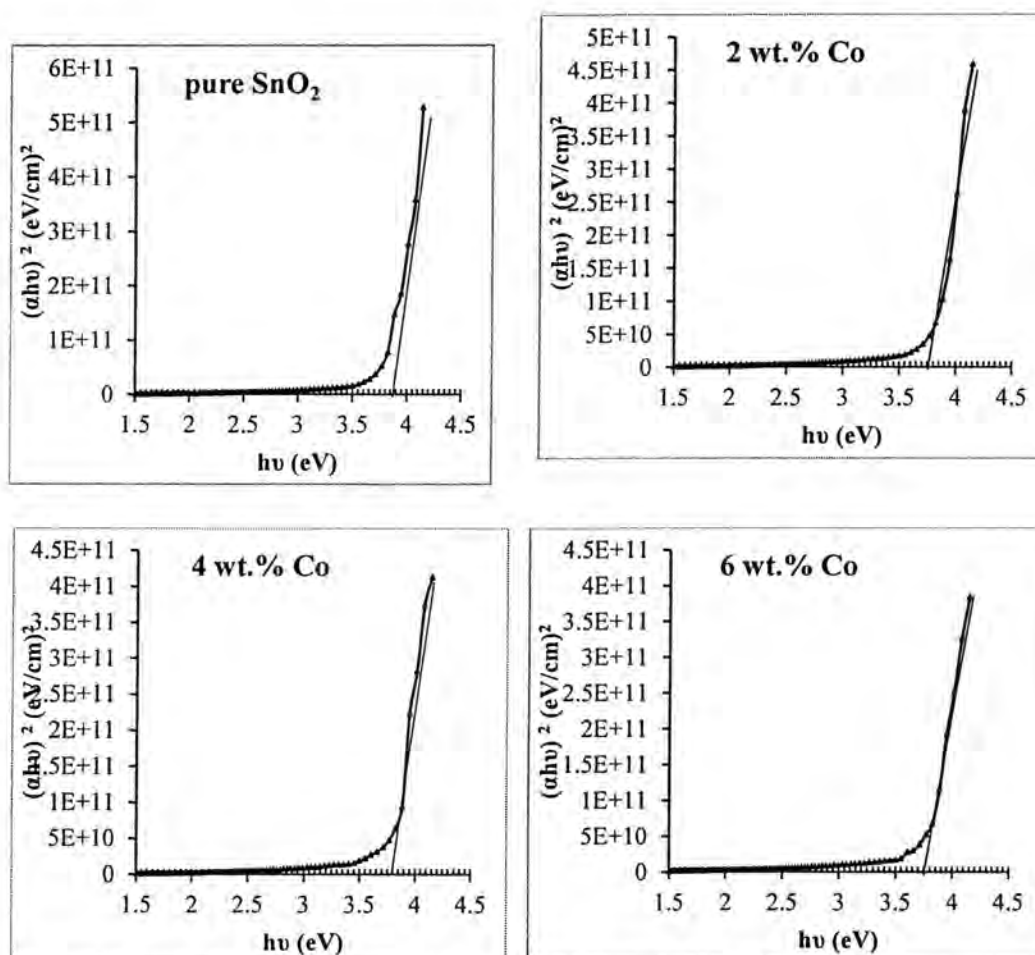


Fig. -7: Plot of  $(\alpha h\nu)^2$  against  $h\nu$  for pure and Co doped  $\text{SnO}_2$  thin films.

The energy gap varies with the doping concentration, Figure (8) shows this variation, it will be decrease with increasing Co concentrations.

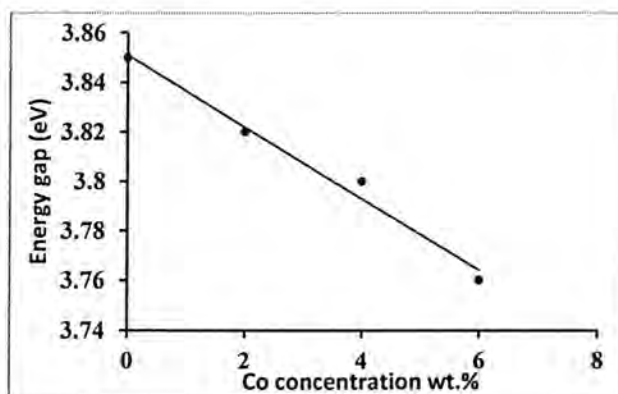


Fig-8 : Energy gap as a function of doping concentration of Co doped  $\text{SnO}_2$  thin films.

## CONCLUSIONS

The structural and optical properties of pure and Co doped SnO<sub>2</sub> thin films prepared spray pyrolysis deposition were investigated. The structural properties show that the growth of the film was preferential in the (101) plan, the average grain size decrease with increase of doping concentration. The surface morphology and the calculated grain size show that the films have a nano scale. The optical constants show that both absorption coefficient and energy gap decrease with increasing Co doping concentration.

The enhancement sprayed Co doped SnO<sub>2</sub> thin films in some structural properties especially crystallite size are much better in comparison to the sprayed Pd doped SnO<sub>2</sub> thin films[2].

## REFERENCES

1. X. Huang, Z. Yu, Sh. Huang, Q. Zhang, D. Li, Y. Luo and Q. Meng, "Preparation of fluorine-doped tin oxide (SnO<sub>2</sub>:F) film on polyethylene terephthalate (PET) substrate", *Mater. Lett.*, 64, 1701 – 1703(2010).
2. M. Boshta, F. A. Mahmoud, and M. H. Sayed, "Characterization of sprayed SnO<sub>2</sub>:Pd thin films for gas sensing applications", *J. Ovonic Research.*, Vol. 6, N. 2, 93 – 98(2010).
3. M. Vaishampayan, R. Deshmukh and I. Mulla, "Influence of Pd doping on morphology and PLG response of SnO<sub>2</sub>", *Sens. Actuat. B:Chem.* 131, 665 – 672(2008).
4. B. Godbole, N. Badera, S. B. Shrivastav, and V. Ganesan, "A simple chemical spray pyrolysis apparatus for thin film preparation", *J. Instrum. Soc. of India*, 39, 1, 42 -45(2009).
5. S. Majumder, S. Hussain, S. Das, R. Bhar and A. Pal, "Silicon doped SnO<sub>2</sub> films for liquid petroleum gas sensor", *Vacuum*, 82, 760 – 770(2008).
6. S. Ray, M. Karanjai, and G. Das, "Tin oxide based transparent semiconducting films deposited by dip-coating technique", *Surf. Coat. Technol.*, 102, 73 – 80(1998).
7. A. J. Mohammed, S. K. Haza'a and A. Neamma, "Some optical properties of the sputtered SnO<sub>2</sub> thin film affected by gamma radiation", *Al-Mus. J. Sci.*, 21, 6, 85 – 89 (2010).
8. S. Ray, P. S. Gupta and G. Singh, "Electrical and optical properties of sol-gel prepared Pd-doped SnO<sub>2</sub> thin films: effect of multiple layers and its use as room temperature methane gas sensor", *J. Ovonic Res.*, 6, 1, 23 – 34 (2010).

## Study Some Of Physical Properties Of Gan/Si(100) For Solar Cell Applications

Wisam Jafer Aziz

Physics Department, College of Science, Al-Mustanseroa University

Received 2/10/2011 – Accepted 18/4/2012

### الخلاصة

في هذا البحث تم صناعة خلية شمسية باستخدام GaN كغطاء مضاد للانعكاس في السطح العلوي على أساس سليكوني نوع p(100). الخصائص السطحية والتركيبية للخلايا الشمسية تمت باستخدام مجهر الماسح الإلكتروني (SEM) ومجهر قياس خشونة السطح (AFM). الانعكاس البصري اخذ بواسطة جهاز (Filmetrics (F20)). قياس الإضاءة الضوئية (PL) أنجز تحت شروط درجة حرارة الغرفة. قياسات كثافة التيار والفولتية تمت دراستها تحت شروط الإضاءة  $80 \text{ mW/cm}^2$ . لقد وجد في هذا البحث ان مادة GaN هي مادة جيدة وفعالة عند استخدامها كغطاء مضاد للانعكاس للأشعة الساقطة مقارنة بالخلية الشمسية السليكونية وأظهرت ماص جيد للأشعة ولمدى (400nm-1000nm) من طيف الطول الموجي. نتائج الفولتية والتيار أظهرت أن كثافة التيار للدائرة هو  $25.2 \text{ mA/cm}^2$  وفولتية الدائرة المفتوحة هو 0.44 وكفاءة التحويل تساوي 11.43%.

### ABSTRACT

In this research the solar cell has been fabricated using GaN as antireflection coating in top surface based on silicon p(100) solar cells. Surface morphology and structural properties of solar cells were investigated using scanning electron microscopy (SEM) and atomic forces microscopy (AFM). Optical reflectance was obtained by using optical reflectometer (Filmetrics (F20)). Photoluminescence (PL) measurement was performed at room temperature. Current density-voltage characterizations were studied under  $80 \text{ mW/cm}^2$  illumination conditions. GaN antireflection coating was found to be an excellent antireflection coating of incident light and exhibited good light-trapping of spectrum at range (400nm-1000nm). The current density-voltage measurements revealed a good values of short circuit current density  $25.2 \text{ mA/cm}^2$ , open circuit voltage 0.44 and conversation efficiency is 11.43%.

### INTRODUCTION

The maximum reported photovoltaic efficiency of 39% at 236 suns is achieved by a triple-junction GaInP/GaInAs/Ge tandem solar cell [1]. While the achievable efficiency of triple-junction tandem solar cells is restricted to about 40%. These structures require band gaps of the top cell to be at least 2.4 eV. GaN has the appropriate optical properties and has been well demonstrated for solar cell applications [2]. The group III-V nitrides such as gallium nitride (GaN) has been actively investigated for the last three decades or so for its promising semiconductor device applications in the electronics as well as optoelectronics operating. The wavelength range of GaN/Si formed by the silicon bandgap 1.12 eV to 3.4 eV for GaN, thus covering the technologically important UV and visible spectral ranges. GaN is an attractive candidate for protective coatings due to its radiation hardness [3], its wide band gap make it go intrinsic at a much higher temperature than materials like Ge, Si and GaAs, i.e. the intrinsic carrier concentration at any given temperature decreases exponentially with



band gap, and therefore GaN and similar wide band gap materials are attractive for high temperature applications. Moreover, due to its many attractive features of GaN like densities, higher mobilities, better charge confinement, higher sheet charge and higher breakdown voltages, also a potential candidate for the application in electronic devices such as high temperature and high power [4,5].

## MATERIALS AND METHODS

The III-nitrides heterostructure of n-type GaN/AlN was grown on Silicon substrate using Veeco model Gen II MBE system. High purity material sources such as gallium and aluminum were used in the Knudsen cells. Nitrogen with high purity was channeled to radio frequency (RF) source to generate reactive nitrogen species. The plasma was operated at typical nitrogen pressure of  $2.5 \times 10^{-5}$  Torr under a discharge power of 300W. The growth of III-nitrides on 7.5cm Si (100) substrate has started with the standard cleaning procedure by using RCA method. The substrate was then mounted on the wafer holder and loaded into the MBE system. The Si substrate was outgassed in the load-lock and buffer chambers. After outgassing, the Si was transferred to the growth chamber. Prior to the growth of the epilayers, surface treatment of the Si substrate was carried out to remove the SiO<sub>2</sub>. Then Si substrate was heated at 1023 ok, and a few monolayers of Ga were deposited on the substrate for the purpose of removing the SiO<sub>2</sub> by formation of GaO<sub>2</sub>. Reflection high energy electron diffraction (RHEED) showed the typical Si (100)  $7 \times 7$  surface reconstruction pattern with the presence of prominent Kikuchi lines, indicating a clean Si (100) surface. Before the growth of nitride epilayers, a few monolayers of Al were also deposited on the Si substrate to avoid the formation of Si<sub>3</sub>N<sub>4</sub> which is deleterious for the growth of the subsequent epilayers. The buffer or wetting layer, AlN was first grown on the Si substrate. To grow AlN buffer layer, the substrate temperature was heated up to 1133 ok, both of the Al and N shutters were opened simultaneously for 15 minutes. Subsequently, GaN epilayer was grown on top of the buffer layer for 50 minutes with substrate temperature set at 1118 ok. Surface morphology and structural properties of GaN/Si structure have been characterized by scanning electron microscopy (SEM) and atomic forces microscopy (AFM). Optical reflectance was obtained by using (Filmetrics (F20)) with wavelength range of 400-1000 nm. Photoluminescence (PL) measurement was performed at room temperature. Current density-voltage characterizations were studied under 80 mW/cm<sup>2</sup> illumination conditions.

## RESULTS AND DISCUSSION

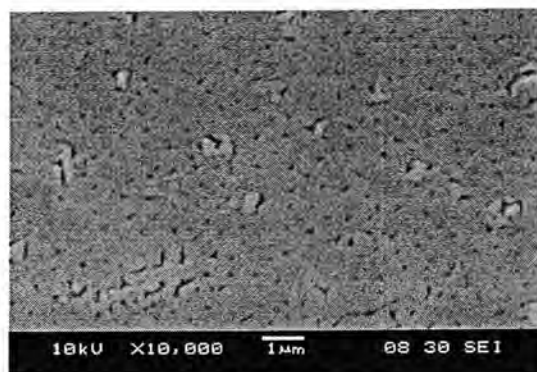


Figure-1: SEM image of the GaN coating.

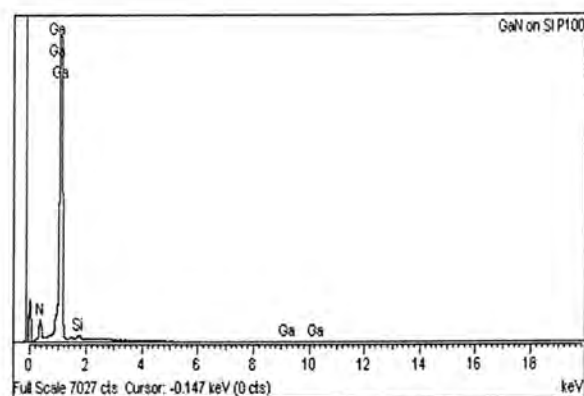


Figure-2: EDX image of GaN/Si coating.

In figure 1, it can be seen that the whole surface is covered by symmetry GaN coating. Figure 2 illustrate the EDX image of GaN/Si contain (Ga=98,01, N=1.78, Si=0.21). Figure 3 shows the roughness of the GaN surface as an antireflection coating based on the c-Si p-type (100) where the root mean square (rms) is 18.35 nm.

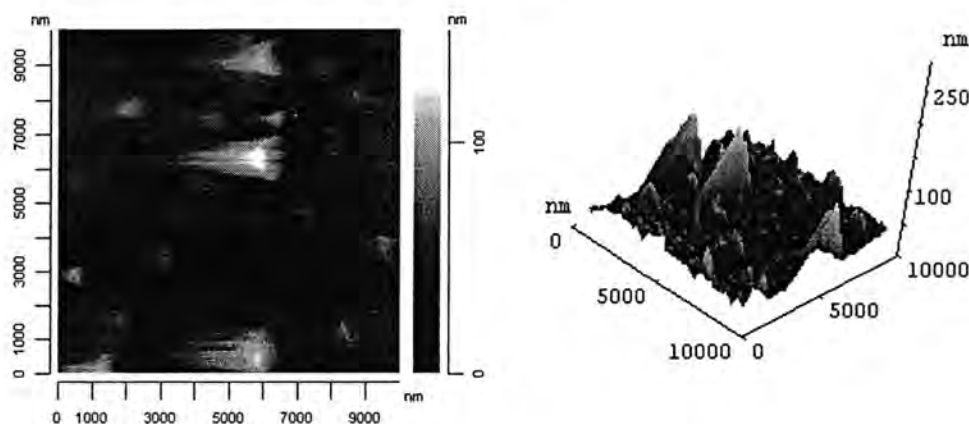


Figure-3: AFM images of GaN coating.



Figure 4 shows PL spectrum of the GaN/Si where the PL spectrum was measured via excitation photon energy of 3.81 eV. Photoluminescence value was observed at 350 nm with FWHM of about 20 nm. Figure 5 shows Raman spectrum of the GaN based on c-Si p-type (100) sample. The sample reveals a sharp line of the spectrum with full width and half maximum (FWHM) of  $8 \text{ cm}^{-1}$  shifted at  $524 \text{ cm}^{-1}$  relative to the laser incident ray. Which is attributed to quantum confinement of the optical phonons.

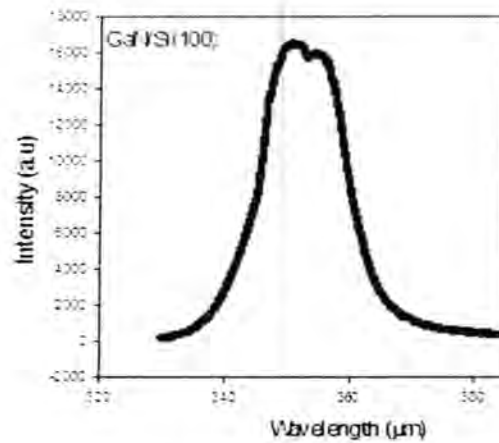


Figure-4: PL spectram of GaN/Si structure.

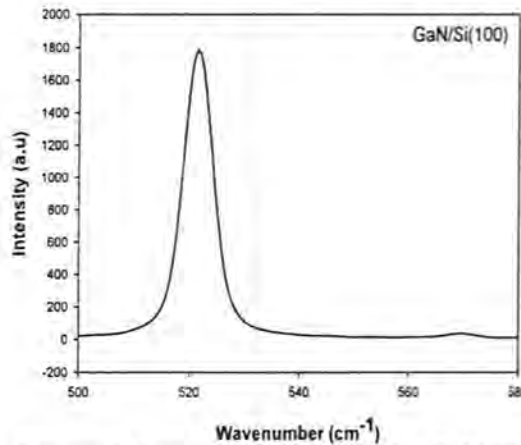


Figure-5: Raman spectram of the GaN/Si structure.

As shown in figure 6, the surface of the GaN based on the c-Si p-type (100) wafer reduced the incoming light reflection and increased light capturing of wide wavelength range where the reflectivity is around 28% compared with the reflectivity of c-Si standard which is 37% [6].

The output of solar cells efficiencies which shown in figure 7 and table 1 are 7.3% of silicon as grown (c-Si) and 11.43% of GaN/Si. These efficiencies indicate that only under high quality of antireflection coating of GaN surface the efficiency can be increased. This is due to a

reduction in the optical losses and in the recombination losses on the surface. In addition, the results of this study revealed that the reduction of reflectivity losses has increased the photovoltage, photocurrent and efficiency.

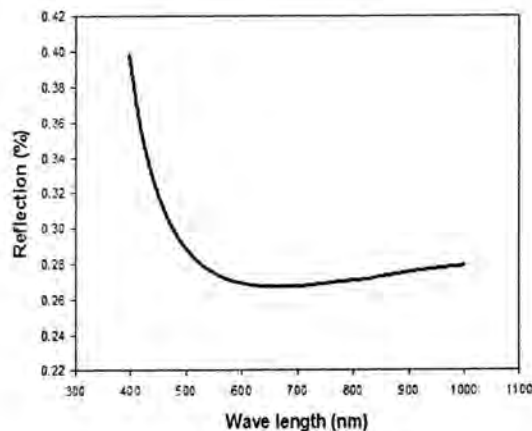


Figure-6: The reflectance spectrum of sample under study

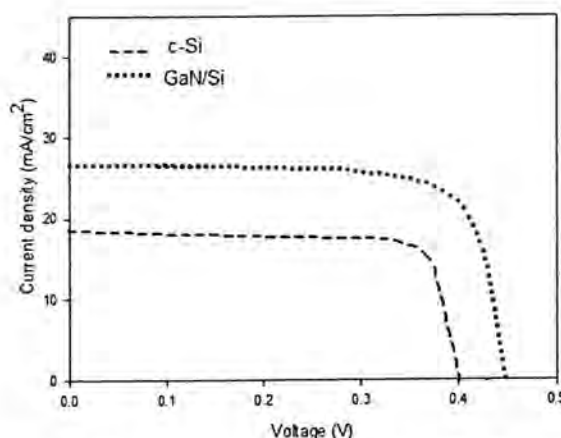


Figure-7: Current density voltage curve of GaN/Si structure.

Table-1: The J-V results of the GaN/Si structure with input power 80 mW/cm<sup>2</sup>.

Sample	V <sub>m</sub> (V)	J <sub>m</sub> (mA/cm <sup>2</sup> )	V <sub>oc</sub> (V)	J <sub>sc</sub> (mA/cm <sup>2</sup> )	FF	η %
c-Si	0.35	16.25	0.4	18.50	79.11	7.30
(GaN/Si)	0.36	24.66	0.44	25.2	82	11.43

## CONCLUSIONS

In this work the GaN material was fabricated and characterized in solar cells. From this study it can be found from the testing that the (J,V) characteristics are very important parameter especially for solar cells because the solar cell which is depend on V<sub>oc</sub> and J<sub>sc</sub> in order to obtain the fill factor (FF) and efficiency (η) values. From figure 7 and table 1 it can be shown that efficiency of silicon as grown (c-Si) is



7.3% and the efficiency of GaN/Si is 11.43%. It can be seen the difference between (c-Si) and GaN/Si values. A photocurrent density of GaN/Si is 25.2 mA/cm<sup>2</sup> and an open-circuit voltage is 0.44 eV.

## REFERENCES

1. R.R. King, D.C. Law, C.M. Fetzer, R.A. Sherif, K.M. Edmondson, S. Kurtz, G.S. Kinsey, H.L. Cotal, D.D. Krut, J.H. Ermer, N.H. Karam, "Pathways to 40% Efficient Concentrator Photovoltaics," Proceedings of the 20th Eu.PVSEC, pp. 118–123 (2005).
2. C.J. Neufeld, Z. Chen, S.C. Cruz, N.G. Toledo, S.P. DenBaars, U.K. Mishra, IEEE Photovoltaic Specialists Conference pp. 2089–2092 (2010).
3. S. Strite, H. Morkoc, J. Vac. Sci. Technology B10, 1242 (1992).
4. S. M. Sze, ed., High-speed semiconductor devices (John Wiley & Sons, New York, 1990), Chapter 5.
5. S. J. Pearton, J. C. Zolper, R. J. Shul, and F. Ren, Appl. Phys. Rev. 86(1), 57-69 (1999).
6. S. Bastide, A. Albu-Yaron, S. Strehlke and C. Levy-Clement, Solar Energy Materials & Solar Cells 57 393-417 (1999).

## Design Fast Feed Forward Neural Network to Solve Initial Value Problems

Luma. N. M. Tawfiq and Yaseen. A. Oraibi

Department of Mathematics, College of Education Ibn Al-Haitham, Baghdad University .

Received 25/10/2011 – Accepted 18/4/2012

### الخلاصة

الهدف من البحث هو تصميم شبكة عصبية ذات تغذية تقدمية مسرعة تمثل طريقة لحل مسائل قيم ابتدائية للمعادلات التفاضلية الاعتيادية وهذا يعني تطوير خوارزمية التدريب بحيث تسرع زمن الحل وتقلل من حالات الفشل في الحصول على الحل و تزيد امكانية الحصول على الحل المثالي الرئيسي واستخدمنا في ذلك عدد من خوارزميات التدريب المختلفة بعضها يمتلك نسبة تقارب سريعة جدا في حالة الشبكات التي تمتلك أحجام معقولة. أخيرا وضحنا الطريقة من خلال حل مثال و قارنا نتائج الشبكة المقترحة مع نتائج حصلنا عليها باستخدام طرق مختلفة أخرى .

### ABSTRACT

The aim of this paper is to design fast feed forward neural network to present a method to solve initial value problems for ordinary differential equations. That is to develop an algorithm which can speedup the solution times, reduce solver failures, and increase possibility of obtaining the globally optimal solution. And we use several different training algorithms many of them having a very fast convergence rate for reasonable size networks. Finally, we illustrate the method by solving model problem and present comparison with solutions obtained using other different methods

**Keyword :** Artificial neural network, Feed Forward neural network, Training Algorithm .

## 1. INTRODUCTION

Many methods have been developed so far for solving differential equations some of them produce a solution in the form of an array that contains the value of the solution at a selected group of points. Others use basis functions to represent the solution in analytic form and transform the original problem usually to a system of algebraic equations.[1]

Most of the previous study in solving differential equations using Artificial neural network(Ann) is restricted to the case of solving the systems of algebraic equations which result from the discretization of the domain. Ann is a simplified mathematical model of the human brain, It can be implemented by both electric elements and computer software. It is a parallel distributed processor with large numbers of connections, it is an information processing system that has certain performance characters in common with biological neural networks. Ann have been developed as generalizations of mathematical models of human cognition or neural biology, based on the assumptions that : [1]  
1- Information processing occurs at many simple elements called neurons that is fundamental to the operation of Ann's.



- 2- Signals are passed between neurons over connection links.
- 3- Each connection link has an associated weight which, in a typical neural net, multiplies the signal transmitted.
- 4- Each neuron applies an action function (usually nonlinear) to its net input (sum of weighted input signals) to determine its output signal [1].

The units in a network are organized into a given topology by a set of connections, or weights .

Ann is Characterized by[2] :

- 1- Architecture: its pattern of connections between the neurons.
- 2- Training Algorithm : its method of determining the weights on the connections.
- 3- Activation function.

Ann's are often classified as single layer or multilayer. In determining the number of layers, the input units are not counted as a layer, because they perform no computation. Equivalently, the number of layers in the net can be defined to be the number of layers of weighted interconnects links between the slabs of neurons [3].

## 2. Multilayer Feed Forward Architecture [4]

In a layered neural network the neurons are organized in the form of layers. We have at least two layers: an input and an output layer. The layers between the input and the output layer (if any) are called hidden layers, whose computation nodes are correspondingly called hidden neurons or hidden units. Extra hidden neurons raise the network's ability to extract higher-order statistics from (input) data .

The Ann is said to be fully connected in the sense that every node in each layer of the network is connected to every other node in the adjacent forward layer , otherwise the network is called partially connected. Each layer consists of a certain number of neurons; each neuron is connected to other neurons of the previous layer through adaptable synaptic weights  $w$  and biases  $b$  .

## 3. Description of the suggest Method

In the proposed approach the model function is expressed as the sum of two terms: the first term satisfies the initial conditions (IC) and contains no adjustable parameters. The second term can be found by using feed forward neural network(FFNN) which is trained so as to satisfy the differential equation and such technique is called collocation neural network. Since it is known that a multilayer FFNN with one hidden layer can approximate any function to arbitrary accuracy[5], [6] , thus our FFNN contains one hidden layer.

In this section we will illustrate how our approach can be used to find an approximate solution of the general form a differential equation of first order :  $y'(x) = F(x, y(x))$  , (1)

subject to certain IC's and  $x = (x_1, x_2, \dots, x_n) \in R^n$ ,  $D \subset R^n$  denotes the domain and  $y(x)$  is the analytic solution to be computed.

If  $y_t(x, p)$  denotes a trial solution with adjustable parameters  $p$ , the problem is transformed to a discretize form :

$$\text{Min}_p \sum_{\bar{x}_i \in D} F(x_i, y_t(x_i, p)) \quad , \quad (2)$$

subject to the constraints imposed by the IC's.

In the our proposed approach, the trial solution  $y_t$  employs a FFNN and the parameters  $p$  correspond to the weights and biases of the neural architecture. We choose a form for the trial function  $y_t(x)$  such that it satisfies the IC's. This is achieved by writing it as a sum of two terms :

$$y_t(x_i, p) = A(x) + G(x, N(x, p)) \quad , \quad (3)$$

where  $N(x, p)$  is a single-output FFNN with parameters  $p$  and  $n$  input units feed with the input vector  $x$ . The term  $A(x)$  contains no adjustable parameters and satisfies the IC's. The second term  $G$  is constructed so as not to contribute to the IC's, since  $y_t(x)$  satisfy them. This term can be formed by using a FFNN whose weights and biases are to be adjusted in order to deal with the minimization problem.

#### 4. Computation of the Gradient

An efficient minimization of (2) can be considered as a procedure of training the FFNN, where the error corresponding to each input vector  $x_i$  is the value  $E(x_i)$  which has to forced near zero. Computation of this error value involves not only the FFNN output but also the derivatives of the output with respect to any of its inputs. Therefore, in computing the gradient of the error with respect to the network weights consider a multi layer FFNN with  $n$  input units (where  $n$  is the dimensions of the domain ) one hidden layer with  $H$  sigmoid units and a linear output unit .

For a given input vector  $x = (x_1, x_2, \dots, x_n)$  the output of the FFNN is :  $N = \sum_{i=1}^H v_i \sigma(z_i)$ , where  $z_i = \sum_{j=1}^n w_{ij} x_j + b_i$

$w_{ij}$  denotes the weight connecting the input unit  $j$  to the hidden unit  $i$   
 $v_i$  denotes the weight connecting the hidden unit  $i$  to the out put unit ,  
 $b_i$  denotes the bias of hidden unit  $i$ , and  
 $\sigma(z)$  is the sigmoid transfer function ( tanhsig. ).

The gradient of FFNN, with respect to the parameters of the FFNN can be easily obtained as :

$$\frac{\partial N}{\partial v_i} = \sigma(z_i) \quad , \quad (4)$$

$$\frac{\partial N}{\partial b_i} = v_i \sigma'(z_i) \quad , \quad (5)$$



$$\frac{\partial N}{\partial w_{ij}} = v_i \sigma'(z_i) x_j, \quad (6)$$

Once the derivative of the error with respect to the network parameters has been defined, then it is a straight forward to employ any minimization technique. It must also be noted, the batch mode of weight updates may be employed.

### 5. Illustration Of The Method

In this section we describe solution of single IVP using FFNN .

To illustrate the method, we will consider the first order IVP

$$dy(x) / dx = f(x, y), \quad (7)$$

where  $x \in [0, 1]$  and the IC :  $y(0) = A$ , a trial solution can be written as :

$$y_t(x) = A + x N(x, p), \quad (8)$$

where  $N(x, p)$  is the output of a FFNN with one input unit for  $x$  and weights  $p$ .

#### Note that

$y_t(x)$  satisfies the IC by construction. The error quantity to be minimized is given by :

$$E[p] = \sum_{i=1}^n \left\{ dy_t(x_i) / dx - f(x_i, y_t(x_i)) \right\}^2, \quad (9)$$

where the  $x_i \in [0, 1]$ . Since :  $dy_t(x) / dx = N(x, p) + x \frac{dN(x, \bar{p})}{dx}$

it is straightforward to compute the gradient of the error with respect to the parameters  $p$  using (4) – (6). The same holds for all subsequent model problems.

### 6. Example

In this section we report numerical result, we use a multi-layer FFNN having one hidden layer with 5 hidden units (neurons) and one linear output unit. The sigmoid activation of each hidden unit is tanhsig, the analytic solution  $y_a(x)$  was known in advance. Therefore we test the accuracy of the obtained solutions by computing the deviation :

$$\Delta y(x) = |y_t(x) - y_a(x)|.$$

In order to illustrate the characteristics of the solutions provided by the neural network method, we provide figures displaying the corresponding deviation  $\Delta y(x)$  both at the few points (training points) that were used for training and at many other points (test points) of the domain of equation. The latter kind of figures are of major importance since they show the interpolation capabilities of the neural solution which to be superior compared to other solution obtained by using other methods. Moreover, we can consider points outside the training interval

in order to obtain an estimate of the extrapolation performance of the obtained numerical solution.

Consider the following first order IVP :

$$dy/dx = x^3 + 2x + x^2 \frac{1+3x^2}{1+x+x^3} - \left( x + \frac{1+3x^2}{1+x+x^3} \right) y$$

with  $y(0) = 1$  and  $x \in [0, 1]$ . The analytic solution is :

$$y_a(x) = \frac{e^{\frac{x^2}{2}}}{1+x+x^3} + x^2, \text{ according to (8) the trial neural form of the}$$

solution is taken to be :  $y_t(x) = 1 + x N(x, p)$ .

The FFNN trained using a grid of ten equidistant points in  $[0, 1]$ . Figure(1) display the analytic and neural solutions with different training algorithm such as : Levenberg – Marquardt (trainlm), conjugate gradient ( traincgf , traincgp ) , quasi – Newton ( trainbfg ) , Bayesian Regulation (trainbr) . The neural results with different types of training algorithm introduced in table (1) and its errors given in table (2), table(4) gives the weight and bias of the designer network ,table(3) gives the performance of the train with epoch and time .

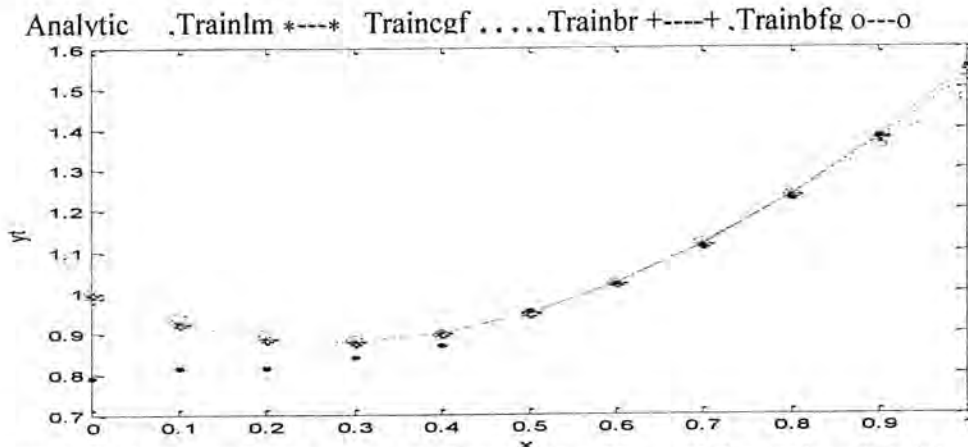


Figure-1: analytic and neural solution of example using : trainlm, traincgf, trainbr and trainbfg training algorithm



Table-1: Analytic and neural solutions of example

$x_i$	$y_a(x)$ (analytic)	trainlm	traincgf	traincgp	trainbfg	trainbr
0.0	1	1	0.790032921	0.997474638	0.999284298	0.984715174
0.1	0.922817911	0.923239090	0.814111397	0.925830028	0.938200116	0.922812329
0.2	0.884537533	0.884537539	0.840088237	0.888248962	0.897608871	0.884547884
0.3	0.878265154	0.878240933	0.869817090	0.881834673	0.882727912	0.877722282
0.4	0.899950182	0.899950199	0.906262886	0.902755242	0.897367528	0.899904677
0.5	0.947322124	0.947322148	0.953892248	0.948625013	0.943275619	0.947431439
0.6	1.019260662	1.019260685	1.018857932	1.018947884	1.019035732	1.019136302
0.7	1.115365302	1.115365329	1.108390156	1.114454634	1.119172120	1.115442881
0.8	1.235643496	1.235745678	1.228482248	1.235804481	1.234755775	1.235625930
0.9	1.380293837	1.380293851	01.37949830	1.381811216	1.355678282	1.374999420
1.0	1.549573756	1.546833461	1.551840247	1.547473024	1.472971587	1.523787407

Table-2 : Accuracy of solutions for example

Error = $ y_t(x) - y_a(x) $				
trainlm	traincgf	traincgp	trainbfg	trainbr
1.008e-08	0.209967078	0.002525361	7.15707e-04	0.015284825
2.422e-04	0.108706514	0.003012116	0.015382205	5.5819e-06
6.588e-09	0.044449295	0.003711429	0.013071338	1.0351e-05
2.422e-05	0.008448064	0.00356951	0.004462757	5.4287e-04
1.706e-08	0.006312704	0.00280506	0.002582654	4.5504e-05
2.363e-08	0.006570123	0.00130288	0.004046505	1.0931e-04
2.343e-08	4.0272034e-04	3.1277e-04	2.2493e-04	1.2435e-04
2.643e-08	0.006975146	9.1066e-04	0.003806818	7.7579e-05
1.021e-04	0.007161248	1.6098e-04	0.8772e-04	1.7566e-05
1.374e-08	7.9553e-5	0.001517378	0.024615555	0.005294417
0.002740295	0.002266490	0.002100732	0.076602169	0.025786349

Table-3 : the performance of the train with epoch and time .

Train code	Performance of train	Epoch	Time
Trainlm	3.47e-10	311	0:00:05
Traincgf	2.99e-6	20	0:00:05
Traincgp	5.59e-06	54	0:00:06
Trainbr	3.60e-08	69	0:00:06
Trainbfg	8.4e-5	38	0:00:01

Table-4: Weight and bias of the network for different training algorithm

Weights and bias for trainbfg		
Net.IW{1,1}	Net.LW{2,1}	Net.B{1}
0.6967	0.0005	0.4795
0.5828	0.8654	0.8013
0.8154	0.6126	0.2278
* 0.8790	0.9900	0.4981
0.9889	0.5277	0.9009

Weights and bias for traincgf		
Net.IW{1,1}	Net.LW{2,1}	Net.B{1}
0.9941	0.6681	0.9596
0.8385	0.4812	0.4421
0.3474	0.2862	0.9620
0.7494	0.5952	0.6764
0.9394	0.3364	0.7061

Weights and bias for trainlm		
Net.IW{1,1}	Net.LW{2,1}	Net.B{1}
0.5085	0.3786	0.8759
0.5108	0.8116	0.5502
0.8176	0.5328	0.6225
0.7948	0.3507	0.5870
0.6443	0.9390	0.2077

Weights and bias for traincgp		
Net.IW{1,1}	Net.LW{2,1}	Net.B{1}
0.3808	0.2836	0.2414
0.7072	0.0406	0.6960
0.2389	0.5514	0.0153
0.1758	0.9425	0.7685
0.2381	0.7878	0.3319

Weights and bias for trainbr		
Net.IW{1,1}	Net.LW{2,1}	Net.B{1}
0.4271	0.5206	0.0864
0.5889	0.9141	0.0408
0.0917	0.6633	0.7516
0.2506	0.4997	0.3238
0.5938	0.6348	0.0665

L. N. M. Tawfiq[7] solve this problem using Ann with radial basis function and unsupervised training algorithm that is Hopfield networks and the results given in table (5) .

Table-5: Results of RBFNN and Hopfield given in [7]

Inputx	Analytic solution $y_a(x)$	RBFNN	Hopfield	Deviation $\Delta y(x) =  y_t(x) - y_a(x) $ , with $e^{-4}$ when used RBFNN	Deviation $\Delta y(x) =  y_t(x) - y_a(x) $ , with $e^{-4}$ when used Hopfield
1.0	1.202176	1.202155	1.202138	0.21	0.38
0.0	1.000000	0.999999	0.999999	0.01	0.01
0.1	0.913735	0.913731	0.613728	0.02	0.07
0.2	0.851422	0.851415	0.851385	0.07	0.37
0.3	0.810420	0.810405	0.810399	0.15	0.23
0.4	0.790543	0.790515	0.790511	0.28	0.32
0.5	0.793075	0.793065	0.793060	0.10	0.15
0.6	0.819950	0.819942	0.819931	0.08	0.19
0.7	0.873115	0.873109	0.873102	0.06	0.13
0.8	0.954078	0.954066	0.954063	0.12	0.15
0.9	1.063699	1.063694	1.063688	0.05	0.11

## 7. Conclusion

From the above problems it is clear that the method is proposed can handle effectively ODE and provide accurate approximate solution throughout the whole domain and not only at the training points. As evident from the tables, the results of proposed method are more precise as compared to RBFNN and Hopfield network.



It is very difficult to know which training algorithm will be the fastest for a given problem. It depends on many factors including the complexity of the problem, the number of data points in the training set, the number of weights and biases in the FFNN, the error goal, and whether the FFNN is being used for pattern recognition (discriminant analysis) or function approximation (regression).

In general, the practical results on FFNN show which contain up to a few hundred weights the Levenberg-Marquardt algorithm (`trainlm`) will have the fastest convergence, then `trainbr` and then `trainbfg`. However, "`trainbr`" it does not perform well on function approximation on problems. The CG algorithms, in particular "`traincgp`", seem to perform well over a wide variety of problems, particularly for FFNN with a large number of weights. The CG algorithms have relatively modest memory requirements, the "`trainbfg`" performance is similar to that of "`trainlm`" some times, it does not require as much storage as "`trainlm`", but the computation required does increase geometrically with the size of the FFNN, since the equivalent of a matrix inverse must be computed at each iteration. Of the CG algorithms, the "`traincgp`" require the most storage, but usually has the fastest convergence. For most situations, we recommend that we try to use the "`trainlm`" algorithm first, if this algorithm require too much memory, then "`trainbfg`" if, easy computed Hessian matrix and then try "`trainbr`" algorithm. The performance of the various algorithms can be affected by the accuracy required of the approximation.

## REFERENCES

1. I. A. Galushkin, "Neural Networks Theory", Berlin Heidelberg, (2007).
2. R. M. Hristev, "The ANN Book", Edition 1, (1998).
3. T. Villmann, U. Seiffert and A. Wismüller, "Theory and Applications of Neural maps", ESANN2004 PROCEEDINGS - European Symposium on Ann, pp.25 - 38, April (2004).
4. L.N.M. Tawfiq and R.S. Naoum, "On Training of Artificial Neural Networks", AL-Fath Jornal, No 23(2005).
5. L.N.M. Tawfiq and R.S. Naoum "Density and approximation by using feed forward Artificial neural networks", Ibn Al-Haitham Journal for Pure & Applied Sciences, Vol. 20 (1) (2007).
6. A. K. Jabber, "On Training Feed Forward Neural Networks for Approximation Problem", MSc Thesis, Baghdad University, College of Education (Ibn Al-Haitham) (2009).
7. L. N. M. Tawfiq, "Design and Training Artificial Neural Networks for Solving Differential Equations", PhD thesis, University of Baghdad, College of Education – Ibn – Al- Haitham, (2004).

## On Optimal Codes

Najm A. M. AL-SERAJI

Dept. of Math.- College of Science - Al-Mustansiriya Univ.- Baghdad

Received 14/9/2011 – Accepted 18/4/2012

### الخلاصة

يقدم هذا البحث استخداما للعلاقة بين الأقواس في فضاء الإسقاط و الرموز المثالية لإيجاد حلول الرموز المثالية. استخدمت لغة GAP كوسيلة لإسناد و برمجة الجانب الرياضي. وقد تم توضيح خواص الرموز الرئيسية مع بعض الأمثلة.

### ABSTRACT

This paper provides, the relation between arcs in a projective space and optimal codes which is used to provide solutions for optimal codes. The main computing tool is the mathematical programming language GAP. The properties of optimal codes with some examples are shown.

### NOTATION

$GF(q)$	Galois field of $q = p^h$ elements, $p$ prime and $h$ positive integer
$PG(n, q)$	$n$ -dimensional Projective space over $GF(q)$
$V(k, q)$	a vector space of dimension $k$ over $GF(q)$
$n$ -arc	set of $n$ points no three of which are collinear
$m(r, q)$	the maximum size of an $n$ -arc in $PG(r, q)$
$\binom{n}{k}$	number of ways of choosing $k$ objects out of $n$
$I_k$	the identity matrix

### INTRODUCTION

The main goal of this work is to introduce concepts and some examples of Codes and arcs also studied the relationship between them. The subject of the study depends on the subject of projective space over Galois field, the vector space and error-correcting codes see [1], [2], [3] and [4].

An  $(n, M, d)_q$  code  $C$  is a set of  $M$  words, each with  $n$  symbols taken from an alphabet of size  $q$ , such that any two words differ in at least  $d$  places. A code  $(n, M, d)_q$  has the following desirable properties:

- Small  $n$ : fast transmission;
- Large  $M$ : many messages;
- Large  $d$ : correct many errors.

If the code is linear, it can more easily be used for encoding and decoding; in this case,  $M = q^k$  for some positive integer  $k$ , the dimension of the code, and  $C$  is called an  $[n, k, d]_q$  code. The main Coding Theory problem is to find codes optimizing one parameter with the other two fixed. Mathematically, such a code can also be viewed as a set of  $n$  points in  $PG(k-1, q)$  with at most  $n-d$  points in a subspace of dimension  $k-2$ .

## PREVIOUS RESULTS

**Definition (1)[4]:** A normal rational curve in  $PG(r, q)$  is any subset of  $PG(r, q)$  which is projectively equivalent to:

$$\{(t^r, t^{r-1}, \dots, t, 1) \in PG(r, q) | t \in GF(q) \cup \{\infty\}\}.$$

For  $r = 2$ , it is a conic; for  $r = 3$ , it is a twisted cubic.

**Definition (2)[1]:** An  $(n, M)$  code  $C$  over  $GF(q)$  is a subset of  $(GF(q))^n$  of size  $M$ . A linear  $[n, k]_q$  code over  $GF(q)$  is a  $k$ -dimensional subspace of  $(GF(q))^n$  and size  $M = q^k$ . The vectors in the linear code  $C$  are called *codewords* and we denote them by  $x = x_1 x_2 \dots x_n$ , where  $x_i \in GF(q)$ .

**Definition (3)[1]:** A generator matrix  $G$  for an  $[n, k]_q$  code  $C$  is any  $k \times n$  matrix  $G$  whose rows form a basis for  $C$ . For any set of  $k$  independent columns of a generator matrix  $G$ , the corresponding set of coordinates forms an information set for  $G$ . If the first  $k$  coordinates form an information set, the code has a unique generator matrix of the form  $[I_k | A]$  where  $I_k$  is the  $k \times k$  identity matrix; such a generator matrix is in *standard form* which means  $[I_k | A]$ .

**Definition (4)[3]:** The ordinary inner product of vectors  $u = u_1 u_2 \dots u_n, v = v_1 v_2 \dots v_n$  in  $(GF(q))^n$  is defined by

$$u \cdot v = \sum_{i=1}^n u_i v_i.$$

**Definition (5)[1]:** The dual of the code  $C$  is the  $[n, n - k]_q$  linear code  $C^\perp$  defined as

$$C^\perp = \{v \in (GF(q))^n | u \cdot v = 0 \forall u \in C\}.$$

**Definition (6)[3]:** A parity check matrix  $H$  of a linear  $[n, k]_q$  code  $C$  is defined to be an  $(n - k) \times n$  generator matrix of  $C^\perp$ .

**Remark (7):** From the previous definition, we deduce that

$$C = \{x \in (GF(q))^n | Hx^T = 0\}.$$

**Theorem (8)[3]:** If  $G = [I_k | A]$  is a generator matrix for  $C$  in standard form, then  $H = [-A^T | I_{n-k}]$  is a parity check matrix for  $C^\perp$ .

**Definition (9)[1]:** The (Hamming) distance  $d(x, y)$  between two vectors  $x, y$  in  $(GF(q))^n$  is defined to be the number of coordinate in which  $x$  and  $y$  differ. The distance  $d$  is a *metric*. The minimum distance

$d$  of a code  $C$  is the smallest distance between any pair of distinct codewords.

**Definition (10)[1]:** The (Hamming) weight  $w(x)$  of a vector  $x$  in  $(GF(q))^n$  is the number of its nonzero coordinates.

**Theorem (11)[1]:** A linear code has minimum distance  $d$  if and only if its parity check matrix has a set of  $d$  linearly dependent columns but there is no set of  $d - 1$  linearly dependent columns.

**Corollary (12)[1]:** For any  $[n, k, d]_q$  code we have  
 $d \leq n - k + 1$ .

**Definition (13)[1]:** A code is *optimal* or *maximum distance separable (MDS)* when  
 $d = n - k + 1$ .

**Lemma (14)[3]:** Let  $r = n - k$ . An  $r \times n$  matrix  $H$  is the parity-check matrix of an optimal code if and only if the  $n$  columns are vector in  $V(r, q)$  with every  $r$  linearly independent.

**Lemma (15)[3]:** An  $[n, k]_q$  code  $C$  has  $d(C) = d$  if and only if the  $n$  columns of a generator matrix  $G$  are vectors in  $V(r, q)$  such that any prime, that is, a subspace of dimension  $k - 1$ , contains at most  $n - d$  of the  $n$  vectors.

**Lemma (16)[3]:** An  $[n, k]_q$  code  $C$  is optimal if and only if the vectors in  $V(r, q)$  given by the  $n$  columns of a generator matrix  $G$  have at most  $k - 1$  in a prime; that is, every  $k$  is linearly independent.

**Theorem (17)[3]:** An  $[n, k]_q$  code  $C$  is optimal if and only if  $C^\perp$  is optimal.

**Example (18)[3]: Reed-Solomon codes**

Let  $GF(q) = \{0, t_1, \dots, t_{q-1}\}$  and, for  $2 \leq r \leq q$ , let

$$M = \begin{bmatrix} 1 & \dots & 1 \\ t_1 & \dots & t_{q-1} \\ t_1^2 & \dots & t_{q-1}^2 \\ \vdots & \vdots & \vdots \\ t_1^{r-1} & \dots & t_{q-1}^{r-1} \end{bmatrix}.$$



The matrix  $M$  is a "Vandermonde matrix". Note that, if  $M'$  is the  $r \times r$  matrix obtained from the first  $r$  columns of  $M$ , then

$$\det M' = \prod_{i>j} (t_i - t_j) \neq 0$$

Hence every  $r$  columns of  $M$  are linearly independent, otherwise  $\det M' = 0$ .

**Definition (19)[3]:** (1) A submatrix of a matrix  $A$  is a matrix obtained by removing a number of rows and columns of  $A$ .

(2) A minor of  $A$  is the determinant of a square submatrix.

**Theorem (20)[3]:** An  $[n, k]_q$  code  $C$  with generator matrix  $G = [I_k A]$  is optimal if and only if every minor of  $A$  is non-zero.

**Theorem (21)[3]:** For  $q \leq k$ ,

$$M(k, q) = k + 1;$$

The corresponding  $[k, k + 1]_q$  code  $C$  is equivalent to one with generator matrix

$$G = [I_k e^T],$$

Where  $e = (11 \dots 1)$ .

## RESULTS AND DISCUSSION

**Theorem (22):**

$$M(3, q) = \begin{cases} q + 2, & q \text{ even;} \\ q + 1, & q \text{ odd.} \end{cases}$$

**Proof:**

(1) There exists  $[q + 1, 3]$  optimal codes for  $q$  odd and  $[q + 2, 3]$  optimal codes

for  $q$  even: since  $N_{q+1}(3)^\perp$  and  $N_{q+2}(3)^\perp$  they have generator matrices as

follows:

$$\begin{bmatrix} 1 & \dots & 1 & 1 & 0 \\ t_1 & \dots & t_{q-1} & 0 & 0 \\ t_1^2 & \dots & t_{q-1}^2 & 0 & 1 \end{bmatrix},$$

$$\begin{bmatrix} 1 & \dots & 1 & 1 & 0 & 0 \\ t_1 & \dots & t_{q-1} & 0 & 0 & 1 \\ t_1^2 & \dots & t_{q-1}^2 & 0 & 1 & 0 \end{bmatrix}.$$

(2) Next, show that  $M(3, q) \leq q + 2$ .

Suppose

$$G = \begin{bmatrix} 1 & 0 & 0 & a_1 & \dots & a_s \\ 0 & 1 & 0 & b_1 & \dots & b_s \\ 0 & 0 & 1 & c_1 & \dots & c_s \end{bmatrix}$$

Let,  $C_1 = \begin{bmatrix} 1 \\ 0 \\ 0 \end{bmatrix}$ ,  $C_2 = \begin{bmatrix} 0 \\ 1 \\ 0 \end{bmatrix}$ ,  $C_3 = \begin{bmatrix} 0 \\ 0 \\ 1 \end{bmatrix}$  and  $C_4 = \begin{bmatrix} a_1 \\ b_1 \\ c_1 \end{bmatrix}$ .

From  $C_2, C_3, C_4$ , it follows that  $a_1 \neq 0$ ; similarly  $a_i \neq 0$ , for all  $i$

So there is an equivalent code with generator matrix  $G'$  and different  $b_i, c_i$  such that

$$G' = \begin{bmatrix} 1 & 0 & 0 & 1 & 1 & 1 & \dots & 1 \\ 0 & 1 & 0 & b_1 & b_2 & b_3 & \dots & b_s \\ 0 & 0 & 1 & c_1 & c_2 & c_3 & \dots & c_s \end{bmatrix}$$

Now, let,  $C_4 = \begin{bmatrix} 1 \\ b_1 \\ c_1 \end{bmatrix}$ ,  $C_5 = \begin{bmatrix} 1 \\ b_2 \\ c_2 \end{bmatrix}$ .

From  $C_1, C_3, C_4$ , we have  $b_1 \neq 0$ ; similarly  $b_i \neq 0$ , for all  $i$ .

From  $C_3, C_4, C_5$ , we have  $b_1 \neq b_2$ ; similarly  $b_i \neq b_j$ , for  $i \neq j$ .

Hence  $\{b_1, \dots, b_s\} \subset GF(q) - \{0\}$ . So  $s \leq q - 1$ .

Hence  $M(3, q) \leq 3 + (q - 1) = q + 2$ .

(3) Suppose for  $q$  odd,  $M(3, q) = q + 2$ .

Hence there exist a generator matrix  $G'$  as above

$$G' = \begin{bmatrix} 1 & 0 & 0 & 1 & 1 & 1 & \dots & 1 \\ 0 & 1 & 0 & b_1 & b_2 & b_3 & \dots & b_{q-1} \\ 0 & 0 & 1 & c_1 & c_2 & c_3 & \dots & c_{q-1} \end{bmatrix}$$

Where  $\{b_1, \dots, b_{q-1}\} = GF(q) - \{0\}$ .

Similarly,  $\{c_1, \dots, c_{q-1}\} = GF(q) - \{0\}$ , since codes  $C_1, C_2, C_4 \rightarrow c_1 \neq 0$  and

Codes  $C_2, C_4, C_5 \rightarrow c_1 \neq c_2$ .

Now codes  $C_1, C_4, C_5 \rightarrow b_1 c_2 - b_2 c_1 \neq 0$

$$\rightarrow b_1 c_1^{-1} \neq b_2 c_2^{-1}$$

Hence  $\{b_1 c_1^{-1}, \dots, b_{q-1} c_{q-1}^{-1}\} = GF(q) - \{0\}$ .

Finally

$$\prod_{\substack{t \neq 0 \\ t \in GF(q)}} t = -1 \quad \dots \quad (1)$$

Hence

$$\prod_{i=1}^{q-1} (b_i c_i^{-1}) = -1$$

But

$$\begin{aligned} \prod_{i=1}^{q-1} (b_i c_i^{-1}) &= (\prod_{i=1}^{q-1} b_i) (\prod_{i=1}^{q-1} c_i^{-1}) \\ &= (\prod_{i=1}^{q-1} b_i) (\prod_{i=1}^{q-1} c_i)^{-1} \\ &= (-1)(-1) = 1 \end{aligned}$$

For  $q$  odd, this is a contradiction with equation (1) ■

**Theorem (23):** In an  $[n, k]_q$  code  $C$  that is MDS, the number of words of minimum weight  $d = n - k + 1$  is

$$(q - 1) \binom{n}{d}.$$

**Proof:** Suppose that

$$G = \begin{bmatrix} a_{11} & \cdots & a_{1n} \\ \vdots & \ddots & \vdots \\ a_{k1} & \cdots & a_{kn} \end{bmatrix}$$

Be a generator matrix for the  $[n, k]_q$  MDS code  $C$ .

Since the first  $k$  columns are linearly independent,

So

$$\text{rank}(G) = k = \dim(C),$$

By row operations give the matrix  $G'$  in standard form

$$G' = \begin{bmatrix} 1 & 0 & 0 & b_1 & b_2 & b_3 & \cdots & b_{q-1} \\ 0 & 1 & 0 & c_1 & c_2 & c_3 & \cdots & c_{q-1} \\ 0 & 0 & 1 & d_1 & d_2 & d_3 & \cdots & d_{q-1} \end{bmatrix} = [I_k A],$$

Which is another generator matrix for  $C$  with  $b_i, c_i, d_i \neq 0$  for all  $i = 1, \dots, q - 1$ .

Hence the number of words of  $C$  with 0 in the first  $k - 1$  positions, and so weight  $n - (k - 1)$ , is

$$\prod_{i=1}^{q-1} d_i = -1 = q - 1;$$

These words are just multiples of the last row of  $G'$ .

Hence the number of words of weight  $n - (k - 1)$  is  
 $(q - 1) \binom{n}{k-1} = (q - 1) \frac{n!}{(n-k+1)!(k-1)!} = (q - 1) \binom{n}{d}$  ■

**Example (24):** the case  $k = 2$  and  $q = 5$ .

$$\text{GF}(5) = \{0, 1, 2, 3, 4\}$$

$$G = \begin{bmatrix} 1 & 0 & 1 & 2 & 3 & 4 \\ 0 & 1 & 1 & 1 & 1 & 1 \end{bmatrix} = [I_k A] = [I_2 A].$$

$$\text{Dim}(C) = k = 2, d = n - k + 1 = 6 - 2 + 1 = 5$$

Hence  $C$  is optimal.

The parity-check matrix is

$$H = \begin{bmatrix} -1 & -1 & 1 & 0 & 0 & 0 \\ -2 & -1 & 0 & 1 & 0 & 0 \\ -3 & -1 & 0 & 0 & 1 & 0 \\ -4 & -1 & 0 & 0 & 0 & 1 \end{bmatrix} = [-A^T I_4].$$

$$\text{Dim}(C^\perp) = n - k = 6 - 2 = 4, d(C^\perp) = d^\perp = 3 = 6 - 4 + 1 = n - k + 1.$$

Hence  $C^\perp$  is optimal code (theorem 17).

**Example (25):** The case  $k = 3$  and  $q = 7$ .

$$\text{GF}(7) = \{0, 1, -1, 2, -2, 3, -3\}$$

$$G = \begin{bmatrix} 1 & 0 & 0 & 1 & -1 & 1 & 3 & 1 \\ 0 & 1 & 0 & 1 & 1 & -3 & -1 & 3 \\ 0 & 0 & 1 & 1 & 3 & 2 & 1 & -1 \end{bmatrix} = [I_k A] = [I_3 A].$$

$$\text{Dim}(C) = k = 3, d = n - k + 1 = 8 - 3 + 1 = 6$$

Hence  $C$  is optimal.

Also, we note that, the elements of finite projective plane of order seven are consider columns of generator matrix  $G$ .

Let  $P_1 = (1, 0, 0), P_2 = (0, 1, 0), P_3 = (0, 0, 1), P_4 = (1, 1, 1), P_5 = (-1, 1, 3), P_6 = (1, -3, 2), P_7 = (3, -1, 1), P_8 = (1, 3, -1)$ .



The 8-arc  $= \{P_1, P_2, \dots, P_8\}$  is a conic and complete, that is not contained in 9-arc.

From *Theorem 22*, the maximum size of an 8-arc in finite projective plane of order seven  $PG(2,7)$  is  $q + 1 = 7 + 1 = 8$ .

The parity-check matrix is

$$H = \begin{bmatrix} -1 & -1 & -1 & 1 & 0 & 0 & 0 & 0 \\ 1 & -1 & -3 & 0 & 1 & 0 & 0 & 0 \\ -1 & 3 & -2 & 0 & 0 & 1 & 0 & 0 \\ -3 & 1 & -1 & 0 & 0 & 0 & 1 & 0 \\ -1 & -3 & 1 & 0 & 0 & 0 & 0 & 1 \end{bmatrix} = [-A^T I_5].$$

$$\text{Dim}(C^\perp) = n - k = 8 - 3 = 5, \quad d(C^\perp) = d^\perp = 4 = 8 - 5 + 1 = n - k + 1.$$

Hence  $C^\perp$  is optimal code (*Theorem 17*).

### Conclusions

- The main computing tool is the mathematical programming language **GAP** and it is used to find the generator matrix in examples (24) and (25).
- The subject of the study is consider the links between error-correcting codes, Projective Space and the vector space over Galois field.
- The columns of the generator matrix of any code consider elements in projective space.
- In future, we can study the subject of almost optimal codes, that is when  $d = n - k$ .
- The geometrical objects considered in this work can be viewed and studied as linear codes defined over a finite field.

### REFERENCES

1. Al-seraji N.A.M, " The Geometry Of The Plane Of Order Seventeen And Its Application To Error-Correcting Codes" Ph.D. Thesis, University of Sussex, UK, (2010).
2. Hirschfeld J.W.P, " *Projective Geometries Over Finite Fields* " *Second Edition*, Oxford University Press, Oxford, (1998).
3. Hirschfeld J.W.P " *Lectures in Coding Theory*" Sussex University, UK, (2008).
4. Hirschfeld J.W.P, Korchmáros G and Torres F, " *Algebraic Curves Over a Finite field*" Oxford University Press, Oxford, (2007).

## A Not on Fully (m,n)-stable modules relative to ideal

Muna Jasim Mohammed Ali

Baghdad University/ College of Science for women/ Department of Mathematics

Received 1/6/2011 – Accepted 20/6/2012

### الخلاصة

لتكن  $R$  حقلية ذات عنصر محايد  $M$  مقاساً أيسراً أحادياً على  $R$  و  $A$  مثالي في الحلقة  $R$ ، كتعميم لمفهوم المقاسات تامة الاستقرار من النمط  $(m,n)$  عرفنا المقاسات تامة الاستقرار من النمط  $(m,n)$  بالنسبة الى مثالي. نقول ان المقاس  $M$  تام الاستقرار من النمط  $(m,n)$  بالنسبة الى  $A$  اذا كان  $\theta(N) \subseteq N + AM^m$  لكل تشاكل مقاسي  $\theta$  من  $N$  الى  $M$  حيث  $N$  مقاس جزئي متولد من النمط  $n$ . في هذا البحث يتم دراسة علاقة صنف المقاسات تامة الاستقرار من النمط  $(m,n)$  بالنسبة الى مثالي باصناف اخرى مثل المقاسات الجدائية من النمط  $(m,n)$ ، المقاسات شبه الغامرة من النمط  $(m,n)$ .

### ABSTRACT

Let  $R$  be a commutative ring with non-zero identity element. For two fixed positive integers  $m$  and  $n$ . A left  $R$ -module  $M$  is called fully  $(m,n)$ -stable relative to ideal  $A$  of  $R$ , if  $\theta(N) \subseteq N + AM^m$  for each  $n$ -generated submodule of  $M^m$  and  $R$ -homomorphism  $\theta: N \rightarrow M^m$ . In this paper we give some characterization theorems and properties of fully  $(m,n)$ -stable modules relative to an ideal  $A$  of  $R$  which generalize the results of fully stable modules relative to an ideal  $A$  of  $R$ .

### 1. Introduction

Throughout,  $R$  is a commutative ring with non-zero identity and all modules are unitary right  $R$ -module. We use the notation  $R^{m \times n}$  for the set of all  $m \times n$  matrices over  $R$ . For  $G \in R^{m \times n}$ ,  $G^T$  will denote the transpose of  $G$ . In general, for an  $R$ -module  $N$ , we write  $N^{m \times n}$  for the set of all formal  $m \times n$  matrices whose entries are elements of  $N$ . Let  $M$  be a right  $R$ -module and  $N$  be a left  $R$ -module. For  $x \in M^{1 \times m}$ ,  $s \in R^{m \times n}$  and  $y \in N^{n \times k}$ , under the usual multiplication of matrices,  $xs$  (resp.  $sy$ ) is a well defined element in  $M^{1 \times n}$  (resp.  $N^{n \times k}$ ). If  $X \in M^{1 \times m}$ ,  $S \in R^{m \times n}$  and  $Y \in N^{n \times k}$ , define

$$\ell_{M^{1 \times m}}(S) = \{ u \in M^{1 \times m} : us = 0, \forall s \in S \}$$

$$\gamma_{N^{n \times k}}(S) = \{ v \in N^{n \times k} : vs = 0, \forall s \in S \}$$

$$\ell_{R^{m \times n}}(Y) = \{ s \in R^{m \times n} : sy = 0, \forall y \in Y \}$$

$$\gamma_{R^{m \times n}}(X) = \{ s \in R^{m \times n} : xs = 0, \forall x \in X \}$$

We will write  $N^n = N^{1 \times n}$ ,  $N_n = N^{n \times 1}$ . Fully stable module relative to an ideal have been discussed in [1], an  $R$ -module  $M$  is called fully stable relative to an ideal, if  $\theta(N) \subseteq N + AM$  for each submodule  $N$  of  $M$  and  $R$ -homomorphism  $\theta: N \rightarrow M$ . It is an easy matter to see that  $M$  is fully stable relative to an ideal, if and only if  $\theta(xR) \subseteq xR + AM$  for each  $x$  in  $M$  and  $R$ -homomorphism  $\theta: xR \rightarrow M$ . In this paper, for two fixed positive integers  $m$  and  $n$ , we introduce the concepts of fully  $(m,n)$ -stable modules relative to an ideal and  $(m,n)$ -Baer criterion relative to an ideal

and we prove that an R-module M is fully (m,n) -stable relative to an ideal if and only if (m,n) -Baer criterion relative to an ideal holds for n-generated submodules of  $M^m$ .

## 2. Main Result

**Definition 2.1 :** An R-module M is called fully (m,n) -stable relative to an ideal A of R, if  $\theta(N) \subseteq N + AM^m$  for each n-generated submodule N of  $M^m$  and R-homomorphism  $\theta: N \rightarrow M^m$ . The ring R is fully (m,n) -stable relative to an ideal, if R is fully (m,n) -stable relative to an ideal as R-module.

It is clear that M is fully (1,1)-stable relative to ideal, if and only if M is fully

stable relative to ideal.

It is an easy matter to see that an R-module M is fully (m,n)-stable relative to ideal, if and only if it is fully (m,q)-stable relative to ideal for all  $1 \leq q \leq n$ , if and only if it is fully (p,n)-stable relative to ideal for all  $1 \leq p \leq m$ , if and only if it is fully (p,q)-stable relative to ideal for all  $1 \leq p \leq m$  and  $1 \leq q \leq n$ .

In [2], an R-module M is called fully-stable, if  $\theta(N) \subseteq N$  for each cyclic submodule N of M and R-homomorphism  $\theta: N \rightarrow M$ . An R-module M is called fully (m,n) -stable, if  $\theta(N) \subseteq N$  for each n-generated submodule N of  $M^m$  and R-homomorphism  $\theta: N \rightarrow M^m$  [3]. It is clear that every fully (m,n)-stable module M is a fully (m,\$)-stable relative to each non-zero ideal A of R for this follows from the fact  $\theta(N) \subseteq N + AM^m$ .

An R-module M is fully (m,n)-stable relative to an ideal A of R, if and only if for each  $\theta: N(\sum_{i=1}^n \alpha_i R) \rightarrow M^m$  (where  $\alpha_i \in M^m$ ) and each  $w \in N$ , there exists  $t = (t_1, \dots, t_n) \in R^n$  such that  $\theta(w) = \sum_{i=1}^n \alpha_i t_i + AM^m = (\alpha_1, \dots, \alpha_n) t^T + AM^m$ , if  $r = (r_1, \dots, r_n) \in R^n$ , then  $\theta((\alpha_1, \dots, \alpha_n) r^T) + AM^m = (\alpha_1, \dots, \alpha_n) t^T + AM^m$ .

**Proposition 2.2 :** An R-module M is fully (m,n)-stable relative to an ideal A of R, if and only if any two m-element subsets  $\{\alpha_1, \dots, \alpha_m\}$  and  $\{\beta_1, \dots, \beta_m\}$  of  $M^n$ , if  $\beta_j \notin \sum_{i=1}^n \alpha_i R + AM^n$ , for each  $j = 1, \dots, m$  implies  $\gamma_{R_n} \{\alpha_1, \dots, \alpha_m\} \subsetneq \gamma_{R_n} \{\beta_1, \dots, \beta_m\}$ .

**Proof :** Assume that M is fully (m,n)-stable module relative to an ideal A of R and there exist two m-element subsets  $\{\alpha_1, \dots, \alpha_m\}$  and  $\{\beta_1, \dots, \beta_m\}$  of  $M^n$  such that  $\beta_j \notin \sum_{i=1}^n \alpha_i R + AM^n$ ,  $\forall j = 1, \dots, m$  and  $\gamma_{R_n} \{\alpha_1$

$\dots, \alpha_m\} \subseteq \gamma_{R_n} \{ \beta_1, \dots, \beta_m \}$ . Define  $f: \sum_{i=1}^n \alpha_i R \rightarrow M^m$  by  $f(\sum_{i=1}^n \alpha_i r_i) = \sum_{i=1}^n \beta_i r_i$ . Let  $\alpha_i = (a_{i1}, a_{i2}, \dots, a_{in})$ . If  $\sum_{i=1}^n \alpha_i r_i = 0$ , then  $\sum_{i=1}^n a_{ij} r_i = 0, j = 1, \dots, m$  implies that  $\alpha_j r^T = 0$  where  $r = (r_1, \dots, r_n)$  and hence  $r^T \in \gamma_{R_n} \{ \alpha_1, \dots, \alpha_m \}$ . By assumption  $\beta_j r^T = 0, j = 1, \dots, m$  so  $\sum_{i=1}^n \beta_i r_i = 0$ . This show that  $f$  is well defined. It is an easy matter to see that  $f$  is  $R$ -homomorphism. Fully  $(m,n)$ -stability relative to an ideal  $A$  of  $M$  implies that there exists  $t = (t_1, \dots, t_n) \in R^n$  and  $w \in AM^n$  such that  $f(\sum_{i=1}^n \alpha_i r_i) = \sum_{k=1}^n (\sum_{i=1}^n \alpha_i r_i t_k) + w$  for each  $\sum_{i=1}^n \alpha_i r_i \in \sum_{i=1}^n \alpha_i R$ . Let  $r_i = (0, \dots, 0, 1, 0, \dots, 0) \in R^n$  where 1 in the  $i$ th position and 0 otherwise.  $\beta_i = f(\alpha_i) = \sum_{k=1}^n \alpha_i t_k + w$  which is contradiction. Conversely assume that there exists  $n$ -generated submodule of  $M^m$  and  $R$ -homomorphism  $\theta: \sum_{i=1}^n \alpha_i R \rightarrow M^m$  such that  $\theta(\sum_{i=1}^n \alpha_i R) \not\subseteq \sum_{i=1}^n \alpha_i R + AM^n$ . Then there exists an element  $\beta (= \sum_{i=1}^n \alpha_i r_i) \in \sum_{i=1}^n \alpha_i R$  such that  $\theta(\beta) \notin \sum_{i=1}^n \alpha_i R + AM^n$ . Take  $\beta_j = \beta, j = 1, \dots, m$ , then we have  $m$ -element subset  $\{\theta(\beta), \dots, \theta(\beta)\}$ , such that  $\theta(\beta) \notin \sum_{i=1}^n \alpha_i R + AM^n, j = 1, \dots, m$ . Let  $\eta = (t_1, \dots, t_n)^T \in \gamma_{R_n} \{ \alpha_1, \dots, \alpha_m \}$  then  $\alpha_j \eta = 0$ , i.e  $\sum_{i=1}^n a_{ij} t_i = 0, \forall j = 1, \dots, m, \alpha_j = (a_{1j}, a_{2j}, \dots, a_{nj})$  and  $\{\theta(\beta), \dots, \theta(\beta)\} \eta = \sum_{k=1}^n \theta(\beta) t_k = \sum_{k=1}^n \theta(\sum_{i=1}^n \alpha_i r_i) t_k = \sum_{k=1}^n (\theta(\sum_{i=1}^n \alpha_i r_i t_k)) = 0$ , hence  $\gamma_{R_n} \{ \alpha_1, \dots, \alpha_m \} \subseteq \gamma_{R_n} \{ \theta(\beta), \dots, \theta(\beta) \}$ , thus  $\gamma_{R_n} \{ \alpha_1, \dots, \alpha_m \} \subseteq \gamma_{R_n} \{ \theta(\beta_1), \dots, \theta(\beta_m) \}$  which is a contradiction. Thus  $M$  is fully  $(m,n)$ -stable module relative to ideal.

**Corollary 2.3 :** Let  $M$  be fully  $(m,n)$ -stable module relative to an ideal  $A$  of  $R$ , then for any two  $m$ -element subsets  $\{ \alpha_1, \dots, \alpha_m \}$  and  $\{ \beta_1, \dots, \beta_m \}$  of  $M^n$ ,  $\gamma_{R_n} \{ \alpha_1, \dots, \alpha_m \} \subseteq \gamma_{R_n} \{ \beta_1, \dots, \beta_m \}$  implies  $\alpha_1 R + \dots + \alpha_m R + AM^n = \beta_1 R + \dots + \beta_m R + AM^n$ .

**Corollary 2.4:** [1] Let  $M$  be a fully stable module relative to an ideal  $A$  of  $R$ , then for each  $x, y$  in  $M, y \notin (x), \gamma_R(x) = \gamma_R(y)$  implies  $(x) + AM = (y) + AM$ .

A submodule  $N$  of an  $R$ -module  $M$  satisfies Baer criterion relative to an ideal  $A$  of  $R$ , if for every  $R$ -homomorphism  $f: N \rightarrow M$ , there exists an element  $r \in R$  such that  $f(n) - rn \in AM$  for each  $n \in N$ . An  $R$ -module  $M$  is said to satisfy Baer criterion relative to  $A$ , if each



submodule of  $M$  satisfies Baer criterion relative to  $A$  and it is proved that an  $R$ -module  $M$  satisfies Baer criterion relative to  $A$  for cyclic submodules, if and only if  $M$  is fully stable relative to  $A$  [1].

**Definition 2.5 :** For a fixed positive integers  $n$  and  $m$ , we say that an  $R$ -module  $M$  satisfies (m,n)-Baer criterion relative to an ideal  $A$  of  $R$ , if for any  $n$ -generated submodule  $N$  of  $M^m$  and any  $R$ -homomorphism  $\theta: N \rightarrow M^m$  there exists  $t \in R$  such that  $\theta(x) - xt \in AM^m$  for each  $x$  in  $N$ .

It is clear that if  $M$  satisfies (m,n) -Baer criterion relative to an ideal  $A$  then  $M$

satisfies (p,q) -Baer criterion relative to an ideal  $A$ ,  $\forall 1 \leq p \leq m$  and  $1 \leq q \leq n$ .

**Proposition 2.6 :** Let  $A$  be an ideal of  $R$  and  $M$  be an  $R$ -module such that  $\gamma_R(N \cap K) = \gamma_R(N) + \gamma_R(K)$  for each two  $n$ -generated submodule of  $M^m$ . If  $M$  satisfies (m,1)-Baer criterion relative to  $A$ . Then  $M$  satisfies (m,n)-Baer criterion relative to  $A$  for each  $n \geq 1$ .

**Proof :** Let  $L = x_1R + x_2R + \dots + x_nR$  be  $n$ -generated submodule of  $M^m$  and  $f: L \rightarrow M^m$  an  $R$ -homomorphism. We use induction on  $n$ . It is clear that  $M$  satisfies (m,n) -Baer criterion, if  $n=1$ . Suppose that  $M$  satisfies (m,n) -Baer criterion for all  $k$ -generated submodule of  $M^m$ , for  $k \leq n-1$ . Write  $N = x_1R$ ,  $K = x_2R + \dots + x_nR$ , then for each  $w_1 \in N$  and  $w_2 \in K$ ,  $f|_N(w_1) = w_1r$ ,  $f|_K(w_2) = w_2s$  for some  $r, s \in R$ . It is clear  $r - s \in \gamma_R(N \cap K) = \gamma_R(N) + \gamma_R(K)$ . Suppose that  $r-s = u+v$  with  $u \in \gamma_R(N)$ ,  $v \in \gamma_R(K)$  and let  $t = r - u = s + v$ . Then for any  $w = w_1 + w_2 \in L$  with  $w_1 \in N$  and  $w_2 \in K$ ,  $f(w) - wt = f(w_1) + f(w_2) - (w_1 + w_2)t = f(w_1) - w_1t + f(w_2) - w_2t = f(w_1) - w_1(r - u) + f(w_2) - w_2(s + v) = f(w_1) - w_1r + w_1u + f(w_2) - w_2s - w_2v = f(w_1) - w_1r + f(w_2) - w_2s \in AM^m$ .

**Proposition 2.7 :** Let  $M$  be an  $R$ -module and  $A$  be an ideal of  $R$ . Then  $M$  satisfies (m,n)-Baer criterion relative to an ideal  $A$ , if and only if  $\ell_{M^n} \gamma_{R_n}(\alpha_1R, \dots, \alpha_nR) \subseteq \alpha_1R + \dots + \alpha_nR + AM^n$  for any  $n$ -element subset  $\{\alpha_1, \dots, \alpha_n\}$  of  $M^n$ .

**Proof :** First assume that (m,n)-Baer criterion relative to an ideal  $A$  holds for  $n$ -generated submodule of  $M^m$ , let  $\alpha_i = (a_{i1}, a_{i2}, \dots, a_{im})$ , for each  $i = 1, \dots, n$  and  $\beta = \{\beta_1, \dots, \beta_n\} \in \ell_{M^n} \gamma_{R_n}(\alpha_1R, \dots, \alpha_nR)$ ,  $\alpha_i = (a_{i1}, a_{i2}, \dots, a_{in})$ . Define  $\theta: \alpha_1R, \dots, \alpha_nR \rightarrow M^m$  by  $\theta(\sum_{i=1}^n \alpha_i r_i) = \sum_{i=1}^n \beta_i r_i$ . If  $\sum_{i=1}^n \alpha_i r_i = 0$ , then  $\sum_{i=1}^n a_{ij} r_i = 0$ ,  $j = 1, \dots, m$ , this implies that  $\alpha_i r^T = 0$  where  $r = (r_1, \dots, r_n)$  and hence  $r^T \in \gamma_{R_n}(\alpha_1R, \dots, \alpha_nR)$ . By assumption  $\beta_i r^T = 0$ ,

$\forall i = 1, \dots, n$  so  $\sum_{i=1}^n \beta_i r_i = 0$ . This show that  $f$  is well defined. It is an easy matter to see that  $\theta$  is  $R$ -homomorphism. By assumption there exists  $t \in R$  such that  $\theta(\sum_{i=1}^n \alpha_i r_i) - (\sum_{i=1}^n \alpha_i r_i)t \in AM^n$  for each  $\sum_{i=1}^n \alpha_i r_i \in \sum_{i=1}^n \alpha_i R$ . Let  $r_i = (0, \dots, 0, 1, 0, \dots, 0) \in R^n$  where 1 in the  $i$ th position and 0 otherwise.  $\beta_i - \alpha_i t = \theta(\alpha_i) - \alpha_i t \in AM^n$  thus  $\beta_i \in \sum_{i=1}^n \alpha_i R + AM^n$  which is contradiction. This implies that  $\ell_{M^n} \gamma_{R_n}(\alpha_1 R, \dots, \alpha_n R) \subseteq \alpha_1 R + \dots + \alpha_n R + AM^n$ . Conversely, assume that  $\ell_{M^n} \gamma_{R_n}(\alpha_1 R, \dots, \alpha_n R) \subseteq \alpha_1 R + \dots + \alpha_n R + AM^n$ , for each  $\{\alpha_1, \dots, \alpha_n\}$  of  $M^n$ . Then for each  $R$ -homomorphism  $f: \alpha_1 R + \dots + \alpha_n R \rightarrow M^n$  and  $s = (s_1, \dots, s_n) \in \gamma_{R_n}(\alpha_1 R + \dots + \alpha_n R)$ ,  $\sum_{k=1}^n (\sum_{i=1}^n \alpha_i r_i) s_k = 0$  for each  $\sum_{i=1}^n \alpha_i r_i \in \sum_{i=1}^n \alpha_i R$ , hence  $\sum_{k=1}^n f(\sum_{i=1}^n \alpha_i r_i) s_k = \sum_{k=1}^n f(\sum_{i=1}^n \alpha_i r_i s_k) = 0$ , thus  $f(\sum_{i=1}^n \alpha_i r_i) \in \ell_{M^n} \gamma_{R_n}(\alpha_1 R, \dots, \alpha_n R) = \alpha_1 R + \dots + \alpha_n R + AM^n$ , then  $f(\sum_{i=1}^n \alpha_i r_i) = f(\alpha_i r_i^T) = f(\alpha_i) r_i^T \in \alpha_1 R + \dots + \alpha_n R + AM^n$ , for some  $r \in R$ . Then  $M$  satisfies  $(m, n)$ -Baer criterion.

**Corollary 2.8:** An  $R$ -module  $M$  is fully  $(m, n)$ -stable relative to an ideal  $A$  of  $R$ , if and only if  $\ell_{M^n} \gamma_{R_n}(\alpha_1 R, \dots, \alpha_n R) \subseteq \alpha_1 R + \dots + \alpha_n R + AM^n$  for any  $n$ -element subset  $\{\alpha_1, \dots, \alpha_n\}$  of  $M^n$ .

We can summarize the above results in the following theorem.

**Theorem 2.9:** The following statements are equivalent for an  $R$ -module  $M$  and an ideal  $A$  of  $R$ .

1.  $M$  is fully  $(m, n)$ -stable relative to  $A$
2. For any two  $m$ -element subsets  $\{\alpha_1, \dots, \alpha_m\}$  and  $\{\beta_1, \dots, \beta_m\}$  of  $M^n$ , if  $\beta_j \notin \sum_{i=1}^n \alpha_i R + AM^n$ , for each  $j = 1, \dots, m$  implies  $\gamma_{R_n} \{\alpha_1, \dots, \alpha_m\} \not\subseteq \gamma_{R_n} \{\beta_1, \dots, \beta_m\}$ .
3.  $(m, n)$ -Baer criterion relative to  $A$  for  $n$ -generated submodules of  $M^n$ .
4.  $\ell_{M^n} \gamma_{R_n}(\alpha_1 R, \dots, \alpha_n R) \subseteq \alpha_1 R + \dots + \alpha_n R + AM^n$  for any  $n$ -element subset  $\{\alpha_1, \dots, \alpha_n\}$  of  $M^n$ .

**Corollary 2.10:** [1] The following statements are equivalent for an  $R$ -module  $M$  and an ideal  $A$  of  $R$ .

1.  $M$  is fully-stable relative to  $A$
2. For each  $x, y$  in  $M$ ,  $y \notin (x)$ ,  $\gamma_R(x) = \gamma_R(y)$  implies  $(x) + AM = (y) + AM$ .
3.  $M$  satisfies Baer criterion to  $A$  for for each cyclic submodule.
4. For each  $x$  in  $M$ ,  $l_M(r_R(x)) \subseteq (x) + AM$ .

Recall that an  $R$ -module  $M$  is  $(m,n)$ -multiplication module if each  $n$ -generated submodule of  $M^m$  is of the form  $IM_n$  for some ideal  $I$  of  $R^{m \times n}$  [3].

**Proposition 2.11 :** Let  $M$  be an  $(m,n)$ -multiplication  $R$ -module. Then  $M$  is fully  $(m,n)$ -stable module if and only if  $M$  is fully  $(m,n)$ -stable relative to each non-zero ideal of  $R$ .

**Proof :**  $\Rightarrow$  It is clear

$\Leftarrow$  Let  $N$  be any  $n$ -generated submodule of  $M^m$  and  $f: N \rightarrow M^m$  be any  $R$ -homomorphism. If  $N = (0)$ , then it is clear that  $M$  is fully  $(m,n)$ -stable. Let  $N \neq (0)$ , and since  $M$  is an  $(m,n)$ -multiplication module, then  $N = IM_n$ , for some non-zero ideal  $I$  of  $R^{m \times n}$ . By hypothesis  $f(N) \subseteq N + IM_n = N + N = N$ . Hence,  $M$  is fully  $(m,n)$ -stable module.

**Corollary 2.12:** [1] Let  $M$  be multiplication  $R$ -module. Then  $M$  is fully stable module if and only if  $M$  is fully stable relative to each non-zero ideal of  $R$ .

Recall that an  $R$ -module  $M$  is  $(m,n)$ -quasi-injective in each  $R$ -homomorphism from an  $n$ -generated submodule of  $M^m$  to  $M$  extends to one from  $M^m$  to  $M$  [4].

The following theorem follows from Theorem(2.14) in [3] and Proposition(2.11).

**Theorem 2.9:** Let  $M$  be an  $(m,n)$ -multiplication  $R$ -module. Then  $M$  is  $(m,n)$ -quasi injective if and only if  $M$  is fully  $(m,n)$ -stable relative to each non-zero ideal of  $R$ .

## REFERENCES

- 1- Anaam M.S, On fully stable modules relative to ideal, MSc. Thesis, College of Science, Mustansiriyah University (2008).
- 2- M. S.Abbas, On fully stable modules, Ph.D. Thesis, College of Science, University of Baghdad (1991).
- 3- M. S.Abbas, M. J. Mohammedali, A note on fully  $(m,n)$ -stable modules, International Electronic Journal of Algebra, vol. 6, 65-73(2009).
- 4- Z. M. Zhu, J. L. Chen, X. X. Zhang, On  $(\$m,n\$)$ -quasi injective modules, Acta Math. Univ. Comenianae, Vol. LXXIV, 1, 25-36(2005).



## Using Semi – Analytic Technique for Solving Heat Conduction Problem in the Human Head

Luma N. M. Tawfiq and Heba W. Rasheed

Department of Mathematics, College of Education Ibn Al-Haitham,

Received 30/11/2011 – Accepted 18/4/2012

### الخلاصة

الهدف من هذا البحث عرض دراسة تحليلية لمسألة التوصيل الحراري حيث اقترحنا التقنية شبه التحليلية باستعمال الاندراج التماسي ذو النقطتين للحصول على الحل كمتعددة حدود، كذلك ناقشنا الخطأ النسبي أو أكبر خطأ نسبي لإثبات سهولة تطبيق وكفاءة أداء الطريقة المقترحة و مقارنة نتائج الطريقة المقترحة مع نتائج طرق أخرى .

### ABSTRACT

This paper presents the solution of heat conduction problem in the human head , semi - analytic technique is proposed using two points osculatory interpolation to construct polynomial solution, and discussed the relative error or the maximum relative defect to demonstrate the applicability and efficiency of the suggested method . The results of proposed method are compared with the results of other methods .

### INTRODUCTION

In the study of nonlinear phenomena in physics, engineering and other sciences, many mathematical models lead to two-point singular boundary value problems (SBVP) associated with nonlinear second order ordinary differential equations (ODE) .

Generally in mathematics, a singularity is an undefined point at which a given mathematical object, or a point of an exceptional set where it fails to be well-behaved in some particular way, such as many problems in varied fields as thermodynamics, electrostatics, physics, and statistics give rise to ordinary differential equation of the form :

$$y''(x) = f(t, y(x), y'(x)) \quad , \quad a < x < b \quad , \quad (1)$$

On some interval of the real line with some boundary conditions.

A two-point BVP associated to the second order differential equation (1) is singular if one of the following situations occurs :

a and/or b are infinite; f is unbounded at some  $x_0 \in [0,1]$  or f is unbounded at some particular value of y or y' [1] .

There are two types of a point  $x_0 \in [0,1]$  : Ordinary point and singular point. Also, there are two types of singular point : Regular and Irregular Points, A function y(x) is analytic at  $x_0$  if it has a power series expansion at  $x_0$  that converges to y(x) on an open interval containing  $x_0$  . A point  $x_0$  is an ordinary point of the ODE (2), if the functions P(x) and Q(x) are analytic at  $x_0$ . Otherwise  $x_0$  is a singular point of the ODE, i.e.

$$y'' + P(x)y' + Q(x)y = 0 \quad , \quad (2)$$



$$P(x) = P_0 + P_1(x-x_0) + P_2(x-x_0)^2 + \dots = \sum_{i=0}^{\infty} p_i (x-x_0)^i, \quad (3)$$

$$Q(x) = Q_0 + Q_1(x-x_0) + Q_2(x-x_0)^2 + \dots = \sum_{i=0}^{\infty} q_i (x-x_0)^i, \quad (4)$$

On the other hand if  $P(x)$  or  $Q(x)$  are not analytic at  $x_0$  then  $x_0$  is said to be a singular. [2]

### Heat Conduction in the Human Head

Morgado and Lima [3] study a class of SBVP :

$$(|y'(x)|^{m-2} y'(x))' + ((N-1)/x) |y'(x)|^{m-2} y'(x) = f(y), \quad 0 < x < 1, \quad (5)$$

where the left hand side represents the radial part of the  $N$  - dimensional degenerate Laplacian, with BC's :  $y'(0) = 0$ ,  $(6)$

$$ay(1) + by'(1) = c, \quad (7)$$

where assume that  $m > 1$  and  $N \geq 1$ ,  $a > 0$ ,  $b \geq 0$  and  $c \geq 0$ . The source function  $f$  has the form :

$$f(y) = -\alpha e^{-\beta y}, \quad \alpha > 0, \quad \beta > 0, \quad (8)$$

The motivation for studying problem (1)-(4) comes from a mathematical model for the distribution of heat sources in the human head. This model was originally described by Flesh and Gray and refer to it in [3]. The problem (5) - (7) is singular, in order to the independent variable, at  $x = 0$  due to the division by zero on the second term of the right-hand side of (5), but also in order to the dependent variable whenever  $m > 2$ , due to the boundary condition (6).

Gazzola, Serrin and Tang [2] studied the behavior of solutions of problem (5) -(7), with  $m > 1$ ,  $f(y)$  given by the following :

$$f(y) = -a y^q + b y^p, \quad a, b > 0 \text{ and } p < q \quad (9)$$

We will also adapt, for this kind of problems, Ribeiro[4] used the shooting algorithms. Morgado and Lima [3] introduced a stable shooting algorithm and finite difference scheme to solve the problem, with the case  $m = 2$ ,  $f(y)$  given in (5) and  $0 \leq p < q \leq 1$ ,  $a, b > 0$ .

Problem (5)-(7), with BC:  $y(0) = y(1) = 0$  and  $f(y) = y - y^3$  has at least one solution, for sufficiently  $m$ , if  $N < 4$  which studied in [5], a theorem about conditions for the existence and uniqueness of solution was also presented in [5], suggested numerical algorithms in [5] used to solve the problem, in the case  $N = 3$ ,  $m = 2$  and the results given in Figure (1).

Lima and Morgado [6] solved this problem in the case  $m = 2$ , i.e.,

$$y'' + ((N-1)/x) y' + f(y) = 0, \quad N \geq 2, \quad 0 < x < 1, \quad (10)$$

$$f(y) = ay^q - by^p, \quad 0 \leq p < q \leq 1, \quad a, b > 0, \quad (11)$$

with BC :  $y'(0) = 0$ ,  $y(1) = y'(1) = y_0$  and the results given in Figure (2).

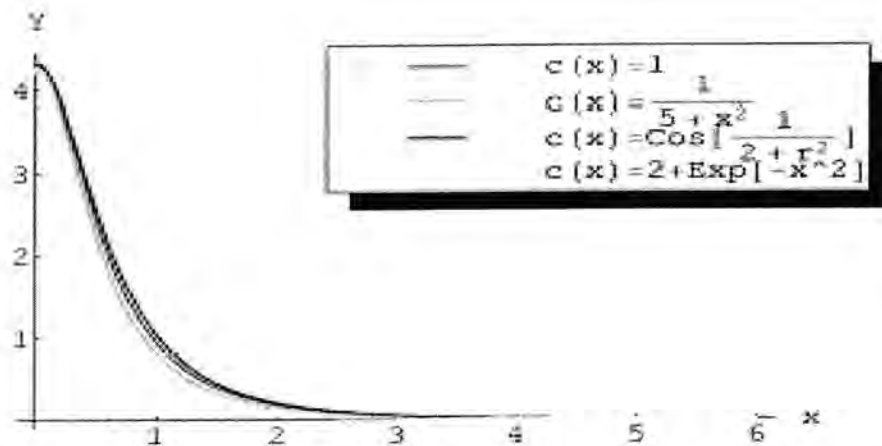


Figure-1-Solution of problem(5)-(7), the case  $f(y) = y - y^3$  which given in [5]

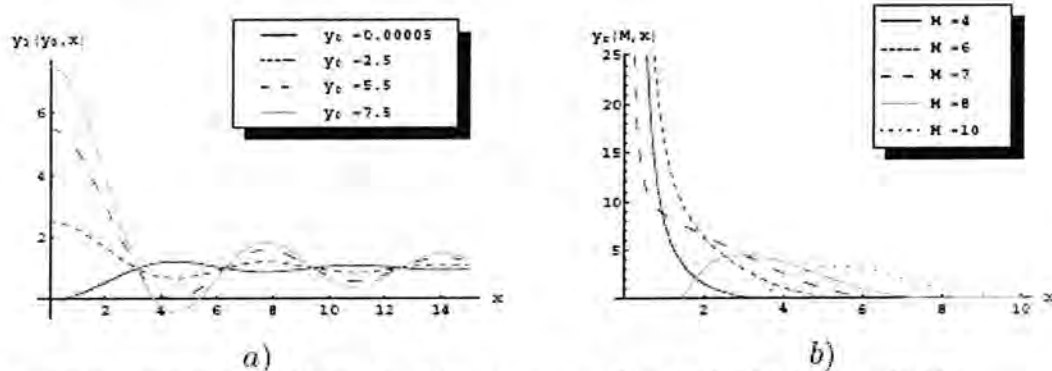


Figure-2: Results of problem(10)-(11) the case  $m=2, a=b=1$  which given in [6] ;  
a)  $N = 3, p = 0, q = 1$  ; b)  $N = 4, p = 0.2, q = 0.8$

### Semi-analytic Technique for Heat Conduction in the Human Head

In this paper we study problem (5) - (8) using semi - analytic technique when  $a = b = 1, c = 0, m = 2, N = 3, \alpha = \beta = 1$ , i.e.,

$$y''(x) + \frac{2}{x}y'(x) + e^{-y} = 0, \quad (12a)$$

$$\text{with B.C : } y'(0) = 0, y(1) + y'(1) = 0, \quad (12b)$$

replace  $y(x)$  in problem (12), or an alternative formulation of it, by a  $P_{2n+1}$  which is polynomial constricted by two-points osculatory interpolation of order  $2n+1$ , where  $n$  is number of fitting function values and derivatives at the two end points of a finite interval, say  $[0, 1]$ , that is :

$$y^{(j)}(0) = P_{2n+1}^{(j)}(0), y^{(j)}(1) = P_{2n+1}^{(j)}(1), j = 0, 1, 2, \dots, n$$

which enables any unknown boundary values or derivatives of  $y(x)$  to be computed .

Therefore, the first step is to construct the  $P_{2n+1}$ , to do this we need the Taylor coefficients of  $y(x)$  at  $x = 0$  :

$$y = a_0 + a_1 x + \sum_{i=2}^{\infty} a_i x^i \quad , \quad (13)$$

where  $y(0) = a_0, y'(0) = a_1, y''(0)/2! = a_2, \dots, y^{(i)}(0)/i! = a_i, i = 3, 4, \dots$   
then insert the series form(13) into(12a) and equate coefficients of powers of  $x$  to obtain  $a_2$ . Also we need Taylor coefficient of  $y(x)$  about  $x = 1$  :

$$y = b_0 + b_1(x-1) + \sum_{i=2}^{\infty} b_i(x-1)^i \quad , \quad (14)$$

where  $y(1) = b_0, y'(1) = b_1, y''(1)/2! = b_2, \dots, y^{(i)}(1)/i! = b_i, i = 3, 4, \dots$   
then insert the series form (14) into (12a) and equate coefficients of powers of  $(x-1)$  to obtain  $b_2$ , then derive equation (12a) with respect to  $x$  and iterate the above process to obtain  $a_3$  and  $b_3$ , now iterate the above process many times to obtain  $a_4, b_4$ , then  $a_5, b_5$  and so on, that is, we can get  $a_i$  and  $b_i$  for all  $i \geq 2$  ( the resulting equations can be solved using MATLAB to obtain  $a_i$  and  $b_i$  for all  $i \geq 2$  ), the notation implies that the coefficients depend only on the indicated unknowns  $a_0, a_1, b_0, b_1$ , we get two of these four unknown by the boundary condition. Now, we can construct a  $P_{2n+1}(x)$  from these coefficients (  $a_i$ 's and  $b_i$ 's ), where a useful and succinct way of writing osculatory interpolant  $P_{2n+1}(x)$  of degree  $2n + 1$  was given for example by Phillips [7] as :

$$P_{2n+1} = \sum_{i=0}^n \{ a_i Q_i(x) + (-1)^i b_i Q_i(1-x) \} \quad , \quad (15)$$

$$\text{where } Q_j(x)/j! = (x^j/j!)(1-x)^{n+1} \sum_{s=0}^{n-j} \binom{n+s}{s} x^s$$

we see that (15) have only two unknowns from  $a_0, b_0, a_1$  and  $b_1$  to find this, integrate equation (12a) on  $[0, x]$  to obtain :

$$x^m y'(x) - m x^{m-1} y(x) + m(m-1) \int_0^x x^{m-2} y(x) dx + \int_0^x f(x, y, y') dx = 0 \quad , \quad (16a)$$

and again integrate equation (16a) on  $[0, x]$  to obtain :

$$x^m y(x) - 2m \int_0^x x^{m-1} y(x) dx + m(m-1) \int_0^x (1-x) x^{m-2} y(x) dx + \int_0^x (1-x) f(x, y, y') dx = 0 \quad , \quad (16b)$$

Putting  $x = 1$  in (16) then gives :

$$b_1 - m b_0 + m(m-1) \int_0^1 x^{m-2} y(x) dx + \int_0^1 f(x, y, y') dx = 0 \quad , \quad (17a)$$

and

$$b_0 - 2m \int_0^1 x^{m-1} y(x) dx + m(m-1) \int_0^1 (1-x) x^{m-2} y(x) dx + \int_0^1 (1-x) f(x, y, y') dx = 0 \quad , \quad (17b)$$

Use  $P_{2n+1}$  as a replacement of  $y(x)$  in ( 17 ) and substitute the boundary conditions (12b) in (17) then, we have only two unknown coefficients  $b_1, b_0$



and two equations (17) so, we can find  $b_1, b_0$  for any  $n$  by solving this system of algebraic equations using MATLAB, so insert  $b_0$  and  $b_1$  into (15), thus (15) represents the solution of (12).

Now from equation (15) we have :

$$P_9 = -0.0000048758 x^9 + 0.0000063574 x^8 - 0.0000210057 x^7 - 0.000161261 x^6 - 0.0000039805 x^5 - 0.0039957442 x^4 - 0.1154086098 x^2 + 0.3675168500$$

For more details ,Table(1) gives the results for different nodes in the domain, for  $n = 4$  and results of method given in [3], we note that there is no difficulty in taking higher values of  $n$  if we wished to refine this value and Figure (3) illustrates the suggested method for  $n = 4$  and methods given in [3].

Table-1: The result of suggested method for  $n=4$  and result of method given in [3]

$a_0$	0.367516850000000		
$b_1$	-0.247927730000742		
$x_i$	Osculatory interpolation $P_9(x)$	Shooting method $y_1(x)$	Finite difference method $y_2(x)$
0	0.367516850000000	0.36751685	0.36751677
0.2	0.362894100567111	0.36289409	0.36289402
0.4	0.348948448563970	0.34894843	0.34894837
0.6	0.325443538301509	0.32544353	0.32544348
0.8	0.291971111816999	0.29197111	0.29197106
1	0.247927730000742	0.24792773	0.24792768

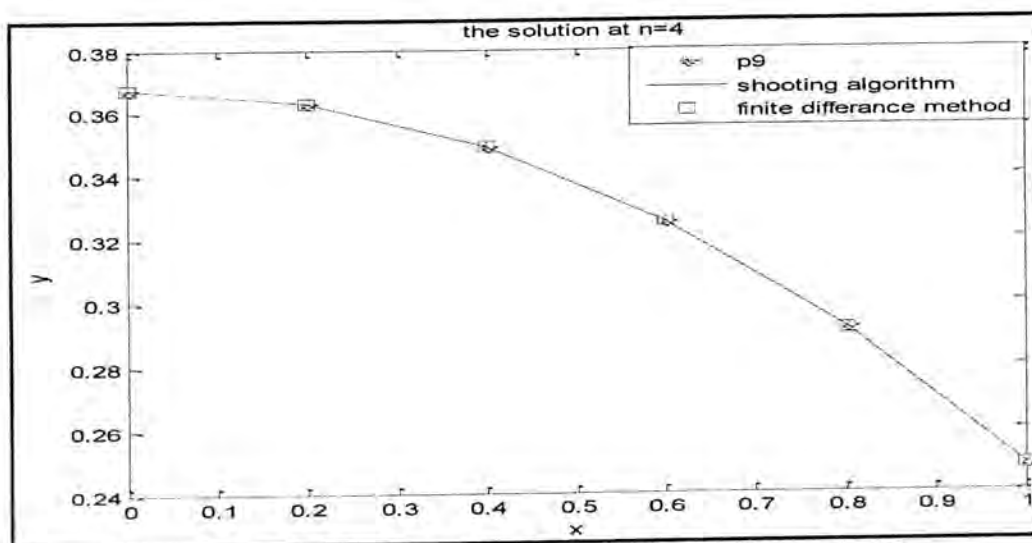


Figure-3: Comparison between  $P_9$  and solutions in [3]



### Error / Defect Weights

Every known BVP software package reports a estimate of either the relative error or the maximum relative defect. The weights used to scale either the error or the maximum defect differ among BVP software. Therefore, the BVP component of pythODE [8] allows users to select the weights they wish to use. The default weights depend on whether an estimate of the error or maximum defect is being used. If the error is being estimated, then the BVP component of pythODE uses :

$$\|y(x) - P(x)\|_{\infty} / (1 + \|P(x)\|_{\infty}) ; 0 \leq x \leq 1 ,$$

where  $y(x)$  is exact solution and  $P(x)$  is suggested solution .

If the maximum defect is being estimated, then the BVP component of pythODE uses :

$$\|P''(x) - f(x, P(x), P'(x))\|_{\infty} / (1 + \|f(x, P(x), P'(x))\|_{\infty}) ; 0 \leq x \leq 1.$$

The relative error estimate of both the error and the maximum defect are slightly modified from the one used in BVP SOLVER.

Now we applied maximum defect on problems (5)-(8), firstly table 2 give the value of  $\|P''(x) - f(x, P(x), P'(x))\|_{\infty}$ , i.e.,  $6.396257166976717 \text{ e-}008$

and  $\|f(x, P(x), P'(x))\|_{\infty} = \text{Max}_i . |f(x, P_9(x_i), P_9'(x_i))| = 0.367516850000000$

then maximum defect is :

$$1.367516850000000 = 4.677278504448934 \text{ e-}008 \quad \text{e-}008 \\ /6.396257166976717$$

Table-2 : Estimate max. error of  $|P_9'' - f(x, P_9(x), P_9'(x))|$

$x_i$	$P_9''$	Error $ P_9'' - f(x, P_9(x), P_9'(x)) $
0	-0.230817219600000	0.000000002628238047217215
0.2	-0.232743818249224	0.00000001054073230455181
0.4	-0.238626143021245	0.0000000527894570136308
0.6	-0.248784833165929	0.00000006396257166976717
0.8	-0.263796257826514	0.00000002756204082023442
1	-0.284560872600000	0.00000000009595692296304748
Max.		6.396257166976717e-008

### CONCLUSION

The result, in this research, for solving Heat conduction in the human head by using semi - analytic technique shown that this method can be used successfully for finding the solution of problem (5)-(8). It may be concluded that this technique is a very powerful and efficient in finding highly accurate solutions for a large class of differential equations.

Another advantage is that it gives the approximate solution on the continuous finite domain whereas other numerical techniques provide the solution on discrete only.

Our results indicate that global error estimation based on higher-order formulas slightly out performs deferred corrections. These results may also be applicable to global - error control software packages .

The results were compared to a finite difference technique and Shooting method applied by Morgado and Lima [3] shown to be more accurate and of high order accuracy. Another advantage of our proposed method that the solution can be estimated within the boundary interval whereas, the finite difference approach approximates the solution solely at the nodal points.

Finally, The bvp4c solver of MATLAB has been modified accordingly so that it can solve some class of SBVP as effectively as it previously solved non-singular BVP .

## REFERENCES

1. L.B. Robert and S. C. Courtney , " Differential Equations A Modeling perspective " , United States of America (1996) .
2. I.Rachůnková ,S.Staněk ,and M.Tvrđý , " Solvability of Nonlinear Singular Problems for Ordinary Differential Equations ",New York, USA, (2008).
3. L. Morgado and P. Lima , " Numerical methods for a singular boundary value problem with application to a heat conduction model in the human head", Proceedings of the International Conference on Computational and Mathematical Methods in Science and Engineering, CMMSE (2009) .
4. M. L. Ribeiro , " Analysis and Numerical Approximation of Singular Boundary Value Problems " , PhD thesis ,Departamento de Matemática , Universidade de Trás-os-Montes e Alto Douro (2007).
5. P. Lima and L. Morgado , " Numerical Approximation of Singular Boundary Value Problems for A Nonlinear Differential Equation " , Proceedings of Equadiff. , Vol.11 , pp. 201–211 (2005).
6. P. Lima and L.Morgado, "Analysis and Numerical Approximation of a Free Boundary Problem for a Singular Ordinary Differential Equation" , TEMA Tend. Mat. Apl. Comput., Vol. 8, No. 2, pp: 259 - 268 (2007).

7. G .M.Phillips , "Explicit forms for certain Hermite approximations ", BIT 13, 177-180(1973).
8. J. J.Boisvert," A Problem-Solving Environment for the Numerical Solution of Boundary Value Problems ,MSC Thesis, Department of Computer Science, University of Saskatchewan ,Saskatoon , Canada , January (2011).

## On Feebly Door spaces

Qays R. Shakir

Technical College of Management, Operations management techniques Department

Received 29/12/2011 – Accepted 18/4/2012

### الخلاصة

في هذا البحث قدمنا مفهوم جديد أسميناه الفضاء البوابي الضئيل، تعريف هذا المفهوم يعتمد على المجموعة المفتوحة الضئيلة، كذلك أعطينا بعض الامثلة والنتائج التي تخص ذلك المفهوم. بالإضافة الى ذلك عرضنا بعض العلاقات بين مختلف الفضاءات المعروفة والفضاء البوابي الضئيل.

### ABSTRACT

In this paper, we introduce a new concept namely feebly door (briefly f-door) space, the definition of this concept depends on feebly open set. Also we give some examples and results concerning this concept. Additionally we investigate some relations between different well-known topological spaces and f-door space.

## 1. INTRODUCTION

### 1.1. Definition [1]:

A set  $B$  in a topological space  $X$  is called semi-open (s.o.) if there exists an open subset  $O$  of  $X$  such that  $O \subseteq B \subseteq \overline{O}$ . The complement of a semi-open set is defined to be semi-closed (s.c.).

### 1.2 Definition [2]:

Let  $X$  be a topological space and  $A \subseteq X$ , then the intersection of all semi-closed subsets of  $X$  which contains  $A$  is called the semi-closure of  $A$  and it is denoted by  $\overline{A}^s$ .

### 1.3. Definition [3]:

A subset of a topological space  $X$  is said to be feebly open briefly (f-open) if the there exists an open subset  $U$  of  $X$  such that  $U \subseteq A \subseteq \overline{U}^s$ . The complement of a feebly open set is defined to be feebly closed (f-closed).

An equivalent definition for being  $A$  is f-open is  $A \subseteq \overline{A^o}^o$  [5].

### 1.4. Remark:

Every open set is f-open but the converse is not true in general, as in the following example:

### 1.5. Example:

Let  $X$  be an infinite set and  $p$  be a fixed point of  $X$ .

Define  $T = \{ U \subset X : U \subset X - \{p\} \text{ and } X - U \text{ is finite} \} \cup \{X\} \cup \{\emptyset\}$ , so  $T$  is topology on  $X$

Let  $x \in X$  with  $x \neq p$ , so the set  $X - \{x\}$  is not open.

But since  $\overline{(X - \{x\})^o}^o = \overline{X - \{x, p\}}^o = X^o = X \Rightarrow X - \{x\} \subset \overline{(X - \{x\})^o}^o = X$  so  $X - \{x\}$  is f-open.



## 1.6. Definition[4]

Let  $X$  be a topological space we say that  $X$  is a door space if every subset of  $X$  is either open or closed set.

## 1.7. Definition:

Let  $(X, \tau)$  be a topological space we say that  $X$  is a f-door space if every subset of  $X$  is either f-open or f-closed set.

## 1.8. Examples:

(1) The discrete topology is f-door space, since every subset of discrete topology is open and closed and so every subset is f-open and f-closed by (1.4).

(2) The either-or topology which is defined on the interval  $X = [-1, 1]$  by declaring a set is open if and only if it either not contains  $\{0\}$  or does contains the interval  $(-1, 1)$ , so the sets  $\{1\}, \{-1\}$  and all sets contain  $\{0\}$  is closed and hence f-closed. The remained subsets of  $X = [-1, 1]$  are open, that is f-closed. Therefore the either-or topology is f-door space.

(3) The set of real numbers with the usual topology is not f-door space, since the set  $[0, 1)$  is neither f-open nor f-closed.

## 1.9. Remark:

Every door space is f-door space but the converse may be not true in general as in the following example.

## 1.10. Example:

The topology defined in (1.5) is f-door space but not door space.

## 1.11. Proposition:

Let  $X$  and  $Y$  be topological spaces, and  $A_1 \subseteq X$ ,  $A_2 \subseteq Y$  be f-open (resp. f-closed) sets. Then  $A_1 \times A_2$  is f-open (resp. f-closed) in  $X \times Y$ .

Proof:

Since  $A_1 \subseteq X$  so  $A_1 \subset \overline{A_1}^o$

Similarly,  $A_2 \subseteq Y$  so  $A_2 \subset \overline{A_2}^o$

$$A_1 \times A_2 \subset \overline{A_1}^o \times \overline{A_2}^o = \left( \overline{A_1 \times A_2}^o \right)^o = \overline{A_1 \times A_2}^o = \overline{(A_1 \times A_2)}^o$$

Hence is  $A_1 \times A_2$  f-open in  $X \times Y$ .

Similar method can be applied on f-closed sets by the complement procedure. ■

## 1.12. Theorem [5]:

Let  $X$  and  $Y$  be topological spaces, and let  $f: X \rightarrow Y$  be a continuous open function. Then the image of any f-open subset of  $X$  is an f-open set in  $Y$ .

The same prove can be applied on f-closed set by the complement procedure.

## 1.13. Definition:

A function  $f : X \rightarrow Y$  is called feebly Quasi-compact if it satisfies the following condition:

If  $U \subset X$  is f-open such that  $f^{-1}(f(U)) = U$  then  $f(U)$  is f-open in  $Y$

## 1.14. Proposition [5]:

Let  $X$  be a topological space and  $Y$  be a subspace of  $X$ . Let  $A \subseteq Y$  be f-open in  $X$ . Then  $A$  is f-open in  $Y$ .

In case  $A$  is f-closed subset in  $X$  then it is f-closed in  $Y$ .

## 1.15. Definition [6]:

A space  $X$  is called f-Hausdorff briefly (f- $T_2$ ) if for any two distinct points  $x, y$  of  $X$  there exists disjoint f-open subsets  $U$  and  $V$  of  $X$  such that  $x \in U, y \in V$ .

## 1.16. Definition [3]:

A point  $x \in X$  is said to be f-accumulation (feebly limit) point of  $A \subset X$  iff for each f-open subset  $U$  of  $X$  with  $x \in U$  implies  $U \cap (A - \{x\}) \neq \emptyset$ .

## 2. MAIN RESULTS

## 2.1. Proposition:

Every subspace of f-door space is f-door.

Proof:

Let  $X$  be an f-door space and  $Y \subset X$  be a subspace of  $X$ . we have to show that  $Y$  is f-door, let  $A \subset Y$ , So  $A \subset X$  then  $A$  is either f-open or f-closed in  $X$ .

If  $A$  is f-open in  $X$  then by (1.14)  $A$  is f-open in  $Y$

If  $A$  is f-closed in  $X$  then by (1.14)  $A$  is f-closed in  $Y$ .

Thus  $Y$  is f-closed. ■

## 2.2. Proposition:

The property of being an f-door space is a topological property.

Proof:

Let  $X$  be an f-door space and let the function  $f : X \rightarrow Y$  be a homeomorphism,

Let  $U$  be a subset of  $Y$  we have to show that  $U$  is either f-open or f-closed

$f^{-1}(U)$  is either f-open or f-closed in  $X$  so by (1.12)

We have that  $f(f^{-1}(U))$  is either f-open or f-closed in  $Y$

But  $f(f^{-1}(U)) = U$  So  $Y$  is f-door space. ■

## 2.3. Remark:

If  $X$  and  $Y$  are f-door spaces then  $X \times Y$  need not be f-door space

## 2.4. Example:

Let  $X=Y=\{1,2\}$  and  $\tau_1=\{\emptyset, \{1\}, X\}$  and  $\tau_2=\{\emptyset, \{2\}, Y\}$  then  $\{2\} \times \{2\} \subset X \times Y$ .

But  $\{2\} \times \{2\}$  neither f-open nor f-closed in  $X \times Y$ . Hence  $X \times Y$  is not f-door space.

## 2.5. Remark:

If  $X \times Y$  is an f-door space then  $Y \times X$  is an f-door space this result derived from the fact that  $X \times Y$  is homeomorphic to  $Y \times X$

## 2.6. Theorem:

Feebly Quasi-compact image of f-door space is f-door space.

Proof:

Suppose that the function  $f: X \rightarrow Y$  is an onto feebly Quasi-compact and  $X$  is f-door space, let  $V \subset Y$ , now we have to show that  $V$  is either f-open or f-closed in  $Y$ .

Since  $X$  is f-door, then  $f^{-1}(V)$  is either f-open or f-closed in  $X$ , let  $f^{-1}(V) = U$

Now suppose that  $U$  is f-open, so  $f(U) \subset V$  and  $f^{-1}(f(U)) \subset f^{-1}(V) = U$

But  $U \subset f^{-1}(f(U))$  Thus  $U = f^{-1}(f(U))$  so  $f(U)$  is f-open.

And since  $f(U) = f(f^{-1}(V)) = V \cap Y = V$

So  $V$  is f-open in  $Y$ .

Assume that  $U$  is f-closed in  $X$ , then  $X \setminus f^{-1}(V) = f^{-1}(Y \setminus V)$  is f-open in  $X$ .

Hence  $(Y \setminus V) \cap f(X) = Y \setminus V$  is f-open in  $Y$ , so  $V$  is f-closed in  $Y$ .

Consequently we get that  $Y$  is f-door space. ■

## 2.7. Theorem:

Every continuous open surjective function is f-Quasi-compact.

Proof

Suppose that  $f: X \rightarrow Y$  be a continuous open surjective function,

Let  $U \subset X$  be an f-open, since  $f$  is surjective, so  $f^{-1}(f(U)) = U$ .

To show that  $f(U)$  is f-open;

$$f(U) \subset f(\overline{U^o}) \subset (f(\overline{U^o}))^o \subset \overline{f(U^o)}^o$$

So  $f(U)$  is f-open.

Hence  $f$  is f-Quasi-compact. ■

## 2.8. Corollary

Every f-closed surjective function is f-Quasi-compact.

2.9. Theorem:

A feebly Hausdorff f-door space has at most one f-accumulation point.

Proof:

Suppose that  $X$  is f-Hausdorff space and  $x, y$  are two different f-accumulation points of  $X$ .

So there are  $U, V$  are f-open subsets of  $X$  such that  $x \in U, y \in V$  and  $U \cap V = \emptyset$ .

Since  $X$  is f-door, so the set  $A = (U \setminus \{x\}) \cup \{y\}$  is either f-open or f-closed.

But  $A \cap V = \{y\}$  this mean that  $\{y\}$  is f-open.

Now if  $A$  is f-closed then  $X \setminus A$  is f-open and so  $(X \setminus A) \cap U = \{x\}$  is f-open

Thus we get at least one of the sets  $\{x\}$  and  $\{y\}$  is f-open.

Now if we say that  $\{x\}$  is f-open this implies  $\{x\} \cap (X - \{x\}) = \emptyset$  i.e.  $x$  is not f-accumulation point of  $X$  which contract our claim, thus we deduce that  $X$  has at most one f-accumulation point. ■

2.10. Theorem:

A topological space  $X$  is maximal f-door space if and only if every continuous bijection function from an f-door space  $(Y, \sigma)$  to  $(X, \tau)$  is a homeomorphism.

Proof:

$\Rightarrow$  suppose  $(X, \tau)$  is maximal f-door space and  $f: (Y, \sigma) \rightarrow (X, \tau)$  is a continuous bijection, then  $\tau' = \{f(U) : U \in \sigma\}$  is topological space and clearly  $f: (Y, \sigma) \rightarrow (X, \tau')$  is homeomorphism, so  $(X, \tau')$  is f-door, now since  $\tau \subset \tau'$  and  $(X, \tau)$  is maximal f-door space so we have  $\tau = \tau'$ .

Consequently we get  $f: (Y, \sigma) \rightarrow (X, \tau)$  is homeomorphism.

$\Leftarrow$  we have to prove that  $(X, \tau)$  is maximal f-door.

If  $(X, \tau)$  is not maximal f-door, so there is  $\tau'$  which is finer than  $\tau$  ( $\tau \subset \tau'$ ) such that  $(X, \tau')$  is f-door.

Now, the identity map  $I: (X, \tau') \rightarrow (X, \tau)$  is a continuous bijection but it is not homeomorphism which is contradiction. ■

## REFERENCES

1. Levine, N., "Semi-open sets and semi-continuity in topological spaces", Amer. Math. Monthly, 70, 36-41, (1963).



2. Dorsett, C., "Semi compactness, "Semi separation axioms", and Product space", Bull. Malaysian Math.Soc.(2) 4, 21-28, (1981).
3. Masheshwart S.N. and Jain P.C., " Some new mappings ", Mathematica, Vol24 (74)(1-2,53-55, (1982).
4. Kelley, J.L., "General Topology", D. Van Nostrand Compony, Inc., Princeton, New Jersey, 1965.
5. Al-Badairy M. H., "On Feebly Proper Actions", M.SC., Thesis, AL-Mustansiriyah university (2005).
6. Maheshwari, S.N. and Thakur, S.S., "On  $\alpha$ -irresolute mappings", Tamkang Math. 11 , 209-214. (1980).

## The Rate of multi Approximation of Unbounded Functions by Means of K-Functional

Saheb Al-Saidy<sup>1</sup> and Ban Mohommed Hassen<sup>2</sup>

<sup>1</sup>Al-mustansiriya University, College of science Department of Mathematics

<sup>2</sup>Al-mustansiriya University, College of Education, Department of Mathematics

Received 16/2/2011 – Accepted 20/6/2012

### الخلاصة

هذا البحث يقدم طريقة لإنشاء المترجمات المباشرة والعكسية للمؤثرات الخطية ممثلة في فضاءات (k-functional) بنائ المتجانسة للدوال الغير مقيدة بواسطة دالة

### ABSTRACT

This paper presents a method for establishing direct and inverse inequalities for linear operators acting on homogeneous Banach space of unbounded functions by means of k-functional

### INTRODUCTION

The direct and inverse inequalities for linear operators acting on homogeneous Banach spaces of unbounded multivariate functions in terms of k- functionals for convolution operators . The method is the best on the behavior of Fourier transform of the kernel of the convolution operator because that the convolution operator have certain good properties of that function. For a classification of inverse inequalities and quite general method of convolution operators for their verification , Yang Zhuyuan, Yang Zougwen and Liu Yonngping [7], they showed that the average widths of Sobolev and Besov classes the classes of functions with bounded moduli of smoothness and Jassim and Bhaya [3] proved direct and inverse inequalities for multi-approximation. Let us also mention the integral transforms [2] and H.S.Shapiro, who first stated such a method for convolution operators[6].

The topic of weighted spaces appears in many different areas of mathematics [4] . Some particular cases were studied in [5] .

### MATERIALS AND METHODS

The space of uniformly continuous and unbounded functions on  $R^d$  , the Lipschitz (Hölder) and Bosov spaces on  $R^d$  as well as their analogy for functions which are  $2\pi$  - periodic in each variable .

First , let us introduce a number of basic notions .

Throughout this sec.  $A = R^d$ ,  $d \in N$  , we denote elements of A by

$x = (x_1, \dots, x_d)$  ; the multiplication of the vector  $x \in R^d$  with scalar  $n \in R$  is denoted by  $nx = (nx_1, \dots, nx_d)$  and  $R_+^d = \{x \in R^d : x_j > 0, j = 1, \dots, d\}$  ,

By Banach space , we denot the set of all functions summable in the Lebesgue sense on A by  $L_\alpha(A)$  with the norm

$$\|f\|_{L_\alpha} = \int_A |f(x).e^{-\alpha x}| dx, \quad f \in L(A)$$

Now we give some definitions which we use in our results:

**Definition (1)** (Shapiro [6]).

A homogeneous Banach space (abbreviated HBS)  $W_\alpha(A)$  on  $A$  is a Banach space of Lebesgue measurable functions on  $A$ , satisfying the conditions :-

a)  $f \in W_\alpha(A)$  and  $t \in A \rightarrow f_t \in W_\alpha(A)$  and

$$\|f_t\|_{W_\alpha} = \|f\|_{W_\alpha} \text{ where } f_t(x) = f(x-t)$$

b)  $f \in W_\alpha(A)$  and  $t, t_0 \in A$

$$\lim_{t \rightarrow t_0} \|f_t - f_{t_0}\|_{W_\alpha} = 0$$

c)  $f \in W_\alpha(A)$  and  $t \in A$

$$\int_{C^d} |f(x-t) \cdot e^{-\alpha}| dx \leq c \|f\|_{W_\alpha},$$

where  $C^d$  denotes the unite cube in  $R^d = \{x \in R^d : 0 \leq x_j \leq 1 \quad j=1, \dots, d\}$ .

Let  $W_\alpha(A)$  be homogeneous Banach space (HBS) on  $A$  and  $\mu_\alpha(A)$  denotes the space of all finite measures  $\mu$  on  $A$  with the norm

$$\|\mu\|_{M_\alpha} = \int_A |e^{-\alpha\mu}| d\mu$$

The convolution of a function  $f \in W_\alpha(A)$  and the measure function  $\mu \in M_\alpha(A)$  are defined by

$$f \cdot d\mu(x) = \int_A f(x-t) e^{-\alpha} d\mu(t)$$

Where the integral is the Lebesgue - Stieltjes one.

As it is known [6],  $f \cdot d\mu(x)$  exists almost every where and

$$\|f \cdot d\mu\|_{W_\alpha} \leq \|\mu\|_{M_\alpha} \|f\|_{W_\alpha}$$

In particular, for a measure  $d\mu(t) = K(t)dt$  with  $K \in L(A)$  we have

$$K \cdot f(x) = \int_A K(t) f(x-t) e^{-\alpha} dt$$

Let  $f(x-t) \cdot e^{-\alpha} = G$ , then

$$\|K \cdot f\|_{W_\alpha} = \|K \cdot G\|_W \leq \|K\|_L \|G\|_W = \|K\|_{L_\alpha} \|f\|_{W_\alpha}$$

### Definition (2) [1]

Let  $d \in N$  and  $n \in R_+^d = \{x \in R^d : x_j > 0, j=1, \dots, d\}$ , the family  $\{K_n(t)\}_{n \in R_+^d}$ , is called an approximate identity on  $A$  if it satisfies the following three conditions:

a) For all  $n \in R_+^d$  we have  $K_n \in L_\alpha(A)$  and  $\int_A K_n(t) dt = 1$

b)  $C$  is a constant such that

$$\|K_n\|_{L_\alpha} \leq C \text{ for all } n \in R_+^d$$

c) For each  $\delta > 0$

$$\lim_{\min_{n,j} n_j \rightarrow \infty} \int_{\{|t| \geq \delta\}} |K_n(t)| dt = 0$$

The function  $K_n(t)$  is called the kernel of the integration.

**Definition (3)[1]**

Let  $W_\alpha(A)$  be HBS on  $A$  and  $n \in \mathbb{R}_+^d$  and  $\{K_n(t)\}_{n \in \mathbb{R}_+^d}$  be an approximate identity on  $A$ . We define the linear operator  $J_{n,\alpha} : W_\alpha(A) \rightarrow W_\alpha(A)$  by

$$J_{n,\alpha} f(x) = K_n \cdot f(x) = \int_A K_n(t) f(x-t) \cdot e^{-\alpha t} dt, x \in A.$$

For bounded measurable function  $f$

$$\lim_{\min_{n,j} n_j \rightarrow \infty} \|f - J_n f\|_p = 0, \quad f \in B_\alpha, \alpha > 0$$

Let  $H(x) = f \cdot e^{-\alpha x}$  then  $\lim_{\min_{n,j} n_j \rightarrow \infty} \|H - J_n(H)\|_p = 0$

$$= \lim_{\min_{n,j} n_j \rightarrow \infty} \|f - J_{n,\alpha}(f)\|_{W_\alpha} = 0, \quad \forall f \in W_\alpha(A),$$

To evaluate the rate of convergence of convolution operator  $J_{n,\alpha}$  by means of the  $k$ -functional defined for  $f \in W_\alpha(A)$  and  $\tau > 0$  is given by

$$K(f, \tau, W_\alpha(A), D) = \inf \{ \|f - g\|_{W_\alpha} + \tau \|Dg\|_{W_\alpha} : g \in D^{-1}(W_\alpha(A)) \},$$

where  $D$  is a linear operator and

$$D^{-1}(W_\alpha(A)) = \{g \in W_\alpha(A) : Dg \in W_\alpha(A)\} \text{ is dense in } W_\alpha(A)$$

Assume that  $D$  satisfies the following condition :

(i)  $K \in L_\alpha(A)$  and  $g \in W_\alpha(A)$

$$D(K \cdot g) = \begin{cases} DK \cdot g, & K \in D^{-1}(L_\alpha(A)) \\ K \cdot Dg, & g \in D^{-1}(W_\alpha(A)) \end{cases}$$

Where either  $K \in D^{-1}(L_\alpha(A))$  or  $g \in D^{-1}(W_\alpha(A))$  implies  $K \cdot g \in D^{-1}(W_\alpha(A))$  as well.

We denote the Fourier transform of a function  $f \in L_\alpha(A)$  by  $\hat{f}$ , more precisely we set

$$\hat{f}(u) = \int_A f(x) \cdot e^{-iux} \cdot e^{-\alpha x} dx, \quad u \in \hat{A},$$

Where  $\hat{A} = \mathbb{R}^d$

The Fourier – Stieltjes transform  $\hat{d}\mu$  of measure  $\mu \in M_\alpha(A)$  is defined as

$$\hat{d}\mu(u) = \int_A e^{-iux} \cdot e^{-\alpha x} d\mu(x), \quad u \in \hat{A}$$

The theorem below contains a version of this comparison principle .

**Theorem (A) [6]**

Let  $W(\mathbb{R}^d)$  be a HBS on  $\mathbb{R}^d$ . Let  $k, \ell \in L(\mathbb{R}^d)$  be such that



$$\int_{R^d} K(t) dt = \int_{R^d} \ell(t) dt = 1 \text{ and } 1 - \hat{K}(u) = (1 - \hat{\ell}(u) d\mu(u)) \text{ for some } \mu \in M(R^d),$$

$$u \in R^d$$

For  $f \in W(R^d)$ ,  $x \in R^d$  and  $n > 0$ ,

$$\text{Let } \mathcal{G}_n f(x) = n^d \int_{R^d} k(nt) f(x-t) e^{-\alpha t} dt \text{ and } \zeta_n f(x) = n^d \int_{R^d} \ell(nt) f(x-t) e^{-\alpha t} dt.$$

$$\text{Then for } f \in W(R^d) \text{ and } n > 0 \text{ with } G = f(x-t) e^{-\alpha t}$$

$$\|f - \mathcal{G}_n(f(x))\|_{w_\alpha} = \|f - G\|_w \leq \|\mu\|_M \|f - G\|_w = \|\mu\|_{M_\alpha} \|f - \zeta_n(f(x))\|_{w_\alpha}$$

## RESULTS AND DISCUSSION

Let us explicitly formulate direct and inverse estimates of the rate of approximation of convolution operators.

### Theorem (1)

Let  $W_\alpha(A)$  be a HBS on  $A$  and  $J_{n,\alpha}$  be given by def. (3.2.3). Let  $D$  satisfies condition (i) and  $D^{-1}(L_\alpha(A))$  be dense in  $L_\alpha(A)$ .

Let also there exist  $\varphi = R_+^d \rightarrow R_+$ ,  $\psi: \hat{A} \rightarrow \mathcal{C}$ ,  $c \in R$  and  $\lambda_n \in M_\alpha(A)$ ,  $n \in R_+^d$ , such that

$$\hat{D}_\eta(u) = \psi_{(u)} \hat{\eta}(u), \quad u \in \hat{A}, \quad \eta \in D^{-1}(L_\alpha(A)) \quad (1)$$

$$1 - \hat{k}_n(u) = \varphi(n) \psi(n) d\hat{\lambda}_n(u), \quad u \in \hat{A}, \quad \forall n \in R_+^d \quad (2)$$

$$\|\lambda_n\|_{M_\alpha} \leq C \quad \forall n \in R_+^d. \quad (3)$$

Then for all  $f \in W_\alpha(A)$  and  $n \in R_+^d$ , we have

$$\|f - J_{n,\alpha}(f)\|_{w_\alpha} \leq CK(f, \varphi(n); W_\alpha(A), D)$$

### Proof

Let  $\mu_0$  be the measure of mass one on  $A$  concentrated at  $x=0$  and let

$d\mu_n = K_n(x) f$  then for every  $f \in W_\alpha(A)$  we have

$$\begin{aligned} f - J_{n,\alpha} f &= f - k_n \cdot f \\ &= f(1 - k_n) = f \cdot d(\mu_0 - \mu_n), \end{aligned} \quad (4)$$

from (1) and (2) we have for every  $\eta \in D^{-1}(L_\alpha(A))$

$$\begin{aligned} \hat{\eta}(d(\mu_0 - \mu_n)) &= \hat{\eta}(1 - \hat{k}_n) = \varphi(n) \psi \hat{\eta} d\hat{\lambda}_n \\ &= \varphi(n) \hat{D} \hat{\eta} d\hat{\lambda}_n \end{aligned}$$

Hence, by the uniqueness of Fourier - Stieltjes transform we get

$$\eta \cdot d(\mu_0 - \mu_n) = \varphi(n) D\eta \cdot d\lambda_n$$

and consequently condition (i) yields

$$g \in D^{-1}(W_\alpha(A)) \text{ and } \eta \in D^{-1}(L_\alpha(A))$$

$$\eta \cdot [g \cdot d(\mu_0 - \mu_n)] = \eta \cdot [\varphi(n) Dg \cdot d\lambda_n]$$

Now , since  $D^{-1}(L_{\alpha}(A))$  is dense in  $L_{\alpha}(A)$ .

We get for every  $g \in D^{-1}(W_{\alpha}(A))$

$g \cdot d(\mu_0 - \mu_n) = \varphi(n) Dg \cdot d\lambda_n$  that is

$$g \cdot (1 - k_n) = g(1 - J_n) = g - J_n g = \varphi(n) Dg d\lambda_n \quad (5)$$

$$\begin{aligned} \|f - J_{n,\alpha} f\|_{W_{\alpha}} &\leq \|f - g\|_{W_{\alpha}} + \|g - J_{n,\alpha} g\|_{W_{\alpha}} + \|J_{n,\alpha} g - J_n f\|_{W_{\alpha}} \\ &\leq \|f - g\|_{W_{\alpha}} + \|g - J_{n,\alpha} g\|_{W_{\alpha}} + \|J_{n,\alpha} f - J_{n,\alpha} g\|_{W_{\alpha}} \\ &\leq \|f - g\|_{W_{\alpha}} + \|g - J_{n,\alpha} g\|_{W_{\alpha}} + J_n \|f - g\|_{W_{\alpha}} \\ &\leq (1 - J_{n,\alpha}) \|f - g\|_{W_{\alpha}} + \varphi(n) \|Dg\|_{W_{\alpha}} \|d\lambda_n\|_{W_{\alpha}} \\ &\leq C \|f - g\|_{W_{\alpha}} + \varphi(n) \|Dg\|_{W_{\alpha}} \end{aligned} \quad \text{from (3)}$$

C is a constant independent of  $f, g$  and  $n$

Now taking an infimum over  $g \in D^{-1}(W_{\alpha}(A))$  then

$$\|f - J_{n,\alpha} f\|_{W_{\alpha}} \leq CK(f, \varphi(n); W_{\alpha}(A), D)$$

### Theorem (2)

Let  $W_{\alpha}(A)$  be a HBS on  $A$  and  $J_{n,\alpha}$  be given as in Definition (3) . Let  $D$  satisfies condition (i) and let there is  $\varphi: R_+^d \rightarrow R_+$  ,  $C \in R$  ,  $m \in N$  and  $\nu_n \in M_{\alpha}(A)$  ,  $n \in R_+^d$  such that

$$K_n^{*m} \in D^{-1}(L_{\alpha}(A)) \quad \forall n \in R_+^d \quad (6)$$

$$\varphi(n) D K_n^{*m} (u) = (1 - K_n(u) d\nu_n(u)) \cdot u \in A, \quad \forall n \in R_+^d \quad (7)$$

and

$$\|\nu_n\|_M \leq C \quad \forall n \in R_+^d \quad (8)$$

Then for all  $f \in W_{\alpha}(f)$  and  $n \in R_+^d$  we have

$$K(f, \varphi(n), W_{\alpha}(A), D) \leq C \|f - J_{n,\alpha}(f)\|_{W_{\alpha}}$$

### Proof

First , let that , in view of property (i) the condition (6) implies that for all  $f \in W_{\alpha}(A)$  and  $n \in R_+^d$  we have

$$K_n^{*m} \cdot f \in D^{-1}(W_{\alpha}(A)) . \quad (9)$$

Further , we shall establish that for  $f \in W_{\alpha}(A)$  and  $n \in R_+^d$  we have

$$\varphi(n) D J_n^m f = (f - J_n f) \cdot d\nu_n \quad (10)$$

$$\begin{aligned} \|f - J_{n,\alpha}^m f\|_{W_{\alpha}} &= \|J_{n,\alpha}^{m-1} + \dots + J_{n,\alpha} + I)(f - J_{n,\alpha} f)\|_{W_{\alpha}} , \quad I \text{ is identity} \\ &\leq (\|J_{n,\alpha}\|^{m-1} + \dots + \|J_{n,\alpha}\| + I) \|f - J_{n,\alpha} f\|_{W_{\alpha}} \\ &\leq C_1 \|f - J_{n,\alpha} f\|_{W_{\alpha}} \end{aligned} \quad (11)$$

On the other hand by (10) we have

$$\varphi(n) \|D J_n^m\|_{W_{\alpha}} \leq \|d\nu_n\|_{W_{\alpha}} \|f - J_n f\|_{W_{\alpha}}$$

$$\leq C_2 \|f - J_n f\|_{w_\alpha}, \quad (12)$$

for every  $f \in W_\alpha(A)$  and  $\alpha > 0$ , inequalities (11), (12) and  $J_n^m f \in L_\alpha(A)$  yield

$$\begin{aligned} K(f, \varphi(n); W_\alpha(A), D) &\leq \|f - J_n^m\|_{w_\alpha} + \varphi(n) \|DJ_n^m\|_{w_\alpha} \\ &\leq C_1 \|f - J_n f\|_{w_\alpha} + C_2 \|f - J_n f\|_{w_\alpha} \\ &\leq C \|f - J_n f\|_{w_\alpha}, \end{aligned}$$

so it remains to verify equation (10). By uniqueness of Fourier transform, equation(7) directly implies

$$\varphi(n) DK_n^{*m} = d\nu_n - K_n * d\nu_n \quad (13)$$

Hence for each  $f \in W_\alpha(A)$ , we have

$$\varphi(n) DK_n^{*m} * f = f * d\nu_n - K_n * f * d\nu_n$$

and finally, condition (i) implies (10). ■

From the theorem (1) and (2) can get the following

### **Corollary (1)**

For  $f \in W_\alpha(A)$ ,  $k \in \mathbb{N}$ , can get

$$\|f - J_{n,\alpha}(f)\| \cong K(f, \varphi(n); W(A), D)$$

### **Proof**

From theorem (1),

$$\|f - J_{n,\alpha}(f)\|_{w_\alpha} \leq CK(f, \varphi(n); W_\alpha(A), D), \text{ and from theorem (2),}$$

$$K(f, \varphi(n); W_\alpha(A), D) \leq C \|f - J_{n,\alpha}(f)\|_{w_\alpha} \text{ then finally we get}$$

$$\|f - J_{n,\alpha}(f)\| \cong K(f, \varphi(n); W(A), D)$$

## **REFERENCE**

1. Butzer, P. L. and Nessel, R. J., "Fourier analysis and approximation" Birkhauser, Verlag, Basel, (1971).
2. Debnath, L. and Bhatta, D., "Integral Transforms and their Application" 2<sup>nd</sup> ed., Chapman and Hall/CRC Taylor and Francis Group, Boca Raton, FL, (2006).
3. Jassim, S. K. and Bhaya, E.S., "Direct and Inverse theorems for best Multi - approximation in  $L_p$ , ( $1 < p < \infty$ )", Mathematics and physics Journal, 17(3), pp. 1-8, (2002).
4. Kilpelainen, H.T., "Weighted Sobolov spaces and capacity", Ann. Acad. Sci. Fenn. Ser. AI. Math., vol. 19, pp.95 - 113, (1994).
5. Rodriguez, R. J. M., "Weierstrass theorem in weighted sobolov spaces", J. Approx. theory, vol. 108, pp. 119 - 160, (2001).
6. Shapiro, H. S., "Topics in approximation theory" in : Lecture notes in Math., vol. 187, Springer - Verlag, Berlin, (1971).
7. Yang Zhuyuan, Yang Zougwen and Liu Yongping, "Average one sided widths of sobolev and Besov classes", Acta. Math. Sci, 30B(1), pp. 148 - 160, (2010).

## A Remark on Generalized Semi- Preregular Closed Sets

Adhiya K. Hussain

Al- Mustansiriyah University, Dept. of Maths., College of Basic Education

E-mail: [aalobiadi@yahoo.com](mailto:aalobiadi@yahoo.com)

Received 8/6/2011 – Accepted 18/4/2012

### الخلاصة

ان الهدف من هذا البحث هو برهنة ان كل مجموعة من فضاء توبولوجي  $(X, \tau)$  تكون مغلقة من النمط  $gspr$

### ABSTRACT

The aim of this note is to show that every subset of a given topological space is a generalized semi- preregular closed set.

## 1. INTRODUCTION.

Navatagi [3] introduced and studied the class of  $gspr$ - closed sets. The notions of  $gspr$ - continuity and  $gspr$ - irresoluteness and  $spr$ -  $T_{1/2}$  are introduced. The purpose of our note is to show that every subset of any topological space is  $gspr$ - closed set and therefore every function  $f: (X, \tau) \rightarrow (Y, \sigma)$  is  $gspr$ - continuous and  $gspr$  irresolute. We have felt the need to point out explicitly this observation since recently several papers have investigated concepts depending on  $gspr$ - closed sets which do not have any nontrivial meaning, we will point out that most results of [3] and [4] are either trivial or false.

Let  $A$  be a subset of a topological  $(X, \tau)$ . If  $A \subset cl(int(cl(A)))$ , then  $A$  is called semi- preopen[2] ( $\beta$ - open[1]) set. The semi- preclosure of a set  $A$ , denoted by  $spcl(A)$ , is the intersection of all semi- preclosed supersets of  $A$ . Since the union of semi- preopen sets is also semi- preopen, the semi-preclosure of every set is in fact a semi- preclosed set. The notion of generalized semi-preregular closed set (briefly  $gspr$ -closed) is introduced in [3], thus a set  $A$  is called a  $gspr$ - closed if  $spcl(A) \subset U$  whenever  $A \subset U$  and  $U$  is regular open in  $X$ . A function  $f: (X, \tau) \rightarrow (Y, \sigma)$  is called  $gspr$ - continuous (resp.  $gspr$ - irresolute) [3] if the preimage of every closed (resp.  $gspr$ - closed) subset of  $Y$  is  $gspr$ -closed in  $X$ .

### 2. Every set is $gspr$ - closed.

The following Lemmas will be useful in the sequel.

#### Lemma 2.1.

For any subset  $A$  of  $X$ , the following result hold.

- (1)  $spcl(A) = A \cup Int(cl(int(A)))[1]$ .
- (2)  $A \subseteq B \Rightarrow spcl(A) \subseteq spcl(B)$ .

The proof of the following result is easy.

#### Lemma 2.2

For every subset  $A$  of  $X$ ,  $int(cl(A)) = int(cl(int(cl(A))))$ .

We have following result

### Proposition 2.3.



If  $A$  is regular open subset of  $X$ , then  $\text{int}(\text{cl}(\text{int}(A))) = \text{int}(\text{cl}(A))$ .

**Proof.**

Since  $A$  is regular open, so  $A = \text{int}(\text{cl}(A))$ . Hence  $\text{int}(\text{cl}(\text{int}(A))) = \text{int}(\text{cl}(\text{int}(\text{cl}(A))))$ . Therefore  $\text{int}(\text{cl}(\text{int}(A))) = \text{int}(\text{cl}(A))$ , by Lemma 2.2.

**Theorem 2.4.**

If  $A$  is a regular open set, then  $\text{spcl}(A) = A$  and hence  $A$  is semi-preclosed.

**Proof.**

Let  $A$  be a regular open subset of  $X$ . Then by Lemma 2.1,  $\text{spcl}(A) = A \cup \text{int}(\text{cl}(\text{int}(A)))$ . Since  $A$  is regular open, so  $\text{int}(\text{cl}(\text{int}(A))) = \text{int}(\text{cl}(A))$ . Hence  $\text{spcl}(A) = A \cup \text{int}(\text{cl}(A)) = A \cup A = A$ . Thus  $A$  is semi-preclosed.

**Corollary 2.5.**

- (1) Every subset  $A$  of a space  $(X, \tau)$  is gspr- closed.
- (2) Every function  $f : (X, \tau) \rightarrow (Y, \sigma)$  is gspr- continuous. Further the definition of gspr- irresolute is trivial.

**Proof.**

- (1) Let  $A$  be a subset of  $X$  and  $U$  be regular open subset of  $X$  such that  $A \subseteq U$ . Then  $\text{spcl}(A) \subseteq \text{spcl}(U)$ . By Theorem 2.4,  $\text{spcl}(U) = U$ . Hence  $\text{spcl}(A) \subseteq U$ . Therefore  $A$  is gspr- closed set.
- (2) Follows from (1).

**Remark 2.5.**

- (1) Corollary 2.5 makes most of the results in [3] and [4] trivial.
- (2) Remark 5.14 and 5.15 from [3] are wrong, since by corollary 2.4, the intersection and the union of gspr- closed sets are gspr- closed.
- (3) Definition 5.22 in [3] becomes: A space  $X$  is semipre- regular  $T_{\frac{1}{2}}$  space if every subset is semipre-closed.
- (4) Theorem 6.10 of [3] is trivial.
- (5) Theorem 6.13, parts (d) and (e) [3] are trivial.
- (6) Remark 2.4 and Example 2.8 from [4] are trivial.

## REFERENCES

1. M. E. El- Monsef, S. N. El- Deeb and R. A. Mahmoud "  $\beta$ - open sets and  $\beta$ - continuous mappings" Bull. Fac. Sci. Assiut. Univ. 12, 77-90(1983).
2. D. Andrijevic, " Semipopn sets" Math. Vesnik 38, no. 1, 24-32(1986).
3. G. B. Navalagi, Semi- Preneighbourhoods and Generalized Semi-Regular- Closed Sets in Topological Spaces" Topology Atlas Preprint #455.
4. M. S. Sarsak and N. Rajesh, "- Generalized Semi- preclosed sets" Int. Math. Fram, 5, no. 12, 573- 578(2010).

## Multi Spectral Scanner "MSS" and Panchromatic Components Difference of Al- Haditha Dam Region Using GIS and Remote Sensing Techniques

Israa J. Muhsin, Faleh Hassan Mahmood and Fouad K. Mashee  
Baghdad University, College of science, Remote Sensing Unit.

Received 17/12/2011 – Accepted 18/4/2012

### الخلاصة

الهدف من الدراسة الحالية هو مراقبة مكونات العناصر الطبوغرافية لمنطقة سد حديثة والتي تشمل على (الماء، الطين، الحشائش او النباتات، التربة والصخور) بواسطة تطبيق تقنية الاستشعار عن بعد. ولتحقيق الدراسة استخدمت صور (MSS) التابع الفضائي Landsat وصور Panchromatic والغرض من استخدام الصورتين الفضائية وبنفس الوقت هو ايجاد محتويات معالم المنطقة وحساب مساحة كل واحدة منها. تم عرض مشاهد مختلفة من منطقة الدراسة وذلك لاغراض المقارنة. علاوة على ذلك هو التحقق من تأثير الحزم لكلا الصورتين الفضائية في دراسة طبوغرافية سد حديثة.

ولانجاز هدف البحث، استعمل التصنيف غير المراقب لتصنيف الصور الفضائية، وهي احدى الطرق في التتبع والتحري للتأثيرات الطبوغرافية بالاعتماد على بيانات الصورة الفضائية، والتي تتكون من الخلايا (تحتوي على عناصر الصورة pixels والتي هي اصغر وحدة في الصورة).

استعمل خوارزمية الخلايا، وتدعى باحصائيات الخلايا، احصائيات المناطق، واحصائيات التجاور. بعد ذلك طبقت اعادة التصنيف ( تصنيف المراقب) لدمج وعزل بعض المناطق التي تعتبر معالم ثانوية او هيجينية لدراستنا مثل المجمعات السكنية، التلال، المسطحات الملحية والتشوهات الموجودة في الصورة ان وجدت.

بالإضافة إلى ذلك تم انجاز حساب المساحات لكل تصنيف للمعلم في الطبيعة الطبوغرافية، للحصول على نتائج سهلة في المقارنة والمراقبة لمحتويات معالم سد حديثة مع الدراسات الأخرى. وهذه النتائج المكتشفة والمحصنة تعطي مصداقية وفائدة بالسيطرة والتخطيط على تطبيقات هذه المناطق، كذلك معرفة والتحقق اي الحزم الطيفية المطبقة جيدة لمراقبة واكتشاف هذه المعالم.

### ABSTRACT

The object of the present study was to monitor the components that had containing topography such as (water, mud, grass or vegetation, soil, and rock) of Al-Haditha Dam region, by applying remote sensing techniques. Satellite Landsat MSS (RGB) and Panchromatic imagery for the same region captured in the same time have been used. The variation of images gives a very good optimizations result and the comparison appears clearly. Moreover, investigate the effects bands in studying of Al- Haditha Dam topography for each satellite images. To fulfill this goal, unsupervised classification techniques have been used to classify, trace and detect the rejoin of the studied area, depended on the dataset of satellite image. Moreover, cell algorithms include statistics cell, statistics zonal, and statistics neighbors have been used to achieve the purpose of the study. Reclassification (supervised classification) has been used to merge and isolated some region, which is secondary considering features or Hybrid, such us building, hills, salt region and distortions. Finally, area calculation for each class of features of topography has been calculated. In order to perform the comparison and monitoring for the container of Al- Haditha Dam with another studies, the results are likely benefits for land-cover mapping and change detection applications, in addition to know which of the used spectral bands are good in detecting and observing these features.



## INTRODUCTION

Remote sensing has made enormous progress over the last decades and a variety of sensors now deliver medium and high-resolution data on an operational basis. Nevertheless, a vast majority of applications still rely on basic image processing concepts developed in the early seventies, classification of single pixels in a multi-dimensional feature space. The spatial context plays a modest role in pixel-based analysis. Consequently, classical algorithms of pixel based image analysis are becoming less important for high resolution classification [1]. Panchromatic (PAN) satellite imagery has been used successfully in different applications such as topographic mapping and terrain modeling. Nevertheless, PAN imagery is still one of the less used digital sources for land-change studies except few processes where the high-resolution of the PAN images is used to improve the visualization quality of the multi-spectral images, The geometrical shape of landsat7 can be shown in figure (1), [2].The additional ETM+ panchromatic band, at a higher spatial resolution of 15 m, improves the spatial accuracy of these applications.15-m panchromatic band spanning the optical wavelengths, increased spatial resolution to (60m) of the thermal band, and a high-gain setting on each channel permitting a 50% increase in the radiometric resolution [3].

Linear array or so-called pushbroom sensors use very sensitive diodes staring constantly at the ground to record the reflected EM energy from the Earth's surface. In comparison to MSS or TM sensors, pushbrooms are more accurate as there is no scanning mirror 189 which in return results in a longer dwelling time for a specific part of the ground surface [4].

SPOT, IRS, and IKONOS are examples of remote sensing images using pushbroom sensors will be explained in more details in the following subsections [6]. Alternatives to a pixel based classification are being currently developed for instance the object oriented approach that takes into account the form. Object based classification starts with the crucial initial step of grouping neighboring pixels into meaningful areas, especially for the end-user. This means that the segmentation and object (topology) generation must be set according to the resolution and the scale of the expected objects.

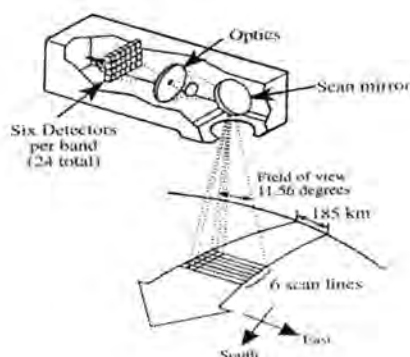


Figure-1 : Show the Landsat 7 MSS techniques (pushbrooms)[2].

The panchromatic data channel of the Landsat 7 scene was combined with the corresponding multispectral data channels. By substituting the higher resolution multispectral and panchromatic data from Landsat 7 for the historic satellite data and aerial photography, respectively, error associated with the rectification of geometric and temporal differences between the data sets was avoided. In using an ideal data set, the results of this experiment are made more applicable for the first objective of this study, to determine the effectiveness with the ECHO algorithm that can be utilized an additional high-resolution spatial information to improve classification accuracy. Then, the accuracy of these classifications had been determined through the statistical analysis of the randomly selected training samples [5].

### MATERAILS AND METHODS

Figure (2) shows the location of region study which has been limited in the west of Iraq to approximate north. It is a large complex of terrain in Iraq, generally, rocks is covert land type. The study area lies in (41.985°E- 42.555°E) latitude and (34.101°N-34.489°N) longitude with UTM-WGS-1984 projection (zone 38). The studied area has been exposed using Landsat Sensor system MSS and Panchromatic image producing in 2002 synchronized in same time perspective, it has survey 578 x 409 kilometers row and column, spatial resolution (30, 15) meters respectively. In order to indicate and point a correct work , a references background map has been used. It is satellite image of landsat TM sensor for bands (1, 2, 4) in 2002 survey which has been produced, spatial resolution 28.5 meter, it is clipping boundary of Iraq by GIS template. The statistical properties of ETM+ and MSS can be shown in table (1) and table (2) respectively.



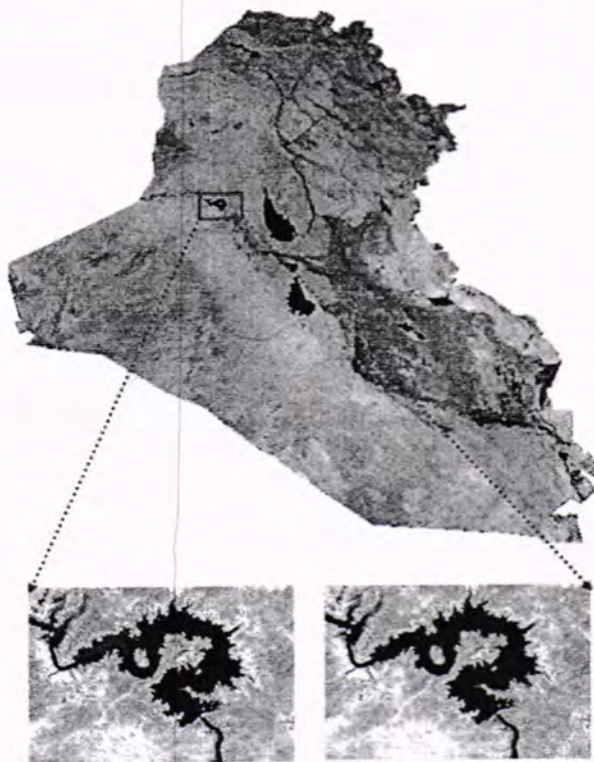


Figure-2 : (a) Source Satellite Landsat MSS image, (b) source Landsat ETM+ Panchromatic Image.

Table-1 : Statistical properties of the Landsat sensor MSS imagery (RGB) 2002, and Panchromatic.

Satellite Sensor	Spectral Band No	Description	Mean ( $\mu$ )	ST.D ( $\sigma$ )	Min	Max
pushbroom sensors MSS	Band 1	Blue	170.93645	83.37099	0	255
pushbroom sensors MSS	Band 2	Green	168.93305	77.15548	0	255
pushbroom sensors MSS	Band 3	Red	176.24549	68.11907	0	255
Landsat ETM+ (Panchromatic)	Band 8	Naturally	152.29267	102.00963	0	255

Table 2 : Statistical properties of the Landsat 7 ETM+ characteristics

Band	Spectral Resolution ( $\mu\text{m}$ )	Spatial resolution (m)	Dynamic Range (bit)
1	0.45-0.515	30 x 30	8
2	0.525-0.605	30 x 30	8
3	0.630-0.690	30 x 30	8
4	0.750-0.900	30 x 30	8
5	1.55-1.75	30 x 30	8
6	10.40-12.50	60 x 60	8
7	2.08-2.35	30 x 30	8
8(Pan)	0.52-0.90	15 x 15	8

The main objectives of the present work consist of three stages; first by , defining the work area from the image source of landscape (Al-Haditha Dam location which lies in the west of Iraq), and geometry

matching will be done with correct coordinate system (WGS\_1984\_UTM\_Zone\_38N). The second stage is done by applying the work in individual band to track and detect the changes of the spectral band on Al- Haditha Dam Topography.

Third, the number of cell or pixels from all scene of images have been selected and applied Spatial Analyst such as, cell statistics, zonal statistics, Neighborhood statistics on them, then apply the classification techniques on satellite Landsat MSS and Panchromatic imagery of each Bands.

Finally, reflect and illustrate results in graphs and tables, in order to find Spectrally bands of satellite Landsat MSS and Panchromatic imagery trace and detect features of Al-Haditha Dam region topography, and determine the cover area of each object (water, mud, grass or vegetation, soil, and rock). Classification technique depends on cell algorithms has been used to separate the satellite image (MSS and panchromatic) into individual bands one, two, and three. After that reclassification using unsupervised manner Automatic color extraction technique has been performed to merge the unimportant regions of the studied area.

## RESULTS AND DISCUSSION

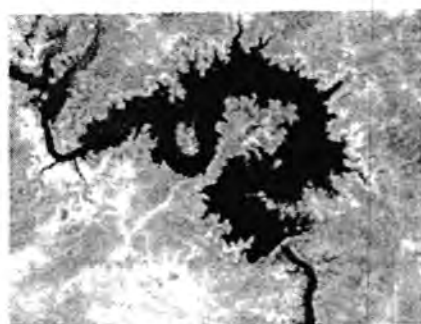
In order to obtain the classification for the correct types of the studied area, the presently methodology has been used. This methodology allowed the creation of thematic maps use classes, which can be used as a cartographic background map for topography studies. The results confirm that the classification of image is a powerful tool for region development, environmental protection, policymaking, risk assessment and planning, [1].

Therefore, Classification of single pixel (smallest object in image) is a multi-dimensional feature space. The spatial context plays a modest role in pixel-based analysis. Consequently, classical algorithms of pixel based image analysis are becoming important for high-resolution classification, alternatives to a pixel-based classification which are develop for instance the object-oriented approach that takes into account the form, textures and spectral information. Object based classification starts with the crucial initial step of grouping neighboring pixels into meaningful. This means that the objects (topology) generation must be set according to the resolution and the scale of the expected objects [5].

Most of all process and analysis image satellite depend on pixel. The cell include summation of all pixels, which allowed image for the processing to determine the statistics on all cell, neighbor cell, zonal include cell, and histogram [6,7].

In this study, different statistical parameters have been adopted. These are standard deviations and means for satellite Landsat MSS

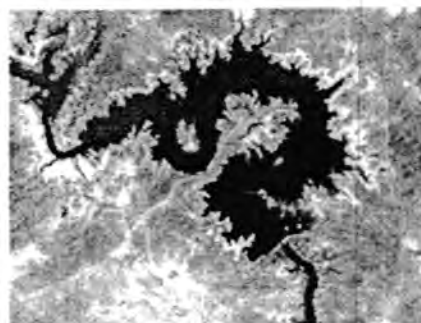
and Panchromatic imagery bands had been used. Figures (3,4,5) represent the work and area and clipping data frame from source imagery respectively.



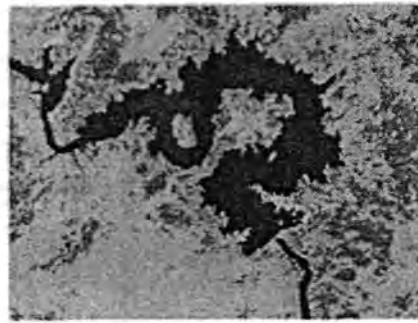
Band1



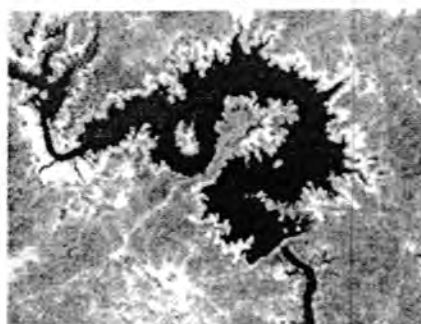
Classified of band1



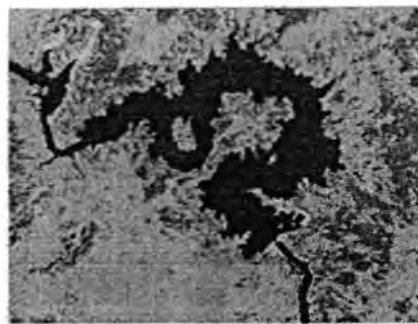
Band2



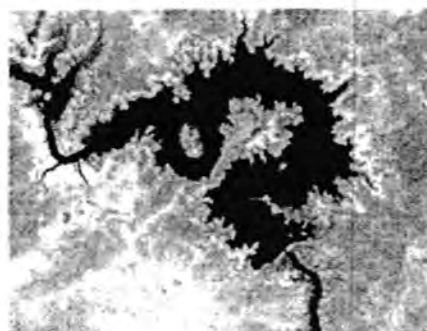
Classified of band2



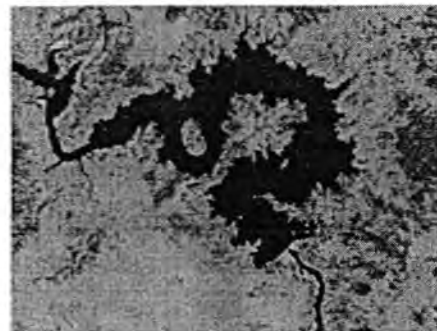
Band3



Classified of band3



Panchromatic image



Classified of panchromatic image

Figure-3 : Illustrations The Satellite Landsate [TM (B1, B2,B3) and panchromatic] with their classification.



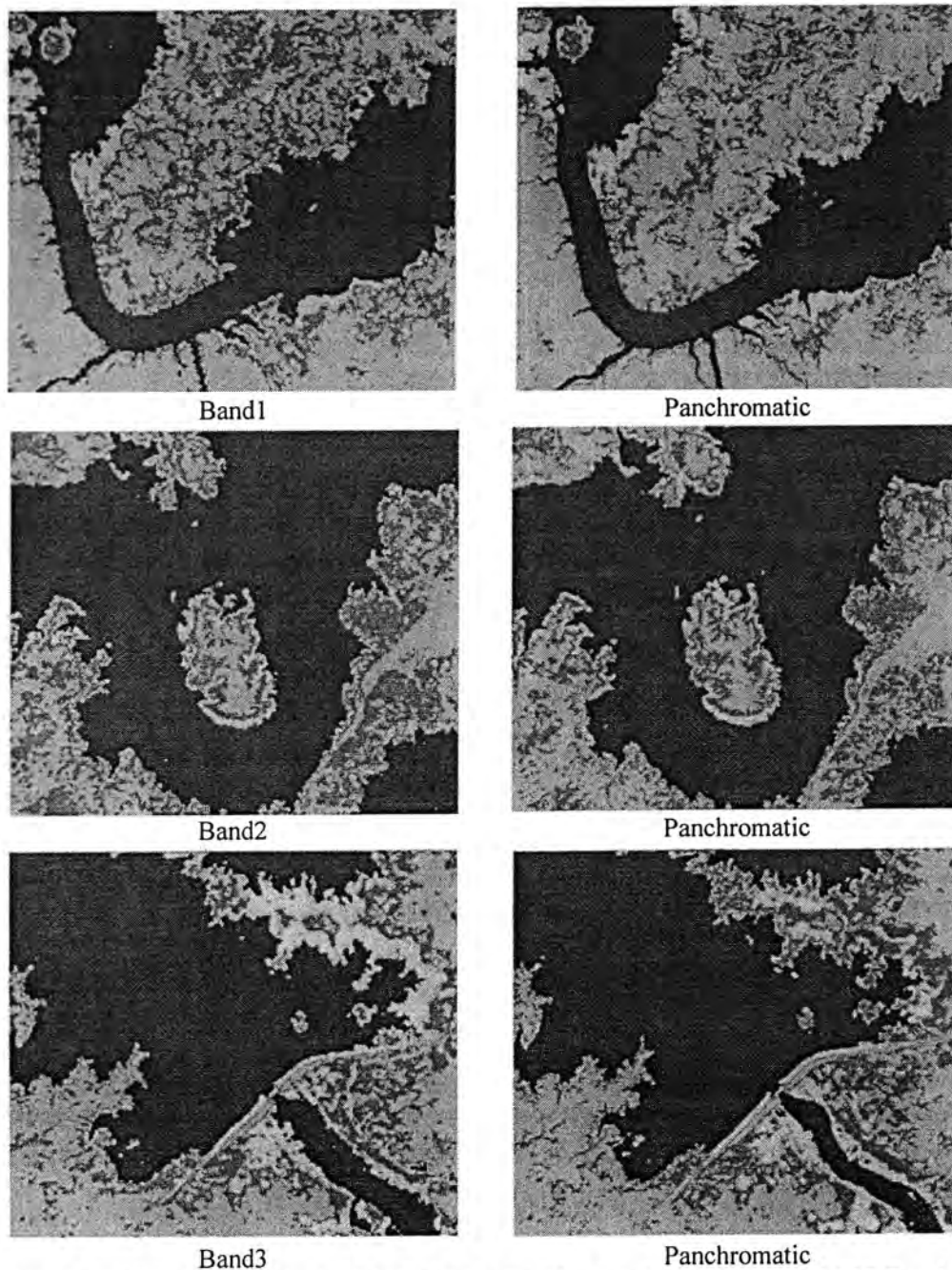


Figure-4 : Illustration, AL- Haditha Dam magnifier section is between MSS Band 1, 2, 3 and Panchromatic sequentially to demonstrate component region topography clearly. Especially Mud (red), Grass (green) and Soil (dark brown).



Multi Spectral Scanner "MSS" and Panchromatic Components Difference of Al- Haditha Dam Region Using GIS and Remote Sensing Techniques

Israa, Faleh and Fouad

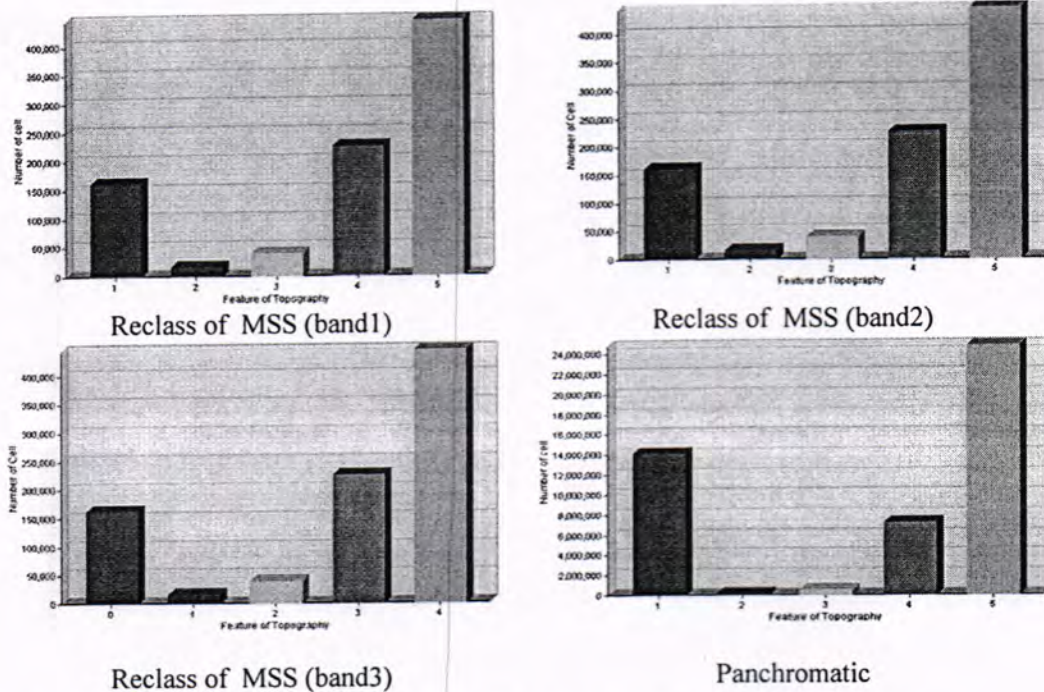


Figure-5 : Representation AL- Haditha Dam regions Topography using MSS (band1, band2, band3) and panchromatic.

Monitoring and Protecting of AL-Haditha Dam region topography (water, mud, grass or vegetation, soil, and rock) is major concerns for many local and state agencies to for solving water world problems. High-resolution satellite remote sensing has important tools that can be apply potentially to gather need information for water, vegetation, and soil area assessments in AL-Haditha Dam region. The presented classification results show the ability of the so far developed rule-sets to distinguish between objects and to generate semantic classes. This is demonstrated with the high value of the overall result accuracy of the classification. Advantages of object-oriented analysis are meaningful statistic and texture calculation. The classification technique of this study depends on extract accurately value of each object cell.

The statistical properties of the feature classes (water, mud, vegetation, soil, rock) for panchromatic and MSS can be shown in figure (5). Where the multispectral data consisted of 6 multispectral channels (30-meter pixel resolution) from Landsate 7. These data had augmented with panchromatic data (15m pixel resolution) from Landsate ETM+ in the first experiment, and with a mosaic of digital aerial photography (1m pixel resolution) in the second. In which the panchromatic data channel from the Landsate 7 scene combined with the corresponding multispectral data channels. By substituting the higher resolution multispectral (consisted of 6 multispectral channels (30-meter pixel resolution) from Landsate 7) and panchromatic data

from Landsate 7 for the historic satellite data and aerial photography, respectively, error associated with the rectification of geometric and temporal differences between the data sets was avoided, [3]. By using an ideal data set, the results of this experiment are more applicable to the first objective of this study, which was to determine the effectiveness with the ECHO algorithm can be utilized an additional high-resolution spatial information to improve classification accuracy.

The results of Classification method using cell algorithm can be shown in figure (3), while the merge of the main features for the container objects of the studied area can be computed using reclassification methods. The area of each object has been calculated to compare each band with other, and to see which of bands work with satellite. The results of the reclassification can be shown in figure (4).

The Bands of Landsate 7 MSS with the objects in the study area can be seen in figures (3, 4). It is unlike to expect that the remain bands of landsate 7 experimented in this study . Because, automation technique of landsate 7 sensor has land survey, in order to produce high resolution, with the same process of landsate 7 panchromatic corresponding with above. Finally, the statistical properties of the MSS (band1,band2,band3)and panchromatic can be listed in table 2,3,4,5 respectively.

Table -2: Characteristics AL-Haditha Dam Topography, when Applied Satellite Landsate MSS 2002 Band 1.

Topography	Number of Cell	Area	Min	Max	Mean	ST.D
Water	161264	19.6098E+07	0	51	8.50828	11.4626
Mud	15960	1.94074E+07	52	102	78.1734	15.1436
Grass	38702	4.70618E+07	103	153	131.881	14.0879
Soil	225621	27.4356E+07	154	204	187.411	12.9581
Rock	442997	53.8686E+07	205	255	228.428	15.1241

Table -3: Characteristics AL-Haditha Dam Topography, when Applied Satellite Landsate MSS 2002 Band 2.

Topography	Number of Cell	Area	Min	Max	Mean	ST.D
Water	161264	19.6098E+07	0	150	22.5891	22.7643
Mud	15960	1.94074E+07	10	215	85.7243	19.4155
Grass	38702	4.70618E+07	40	239	131.477	18.5473
Soil	225621	27.4356E+07	63	255	180.036	16.3998
Rock	442997	53.8686E+07	126	255	222.822	19.5481

Table -4: Characteristics AL-Haditha Dam Topography, when Applied Satellite Landsate MSS 2002 Band 3.

Topography	Number of Cell	Area	Min	Max	Mean	ST.D
Water	161264	19.6098E+07	0	188	48.4997	23.1006
Mud	15960	1.94074E+07	29	255	110.066	24.5846
Grass	38702	4.70618E+07	67	255	153.148	25.2354
Soil	225621	27.4356E+07	85	255	187.516	21.9706
Rock	442997	53.8686E+07	132	255	221.411	22.3188



Table-5: Characteristics AL-Haditha Dam Topography, when Applied Satellite Landsat ETM+ Panchromatic.

Topography	Number of Cell	Area	Min	Max	Mean	ST.D
Water	14116127	410.817E+07	0	51	0.652554	3.93657
Mud	122303	3.55934E+07	52	102	83.0989	14.9886
Grass	494786	14.3996E+07	103	153	134.039	14.4346
Soil	7209475	209.815E+07	154	204	190.093	11.7997
Rock	24730719	719.729E+07	205	255	228.536	14.1058

## REFERENCES

1. Antunes, A. F. B., Lingnau, C., Da Silva, J. C., Object Oriented Analysis and Semantic Network For High Resolution Image Classification, Anais XI SBSR. Belo Horizonte, Brasil, INPE, p. 273-279, (2003).
2. Ahmed Shaker, A., W.Y. Yan a, b, M.S. Wong c, Nagwa El-Ashmawy d, Bahaaeddin IZ Alhaddad e, Flood Hazard Assessment Using Panchromatic Satellite Imagery, The International Archives of the Photogrammetry, Remote Sensing and Spatial Information Sciences". XXXVII, Vol., Part B7, pp: 881-886, (2008).
3. Robert B., Julian D., Dorothy H., Jan-Gunnar W., Glaciological applications with Landsat-7 imagery: Early assessments, Elsevier, Remote Sensing of Environment, 78 (2001) 163–179, (2000).
4. Jensen, J.R., Cowen, D.C., Remote Sensing of Urban/suburban Infrastructure and Socio-Economic Attributes, Photogrammetric Engineering and Remote Sensing, Vol. 65, pp. 611-622, (1999).
5. Daniel J. Getman<sup>1</sup>, Jonathan M. Harbor, Chris J. Johannsen, Bernard A. Engel, & Goufan S. (Improving the Accuracy of Historic Satellite Image Classification by Combining Low-Resolution Multispectral Data with High-Resolution Panchromatic Data), Terrestrial Observation, Volume 1 Number (1), pp. 70-87, (2008).
6. Mohammad A. Rajabi, "Spatial Enhancement of Digital Terrain Models Using Shape from Shading with Single Satellite Imagery". Geomatics Engineering, UCGE Reports Number 20182: pp:183-190, (2003).
7. Antunes, A. F. B., Lingnau, C., Da Silva, J. C., "Object Oriented Analysis and Semantic Network For High Resolution Image Classification". Anais XI SBSR. Belo Horizonte, Brasil, INPE, p. 273-279, (2003).

## مجلة علوم المستنصرية

هي مجلة علمية رصينة تصدر عن عمادة كلية العلوم في الجامعة المستنصرية في تخصصات الكيمياء والفيزياء وعلوم الحياة وعلوم الحاسبات وعلوم الجوّ. تقوم المجلة بنشر البحوث العلمية التي لم يسبق نشرها في مكان آخر بعد إخضاعها للتقويم العلمي من قبل مختصين وباللغتين العربية أو الانكليزية وتُصدر المجلة عددين سنوياً بكلا اللغتين.

### تعليمات النشر في المجلة

1. يقدم الباحث طلباً تحريرياً لنشر البحث في المجلة ويكون مرفقاً بأربع نسخ من البحث مطبوعة على ورق ابيض قياس (A4, 21.6×27.9 cm) مع ترك حاشية بمسافة انج واحد لكل اطراف الصفحة ومطبوعة باستخدام برنامج (Microsoft Word, 97-2003) بصيغة (doc.).
2. يرفق مع البحث ملخص باللغة العربية وآخر باللغة الإنجليزية على ان لا تزيد كلمات الملخص عن (150) كلمة.
3. عدد صفحات البحث لا تتجاوز 10 صفحة بضمنها الاشكال والجداول على ان تكون الاحرف بقياس 14 نوع (Time New Roman) وبمسافة مزدوجة بين الاسطر. وينبغي ترتيب اجزاء البحث دون ترقيم وبالخط العريض (Bold) كالآتي: صفحة العنوان، الخلاصة باللغة العربية، الخلاصة باللغة الإنجليزية، مقدمة، المواد وطرائق العمل (الجزء العملي)، النتائج والمناقشة، الاستنتاجات وقائمة المراجع.
4. يطبع عنوان البحث واسماء الباحثين (كاملة) وعناوينهم باللغتين العربية والانكليزية على ورقة منفصلة شرط ان لا تكتب اسماء الباحثين وعناوينهم في أي مكان اخر من البحث، وتعاد كتابة عنوان البحث فقط على الصفحة الاولى من البحث.
5. ترقم الجداول والاشكال على التوالي حسب ورودها في المخطوط، وتزود بعناوين، ويشار إلى كل منها بالتسلسل نفسه في متن البحث.
6. يشار الى المصدر برقم يوضع بين قوسين بمستوى السطر نفسه بعد الجملة مباشرة [1]، [2]، [3] وهكذا. تطبع المصادر على ورقة منفصلة، ويستخدم الاسلوب الدولي المتعارف عليه عند ذكر مختصرات اسماء المجلات.
7. يتبع الاسلوب الاتي عند كتابة قائمة المصادر على الصفحة الاخيرة كالآتي: ترقيم المصادر حسب تسلسل ورودها في البحث، يكتب الاسم الاخير (اللقب) للباحث او الباحثين ثم مختصر الاسمين الاولين فعنوان البحث، مختصر اسم المجلة، المجلد، العدد، الصفحات الاولى والاخيرة، سنة نشر البحث. وفي حالة كون المصدر كتاباً يكتب بعد اسم المؤلف او المؤلفين عنوان الكتاب، الطبعة، الصفحات، سنة النشر، المؤسسة الناشرة، الدولة مكان الطبع. بخصوص اجور النشر يتم دفع مبلغ (50000) خمسون الف دينار عند تقديم البحث للنشر وهي غير قابلة للرد ومن ثم يدفع الباحث (25000) عشرون الف دينار اخرى عند قبول البحث للنشر.

جميع البحوث ترسل الى:

رئيس تحرير المجلة

أ.د. رضا ابراهيم البياتي

كلية العلوم- الجامعة المستنصرية

البريد الالكتروني: mustjsci@yahoo.com



# مجلة علوم المستنصرية

تصدر عن كلية العلوم الجامعة المستنصرية

رئيس التحرير  
أ.د. رضا ابراهيم البياتي

مدير التحرير  
أ.د. خضر حسن علي

## هيئة التحرير

عضوا  
عضوا  
عضوا  
عضوا  
عضوا  
عضوا  
عضوا  
عضوا

د. انعام عبد الرحمن ملوكي  
د. فائق فاضل القزاز  
د. ايمان ناطق ناجي  
د. احمد عزيز احمد  
د. منعم حكيم خلف  
د. عمر عباس حسن  
د. كريم قاسم حسين  
د. سعد عويد بديوي

## الهيئة الاستشارية

رئيسا  
عضوا  
عضوا  
عضوا  
عضوا  
عضوا

أ. د. طارق صالح عبد الرزاق  
أ. د. حسن هاشم سلمان  
أ. د. طارق سهيل نجم  
أ. د. علي حسين دحية  
أ. د. عبد المنعم صالح رحمن  
أ. د. ليلى صالح العلي